

Fig. 1 (old) Starting design of the long propellant tank with two sets of struts, aft and forward, with 4 pairs of struts in each of these two sets. Compare with the optimized configuration shown in Fig. 4. (NOTE: In this elevation view only one of the four pairs of struts is displayed)

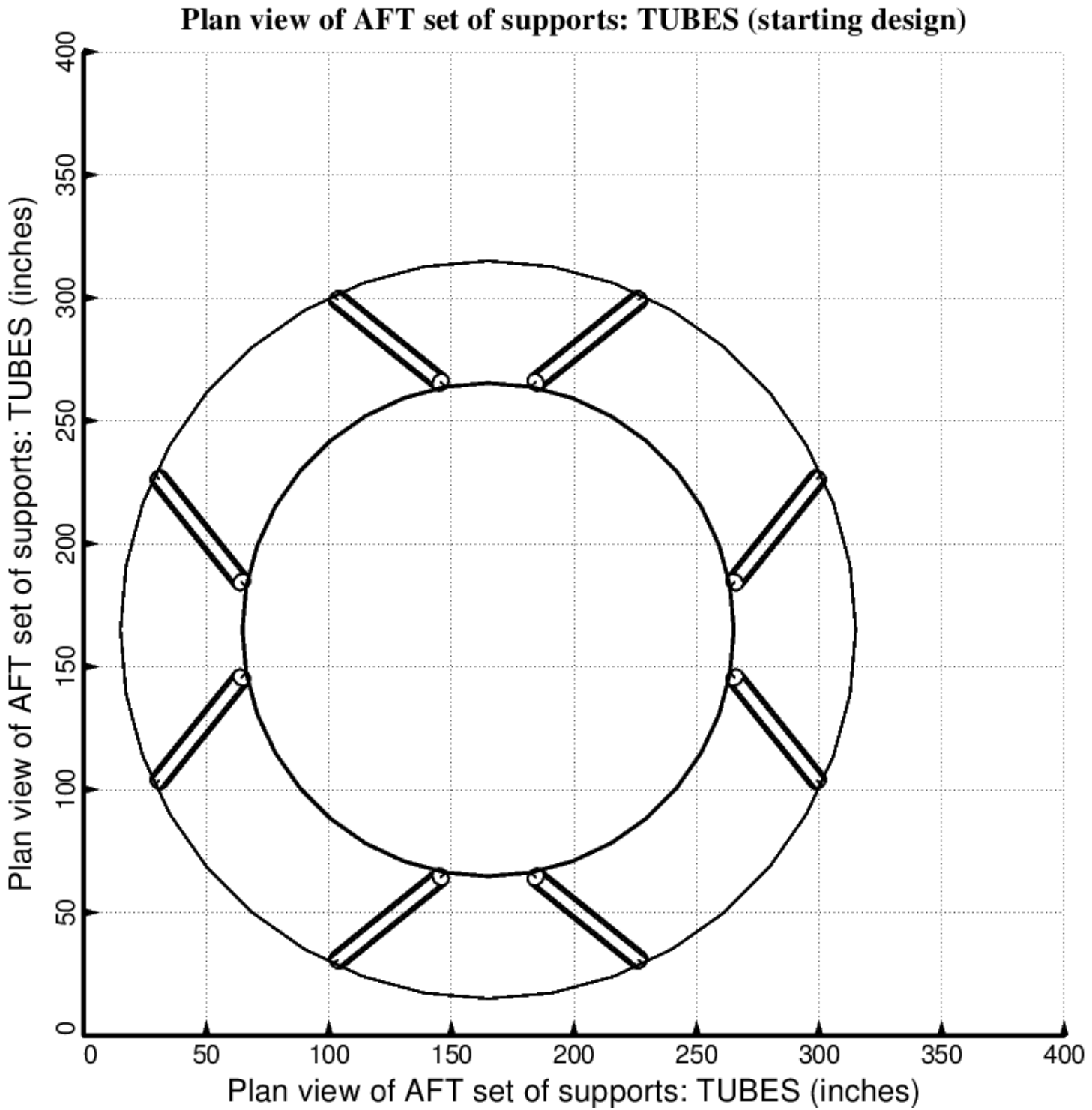


Fig. 2 (old) Starting design of the long propellant tank with two sets of struts, aft and forward, with 4 pairs of struts in each of these two sets. Compare with the optimized configuration shown in Fig. 5.

**Plan view of FWD set of supports: TUBES (starting design)**

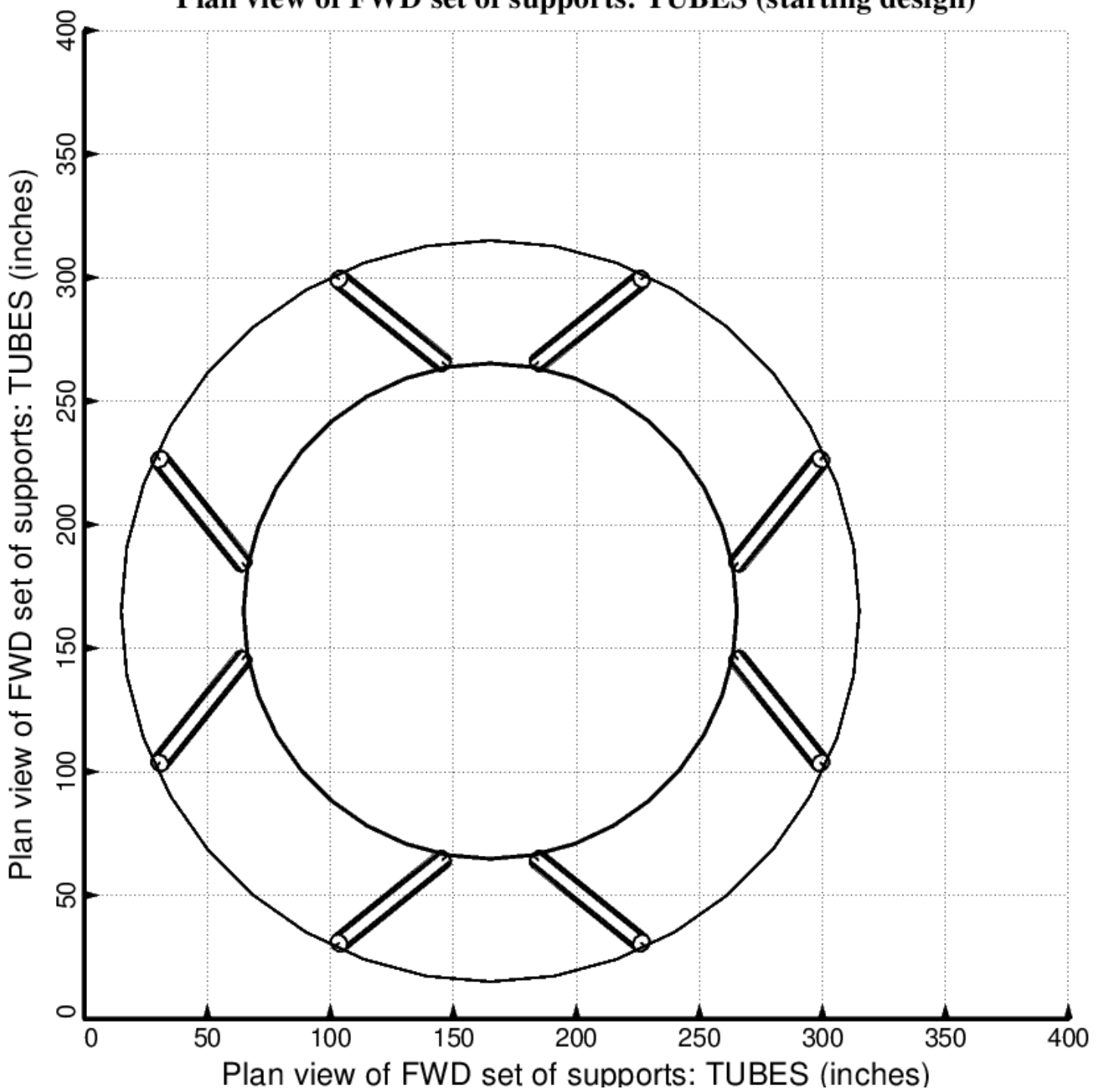


Fig. 3 (old) Starting design of the long propellant tank with two sets of struts, aft and forward, with 4 pairs of struts in each of these two sets. Compare with the optimized configuration shown in Fig. 6.

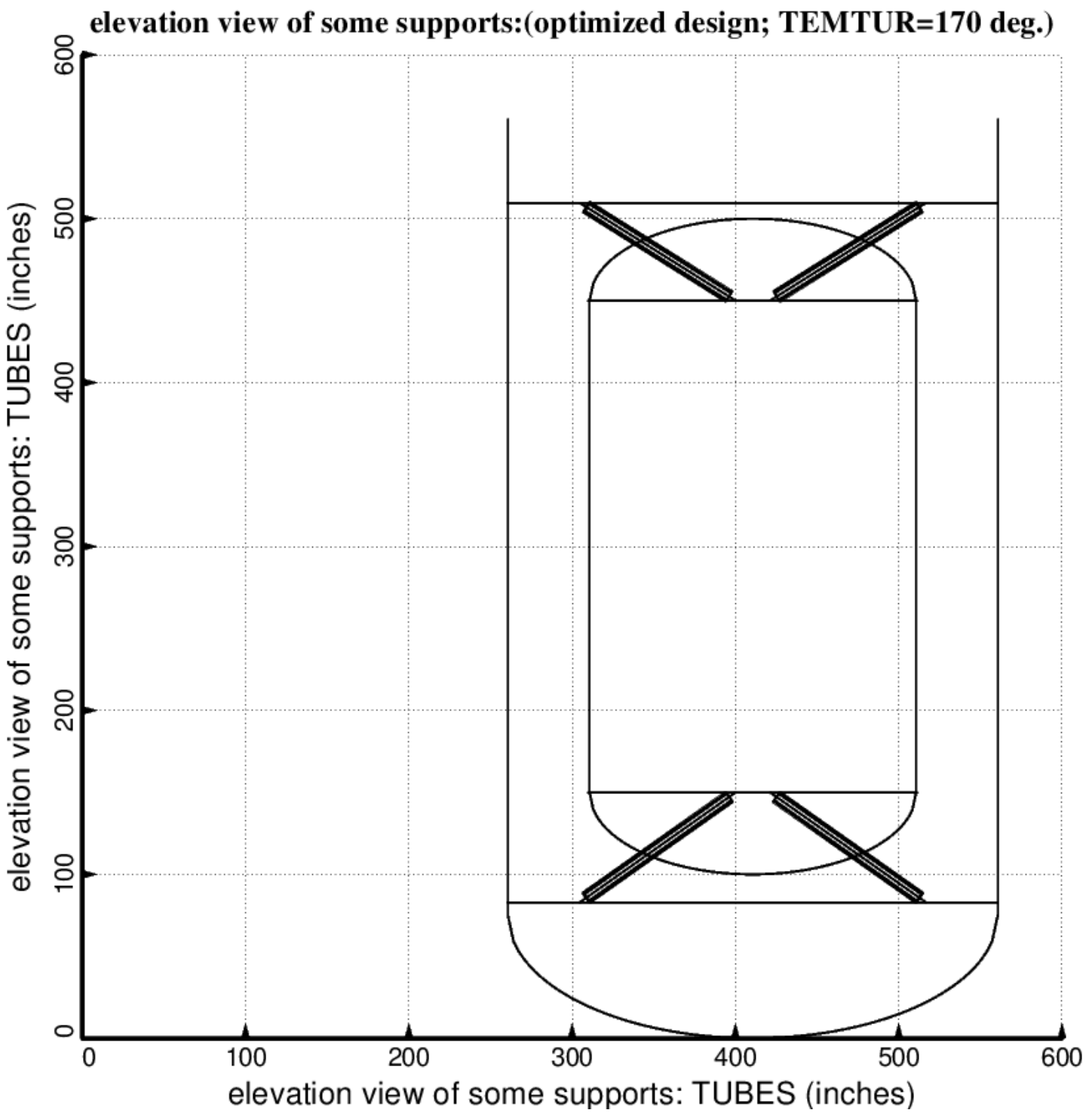


Fig. 4 (old) Optimum design of the long propellant tank with two sets of struts, aft and forward, with 4 pairs of struts in each of these two sets. Compare with the starting configuration shown in Fig. 1. (NOTE: In this elevation view only one of the four pairs of struts is displayed)

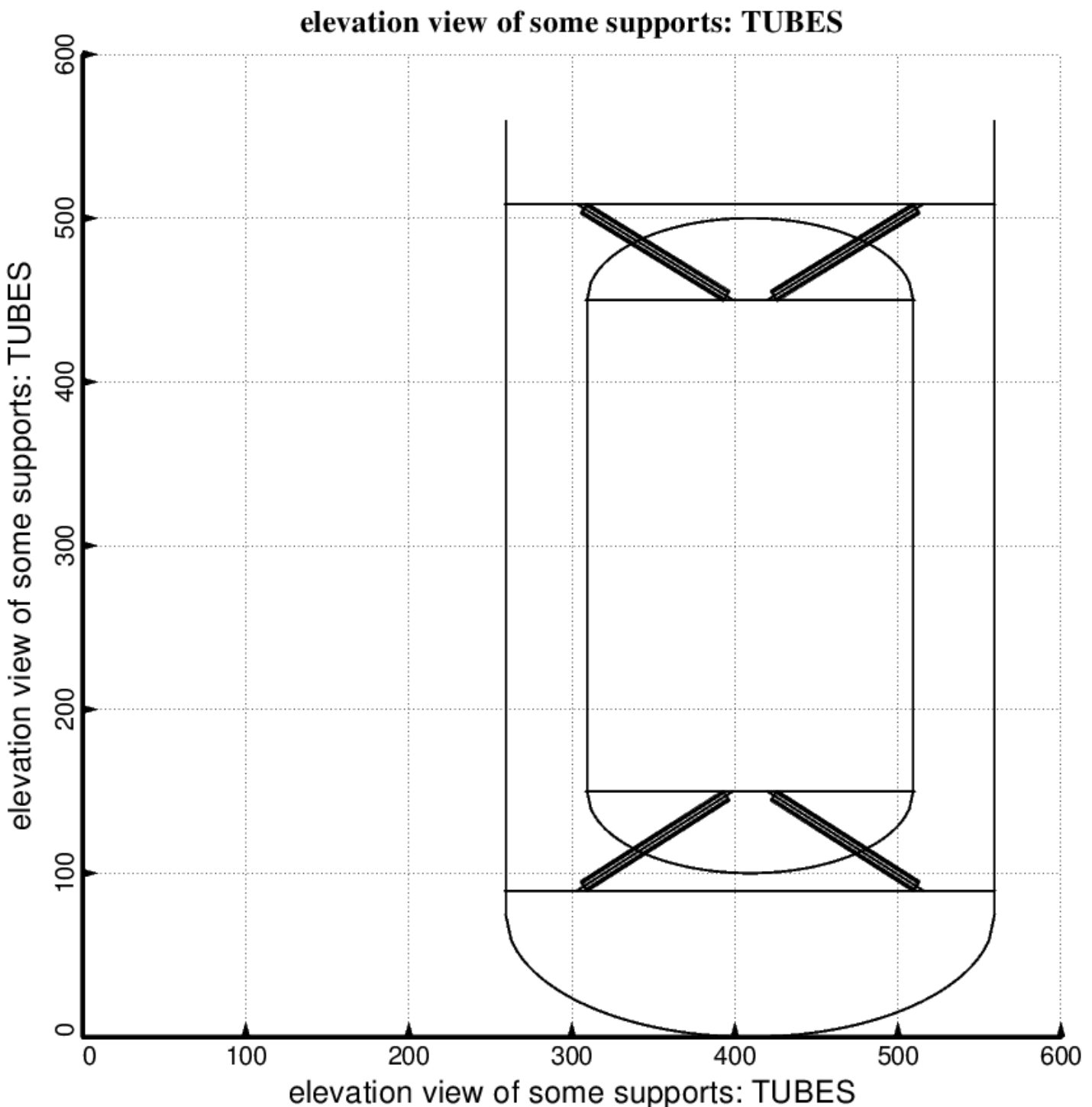


Fig. 4 (new) Optimum design of the long propellant tank with two sets of struts, aft and forward, with 4 pairs of struts in each of these two sets. Compare with the starting configuration shown in Fig. 1. (NOTE: In this elevation view only one of the four pairs of struts is displayed). This optimum design was found with use of the “temporary” (varying density) versions of bosdec (bosdec.density.var) and addbosor4 (addbosor4.density.var).

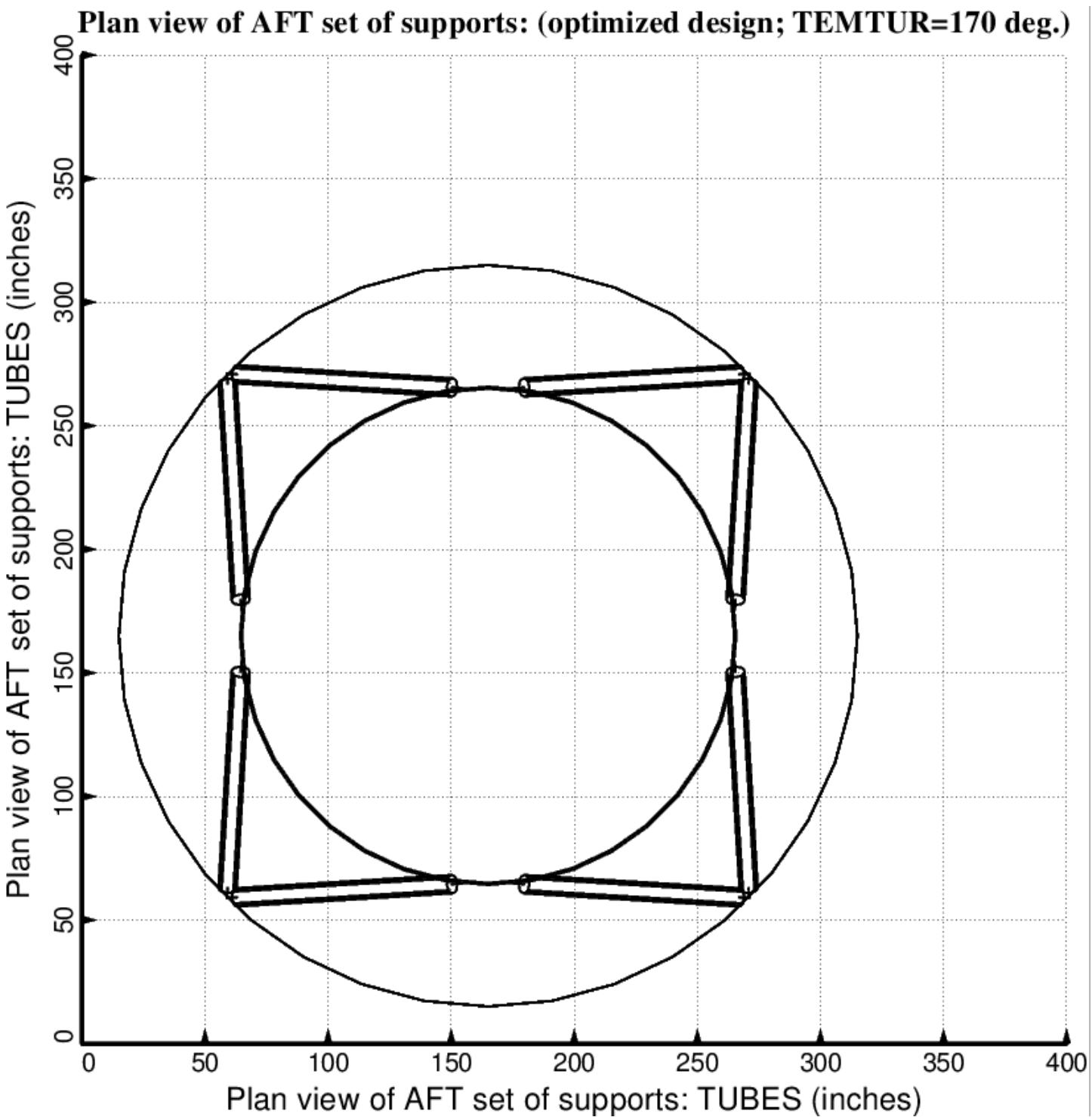


Fig. 5 (old) Optimized design of the long propellant tank with two sets of struts, aft and forward, with 4 pairs of struts in each of these two sets. Compare with the starting configuration shown in Fig. 2.

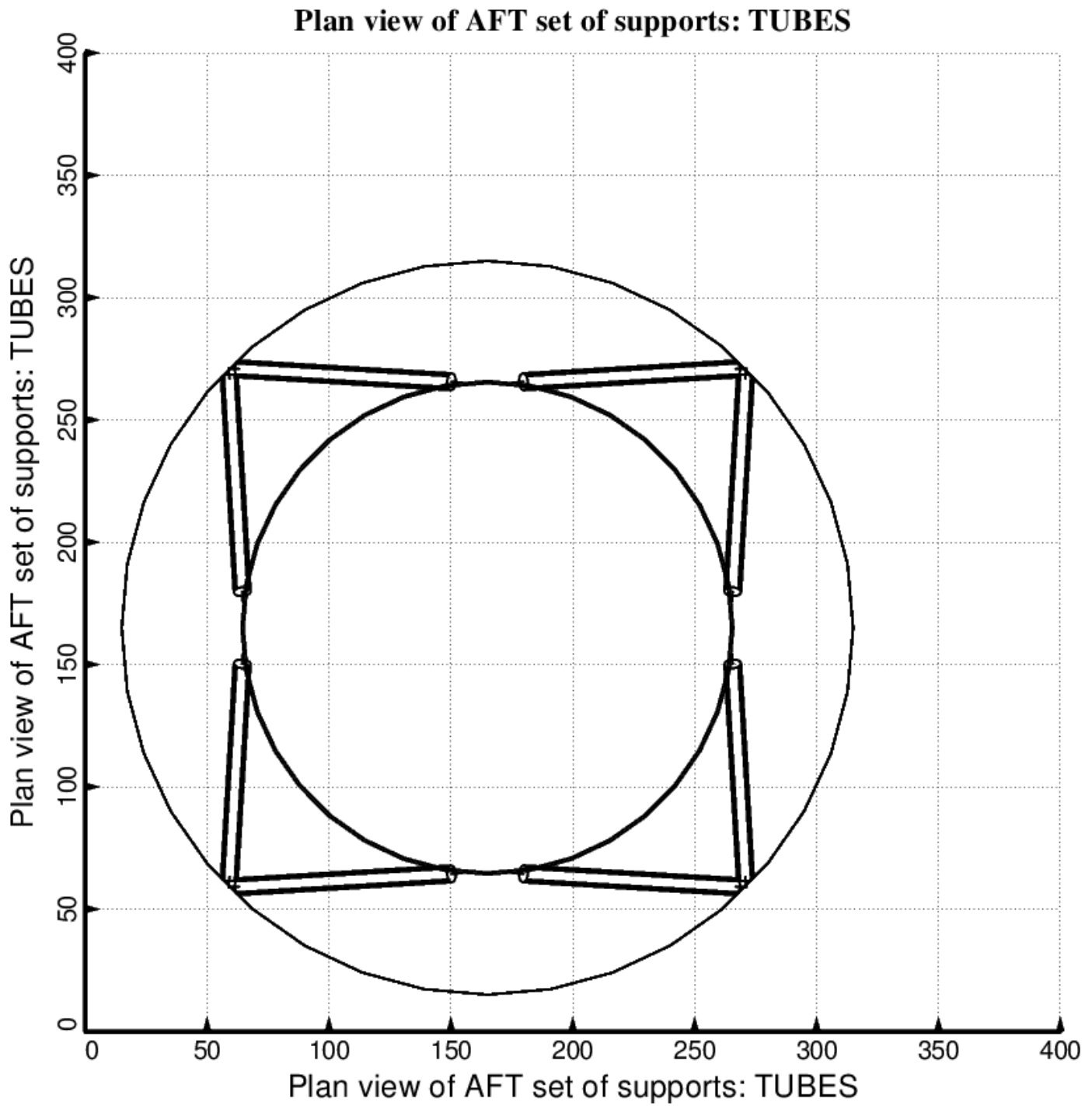


Fig. 5 (new) Optimized design of the long propellant tank with two sets of struts, aft and forward, with 4 pairs of struts in each of these two sets. Compare with the starting configuration shown in Fig. 2. This optimum design was found with use of the “temporary” (varying density) versions of bosdec (bosdec.density.var) and addbosor4 (addbosor4.density.var).

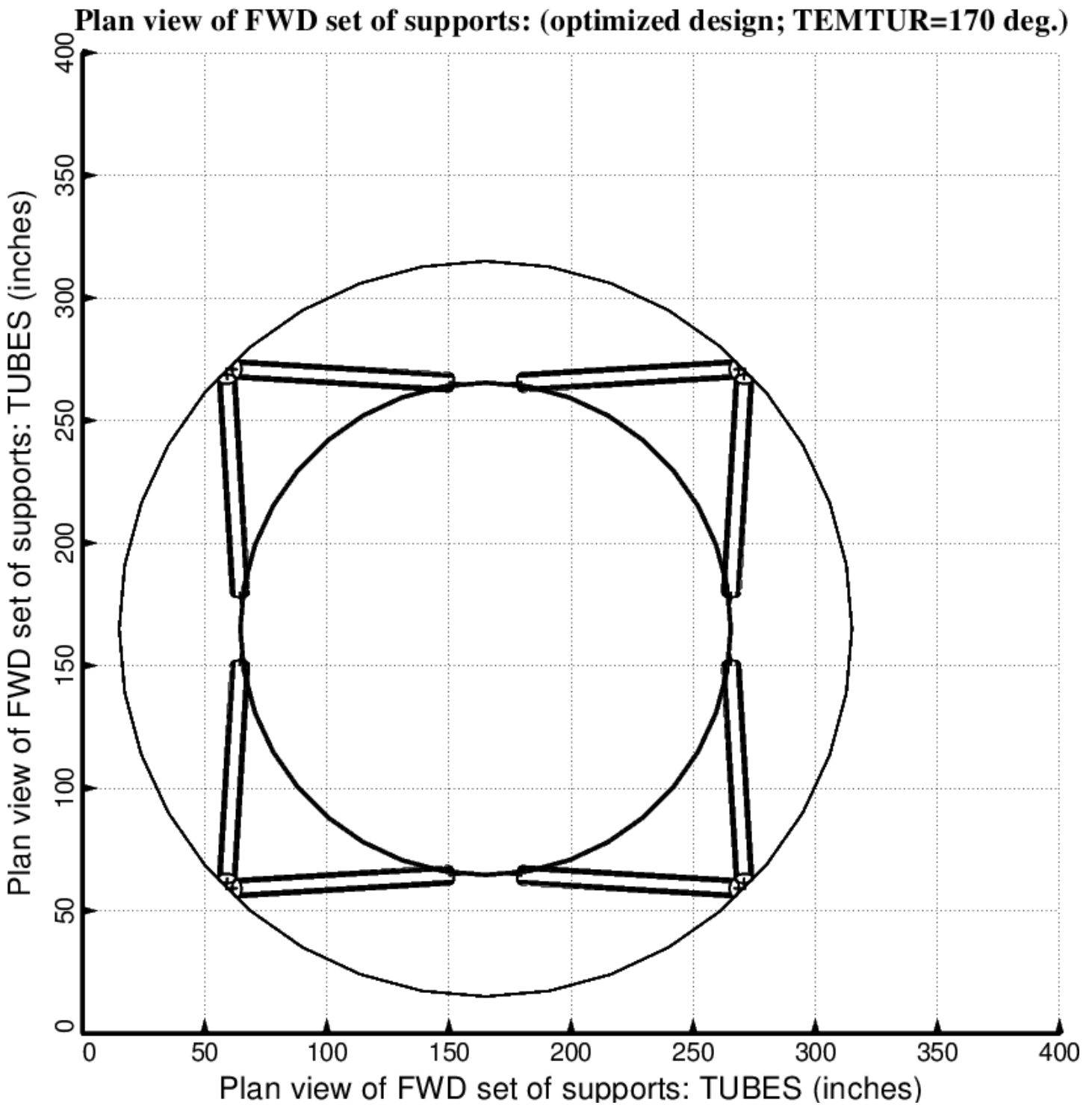


Fig. 6 (old) Optimized design of the long propellant tank with two sets of struts, aft and forward, with 4 pairs of struts in each of these two sets. Compare with the optimized configuration shown in Fig. 3.

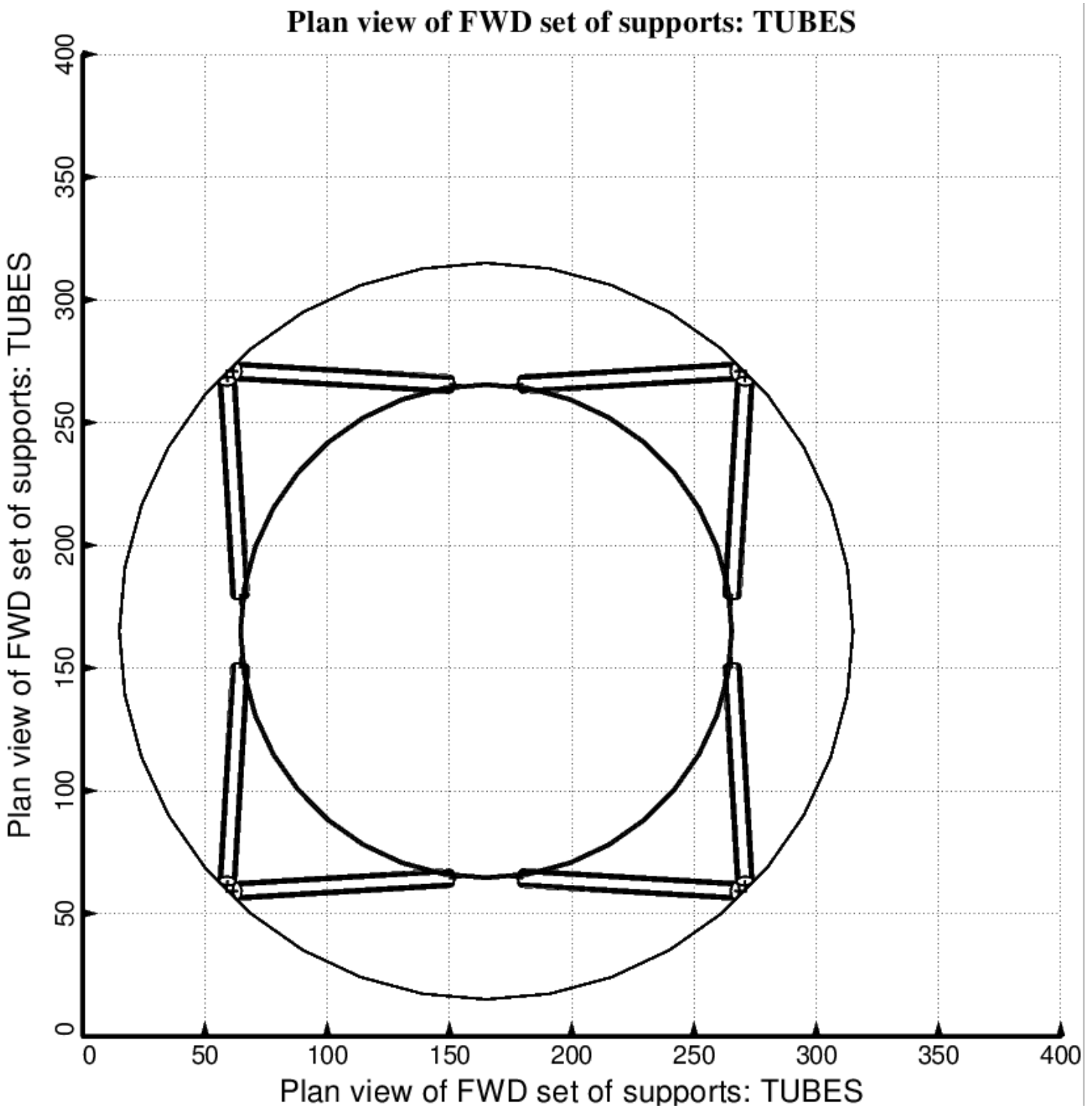


Fig. 6 (new) Optimized design of the long propellant tank with two sets of struts, aft and forward, with 4 pairs of struts in each of these two sets. Compare with the optimized configuration shown in Fig. 3. This optimum design was found with use of the “temporary” (varying density) versions of bosdec (bosdec.density.var) and addbosor4 (addbosor4.density.var).

### elevation view of some supports: TUBES (starting design)

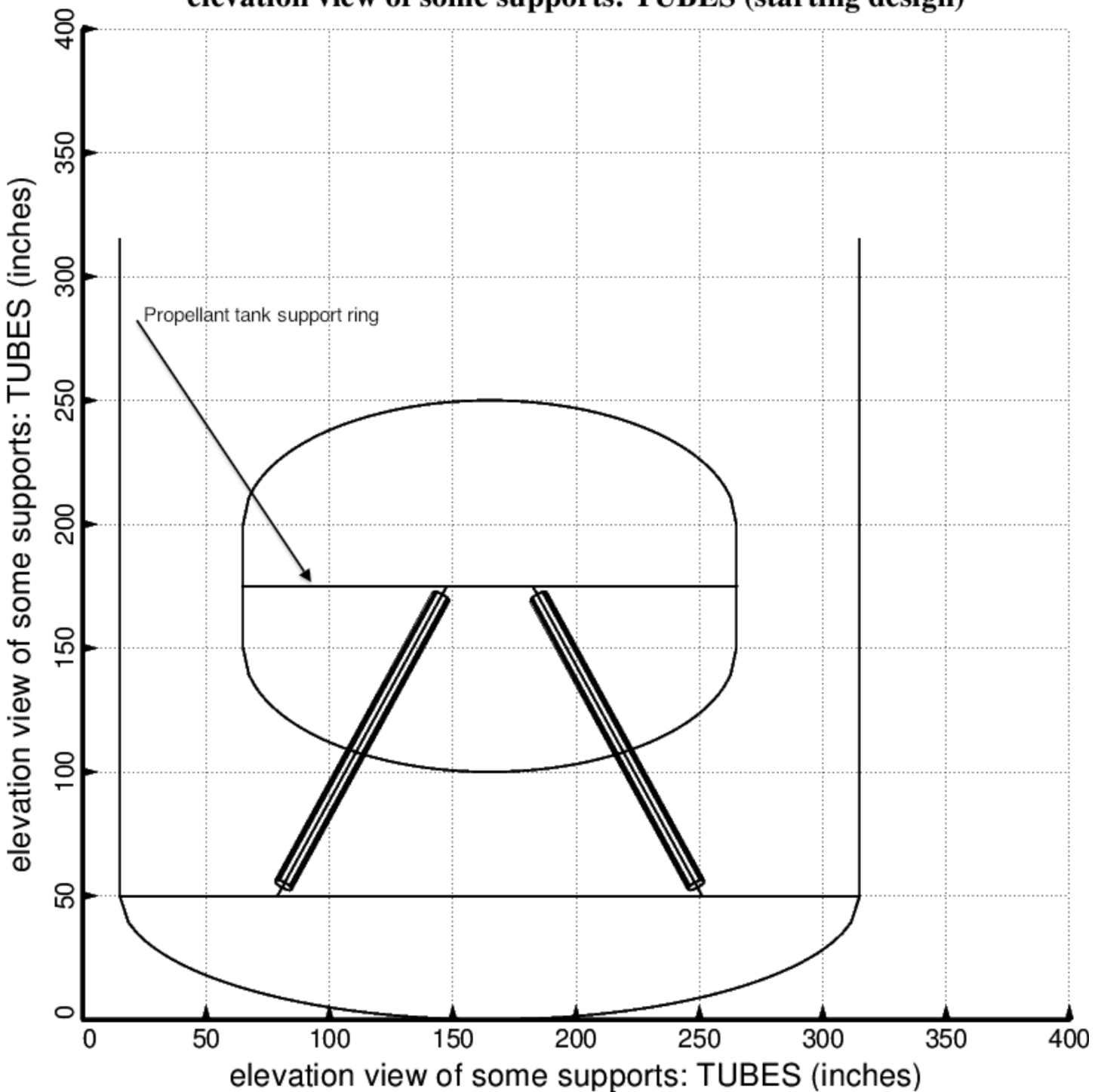


Fig. 7 (old) Starting design of the short propellant tank with one set of struts, called “aft”, with 4 pairs of struts in this one set. Compare with the optimized configuration shown in Fig. 9. (NOTE: In this elevation view only one of the four pairs of struts is displayed)

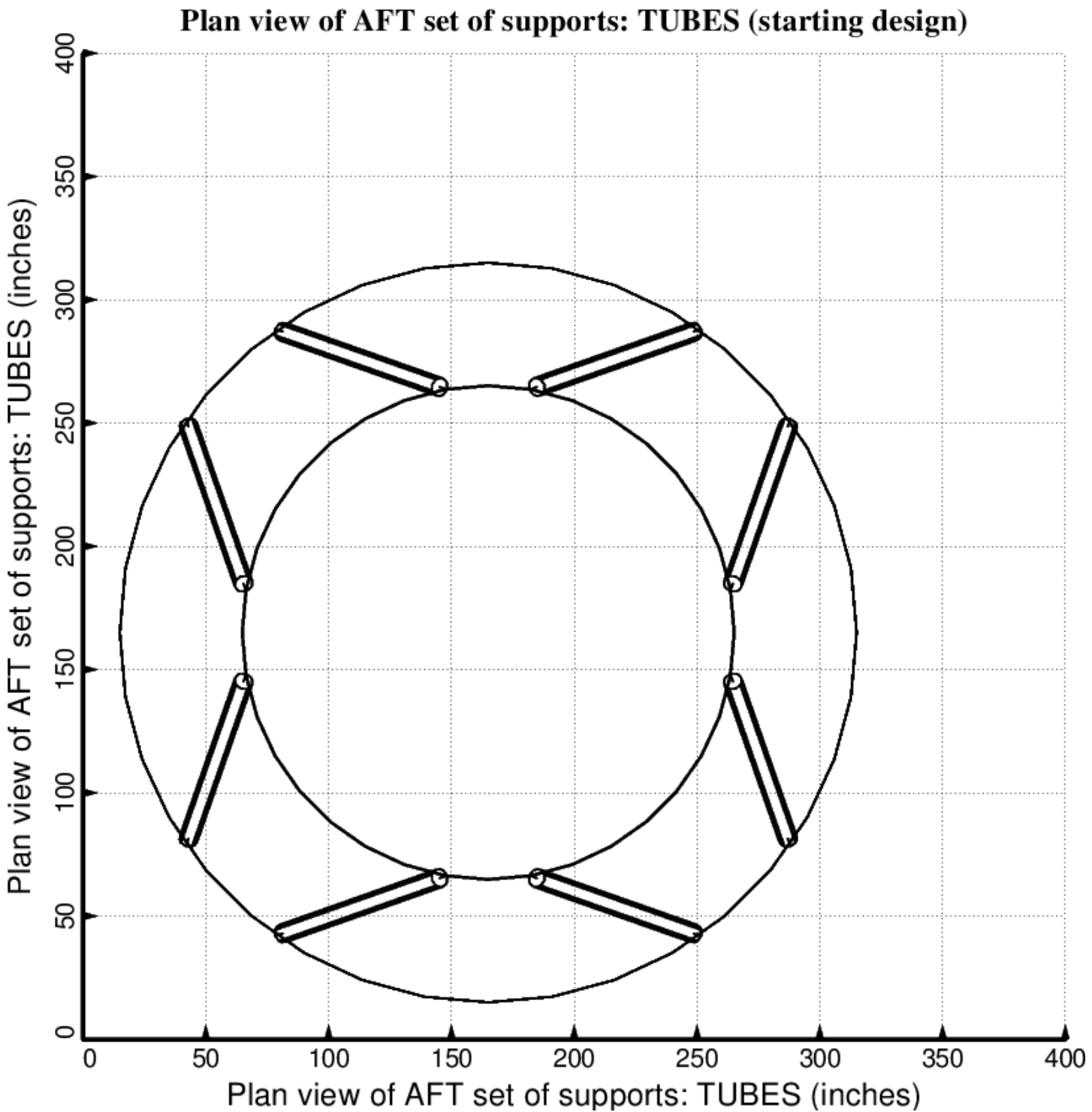


Fig. 8 (old) Starting design of the short propellant tank with one set of struts, called “aft”, with 4 pairs of struts in this one set. Compare with the optimized configuration shown in Fig. 10.

### elevation view of some supports: TUBES (optimized design)

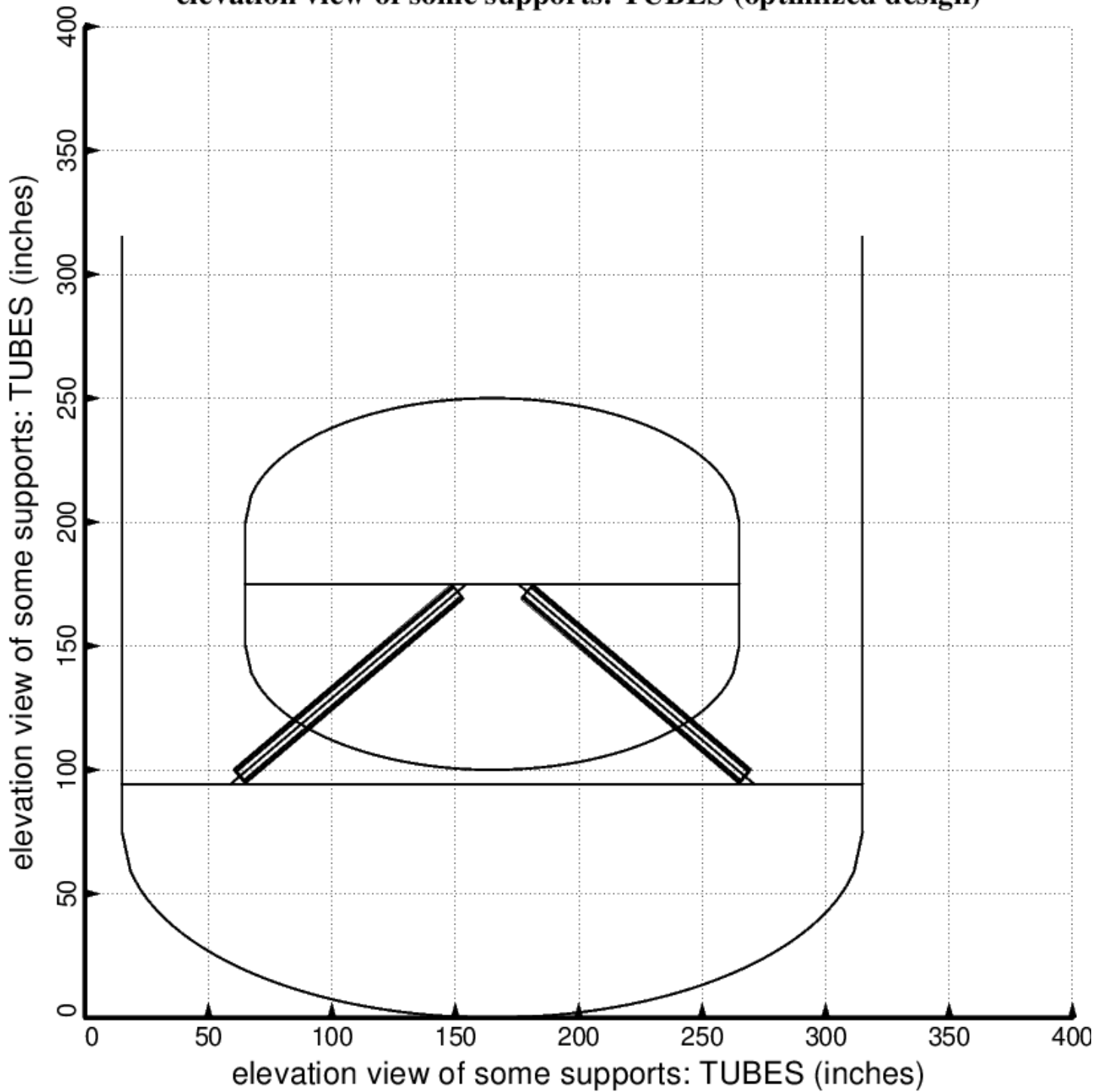


Fig. 9 (old) Optimized design of the short propellant tank with one set of struts, called “aft”, with 4 pairs of struts in this one set. Compare with the starting configuration shown in Fig. 7. (NOTE: In this elevation view only one of the four pairs of struts is displayed)

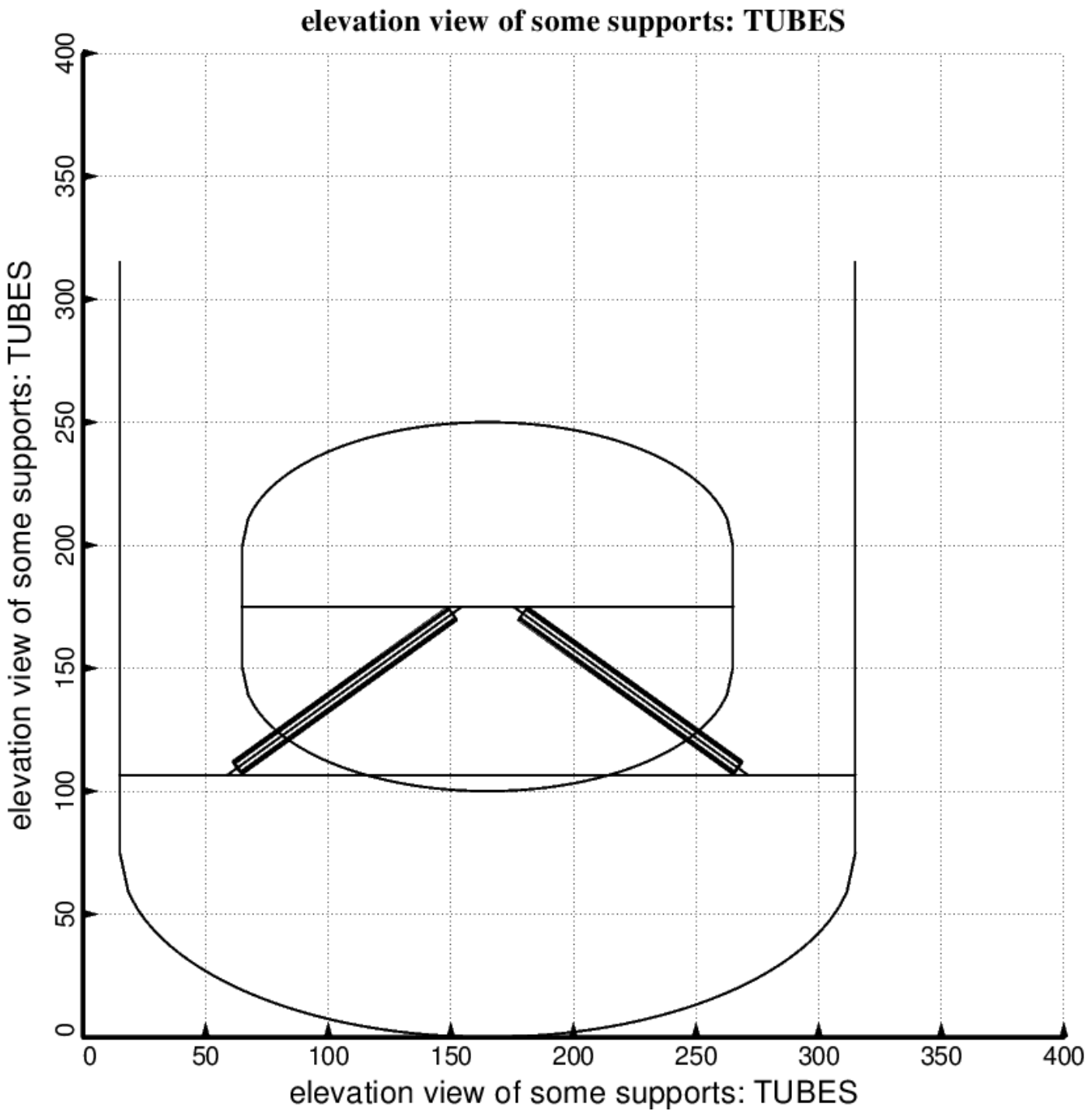


Fig. 9 (new) Optimized design of the short propellant tank with one set of struts, called “aft”, with 4 pairs of struts in this one set. Compare with the starting configuration shown in Fig. 7. (NOTE: In this elevation view only one of the four pairs of struts is displayed). This optimum design was found with use of the “temporary” (varying density) versions of bosdec (bosdec.density.var) and addbosor4 (addbosor4.density.var).

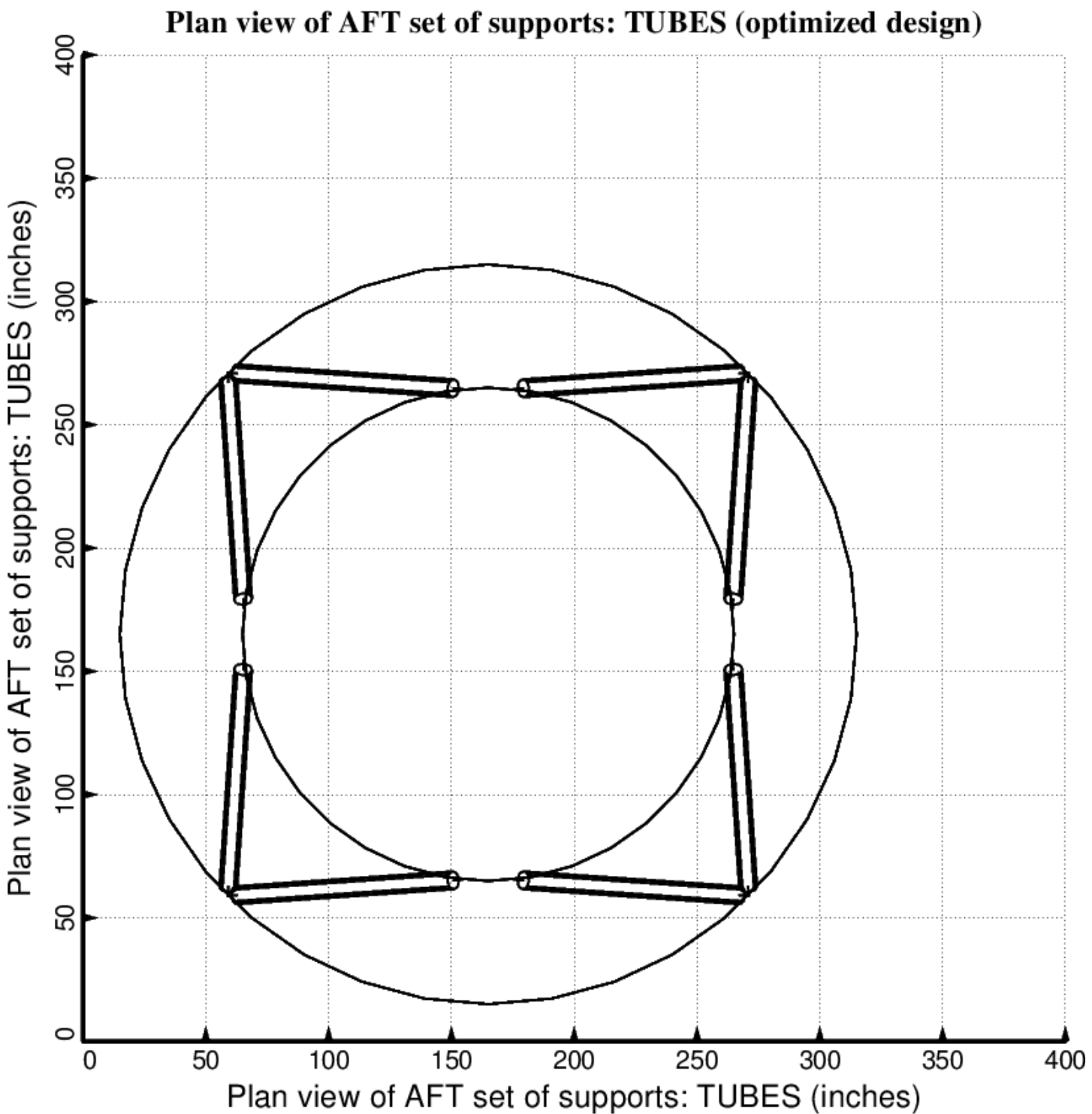


Fig. 10 (old) Optimized design of the short propellant tank with one set of struts, called “aft”, with 4 pairs of struts in this one set. Compare with the starting configuration shown in Fig. 8.

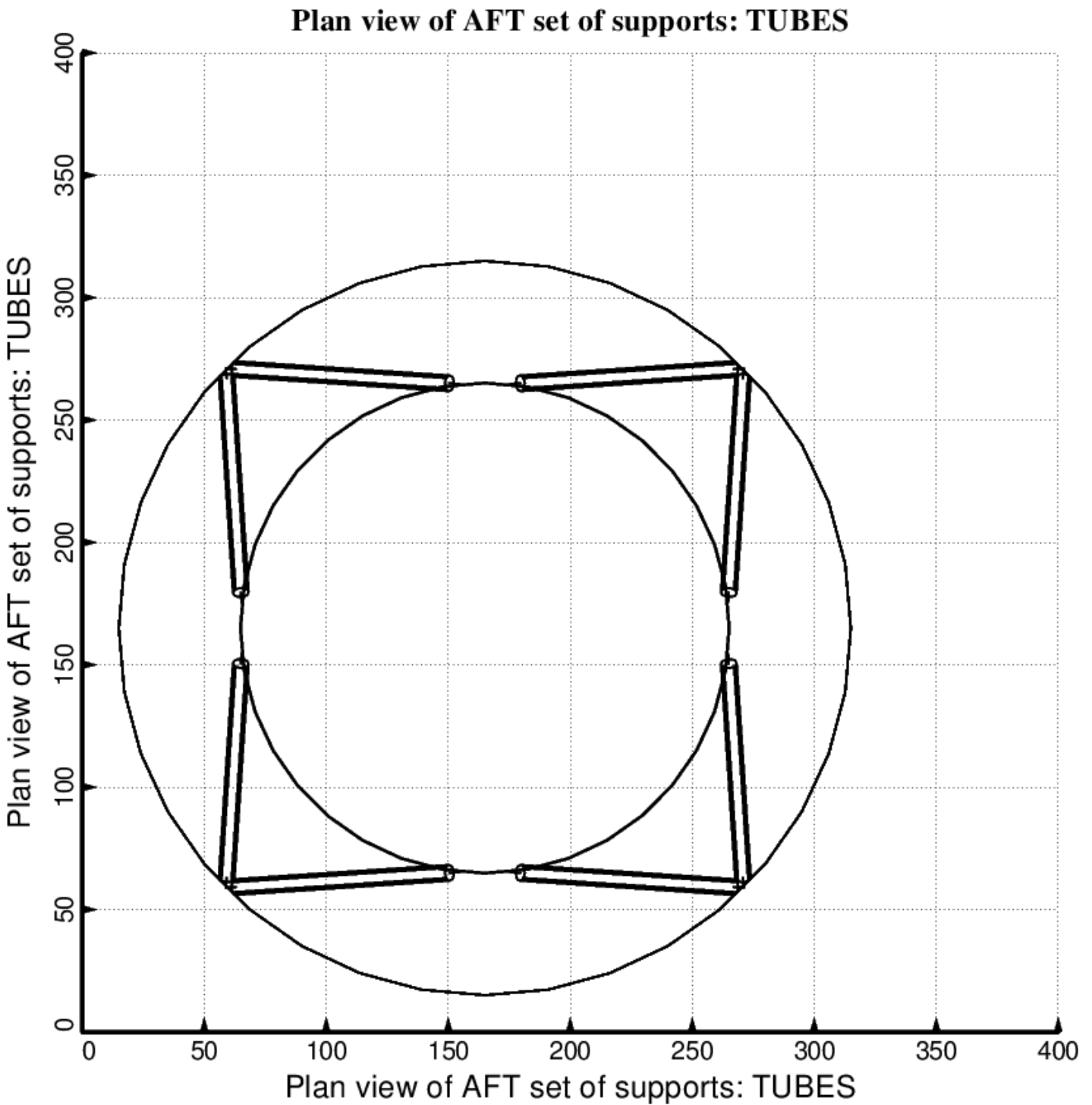


Fig. 10 (new) Optimized design of the short propellant tank with one set of struts, called “aft”, with 4 pairs of struts in this one set. Compare with the starting configuration shown in Fig. 8. This optimum design was found with use of the “temporary” (varying density) versions of bosdec (bosdec.density.var) and addbosor4 (addbosor4.density.var).

### Plan view of AFT set of supports: TUBES (superopt2; WGT = 0.5)

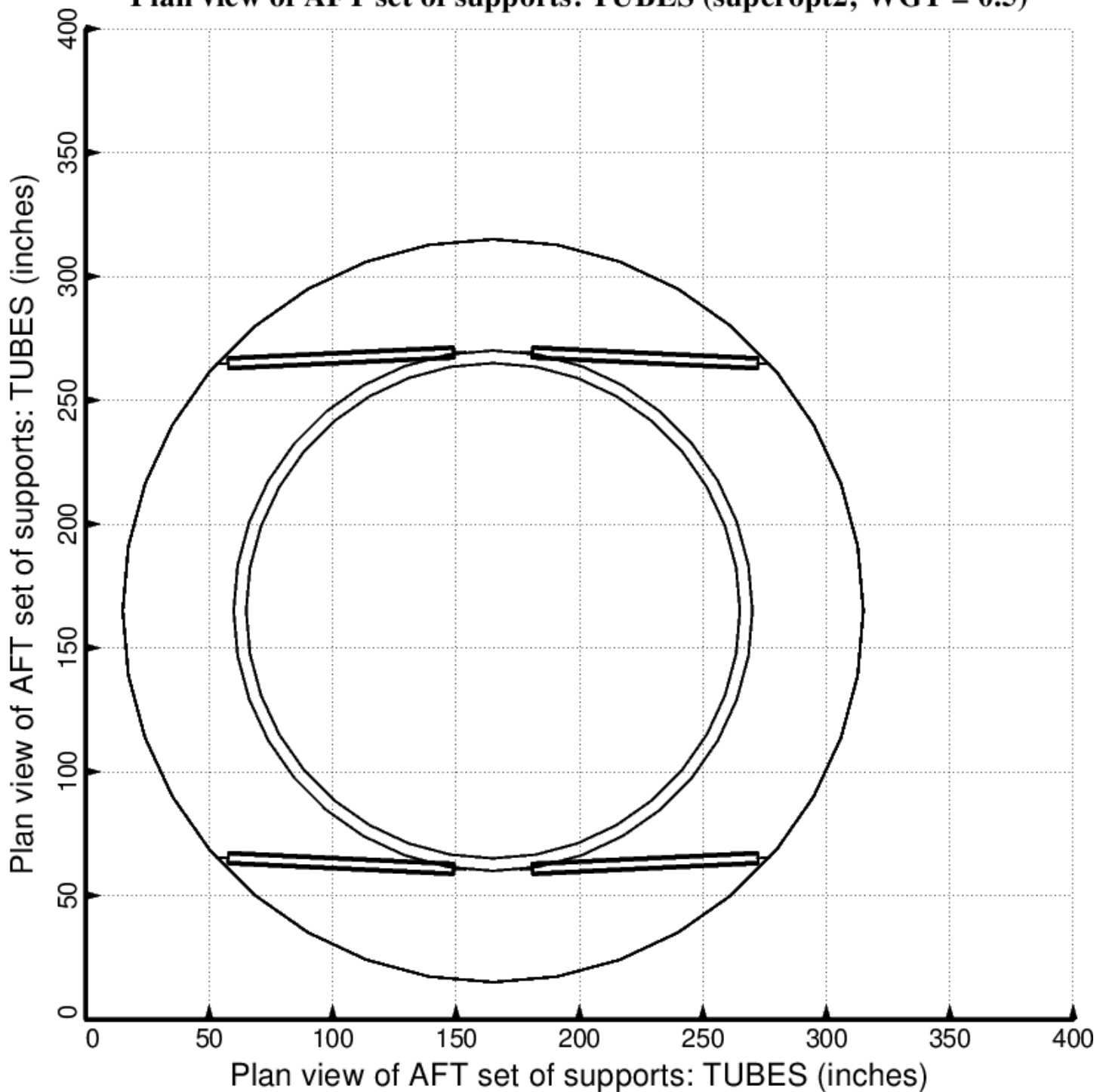


Fig. 11 (old) Optimized design of the long propellant tank with two sets of struts, aft and forward, with 2 pairs of struts in each of these two sets.

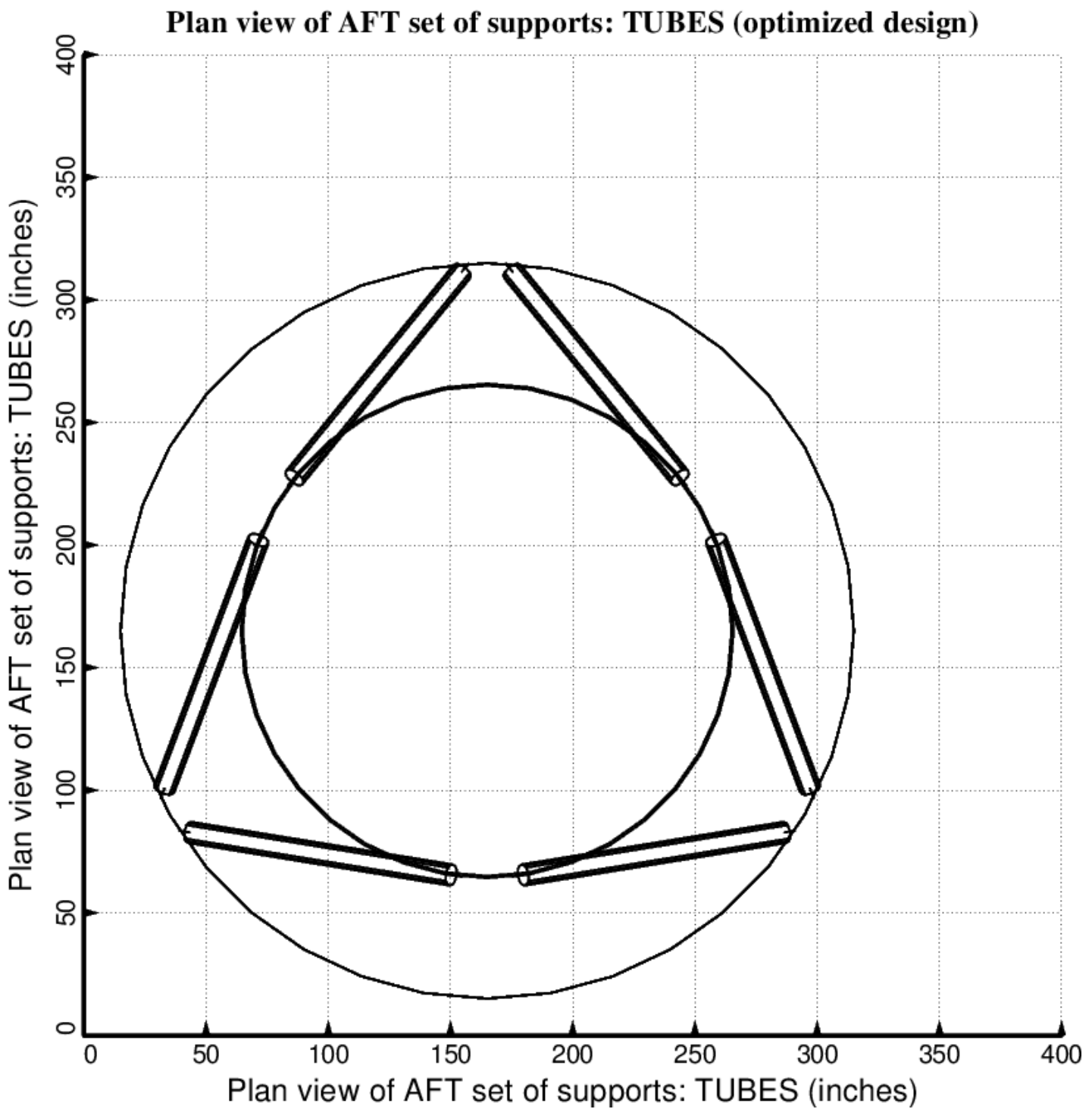


Fig. 12 (old) Optimized design of the long propellant tank with two sets of struts, aft and forward, with 3 pairs of struts in each of these two sets. Notice that there is a small clearance problem at the end of the struts attached to the propellant tank. In the work reported here no constraint was introduced to avoid clearance problems of this type.

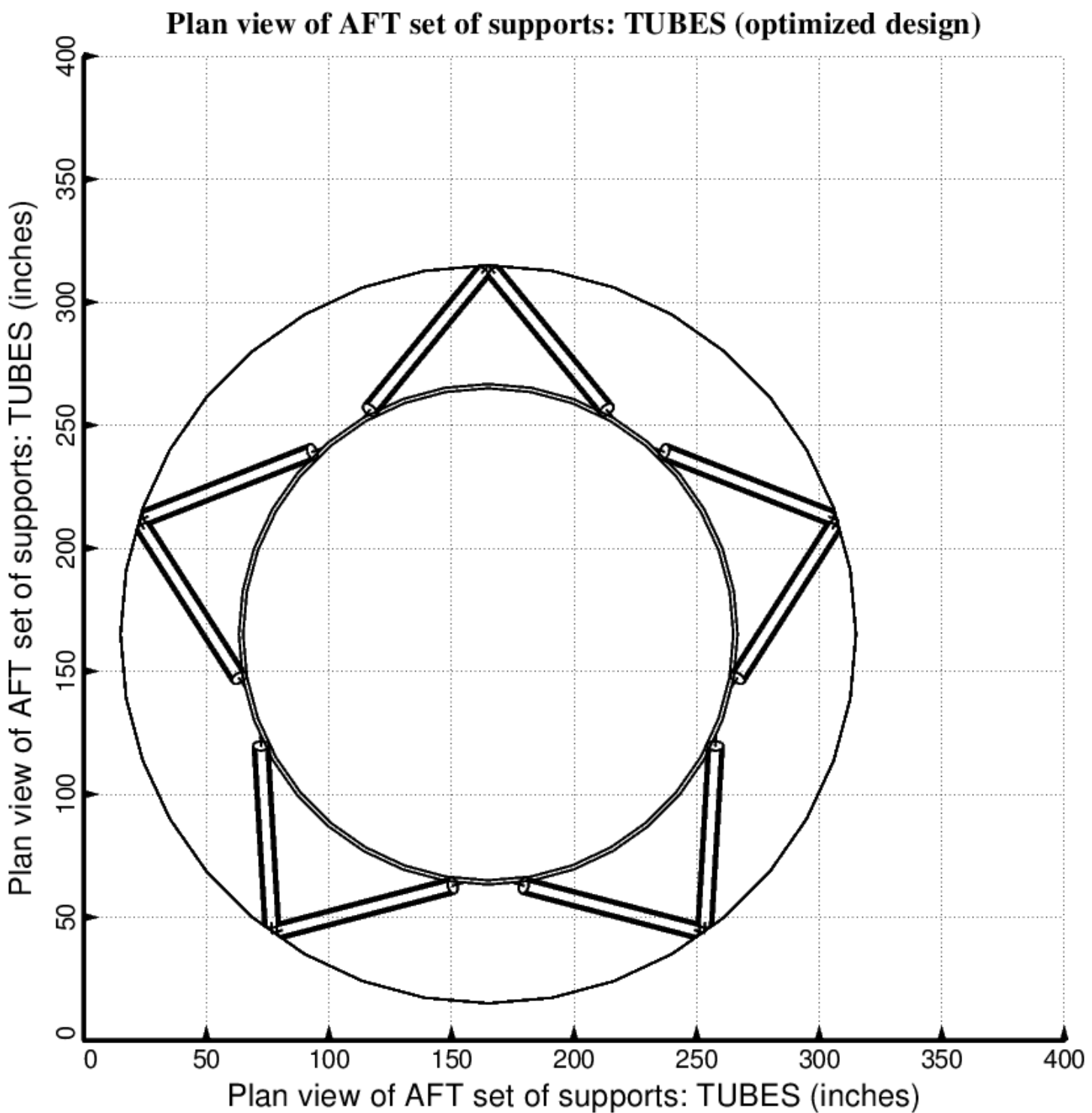


Fig. 13 (old) Optimized design of the long propellant tank with two sets of struts, aft and forward, with 5 pairs of struts in each of these two sets.

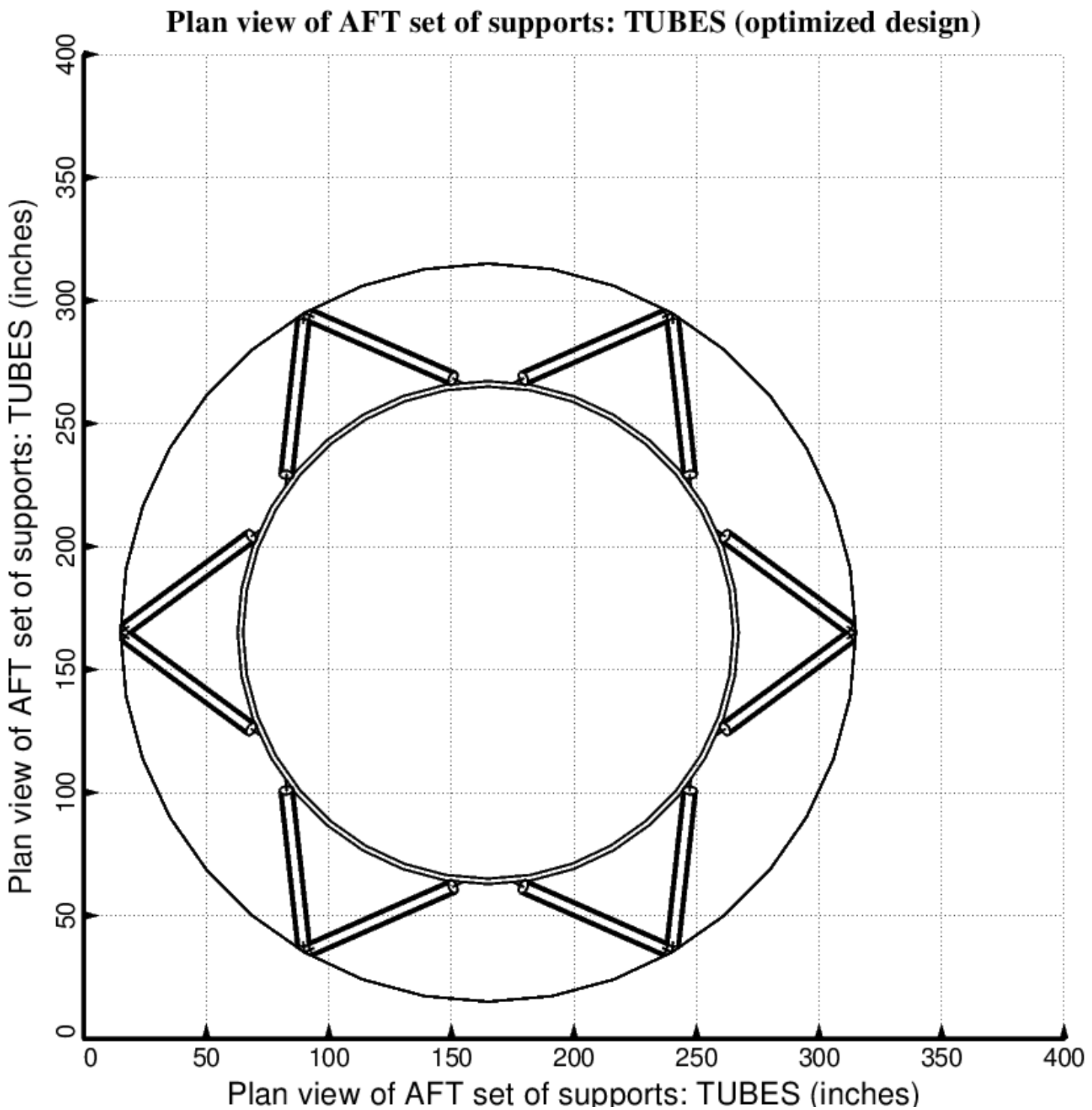


Fig. 14 (old) Optimized design of the long propellant tank with two sets of struts, aft and forward, with 6 pairs of struts in each of these two sets.

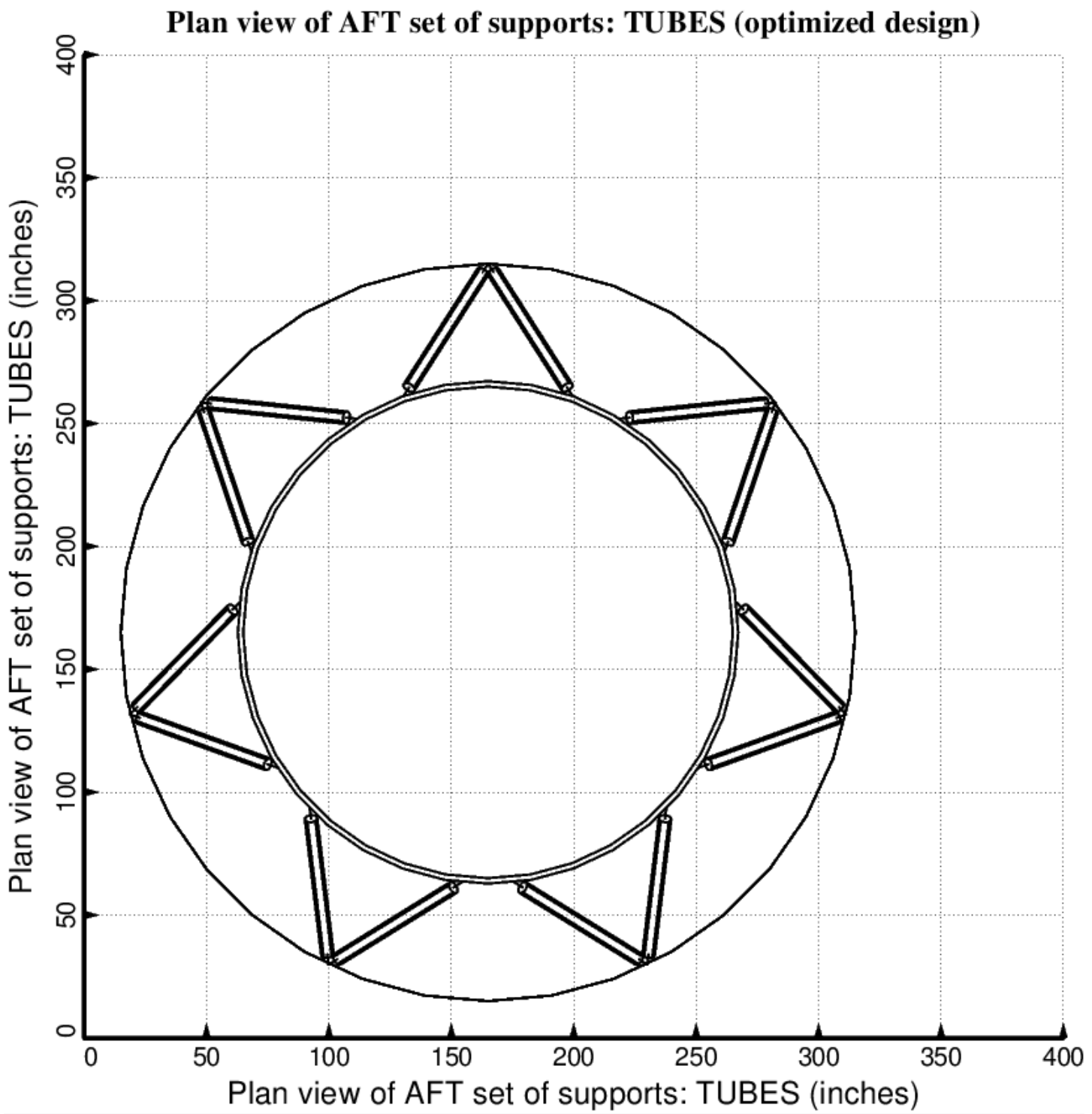


Fig. 15 (old) Optimized design of the long propellant tank with two sets of struts, aft and forward, with 7 pairs of struts in each of these two sets.

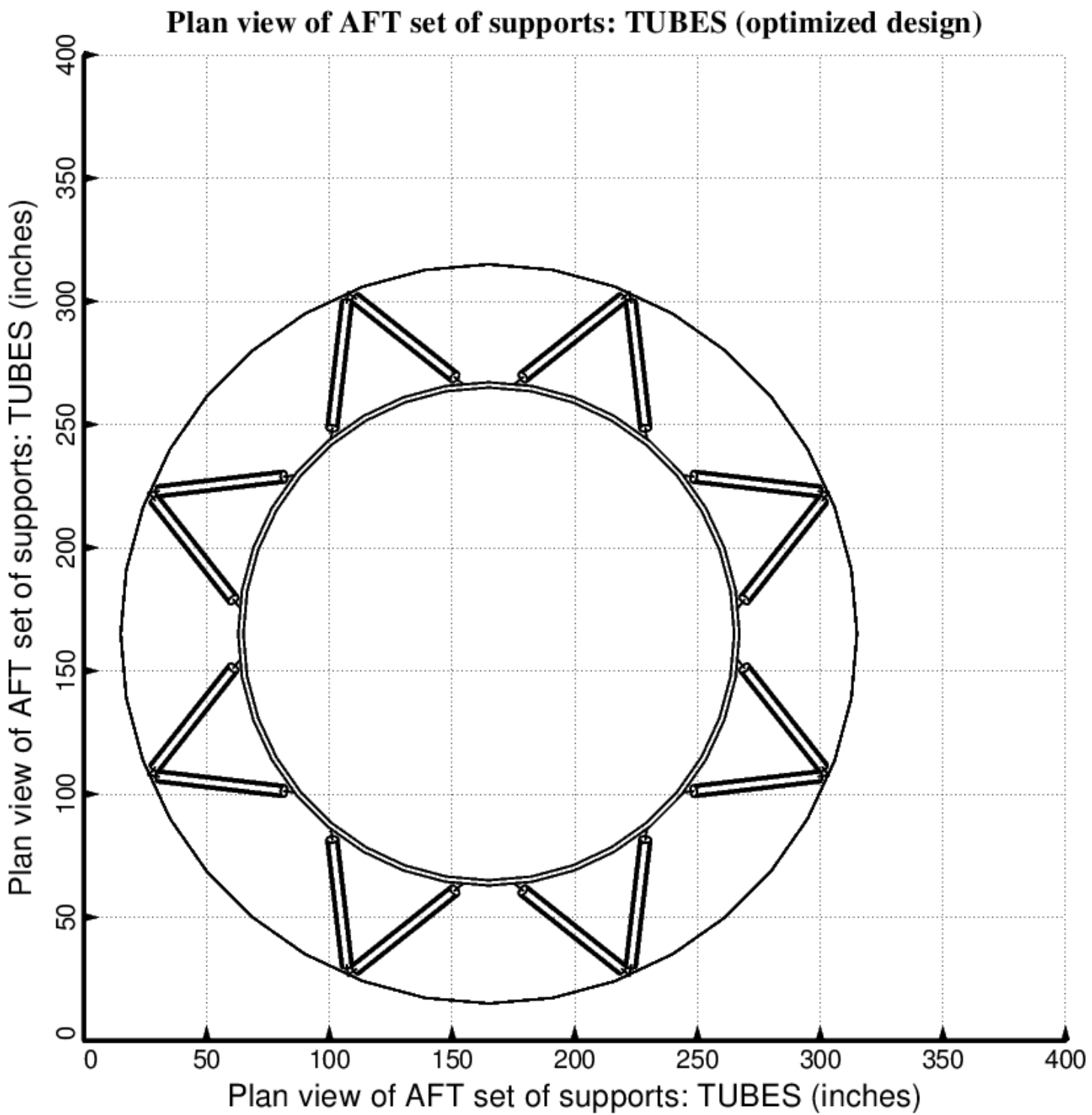


Fig. 16 (old) Optimized design of the long propellant tank with two sets of struts, aft and forward, with 8 pairs of struts in each of these two sets.

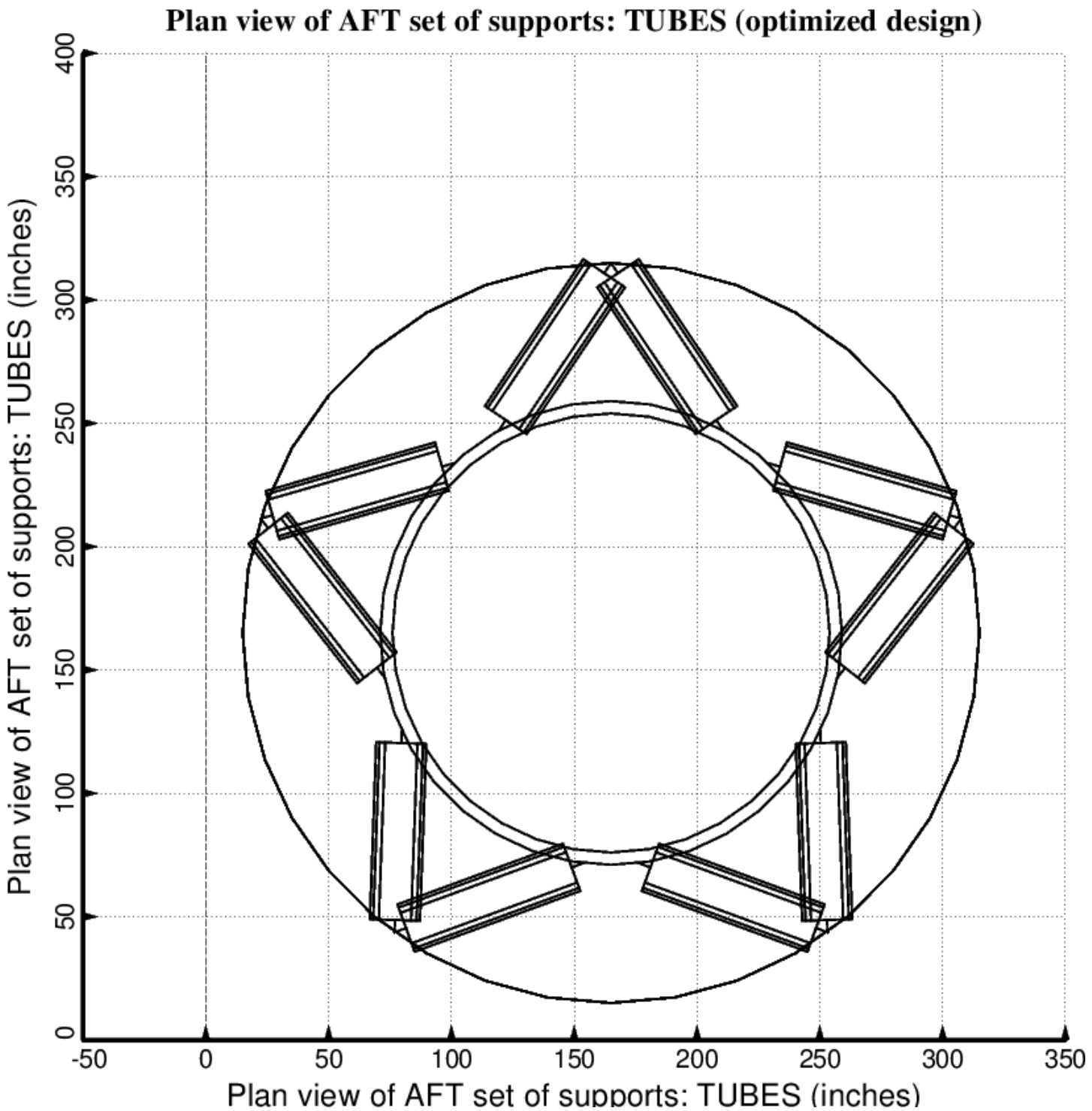


Fig. 17 (old) Optimized design of the long propellant tank with two sets of struts, aft and forward, with 5 pairs of struts in each of these two sets. The ends of the struts attached to the propellant tank are attached within the end domes, not at the junctions between the domes and the cylindrical part of the tank. This is a poor design: corresponding to high values of the empty tank mass and the total conductance.

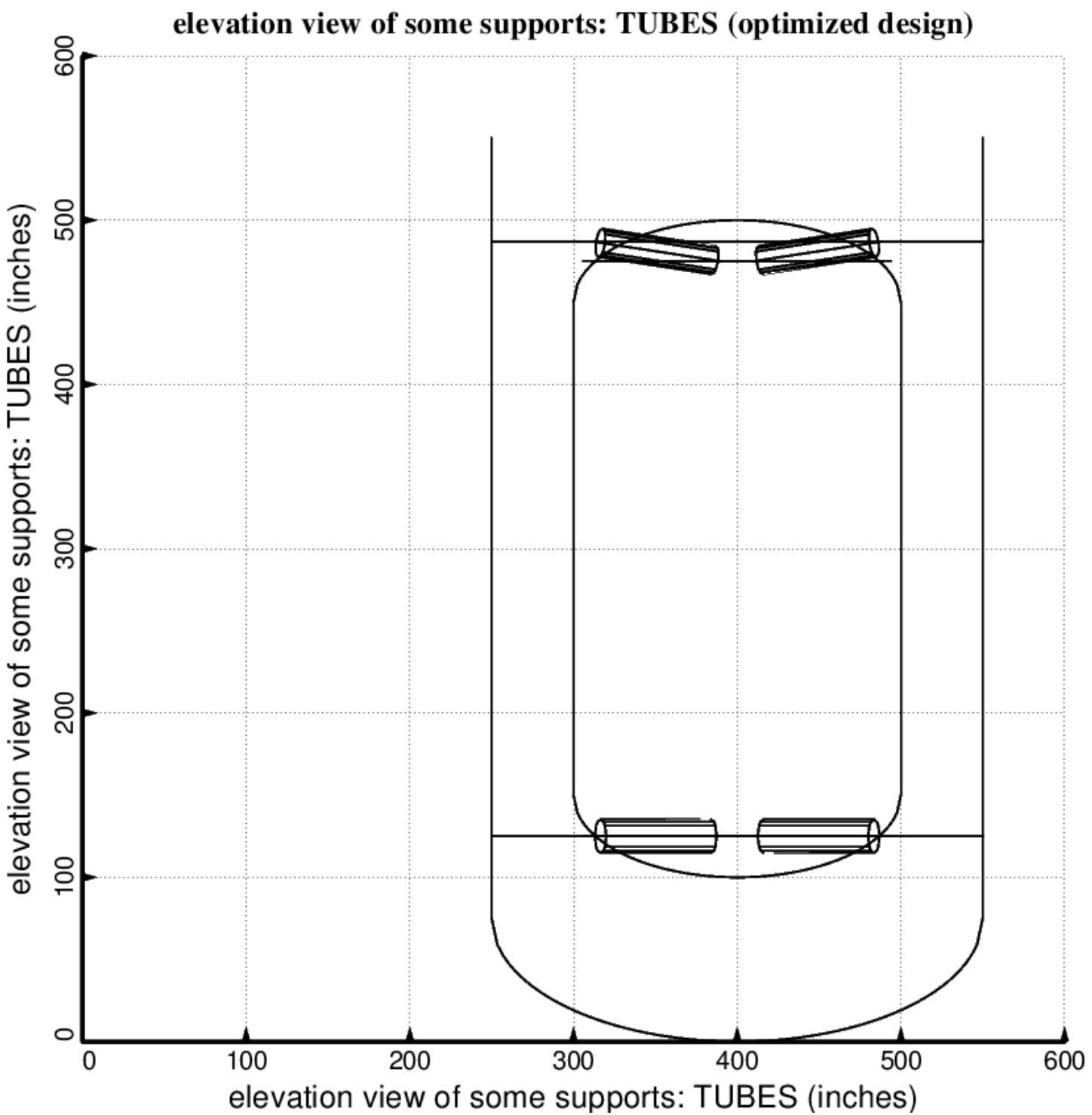


Fig. 18 (old) Optimum design of the long propellant tank with two sets of struts, aft and forward, with 5 pairs of struts in each of these two sets (NOTE: In this elevation view only one of the five pairs of struts is displayed)  
This is a poor design because the tank-ends of the struts are attached within the domes, not at the junctions between the domes and the cylindrical part of the tank.

- - - Undeformed; optimized design found with the use of the temporary BIGBOSOR4/BOSDEC  
 — Deformed; Load Case 2 (lateral 10g acceleration); curing temperature, TEMTUR = 170 degrees

**test: vibration mode1; freq.=10.957; n=0 circ.waves; permanent bigbosor4**

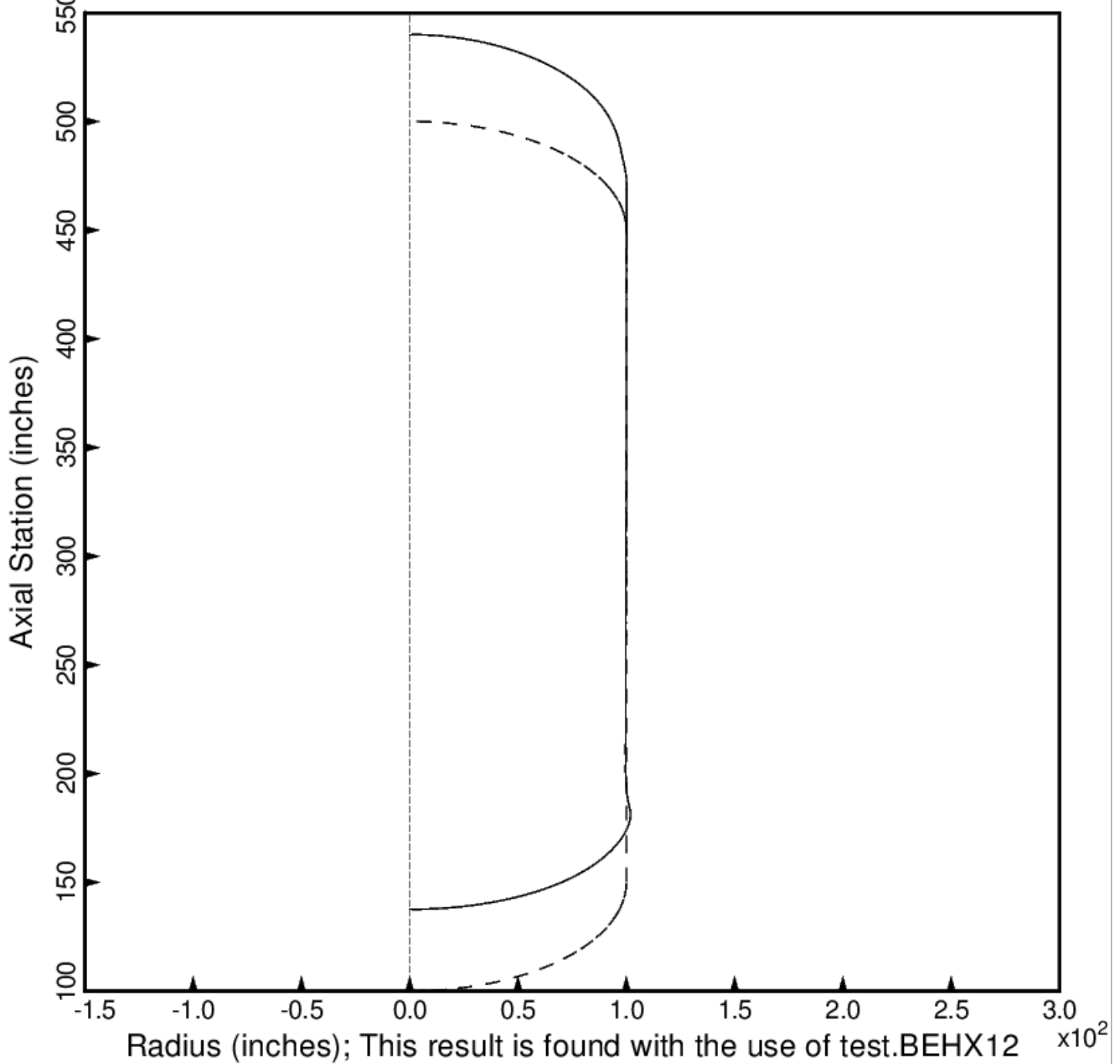


Fig. 19 (old) Free vibration mode of the optimized tank/strut system for the long propellant tank with aft and forward sets of struts, 4 strut pairs in each set. The struts are present in the BIGBOSOR4 model but are not plotted here because BIGBOSOR4 does not yet have the capability to plot springs. This mode corresponds to axial motion.

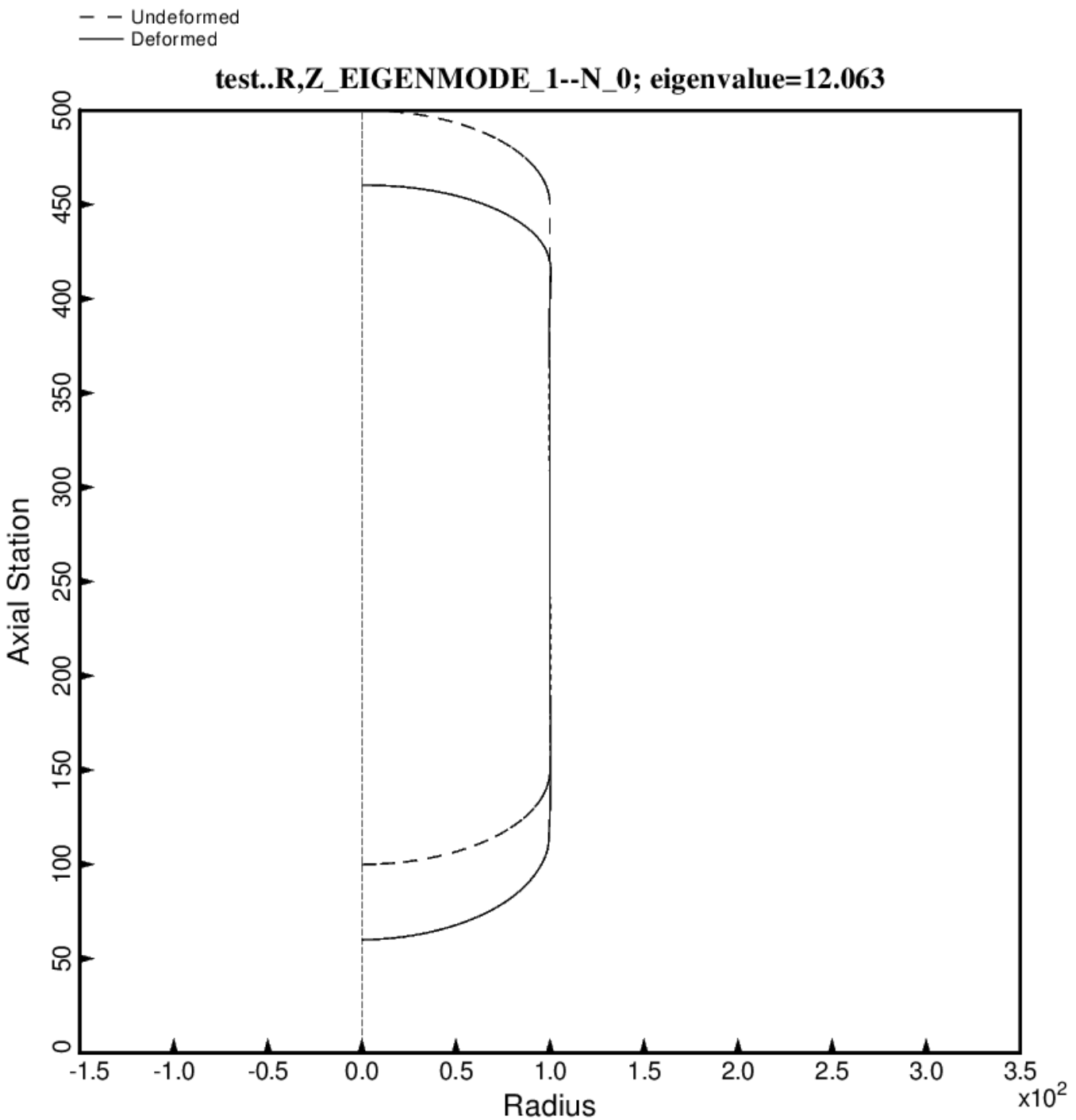


Fig. 19 (new) Free vibration mode of the optimized tank/strut system for the long propellant tank with aft and forward sets of struts, 4 strut pairs in each set, Load Case 2 (test.BEHX12). The struts are present in the BIGBOSOR4 model but are not plotted here because BIGBOSOR4 does not yet have the capability to plot springs. This mode corresponds to axial motion. This optimum design was found with use of the “permanent” (constant density) versions of bosdec (bosdec.tank) and addbosor4 (addbosor4.tank).

- - Undeformed; optimized design found with the use of the temporary BIGBOSOR4/BOSDEC  
 — Deformed; Load Case 2 (lateral 10g acceleration); curing temperature, TEMTUR = 170 degrees

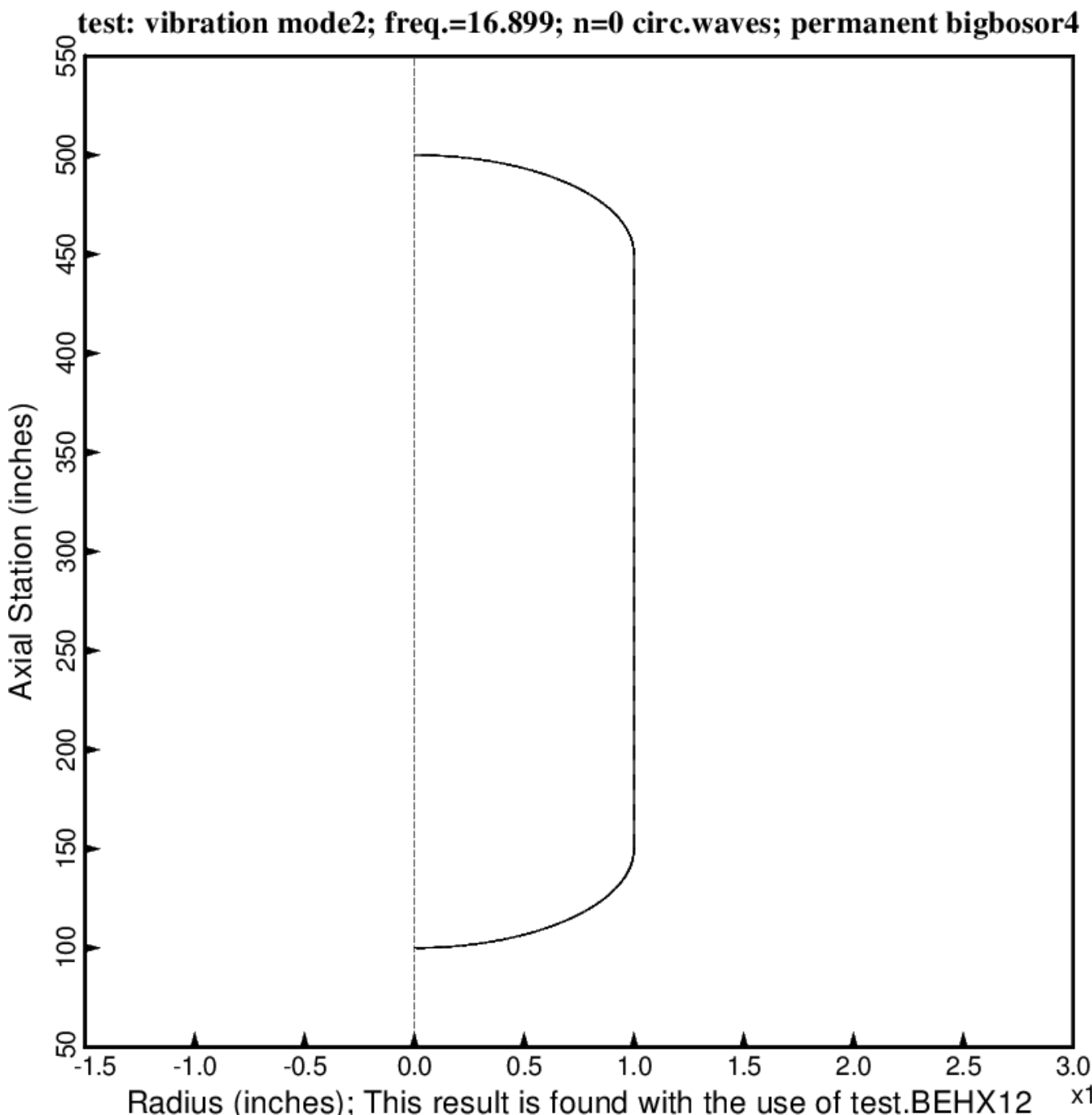


Fig. 20 (old) Free vibration mode of the optimized tank/strut system for the long propellant tank with aft and forward sets of struts, 4 strut pairs in each set. The struts are present in the BIGBOSOR4 model but are not plotted here because BIGBOSOR4 does not yet have the capability to plot springs. This mode corresponds to rolling motion.

- - Undeformed; optimized design found with the use of the temporary BIGBOSOR4/BOSDEC  
 — Deformed; Load Case 2 (lateral 10g acceleration); curing temperature, TEMTUR = 170 degrees

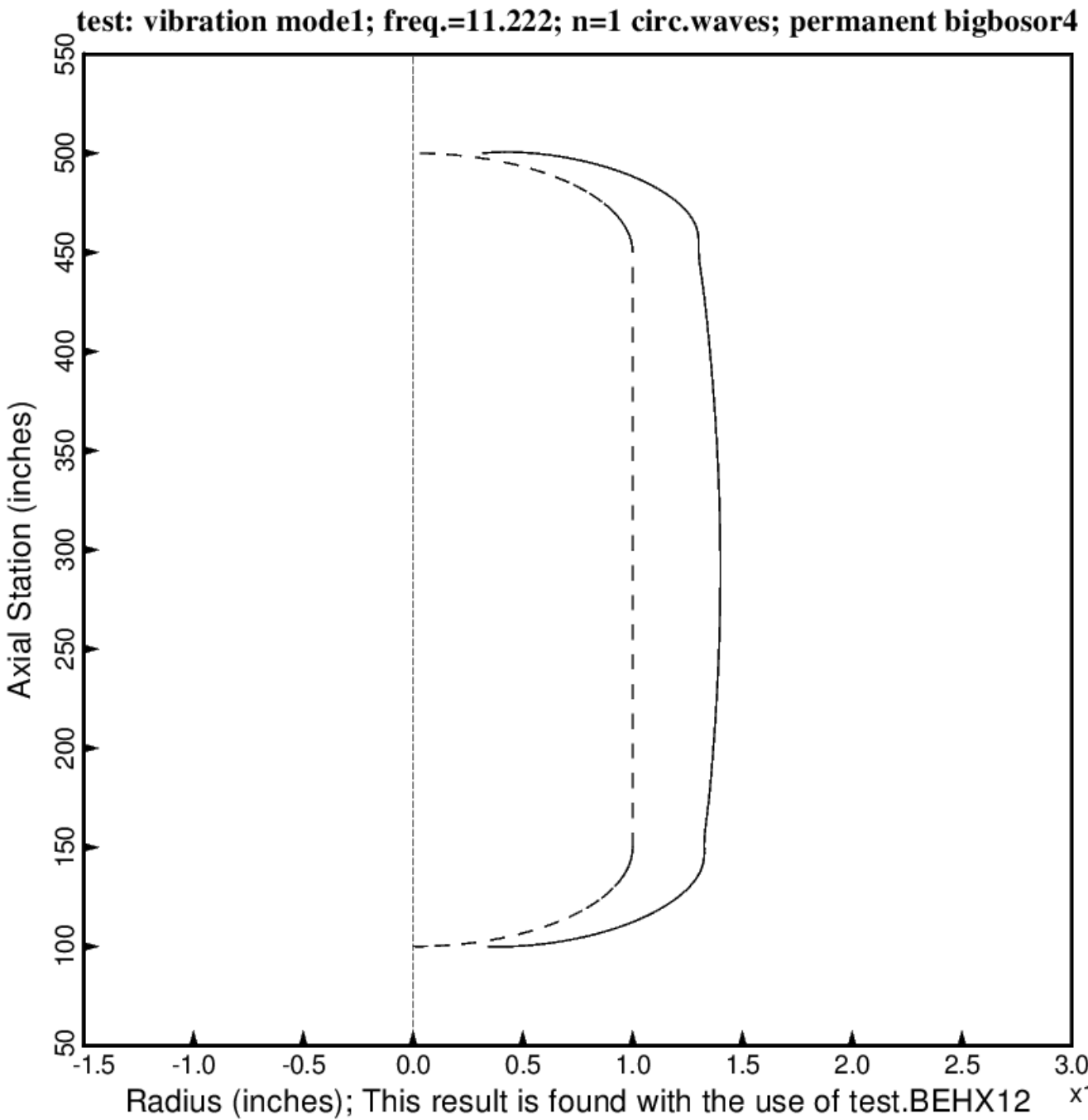


Fig. 21 (old) Free vibration mode of the optimized tank/strut system for the long propellant tank with aft and forward sets of struts, 4 strut pairs in each set. The struts are present in the BIGBOSOR4 model but are not plotted here because BIGBOSOR4 does not yet have the capability to plot springs. This mode corresponds to the first lateral/pitching mode, almost pure lateral motion here because the tank/strut system is essentially symmetric.

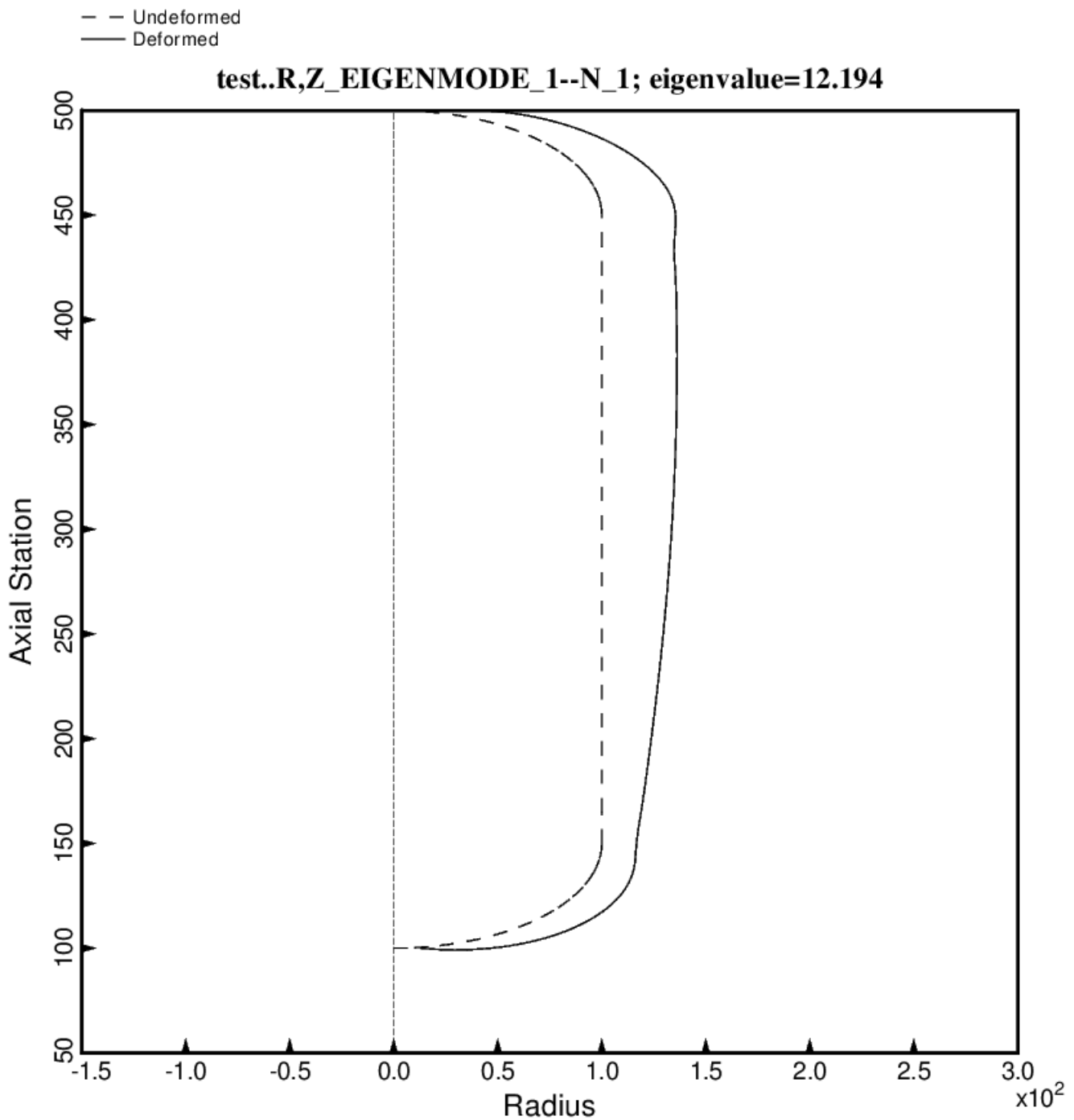
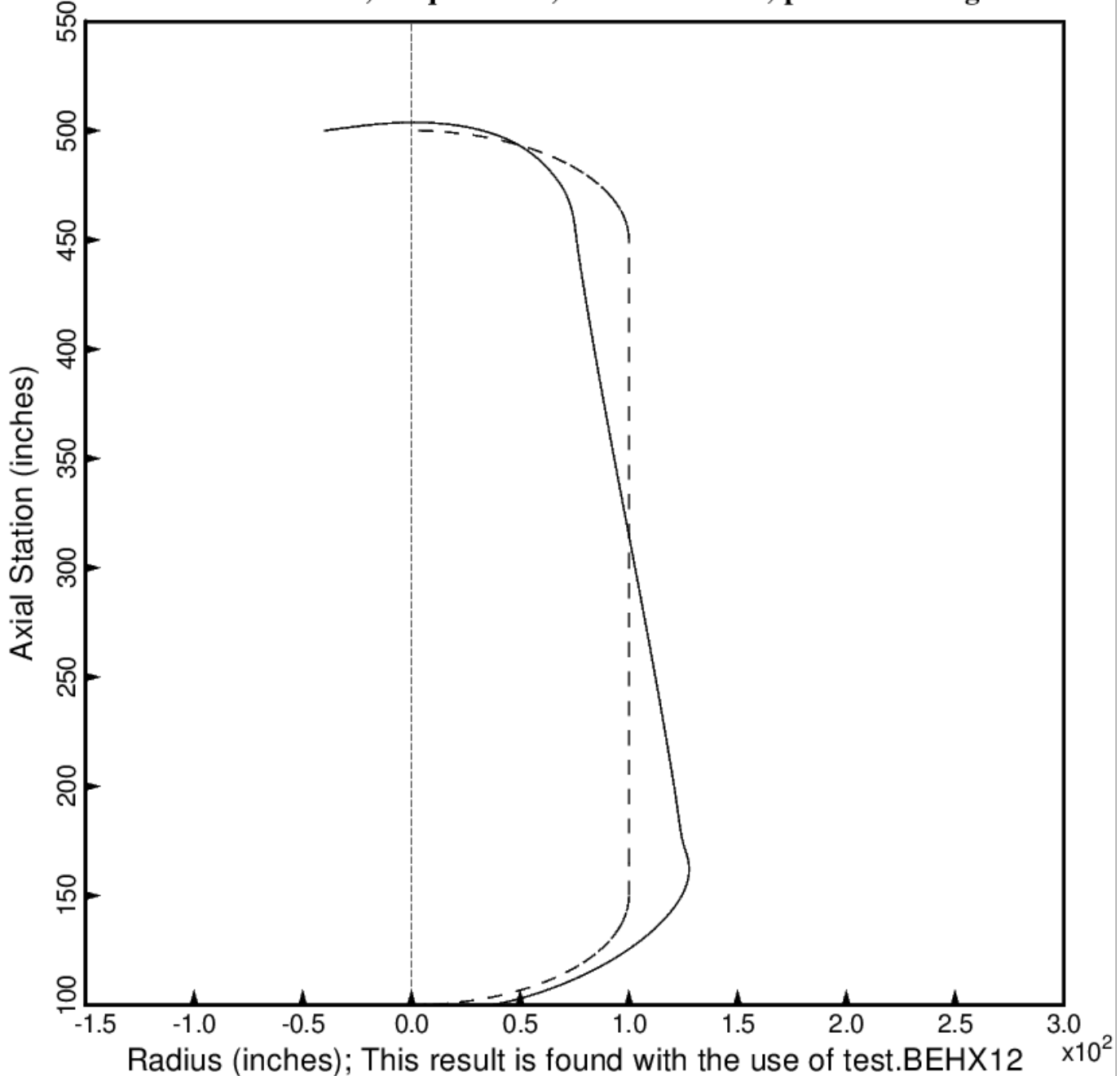


Fig. 21 (new) Free vibration mode of the optimized tank/strut system for the long propellant tank with aft and forward sets of struts, 4 strut pairs in each set, Load Case 2 (test.BEHX12). The struts are present in the BIGBOSOR4 model but are not plotted here because BIGBOSOR4 does not yet have the capability to plot springs. This mode corresponds to the first lateral/pitching mode, mostly pure lateral motion here because the tank/strut system is fairly symmetric. This optimum design was found with use of the “permanent” (constant density) versions of bosdec (bosdec.tank) and addbosor4 (addbosor4.tank).

— — Undeformed; optimized design found with the use of the temporary BIGBOSOR4/BOSDEC  
 — Deformed; Load Case 2 (lateral 10g acceleration); curing temperature, TEMTUR = 170 degrees

**test: vibration mode2; freq.=12.663; n=1 circ.waves; permanent bigbosor4**



**Radius (inches); This result is found with the use of test.BEHX12  $\times 10^2$**

Fig. 22 (old) Free vibration mode of the optimized tank/strut system for the long propellant tank with aft and forward sets of struts, 4 strut pairs in each set. The struts are present in the BIGBOSOR4 model but are not plotted here because BIGBOSOR4 does not yet have the capability to plot springs. This mode corresponds to the second lateral/pitching mode, almost pure pitching motion here because the tank/strut system is essentially symmetric.

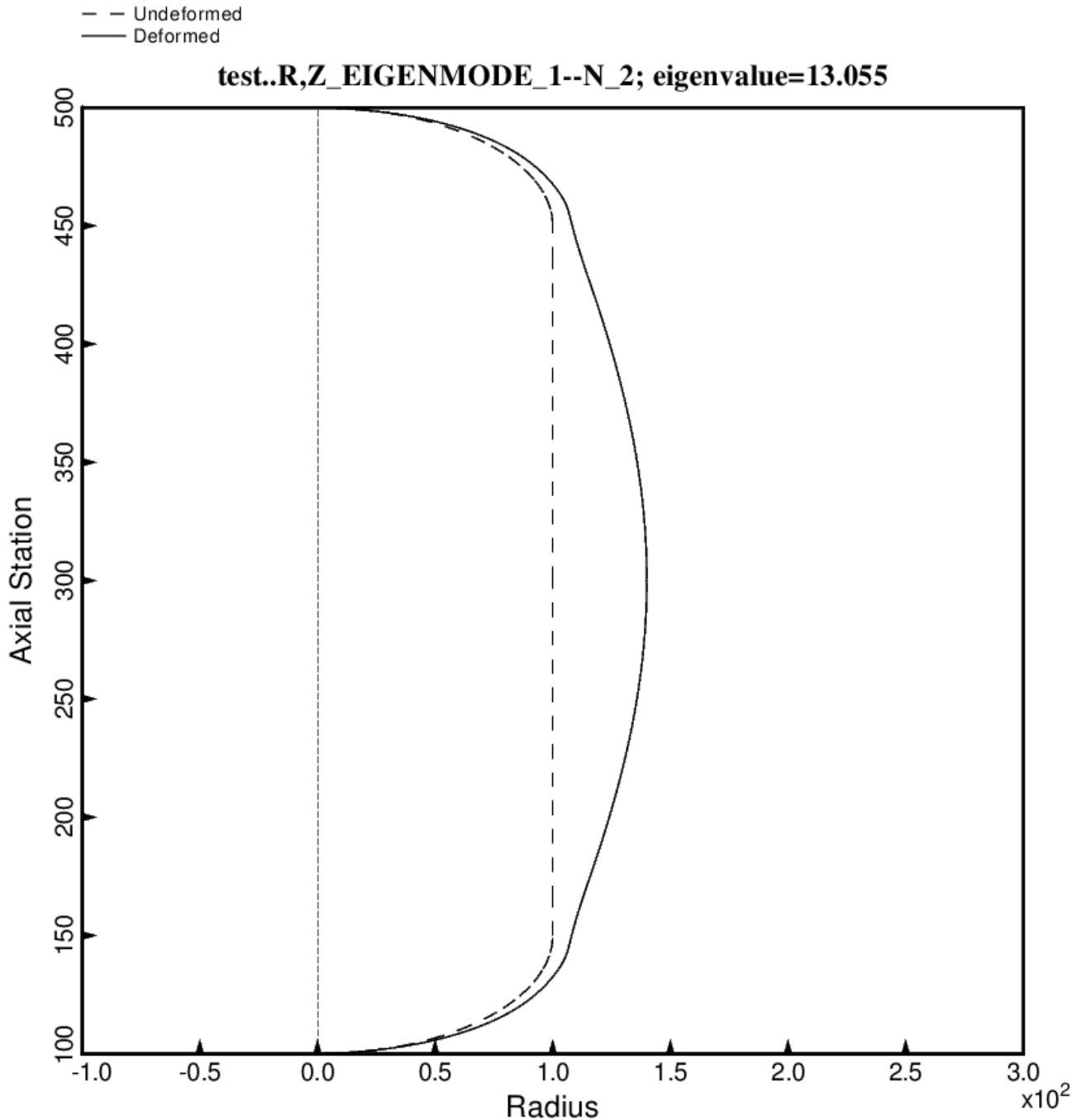


Fig. 22b (new) Free vibration mode of the optimized tank/strut system for the long propellant tank with aft and forward sets of struts, 4 strut pairs in each set, Load Case 2 (test.BEHX12). The struts are present in the BIGBOSOR4 model but are not plotted here because BIGBOSOR4 does not yet have the capability to plot springs. This mode corresponds to  $N = 2$  circumferential waves. This is a “shell” vibration mode the frequency of which is not sensitive to the type of propellant “lumping” model: constant density or varying density, because most of the motion occurs in the cylindrical portion of the propellant tank in which the “lumped” propellant density does not depend on the location along the cylindrical shell. This optimum design was found with use of the “permanent” (constant density) versions of bosdec (bosdec.tank) and addbosor4 (addbosor4.tank).

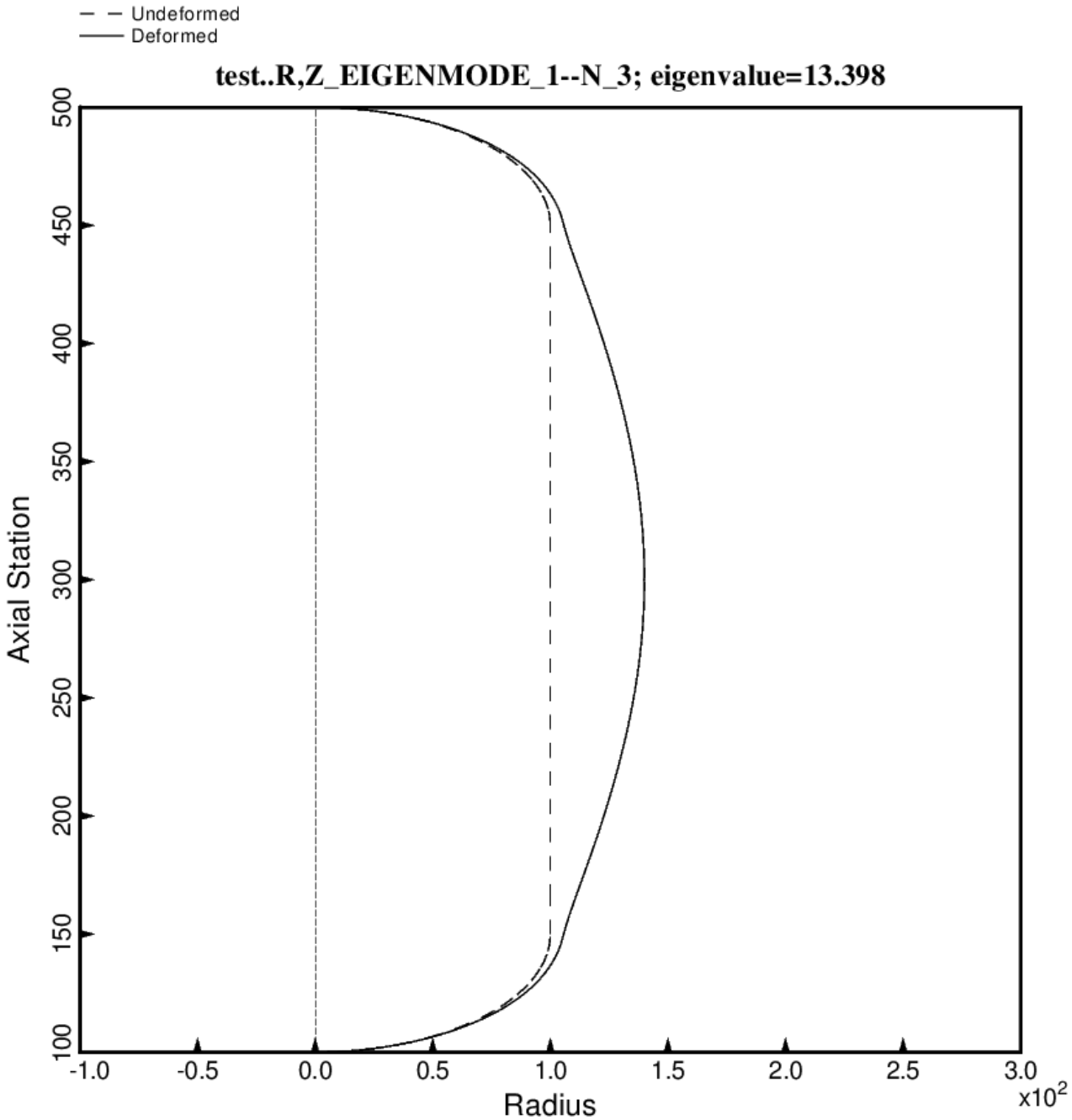


Fig. 22c (new) Free vibration mode of the optimized tank/strut system for the long propellant tank with aft and forward sets of struts, 4 strut pairs in each set, Load Case 2 (test.BEHX12). The struts are present in the BIGBOSOR4 model but are not plotted here because BIGBOSOR4 does not yet have the capability to plot springs. This mode corresponds to  $N = 3$  circumferential waves. This is a “shell” vibration mode the frequency of which is not sensitive to the type of propellant “lumping” model: constant density or varying density, because most of the motion occurs in the cylindrical portion of the propellant tank in which the “lumped” propellant density does not depend on the location along the cylindrical shell. This optimum design was found with use of the “permanent” (constant density) versions of bosdec (bosdec.tank) and addbosor4 (addbosor4.tank).

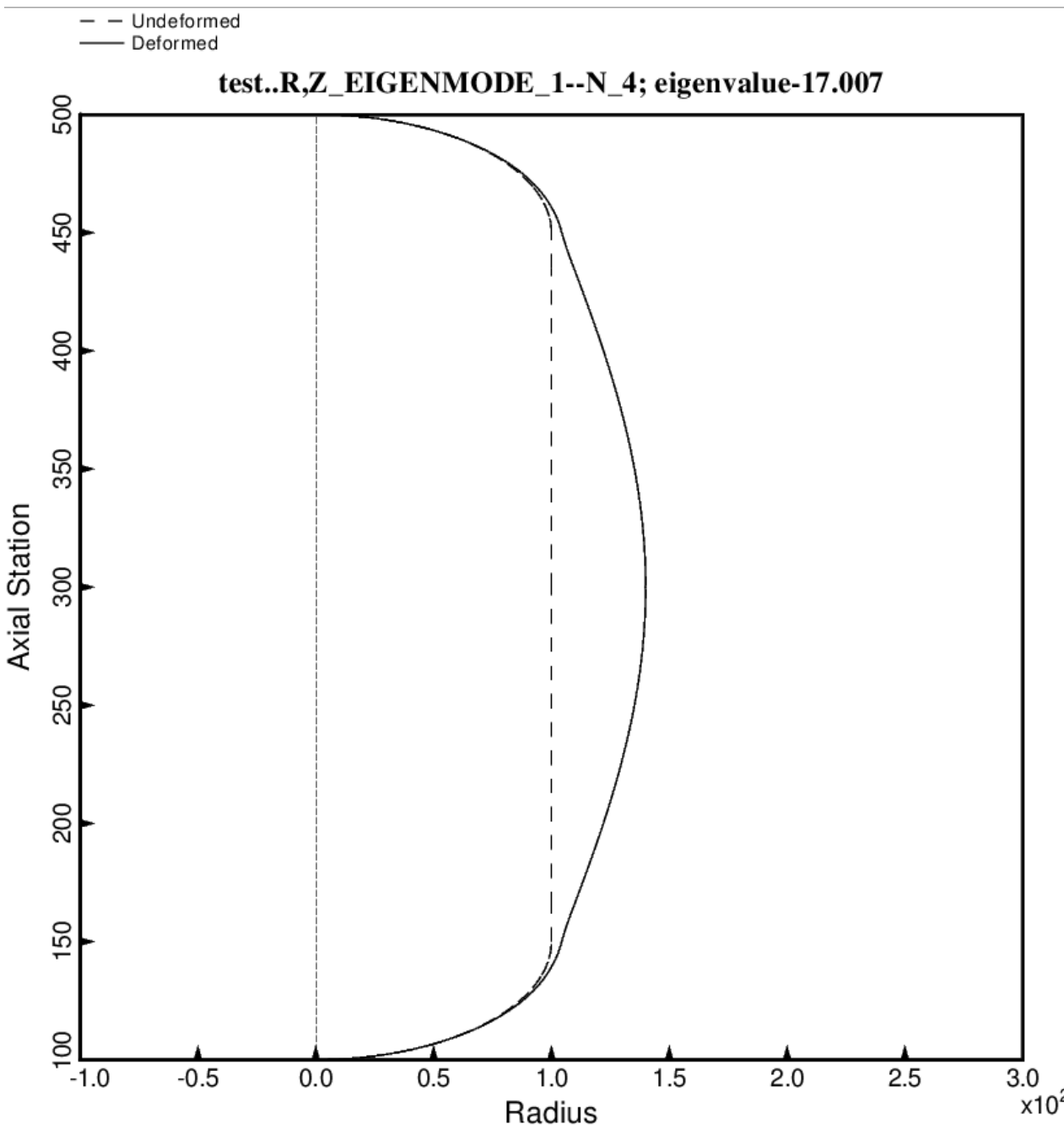


Fig. 22d (new) Free vibration mode of the optimized tank/strut system for the long propellant tank with aft and forward sets of struts, 4 strut pairs in each set, Load Case 2 (test.BEHX12). The struts are present in the BIGBOSOR4 model but are not plotted here because BIGBOSOR4 does not yet have the capability to plot springs. This mode corresponds to  $N = 4$  circumferential waves. This is a “shell” vibration mode the frequency of which is not sensitive to the type of propellant “lumping” model: constant density or varying density, because most of the motion occurs in the cylindrical portion of the propellant tank in which the “lumped” propellant density does not depend on the location along the cylindrical shell. This optimum design was found with use of the “permanent” (constant density) versions of bosdec (bosdec.tank) and addbosor4 (addbosor4.tank).

— — Undeformed; optimized design found with the use of the temporary BIGBOSOR4/BOSDEC  
— Deformed; Load Case 1 (axial 10g acceleration); curing temperature, TEMTUR = 170 degrees

**test: buckling mode; Eigen.=5.2366; n=35 circ.waves; meridian=6.0 deg.**

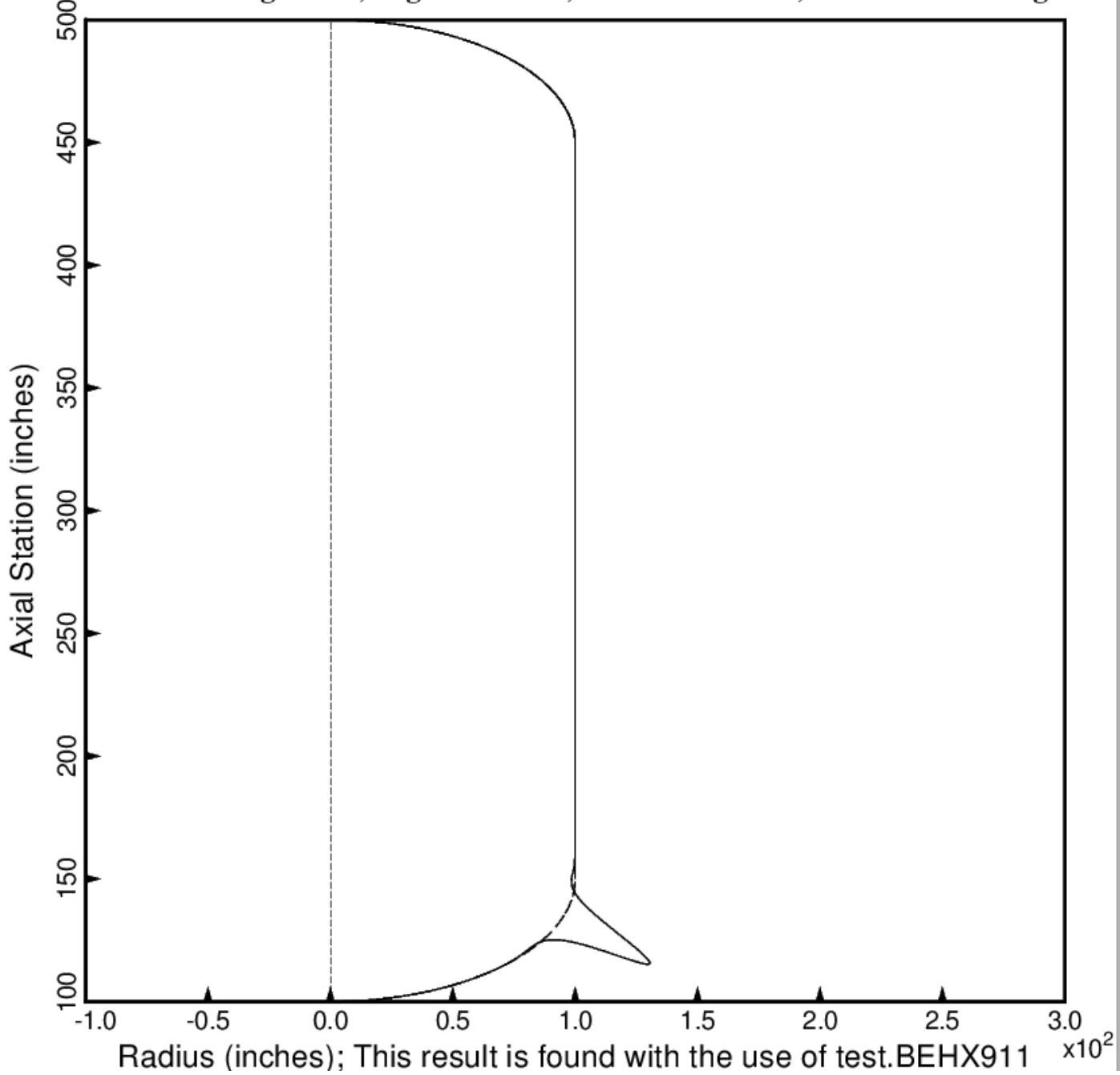


Fig. 23 (old) Buckling of the long optimized tank with aft and forward sets of struts, 4 strut pairs in each set. The loading is Load Case 1: axial acceleration = 10 g, 25 psi ullage pressure, 200 deg. tank cool-down. Buckling in the aft 2:1 ellipsoidal dome is caused by the narrow band of hoop compression in the dome knuckle region.

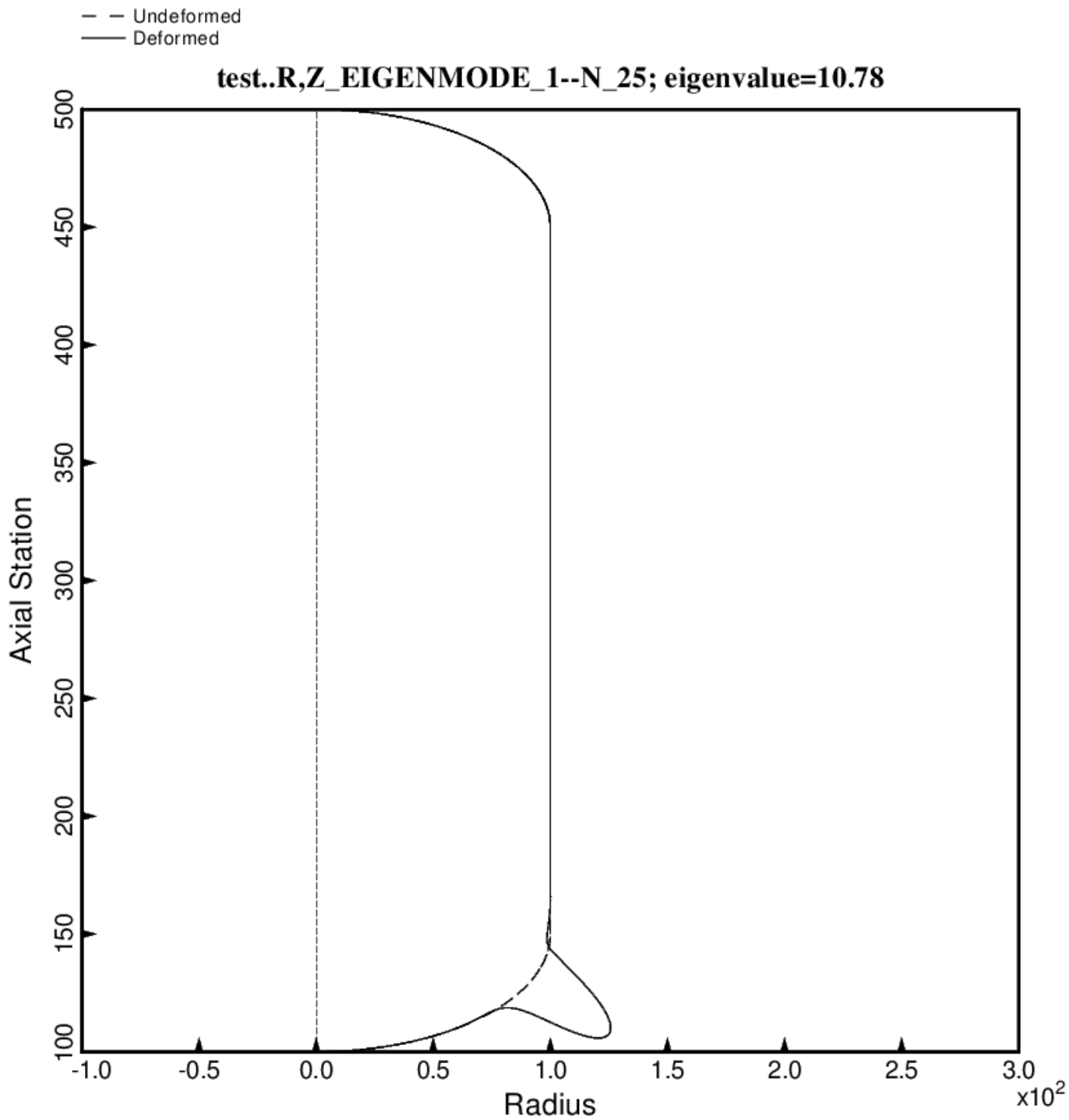


Fig. 23 (new) Buckling of the long optimized tank with aft and forward sets of struts, 4 strut pairs in each set. The loading is Load Case 1: axial acceleration = 10 g, 25 psi ullage pressure, 200 deg. tank cool-down. Buckling in the aft 2:1 ellipsoidal dome is caused by the narrow band of hoop compression in the dome knuckle region. This optimum design was found with use of the “temporary” (varying density) versions of bosdec (bosdec.density.var) and addbosor4 (addbosor4.density.var).

- - - Undeformed; optimized design found with the use of the temporary BIGBOSOR4/BOSDEC  
 — Deformed; Load Case 2 (lateral 10g acceleration); curing temperature, TEMTUR = 170 degrees

**test: buckling mode; Eigen.=4.1087; n=30 circ.waves; meridian=84 deg.**

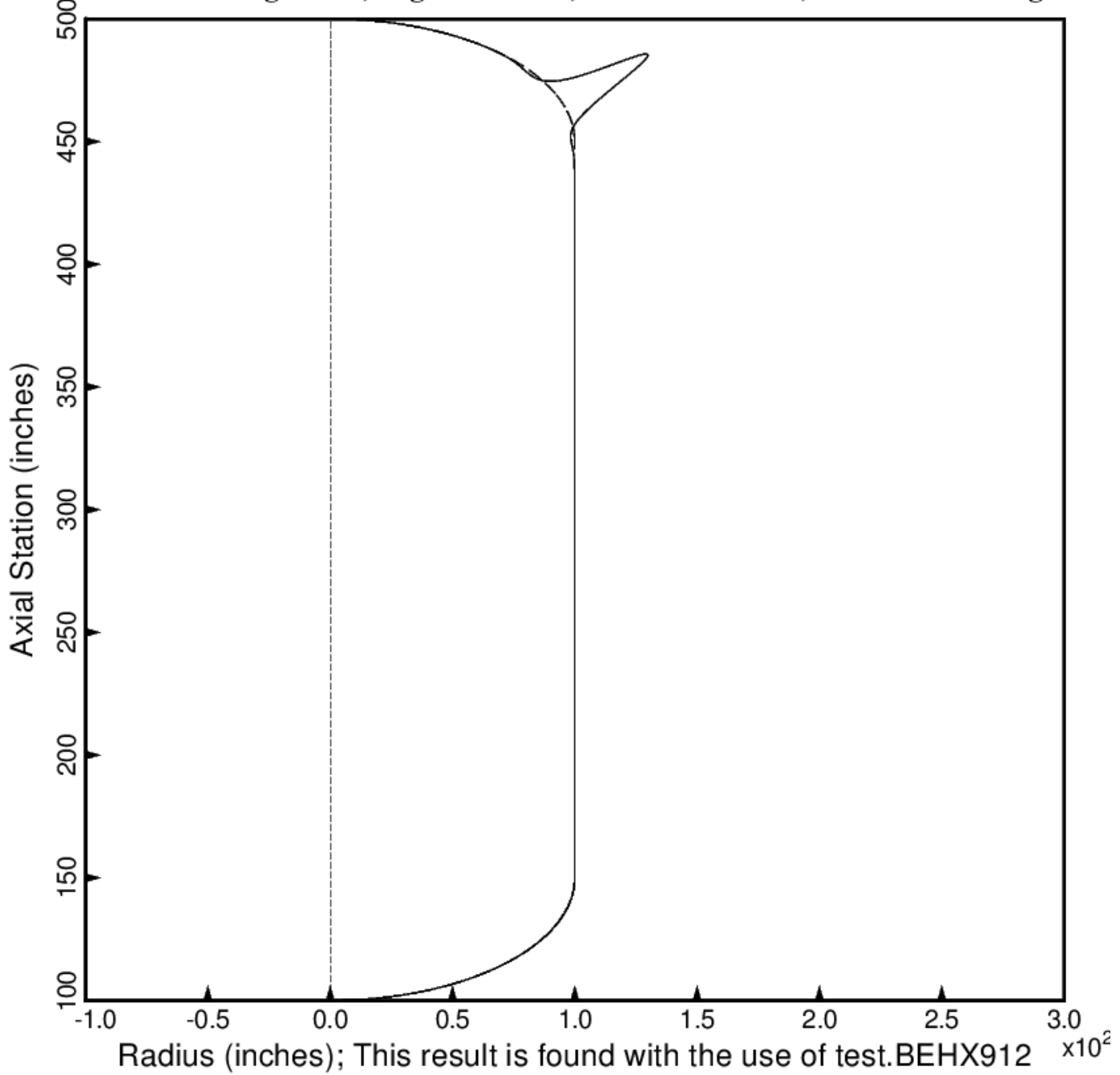


Fig. 24 (old) Buckling of the long optimized tank with aft and forward sets of struts, 4 strut pairs in each set. The loading is Load Case 2: lateral acceleration = 10 g, 25 psi ullage pressure, 200 deg. tank cool-down. Buckling in the forward 2:1 ellipsoidal dome is caused partly by the narrow band of hoop compression in the dome knuckle region and partly from concentrated compression caused by the struts “poking” into the tank.

— — Undeformed; optimized design found with the use of the temporary BIGBOSOR4/BOSDEC  
— Deformed; BIGBOSOR4 model of a strut tube; Euler model gets Eigen.=1.001 compared to 1.8972

**test: buckling of strut tube as a column; Eigen.=1.8972 from bigbosor4**

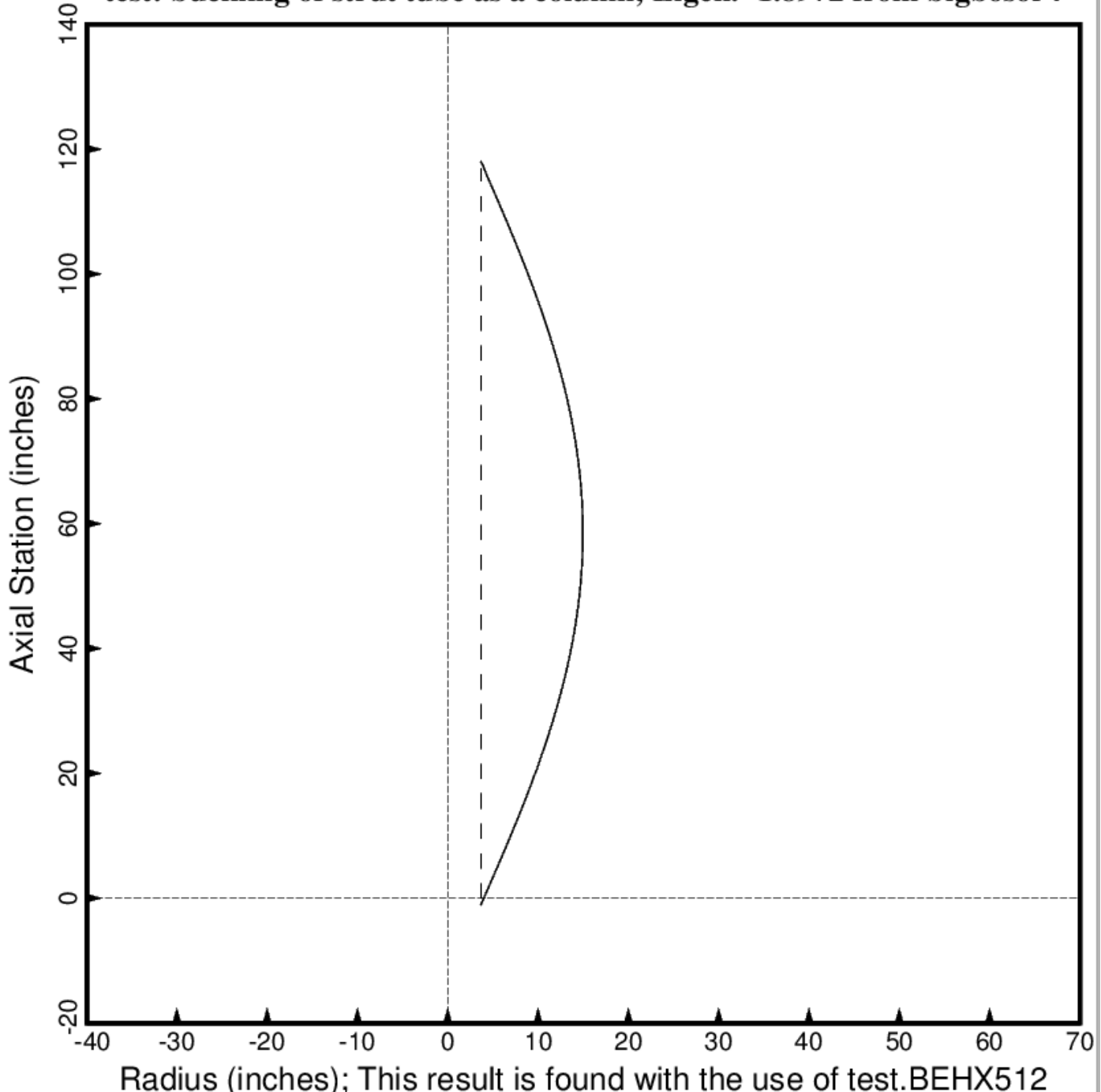
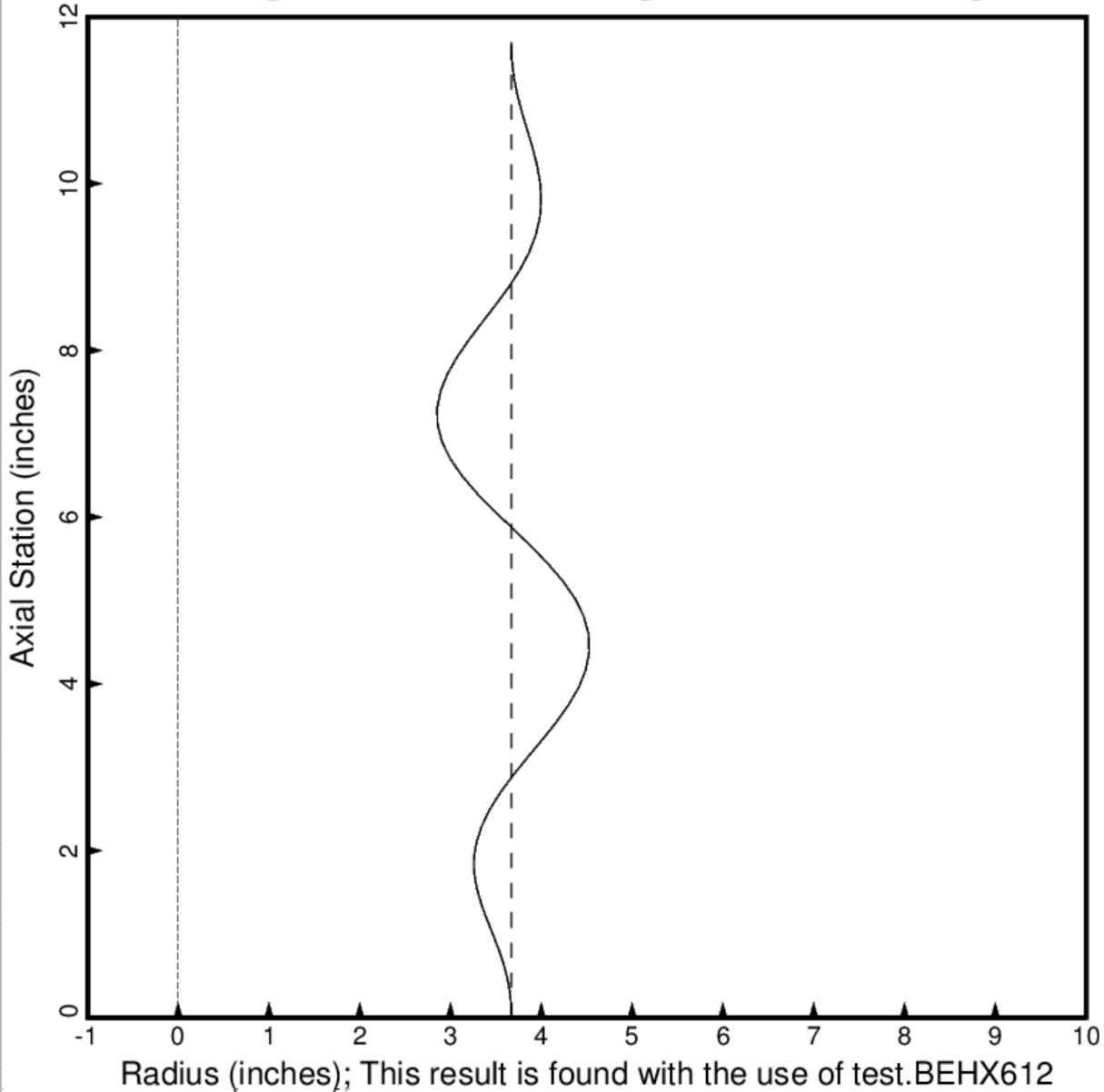


Fig. 25 (old) Buckling of the most highly compressed strut as a column from the BIGBOSOR4 model. The BIGBOSOR4 model does not include the “softening” effect of the tank flexibility on the effective axial stiffness of the struts.

— — Undeformed; optimized design found with the use of the temporary BIGBOSOR4/BOSDEC  
 — Deformed; BIGBOSOR4 model of a strut tube; PANDA2 model gets Eigen.=1.984 compared to 2.649!

**test: buckling of strut tube as a shell; Eigen.=2.6495,n=6 from bigbosor4**



Radius (inches); This result is found with the use of test.BEHX612

Fig. 26 (old) Buckling of the most highly compressed strut as a thin axially compressed cylindrical shell from the BIGBOSOR4 model. Only part of the total strut length is included in this BIGBOSOR4 model. The BIGBOSOR4 model does not include the effects of anisotropy or transverse shear deformation, and therefore overestimates the shell buckling load factor. However, a PANDA model of shell buckling is also included in the GENOPT model reported here. The PANDA model includes anisotropy and transverse shear deformation. Therefore, it yields a lower shell buckling load factor than the BIGBOSOR4 model. A factor of safety of 2.0 is used for the shell buckling behavior in order to account for the effect of unavoidable initial imperfections in the cylindrical shape of the laminated composite strut tube.

- - Undeformed; optimized design found with the use of the temporary BIGBOSOR4/BOSDEC  
 — Deformed; Load Case 1 (axial 10g acceleration); curing temperature, TEMTUR = 170 degrees

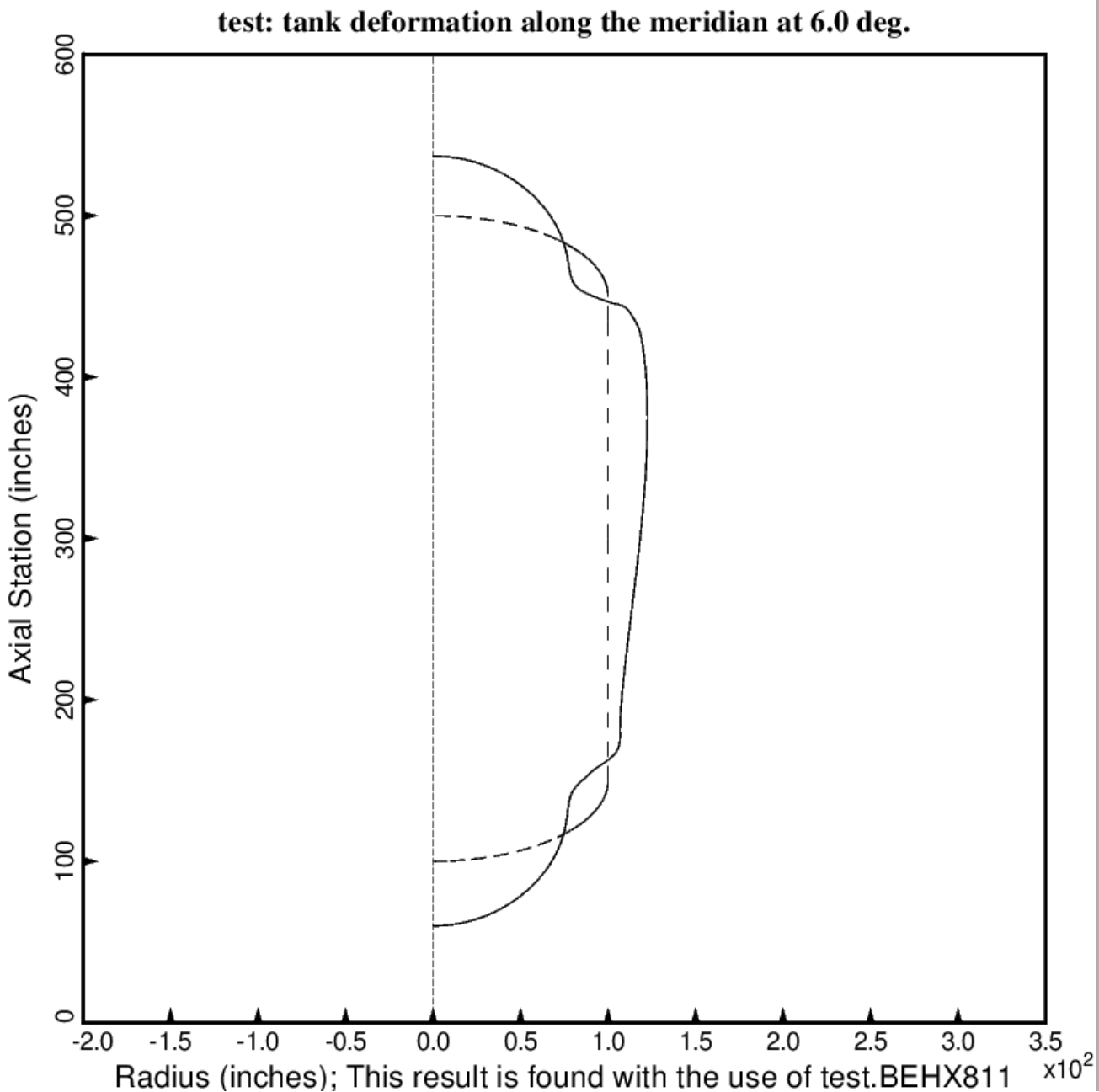


Fig. 27 (old) Load Case 1 (10 g axial acceleration, 25 psi ullage pressure, 200 deg. tank cool-down): Deformation along meridian 1 of the long propellant tank with aft and forward struts, 4 strut pairs in each set of struts. In this BIGBOSOR4 model, from which the maximum stresses in the propellant tank are computed, the struts (springs) are replaced by the concentrated loads that these springs apply to the tank. The concentrated loads are represented in the BIGBOSOR4 model as Fourier series expansions of circumferential line loads. The non-axisymmetric linear equilibrium state is obtained by superposition of the displacements and stresses from each Fourier component.

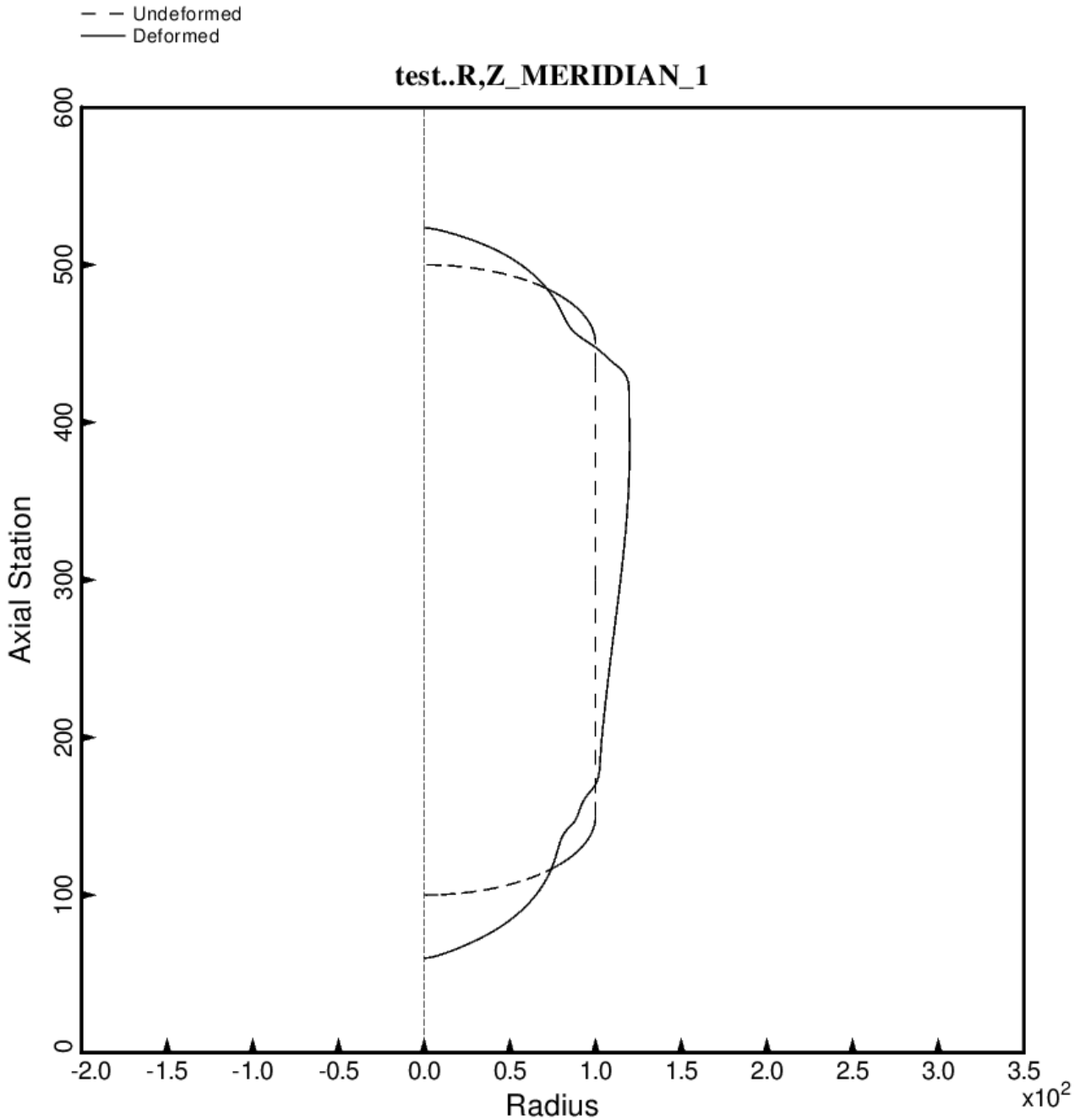


Fig. 27a (new) Load Case 1 (10 g axial acceleration, 25 psi ullage pressure, 200 deg. tank cool-down): Deformation along the meridian at zero degrees of the long propellant tank with aft and forward struts, 4 strut pairs in each set of struts. In this BIGBOSOR4 model, from which the maximum stresses in the propellant tank are computed, the struts (springs) are replaced by the concentrated loads that these springs apply to the tank. The concentrated loads are represented in the BIGBOSOR4 model as Fourier series expansions of circumferential line loads. The non-axisymmetric linear equilibrium state is obtained by superposition of the displacements and stresses from each Fourier component. This optimum design was found with use of the “temporary” (varying density) versions of bosdec (bosdec.density.var) and addbosor4 (addbosor4.density.var).

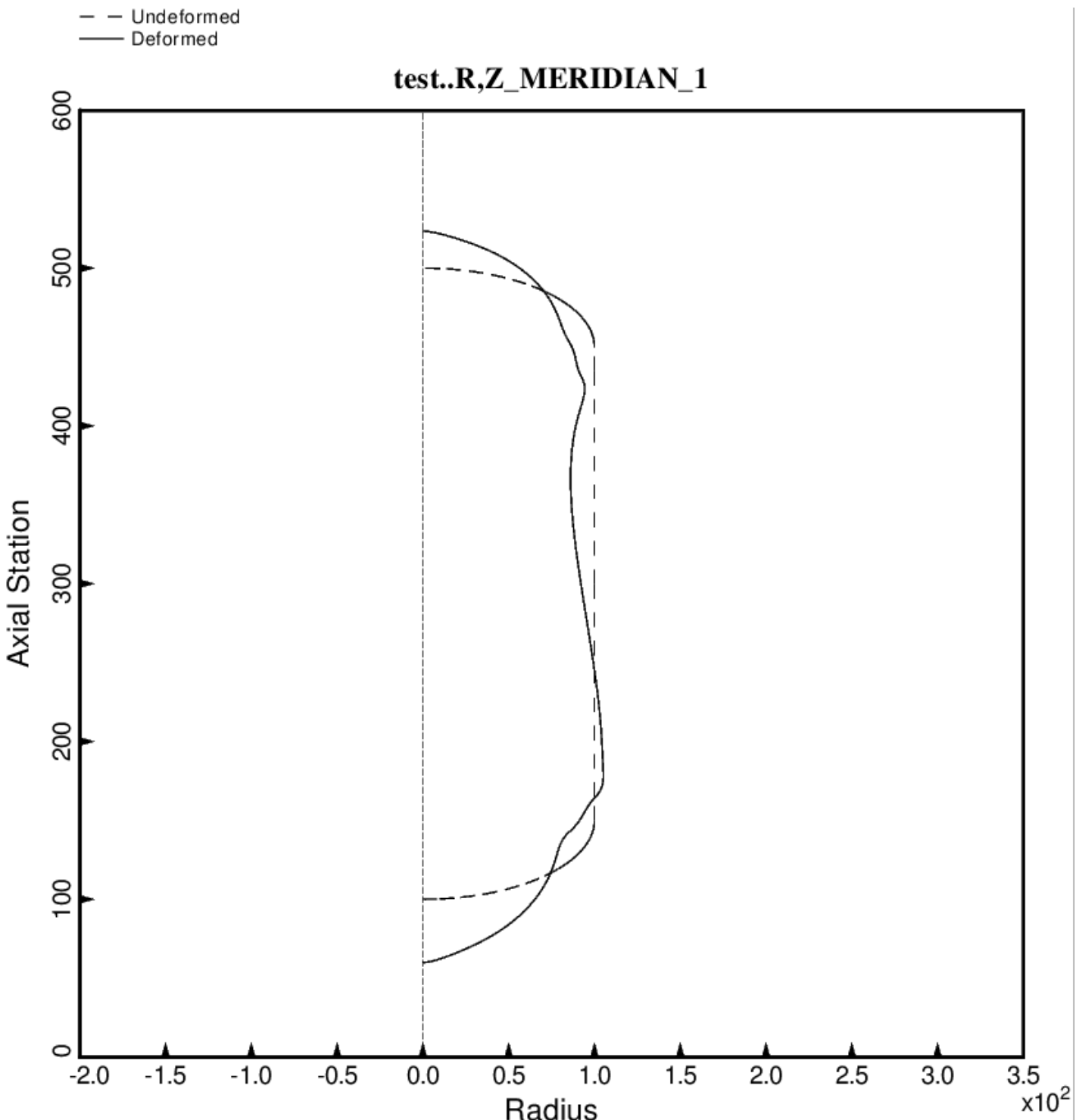


Fig. 27b (new) Load Case 1 (10 g axial acceleration, 25 psi ullage pressure, 200 deg. tank cool-down): Deformation along the meridian at 45 degrees of the long propellant tank with aft and forward struts, 4 strut pairs in each set of struts. This optimum design was found with use of the “temporary” (varying density) versions of bosdec (bosdec.density.var) and addbosor4 (addbosor4.density.var).

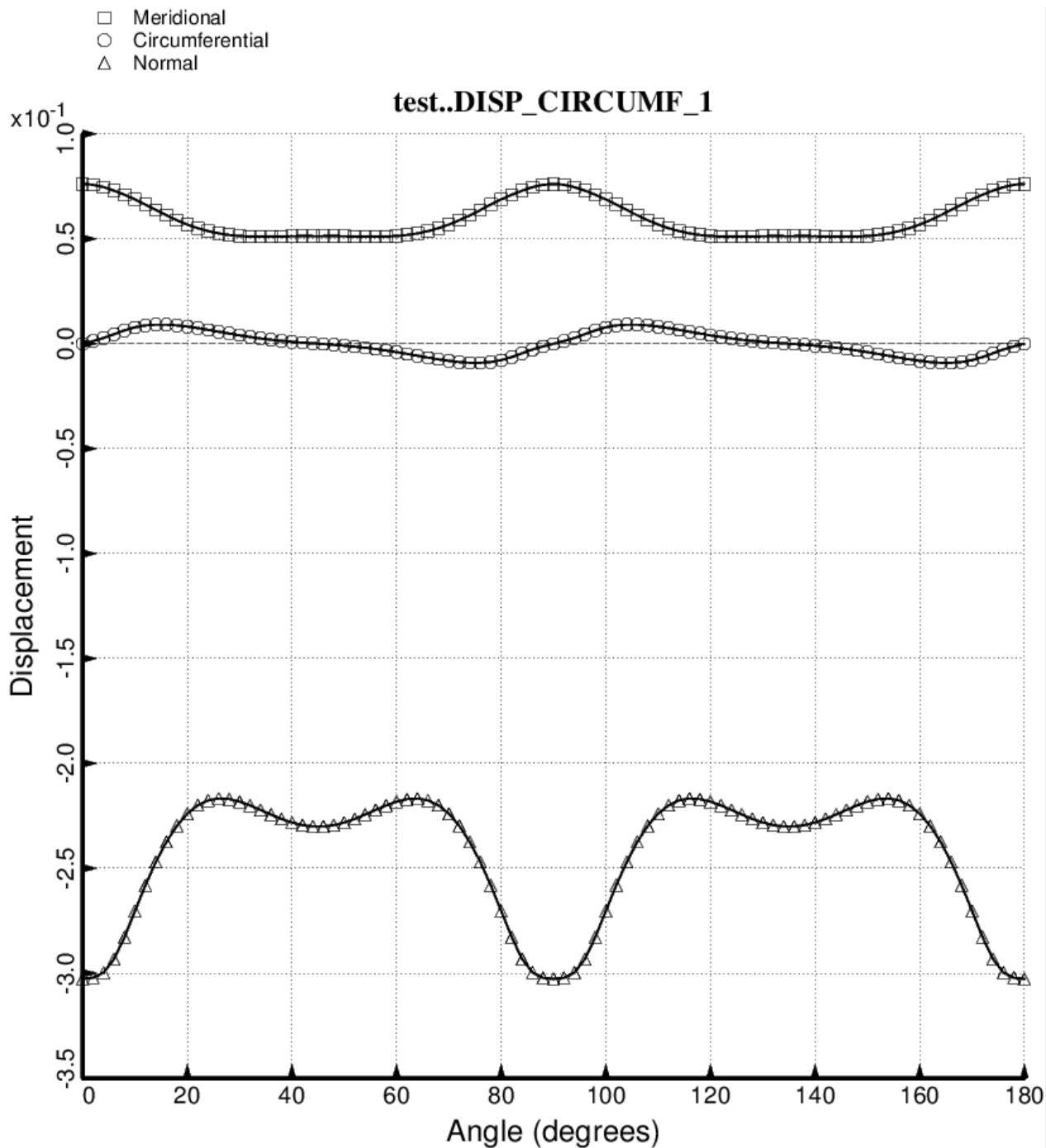


Fig. 27c (new) Load Case 1 (10 g axial acceleration, 25 psi ullage pressure, 200 deg. tank cool-down): Deformation along 180 degrees of the circumference at the aft dome/cylinder junction of the long propellant tank with aft and forward struts, 4 strut pairs in each set of struts. This optimum design was found with use of the “temporary” (varying density) versions of bosdec (bosdec.density.var) and addbosor4 (addbosor4.density.var).

□ Meridional  
 ○ Circumferential  
 △ Normal

### test..DISP\_CIRCUMF\_1

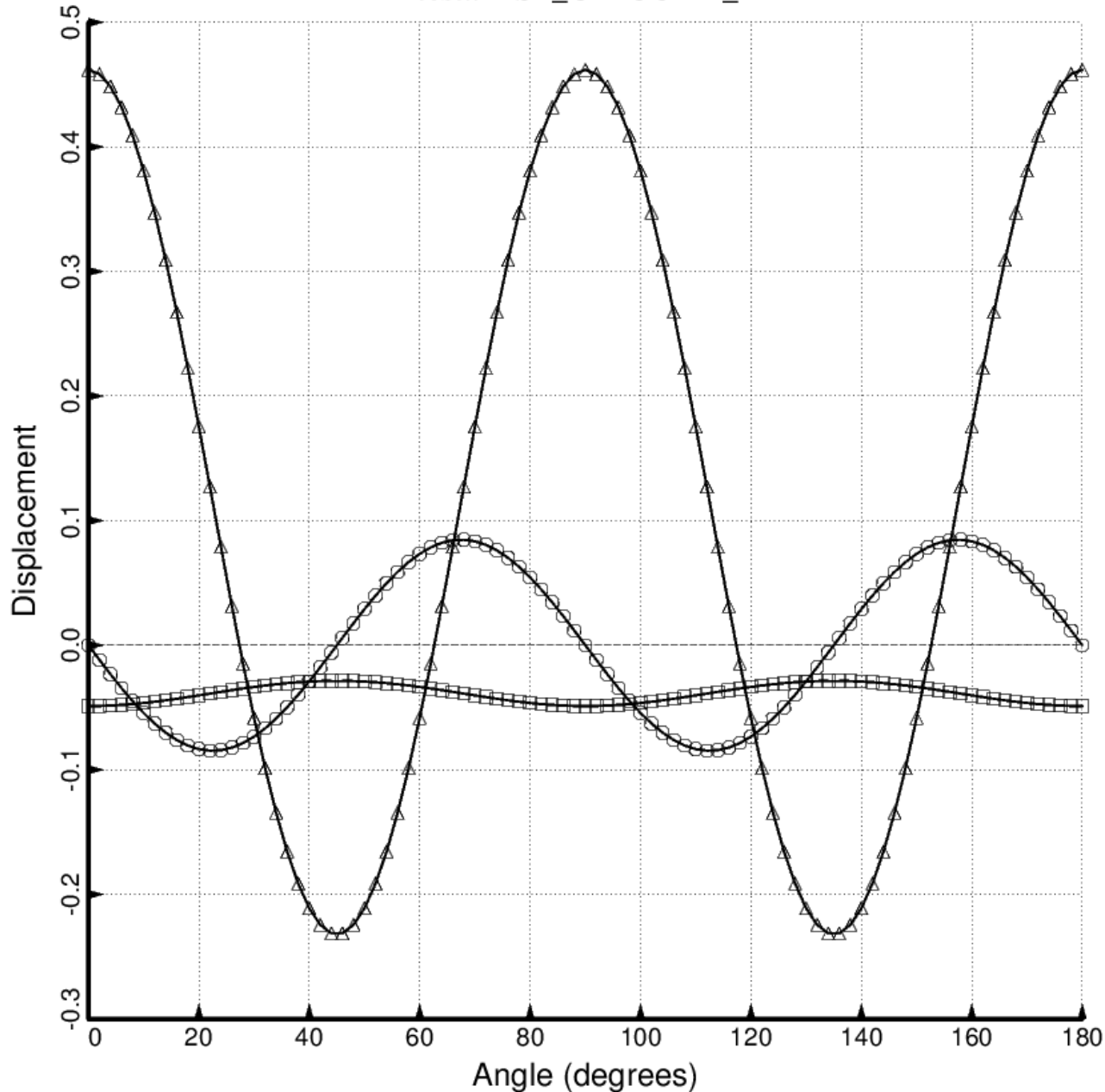


Fig. 27d (new) Load Case 1 (10 g axial acceleration, 25 psi ullage pressure, 200 deg. tank cool-down): Deformation along 180 degrees of the circumference at the midlength of the cylindrical part of the long propellant tank with aft and forward struts, 4 strut pairs in each set of struts. This optimum design was found with use of the “temporary” (varying density) versions of bosdec (bosdec.density.var) and addbosor4 (addbosor4.density.var).

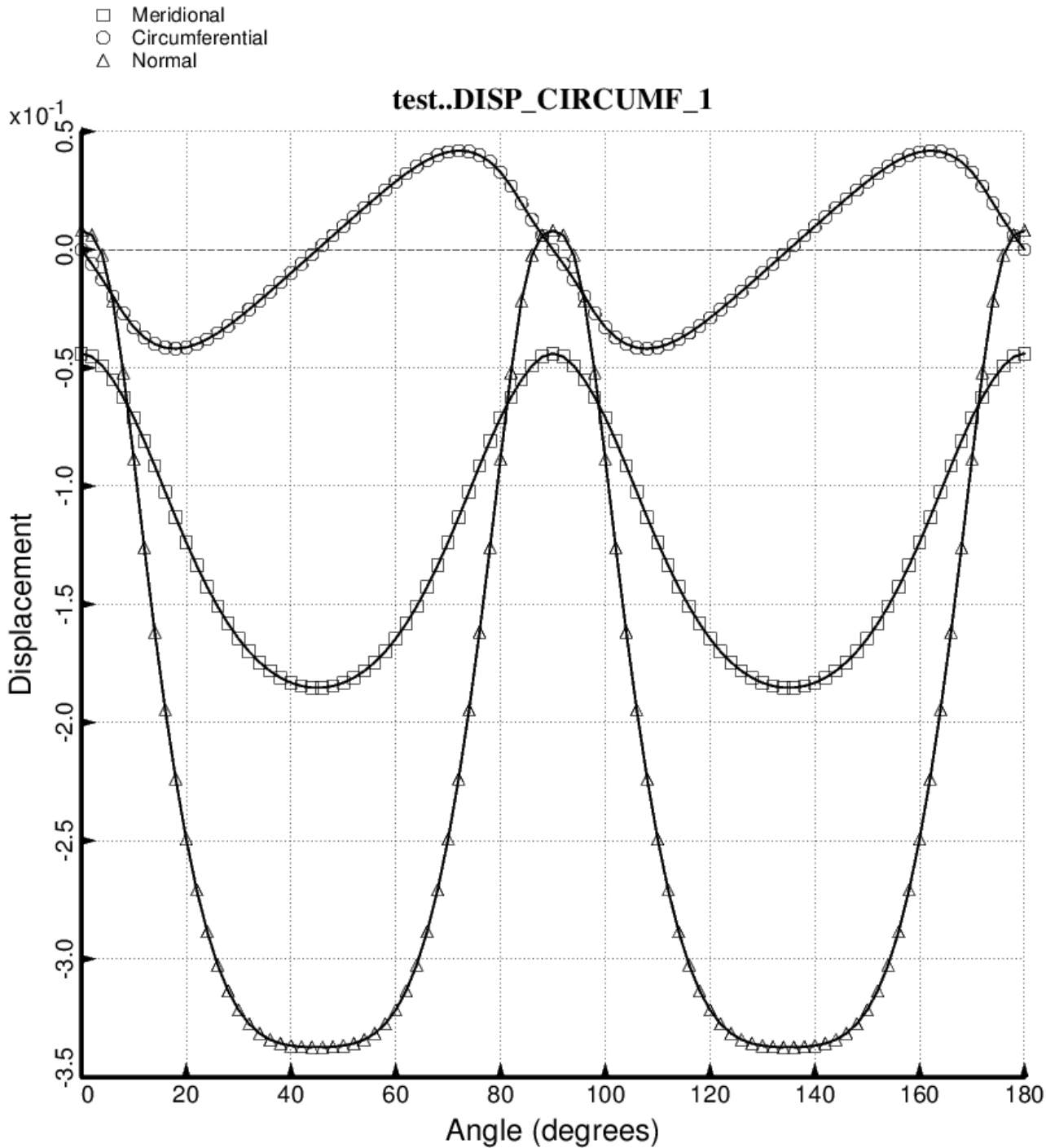


Fig. 27e (new) Load Case 1 (10 g axial acceleration, 25 psi ullage pressure, 200 deg. tank cool-down): Deformation along 180 degrees of the circumference at the forward dome/cylinder junction of the long propellant tank with aft and forward struts, 4 strut pairs in each set of struts. This optimum design was found with use of the “temporary” (varying density) versions of bosdec (bosdec.density.var) and addbosor4 (addbosor4.density.var).

— — Undeformed; optimized design found with the use of the temporary BIGBOSOR4/BOSDEC  
 — Deformed; Load Case 2 (lateral 10g acceleration); curing temperature, TEMTUR = 170 degrees

### test: tank deformation along the meridian at 84.0 degrees

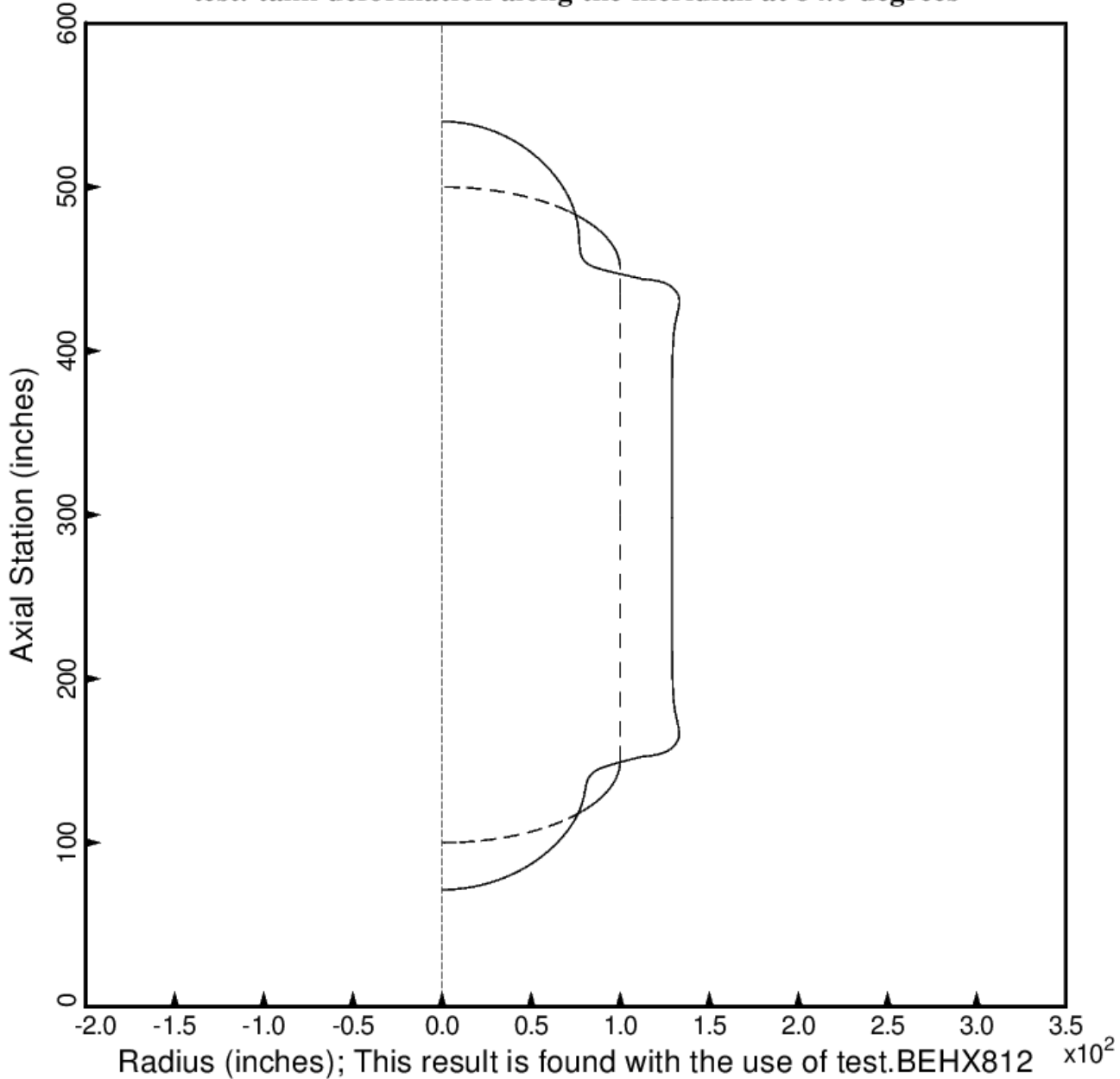


Fig. 28 (old) Load Case 2 (10 g lateral acceleration, 25 psi ullage pressure, 200 deg. tank cool-down): Deformation along meridian 1 of the long propellant tank with aft and forward struts, 4 strut pairs in each set of struts. In this BIGBOSOR4 model, from which the maximum stresses in the propellant tank are computed, the struts (springs) are replaced by the concentrated loads that these springs apply to the tank. The concentrated loads are represented in the BIGBOSOR4 model as Fourier series expansions of circumferential line loads. The non-axisymmetric linear equilibrium state is obtained by superposition of the displacements and stresses from each Fourier component.

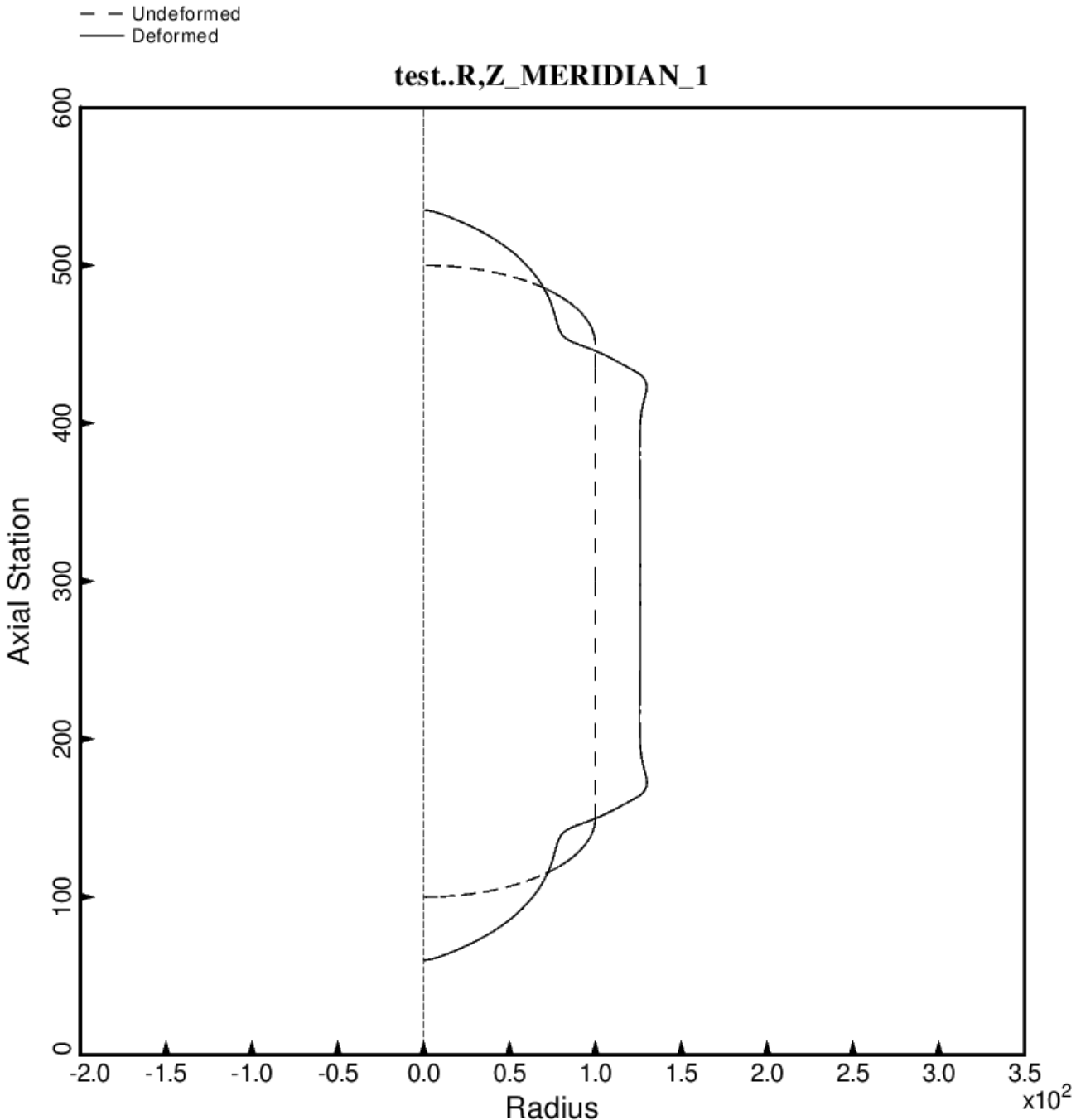


Fig. 28a (new) Load Case 2 (10 g lateral acceleration, 25 psi ullage pressure, 200 deg. tank cool-down): Deformation along the meridian at 84 degrees of the long propellant tank with aft and forward struts, 4 strut pairs in each set of struts. In this BIGBOSOR4 model, from which the maximum stresses in the propellant tank are computed, the struts (springs) are replaced by the concentrated loads that these springs apply to the tank. The concentrated loads are represented in the BIGBOSOR4 model as Fourier series expansions of circumferential line loads. The non-axisymmetric linear equilibrium state is obtained by superposition of the displacements and stresses from each Fourier component. This optimum design was found with use of the “temporary” (varying density) versions of bosdec (bosdec.density.var) and addbosor4 (addbosor4.density.var).

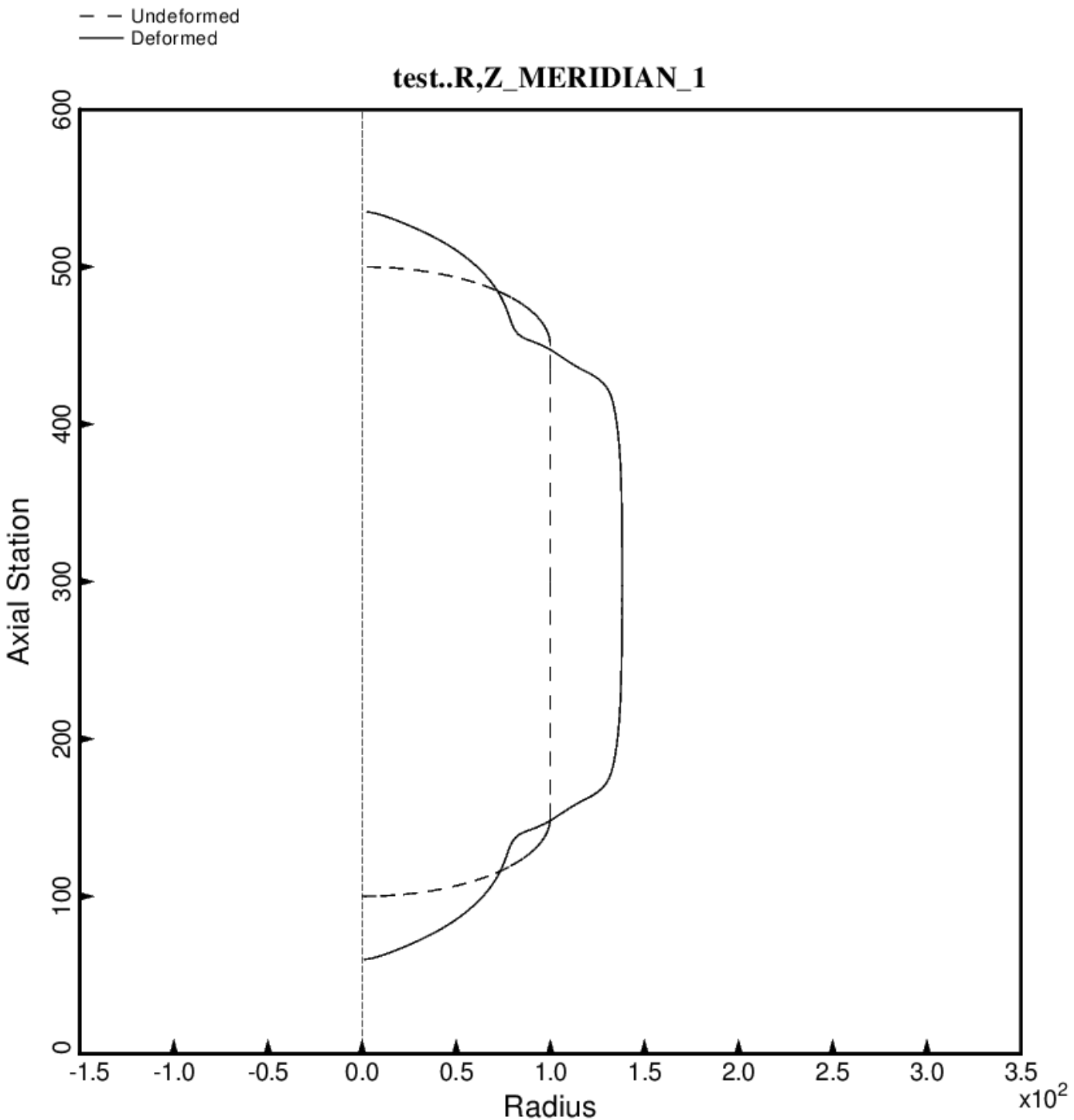


Fig. 28b (new) Load Case 2 (10 g lateral acceleration, 25 psi ullage pressure, 200 deg. tank cool-down): Deformation along the meridian at 70 degrees of the long propellant tank with aft and forward struts, 4 strut pairs in each set of struts. This optimum design was found with use of the “temporary” (varying density) versions of bosdec (bosdec.density.var) and addbosor4 (addbosor4.density.var).

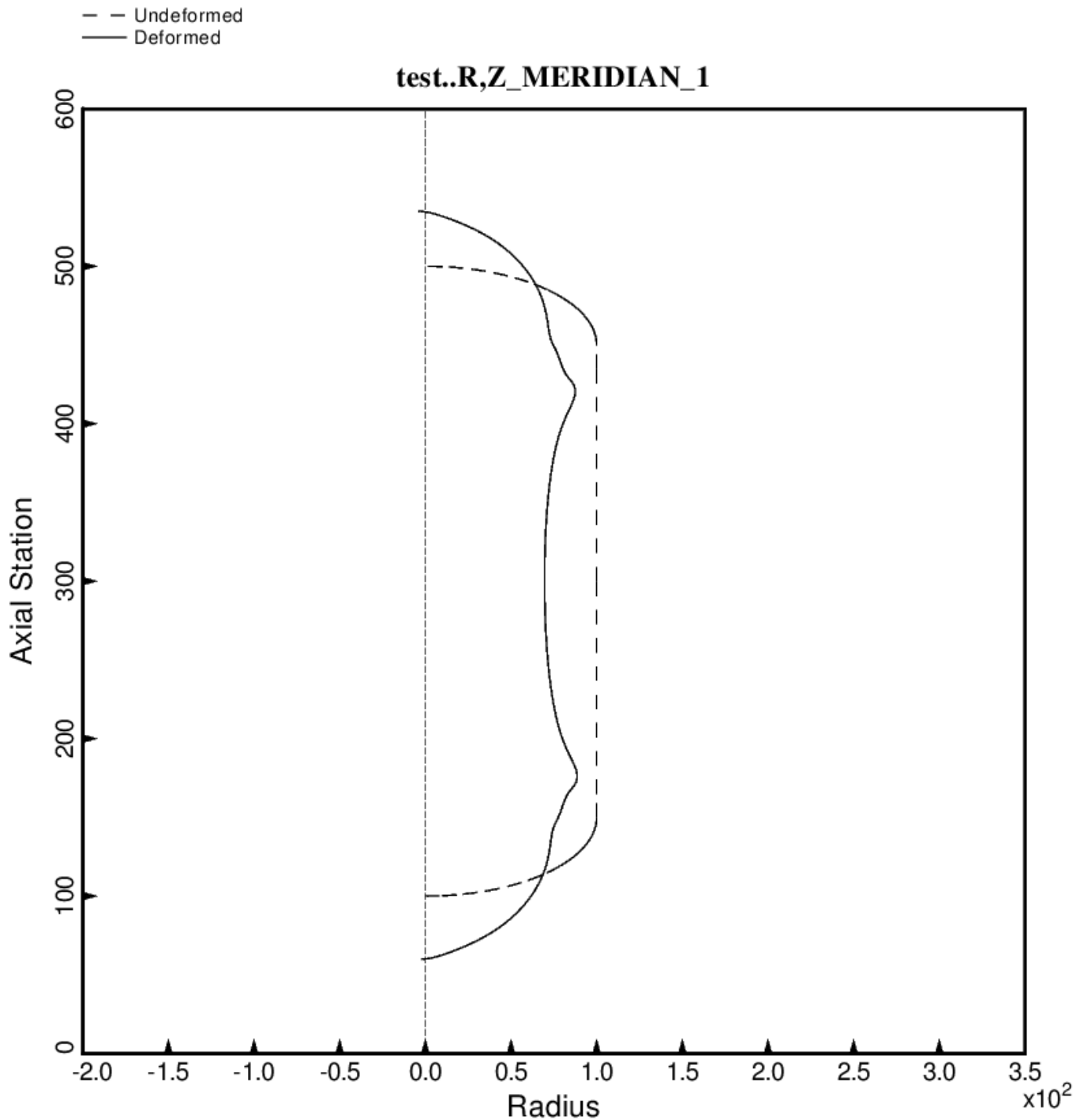


Fig. 28c (new) Load Case 2 (10 g lateral acceleration, 25 psi ullage pressure, 200 deg. tank cool-down): Deformation along the meridian at 120 degrees of the long propellant tank with aft and forward struts, 4 strut pairs in each set of struts. This optimum design was found with use of the “temporary” (varying density) versions of bosdec (bosdec.density.var) and addbosor4 (addbosor4.density.var).

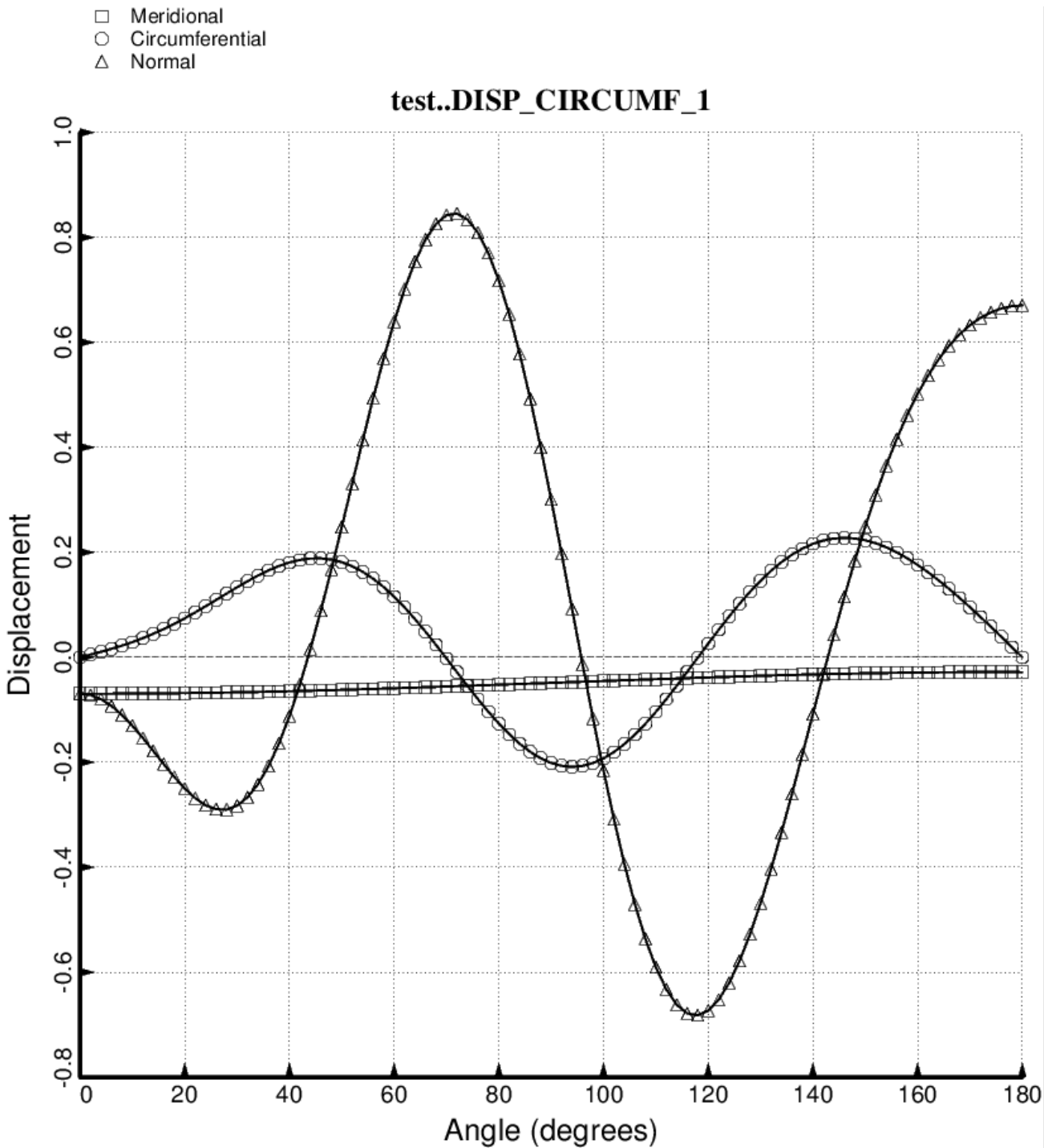


Fig. 28d (new) Load Case 2 (10 g lateral acceleration, 25 psi ullage pressure, 200 deg. tank cool-down): Deformation along 180 degrees of the circumference at the midlength of the cylindrical part of the long propellant tank with aft and forward struts, 4 strut pairs in each set of struts. This optimum design was found with use of the “temporary” (varying density) versions of bosdec (bosdec.density.var) and addbosor4 (addbosor4.density.var).

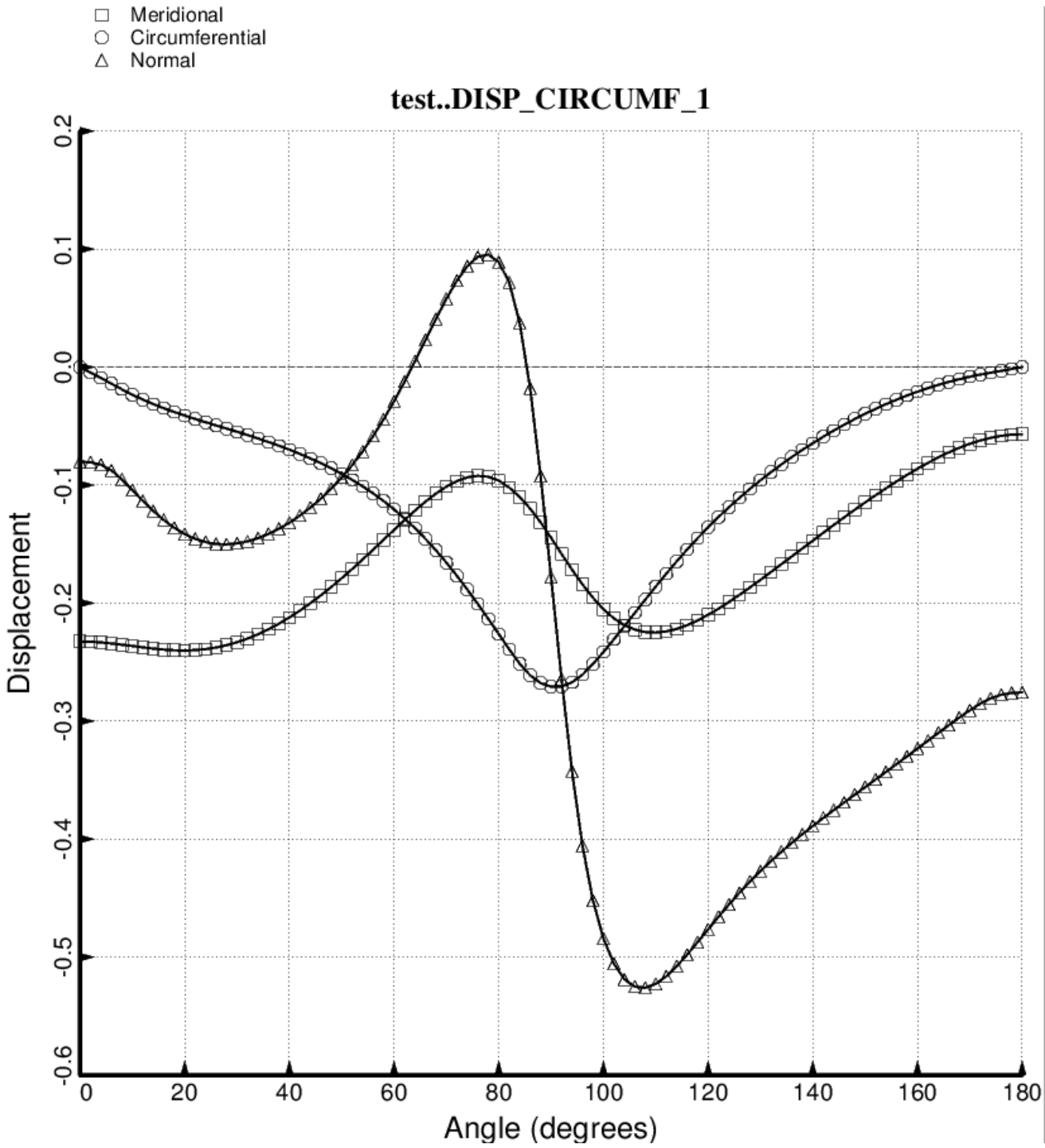


Fig. 28e (new) Load Case 2 (10 g lateral acceleration, 25 psi ullage pressure, 200 deg. tank cool-down): Deformation along 180 degrees of the circumference at the forward dome/cylinder junction of the long propellant tank with aft and forward struts, 4 strut pairs in each set of struts. This optimum design was found with use of the “temporary” (varying density) versions of bosdec (bosdec.density.var) and addbosor4 (addbosor4.density.var).

□ Objective=0.5x(TOTMAS/10.) +0.5x(CONDCT/0.002); temporary bigbosor4/bosdec; TEMTUR=170

### test: objective vs design iterations; curing temperature=170 degrees

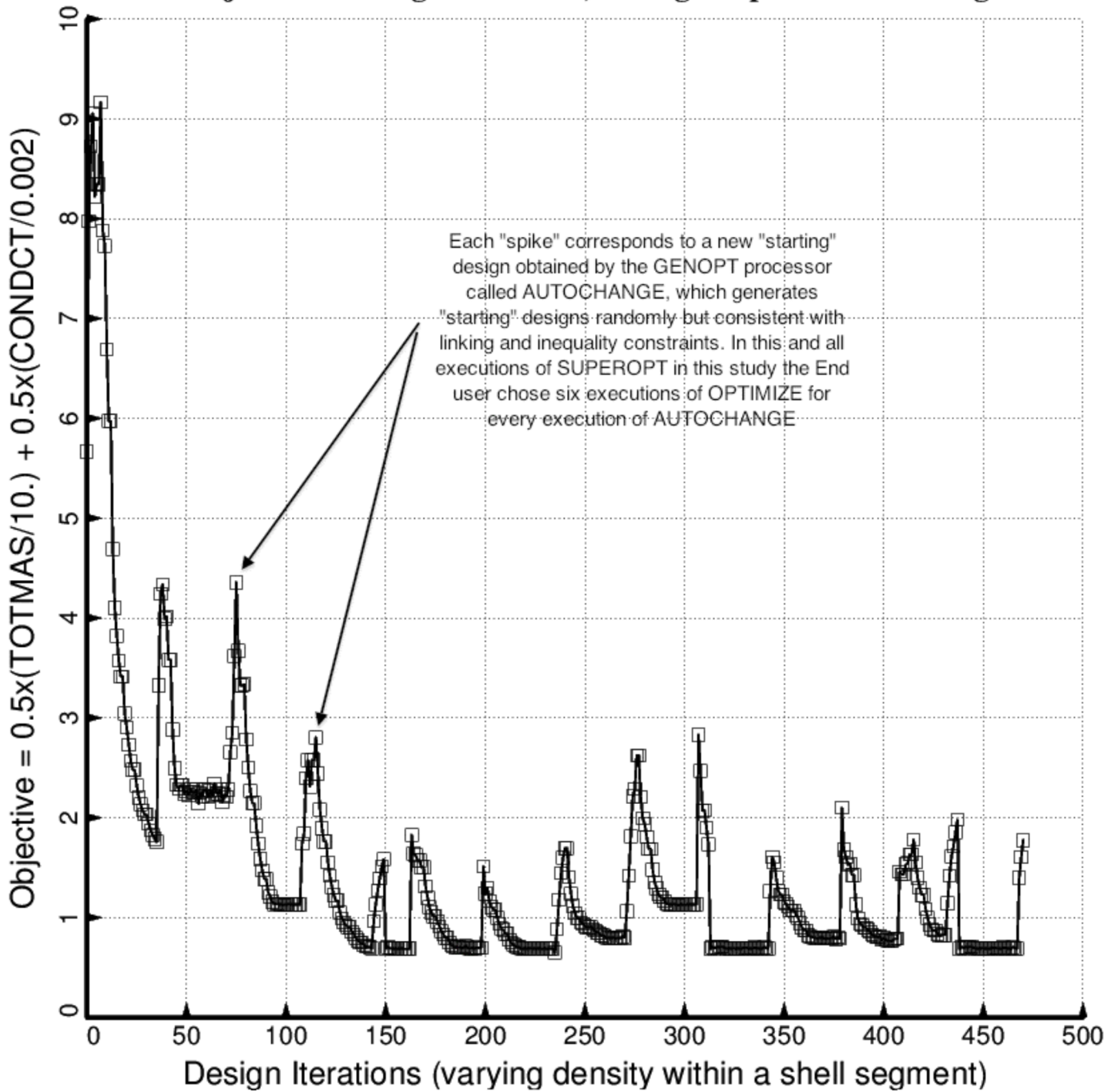


Fig. 29 (old) Evolution of the objective during the first execution of the GENOPT processor, SUPEROPT, for the long tank/strut system with aft and forward sets of struts. Notice that during the long SUPEROPT process (24 hours of computer time on the writer's very fast computer) the objective converges to more than one local minimum. This behavior makes it difficult to find a “global” optimum design.

□ WGTxTOTMAS/TNKNRM +(1-WGT)xCONDCT/CONNRM: CONDCT

### GENOPT test: objective vs design iterations

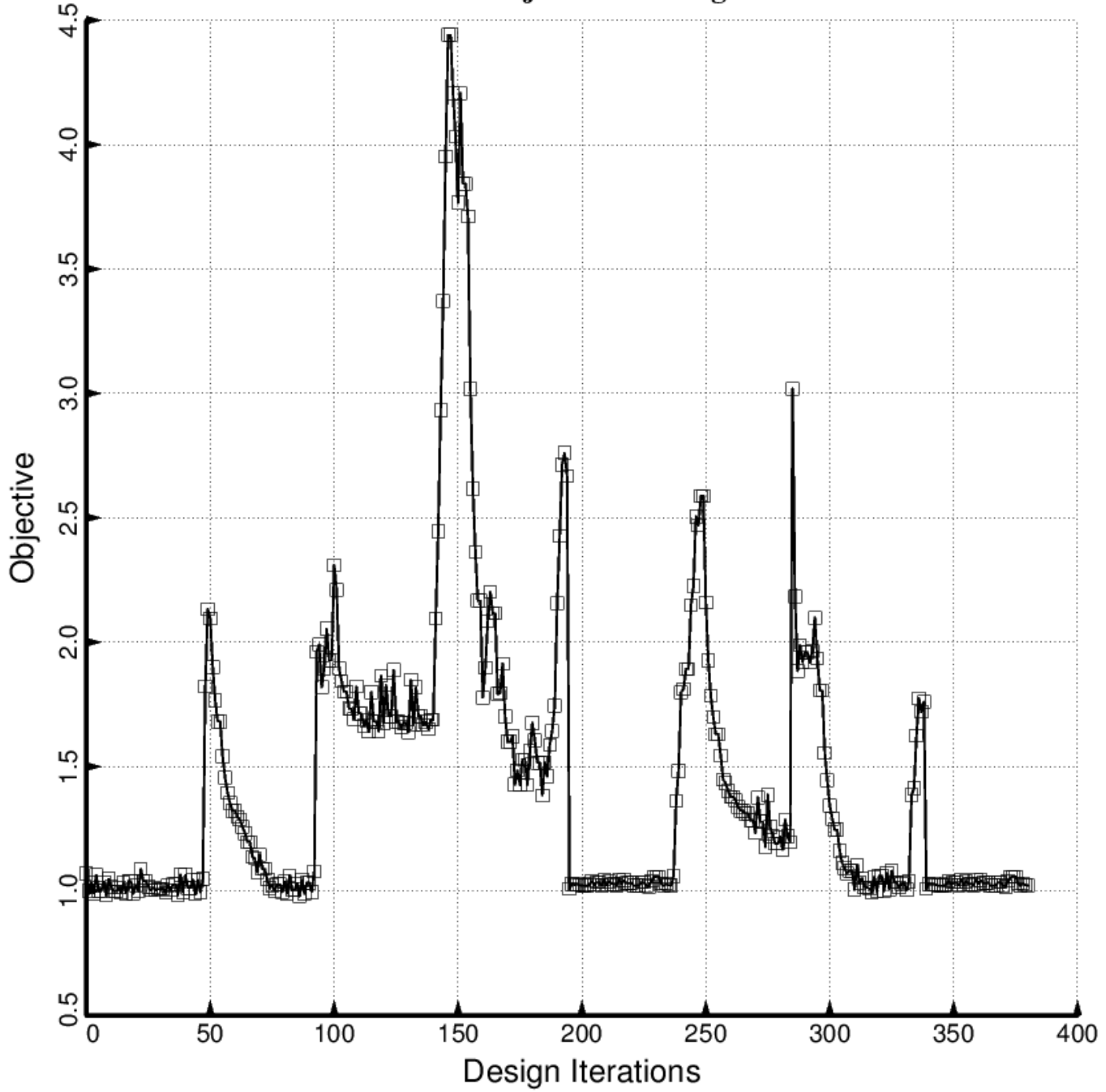


Fig. 29a (new) Evolution of the objective during a partial execution of the GENOPT processor, SUPEROPT, for the long tank/strut system with aft and forward sets of struts. This optimum design was found with use of the “temporary” (varying density) versions of bosdec (bosdec.density.var) and addbosor4 (addbosor4.density.var).

□ WGTxTOTMAS/TNKNRM +(1-WGT)xCONDCT/CONNRM: CONDCT

### GENOPT test: objective vs design iterations

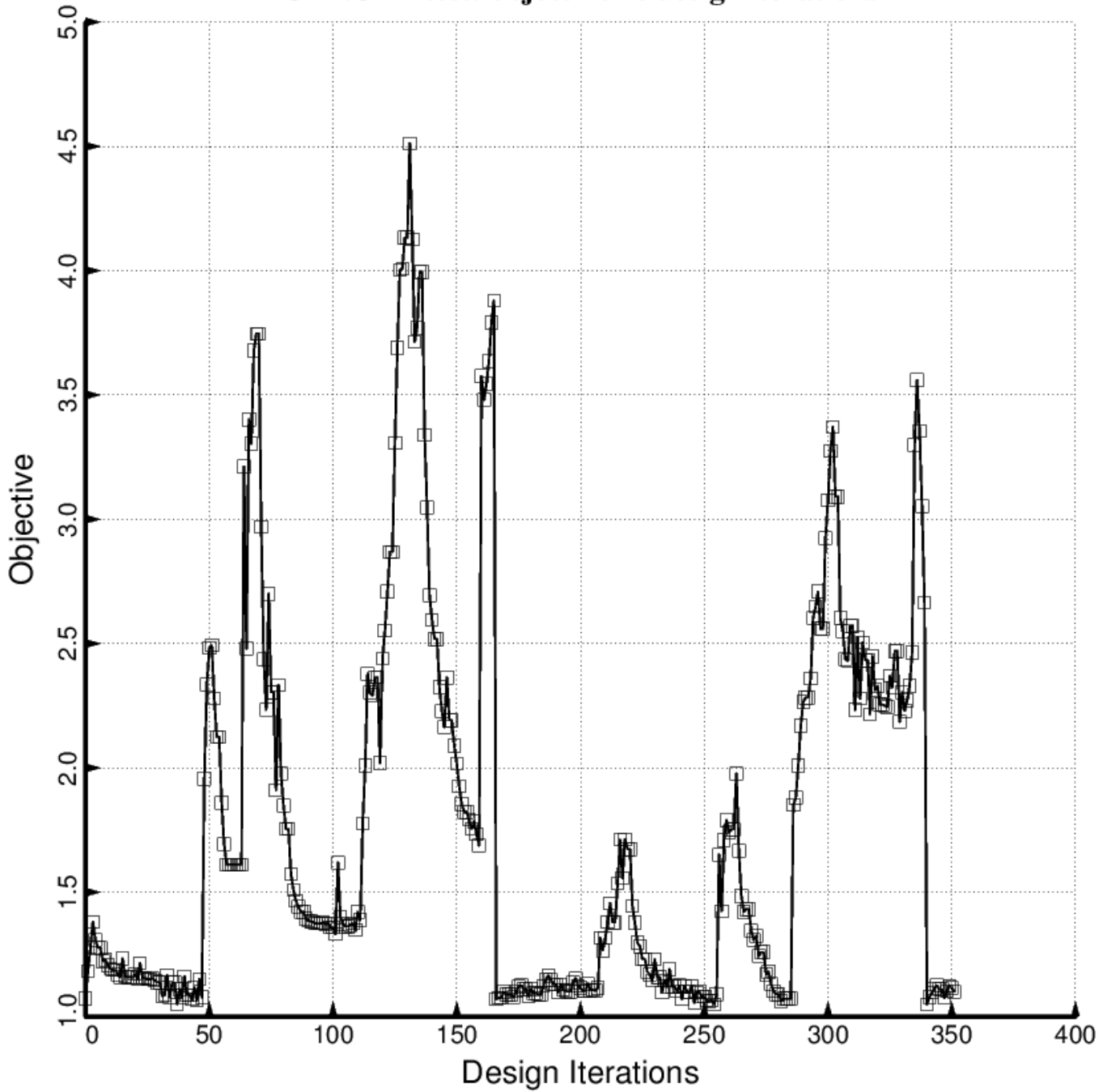


Fig. 29b (new) Evolution of the objective during a partial execution of the GENOPT processor, SUPEROPT, for the long tank/strut system with aft and forward sets of struts. This optimum design was found with use of the “permanent” (constant density) versions of bosdec (bosdec.tank) and addbosor4 (addbosor4.regular). Notice that during the long SUPEROPT process the objective converges to more than one local minimum. This behavior makes it difficult to find a “global” optimum design.

□ (FREQ(1,1)/FREQA(1,1)) / FREQF(1,1)-1; F.S.= 1.20  
 ○ (FREQ(1,2)/FREQA(1,2)) / FREQF(1,2)-1; F.S.= 1.20  
 △ (FREQ(1,3)/FREQA(1,3)) / FREQF(1,3)-1; F.S.= 1.20  
 + (FREQ(1,4)/FREQA(1,4)) / FREQF(1,4)-1; F.S.= 1.20  
 × (STRES2A(1,3)/STRES2(1,3)) / STRES2F(1,3)-1; F.S.= 1.50  
 ◇ (TNKSTRA(1,1)/TNKSTR(1,1)) / TNKSTRF(1,1)-1; F.S.= 1.00

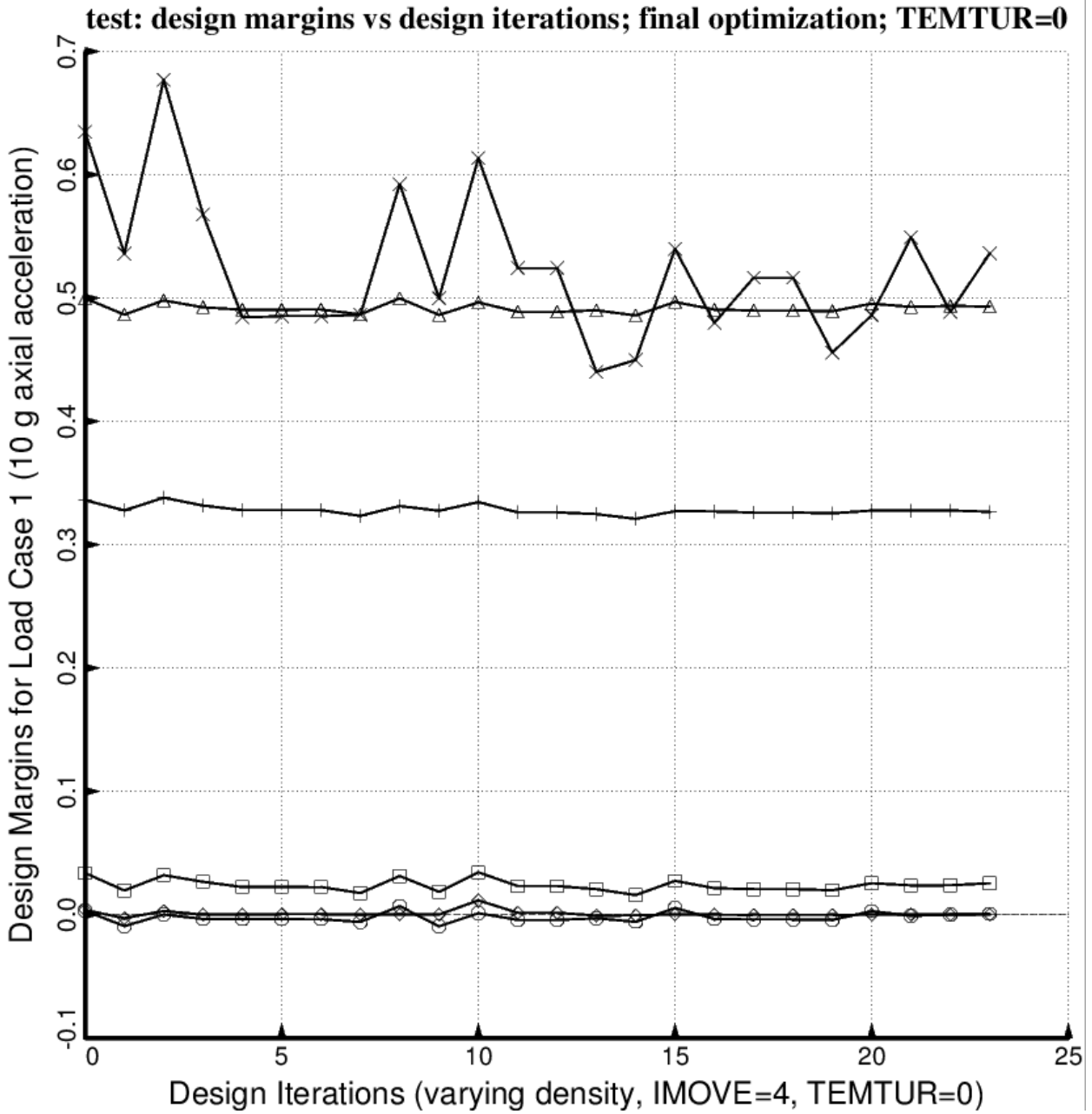


Fig. 30 (old) Load Case 1 = 10g axial acceleration, 25 psi ullage pressure, 200 degrees propellant tank cool-down. Shown here are the most critical margins as a function of design iterations for a partial execution of the GENOPT processor, SUPEROPT. (The index, IMOVE, governs how large a change in the design is permitted by the ADS optimizer at each optimization cycle. IMOVE = 4 is quite restrictive.)

- $\square$  (FREQ(2,1)/FREQA(2,1)) / FREQF(2,1)-1; F.S.= 1.20
- $\circ$  (FREQ(2,2)/FREQA(2,2)) / FREQF(2,2)-1; F.S.= 1.20
- $\triangle$  (FREQ(2,3)/FREQA(2,3)) / FREQF(2,3)-1; F.S.= 1.20
- $+$  (FREQ(2,4)/FREQA(2,4)) / FREQF(2,4)-1; F.S.= 1.20
- $\times$  (STRES1A(2,2)/STRES1(2,2)) / STRES1F(2,2)-1; F.S.= 1.50
- $\diamond$  (STRES1A(2,3)/STRES1(2,3)) / STRES1F(2,3)-1; F.S.= 1.50
- $\triangledown$  (STRES2A(2,2)/STRES2(2,2)) / STRES2F(2,2)-1; F.S.= 1.50
- $\boxtimes$  (STRES2A(2,3)/STRES2(2,3)) / STRES2F(2,3)-1; F.S.= 1.50
- $\times$  (COLBUK(2,1)/COLBUKA(2,1)) / COLBUKF(2,1)-1; F.S.= 1.00
- $\diamond$  (COLBUK(2,2)/COLBUKA(2,2)) / COLBUKF(2,2)-1; F.S.= 1.00
- $\oplus$  (SHLBUK(2,1)/SHLBUKA(2,1)) / SHLBUKF(2,1)-1; F.S.= 2.00
- $\boxtimes$  (SHLBUK(2,2)/SHLBUKA(2,2)) / SHLBUKF(2,2)-1; F.S.= 2.00
- $\boxplus$  (FORCEA(2,2)/FORCE(2,2)) / FORCEF(2,2)-1; F.S.= 1.00
- $\boxtimes$  (TNKSTRA(2,1)/TNKSTR(2,1)) / TNKSTRF(2,1)-1; F.S.= 1.00
- $\boxtimes$  (TNKSTRA(2,2)/TNKSTR(2,2)) / TNKSTRF(2,2)-1; F.S.= 1.00

**test: design margins vs design iterations; final optimization; TEMTUR=0**

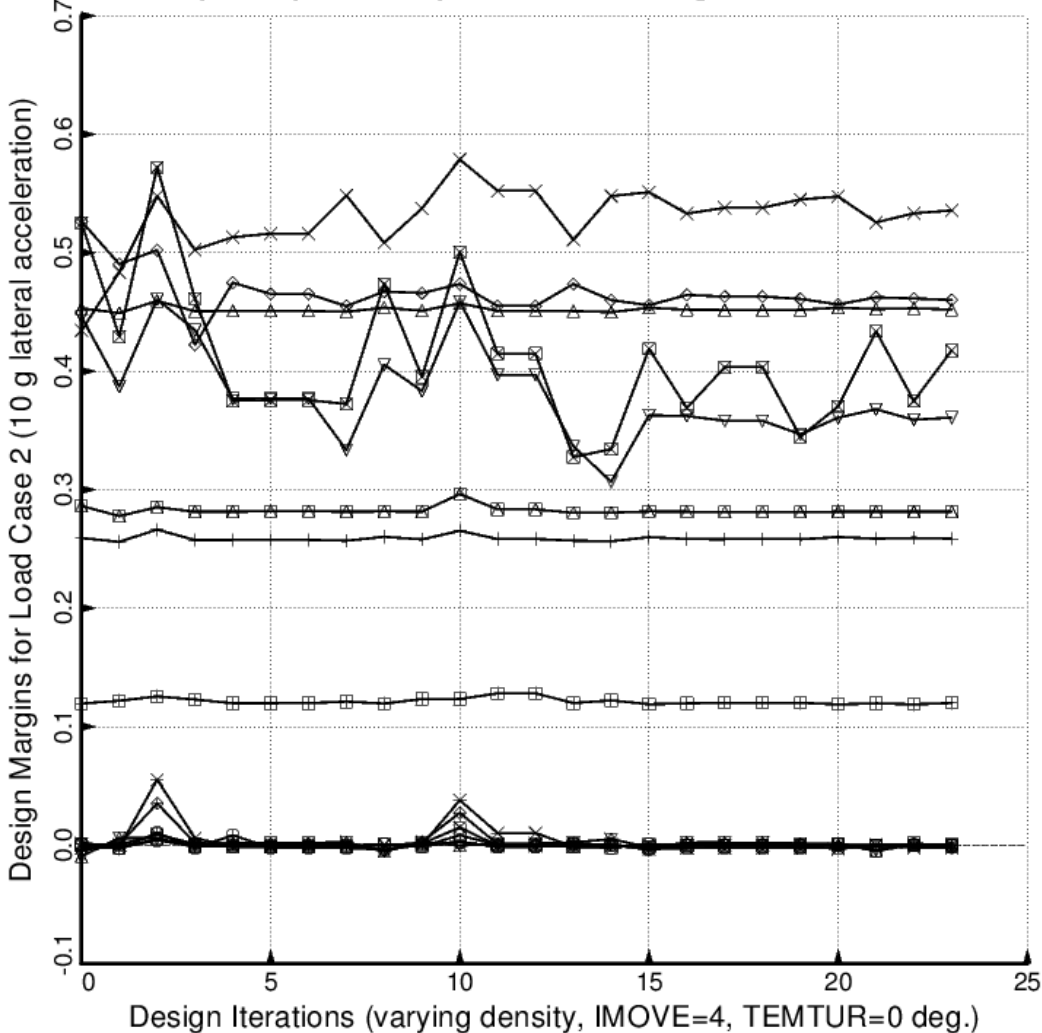


Fig. 31 (old) Load Case 2 = 10g lateral acceleration, 25 psi ullage pressure, 200 degrees propellant tank cooldown. Shown here are the most critical margins as a function of design iterations for a partial execution of the GENOPT processor, SUPEROPT. (The index, IMOVE, governs how large a change in the design is permitted by the ADS optimizer at each optimization cycle. IMOVE = 4 is quite restrictive.) Compare with the previous figure. More of the design margins are critical under Load Case 2 than under Load Case 1.

□ (FREQ(1,1)/FREQA(1,1)) / FREQF(1,1)-1; F.S.= 1.20  
 ○ (FREQ(1,2)/FREQA(1,2)) / FREQF(1,2)-1; F.S.= 1.20  
 △ (STRES2A(1,3)/STRES2(1,3)) / STRES2F(1,3)-1; F.S.= 1.50  
 + (FORCEA(1,2)/FORCE(1,2)) / FORCEF(1,2)-1; F.S.= 1.00  
 × (TNKSTRA(1,1)/TNKSTR(1,1)) / TNKSTRF(1,1)-1; F.S.= 1.00  
 ◊ (FREQ(2,1)/FREQA(2,1)) / FREQF(2,1)-1; F.S.= 1.20  
 ▽ (FREQ(2,2)/FREQA(2,2)) / FREQF(2,2)-1; F.S.= 1.20  
 ▨ (STRES1A(2,3)/STRES1(2,3)) / STRES1F(2,3)-1; F.S.= 1.50  
 ✕ (STRES2A(2,3)/STRES2(2,3)) / STRES2F(2,3)-1; F.S.= 1.50  
 ♦ (COLBUK(2,2)/COLBUKA(2,2)) / COLBUKF(2,2)-1; F.S.= 1.00  
 ▨ (SHLBUK(2,1)/SHLBUKA(2,1)) / SHLBUKF(2,1)-1; F.S.= 2.00  
 ✕ (SHLBUK(2,2)/SHLBUKA(2,2)) / SHLBUKF(2,2)-1; F.S.= 2.00  
 (FORCEA(2,2)/FORCE(2,2)) / FORCEF(2,2)-1; F.S.= 1.00  
 ✕ (TNKSTRA(2,1)/TNKSTR(2,1)) / TNKSTRF(2,1)-1; F.S.= 1.00

### GENOPT test: design margins vs THKAFT

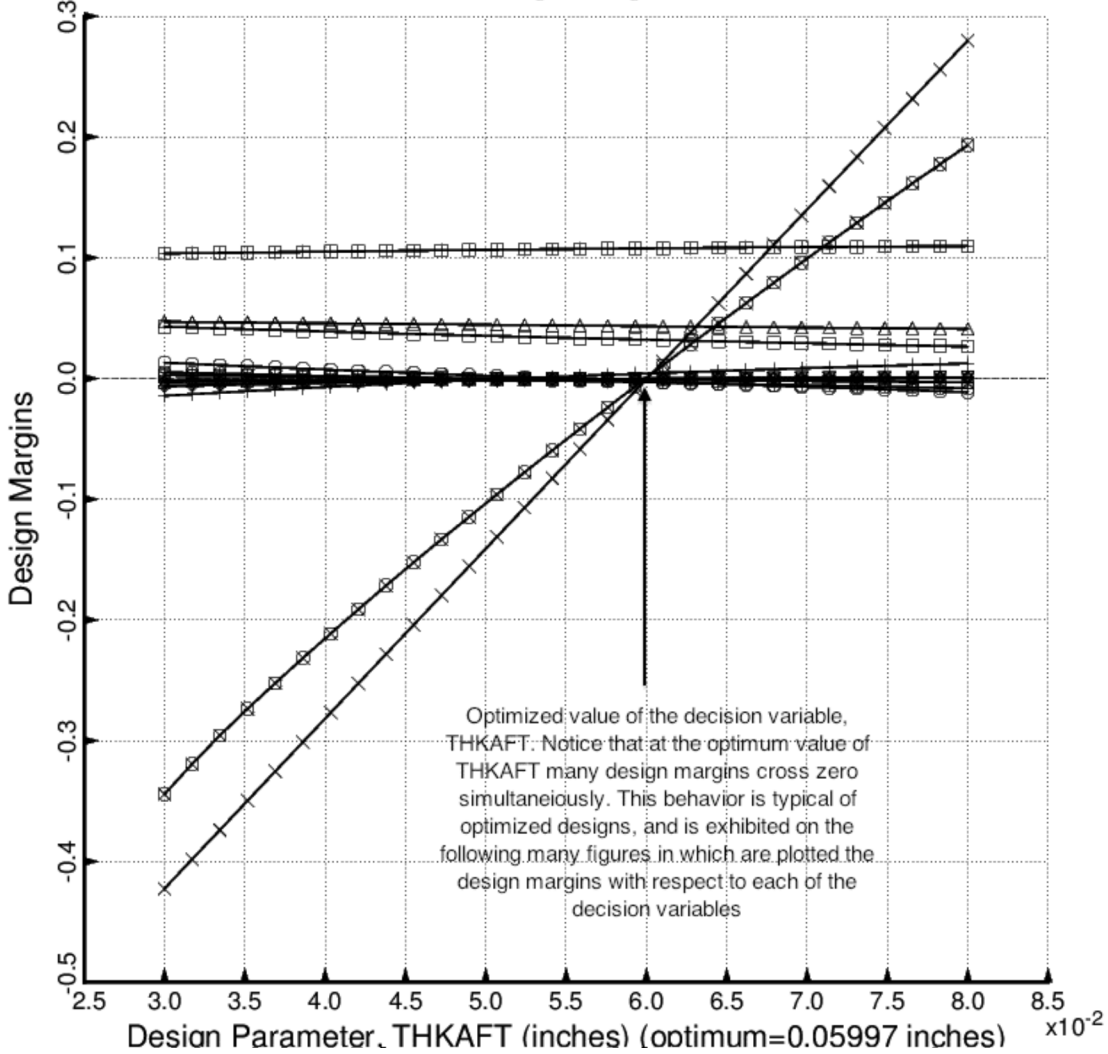


Fig. 32 (old) Design sensitivity of the optimized long propellant tank with aft and forward struts, 4 strut pairs in each set of struts. Here we have the design sensitivity with respect to the decision variable, THKAFT = uniform thickness of the middle layer of the 3-layered aft ellipsoidal dome. Design sensitivity is conducted by GENOPT whenever the End user chooses ITYPE = 3 for the analysis type during the MAINSETUP interactive session. See Table 7 for an example of typical input data for MAINSETUP when ITYPE = 3.

- 
- (FREQ(1,1)/FREQA(1,1)) / FREQF(1,1)-1; F.S.= 1.20  
 ○ (FREQ(1,2)/FREQA(1,2)) / FREQF(1,2)-1; F.S.= 1.20  
 △ (STRES2A(1,3)/STRES2(1,3)) / STRES2F(1,3)-1; F.S.= 1.50  
 + (FORCEA(1,2)/FORCE(1,2)) / FORCEF(1,2)-1; F.S.= 1.00  
 × (TNKSTRA(1,1)/TNKSTR(1,1)) / TNKSTRF(1,1)-1; F.S.= 1.00  
 ◇ (FREQ(2,1)/FREQA(2,1)) / FREQF(2,1)-1; F.S.= 1.20  
 ▽ (FREQ(2,2)/FREQA(2,2)) / FREQF(2,2)-1; F.S.= 1.20  
 ▨ (STRES1A(2,3)/STRES1(2,3)) / STRES1F(2,3)-1; F.S.= 1.50  
 ✕ (STRES2A(2,3)/STRES2(2,3)) / STRES2F(2,3)-1; F.S.= 1.50  
 ♦ (COLBUK(2,2)/COLBUKA(2,2)) / COLBUKF(2,2)-1; F.S.= 1.00  
 ⊕ (SHLBUK(2,1)/SHLBUKA(2,1)) / SHLBUKF(2,1)-1; F.S.= 2.00  
 ✋ (SHLBUK(2,2)/SHLBUKA(2,2)) / SHLBUKF(2,2)-1; F.S.= 2.00  
 ▨ (FORCEA(2,2)/FORCE(2,2)) / FORCEF(2,2)-1; F.S.= 1.00  
 ✎ (TNKSTRA(2,1)/TNKSTR(2,1)) / TNKSTRF(2,1)-1; F.S.= 1.00

**GENOPT test: design margins vs THKMID**

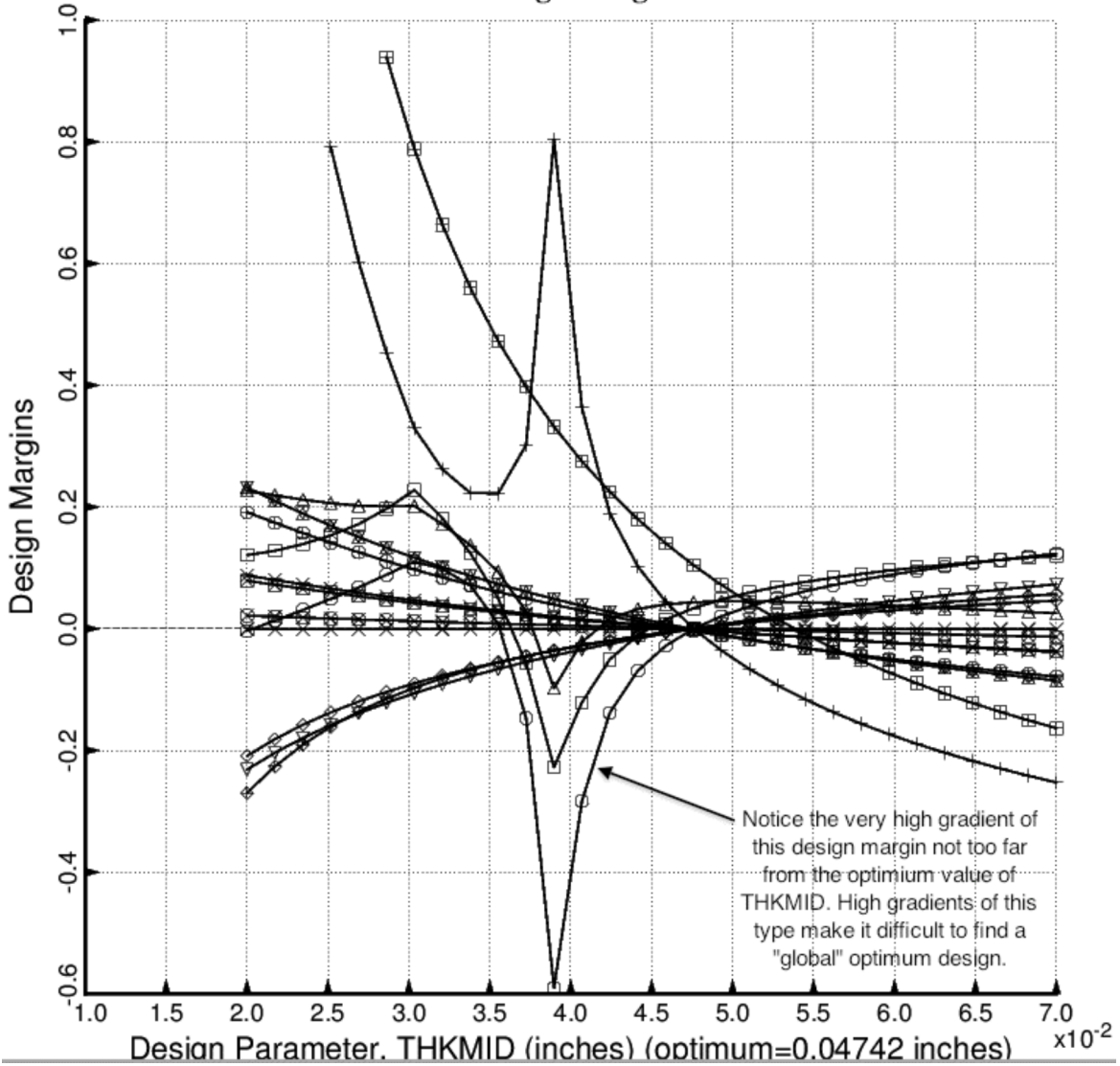


Fig. 33 (old) Design sensitivity of the optimized long propellant tank with aft and forward struts, 4 strut pairs in each set of struts. Here we have the design sensitivity with respect to the decision variable, THKMID = uniform thickness of the middle layer of the 3-layered cylindrical part of the tank.

- $\square$   $(\text{FREQ}(1,1)/\text{FREQA}(1,1)) / \text{FREQH}(1,1) - 1$ ; F.S. = 1.20
- $\circ$   $(\text{FREQ}(1,2)/\text{FREQA}(1,2)) / \text{FREQF}(1,2) - 1$ ; F.S. = 1.20
- $\triangle$   $(\text{STRES2A}(1,3)/\text{STRES2}(1,3)) / \text{STRES2F}(1,3) - 1$ ; F.S. = 1.50
- $+$   $(\text{FORCEA}(1,2)/\text{FORCE}(1,2)) / \text{FORCEF}(1,2) - 1$ ; F.S. = 1.00
- $\times$   $(\text{TNKSTRA}(1,1)/\text{TNKSTR}(1,1)) / \text{TNKSTRF}(1,1) - 1$ ; F.S. = 1.00
- $\diamond$   $(\text{FREQ}(2,1)/\text{FREQA}(2,1)) / \text{FREQF}(2,1) - 1$ ; F.S. = 1.20
- $\triangledown$   $(\text{FREQ}(2,2)/\text{FREQA}(2,2)) / \text{FREQF}(2,2) - 1$ ; F.S. = 1.20
- $\blacksquare$   $(\text{STRES1A}(2,3)/\text{STRES1}(2,3)) / \text{STRES1F}(2,3) - 1$ ; F.S. = 1.50
- $\times$   $(\text{STRES2A}(2,3)/\text{STRES2}(2,3)) / \text{STRES2F}(2,3) - 1$ ; F.S. = 1.50
- $\diamond$   $(\text{COLBUK}(2,2)/\text{COLBUKA}(2,2)) / \text{COLBUKF}(2,2) - 1$ ; F.S. = 1.00
- $\oplus$   $(\text{SHLBUK}(2,1)/\text{SHLBUKA}(2,1)) / \text{SHLBUKF}(2,1) - 1$ ; F.S. = 2.00
- $\blacksquare$   $(\text{SHLBUK}(2,2)/\text{SHLBUKA}(2,2)) / \text{SHLBUKF}(2,2) - 1$ ; F.S. = 2.00
- $\blacksquare$   $(\text{FORCEA}(2,2)/\text{FORCE}(2,2)) / \text{FORCEF}(2,2) - 1$ ; F.S. = 1.00
- $\blacksquare$   $(\text{TNKSTRA}(2,1)/\text{TNKSTR}(2,1)) / \text{TNKSTRF}(2,1) - 1$ ; F.S. = 1.00

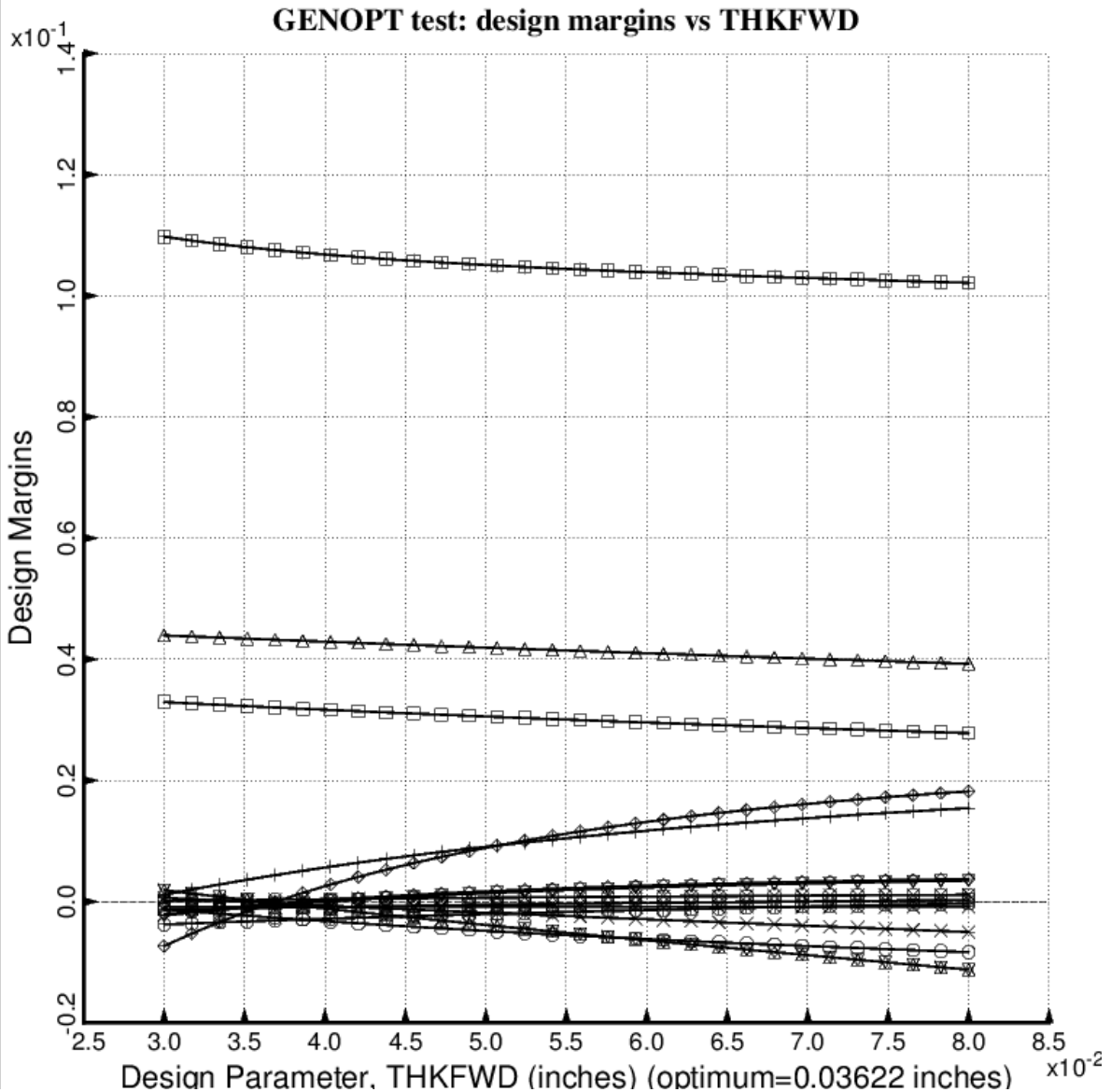


Fig. 34 (old) Design sensitivity of the optimized long propellant tank with aft and forward struts, 4 strut pairs in each set of struts. Here we have the design sensitivity with respect to the decision variable, THKFWD = uniform thickness of the middle layer of the 3-layered forward ellipsoidal dome.

- 
- (FREQ(1,1)/FREQA(1,1)) / FREQF(1,1)-1; F.S.= 1.20  
 ○ (FREQ(1,2)/FREQA(1,2)) / FREQF(1,2)-1; F.S.= 1.20  
 △ (STRES2A(1,3)/STRES2(1,3)) / STRES2F(1,3)-1; F.S.= 1.50  
 + (FORCEA(1,2)/FORCE(1,2)) / FORCEF(1,2)-1; F.S.= 1.00  
 × (TNKSTRA(1,1)/TNKSTR(1,1)) / TNKSTRF(1,1)-1; F.S.= 1.00  
 ◇ (FREQ(2,1)/FREQA(2,1)) / FREQF(2,1)-1; F.S.= 1.20  
 ▽ (FREQ(2,2)/FREQA(2,2)) / FREQF(2,2)-1; F.S.= 1.20  
 (STRES1A(2,3)/STRES1(2,3)) / STRES1F(2,3)-1; F.S.= 1.50  
 (STRES2A(2,3)/STRES2(2,3)) / STRES2F(2,3)-1; F.S.= 1.50  
 ♦ (COLBUK(2,2)/COLBUKA(2,2)) / COLBUKF(2,2)-1; F.S.= 1.00  
 ⊕ (SHLBUK(2,1)/SHLBUKA(2,1)) / SHLBUKF(2,1)-1; F.S.= 2.00  
 × (SHLBUK(2,2)/SHLBUKA(2,2)) / SHLBUKF(2,2)-1; F.S.= 2.00  
 ▨ (FORCEA(2,2)/FORCE(2,2)) / FORCEF(2,2)-1; F.S.= 1.00  
 □ (TNKSTRA(2,1)/TNKSTR(2,1)) / TNKSTRF(2,1)-1; F.S.= 1.00

**GENOPT test: design margins vs STRSPC**

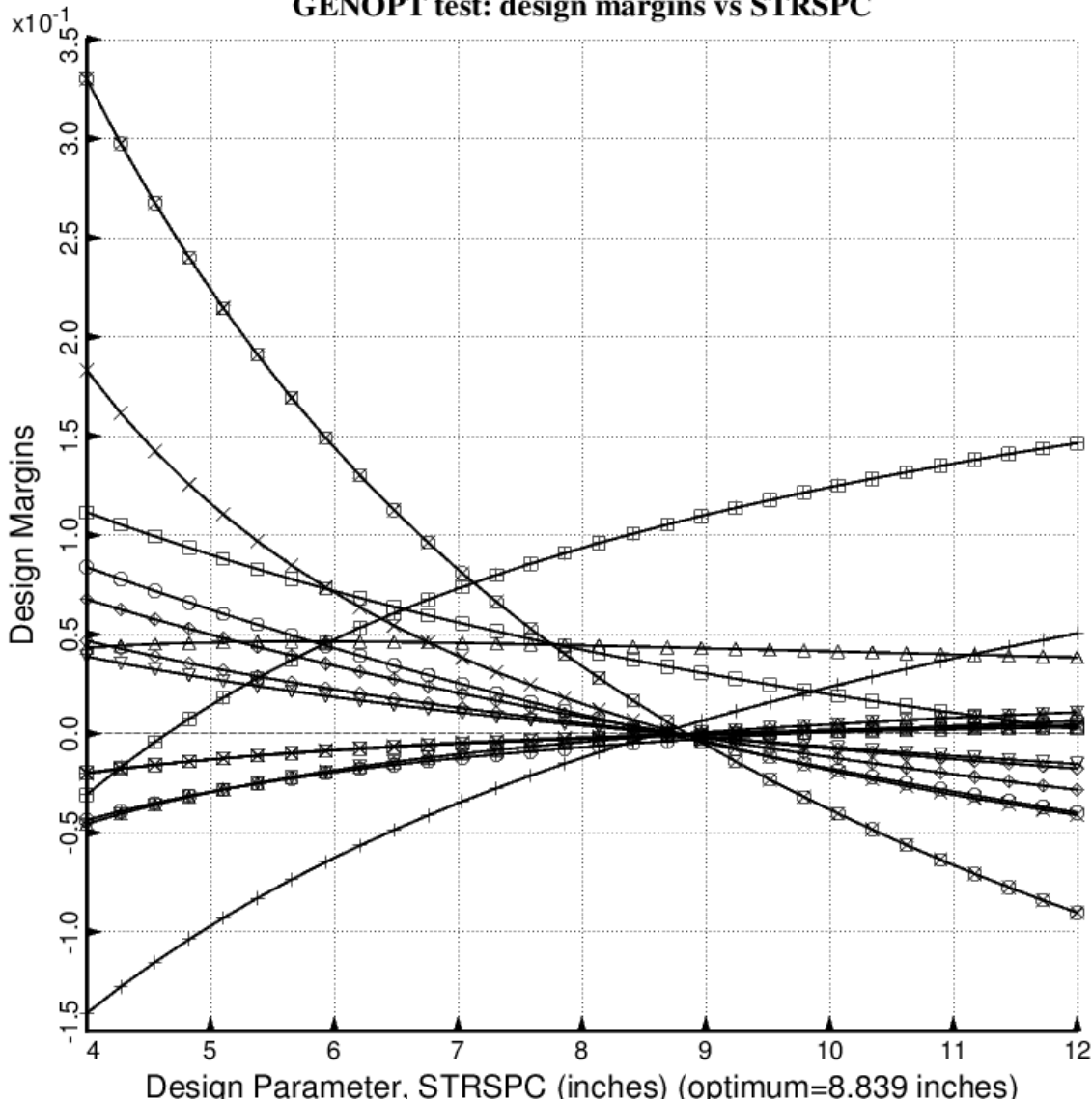


Fig. 35 (old) Design sensitivity of the optimized long propellant tank with aft and forward struts, 4 strut pairs in each set of struts. Here we have the design sensitivity with respect to the decision variable, STRSPC = uniform spacing of the stiffeners in the internal smeared orthogrid “layer” of the propellant tank.

- $\square$  (FREQ(1,1)/FREQA(1,1)) / FREQF(1,1)-1; F.S.= 1.20
- $\circ$  (FREQ(1,2)/FREQA(1,2)) / FREQF(1,2)-1; F.S.= 1.20
- $\triangle$  (STRES2A(1,3)/STRES2(1,3)) / STRES2F(1,3)-1; F.S.= 1.50
- $+$  (FORCEA(1,2)/FORCE(1,2)) / FORCEF(1,2)-1; F.S.= 1.00
- $\times$  (TNKSTRA(1,1)/TNKSTR(1,1)) / TNKSTRF(1,1)-1; F.S.= 1.00
- $\diamond$  (FREQ(2,1)/FREQA(2,1)) / FREQF(2,1)-1; F.S.= 1.20
- $\triangledown$  (FREQ(2,2)/FREQA(2,2)) / FREQF(2,2)-1; F.S.= 1.20
- $\blacksquare$  (STRES1A(2,3)/STRES1(2,3)) / STRES1F(2,3)-1; F.S.= 1.50
- $\times$  (STRES2A(2,3)/STRES2(2,3)) / STRES2F(2,3)-1; F.S.= 1.50
- $\diamond$  (COLBUK(2,2)/COLBUKA(2,2)) / COLBUKF(2,2)-1; F.S.= 1.00
- $\oplus$  (SHLBUK(2,1)/SHLBUKA(2,1)) / SHLBUKF(2,1)-1; F.S.= 2.00
- $\boxtimes$  (SHLBUK(2,2)/SHLBUKA(2,2)) / SHLBUKF(2,2)-1; F.S.= 2.00
- $\blacksquare$  (FORCEA(2,2)/FORCE(2,2)) / FORCEF(2,2)-1; F.S.= 1.00
- $\blacksquare$  (TNKSTRA(2,1)/TNKSTR(2,1)) / TNKSTRF(2,1)-1; F.S.= 1.00

GENOPT test: design margins vs STRTHK

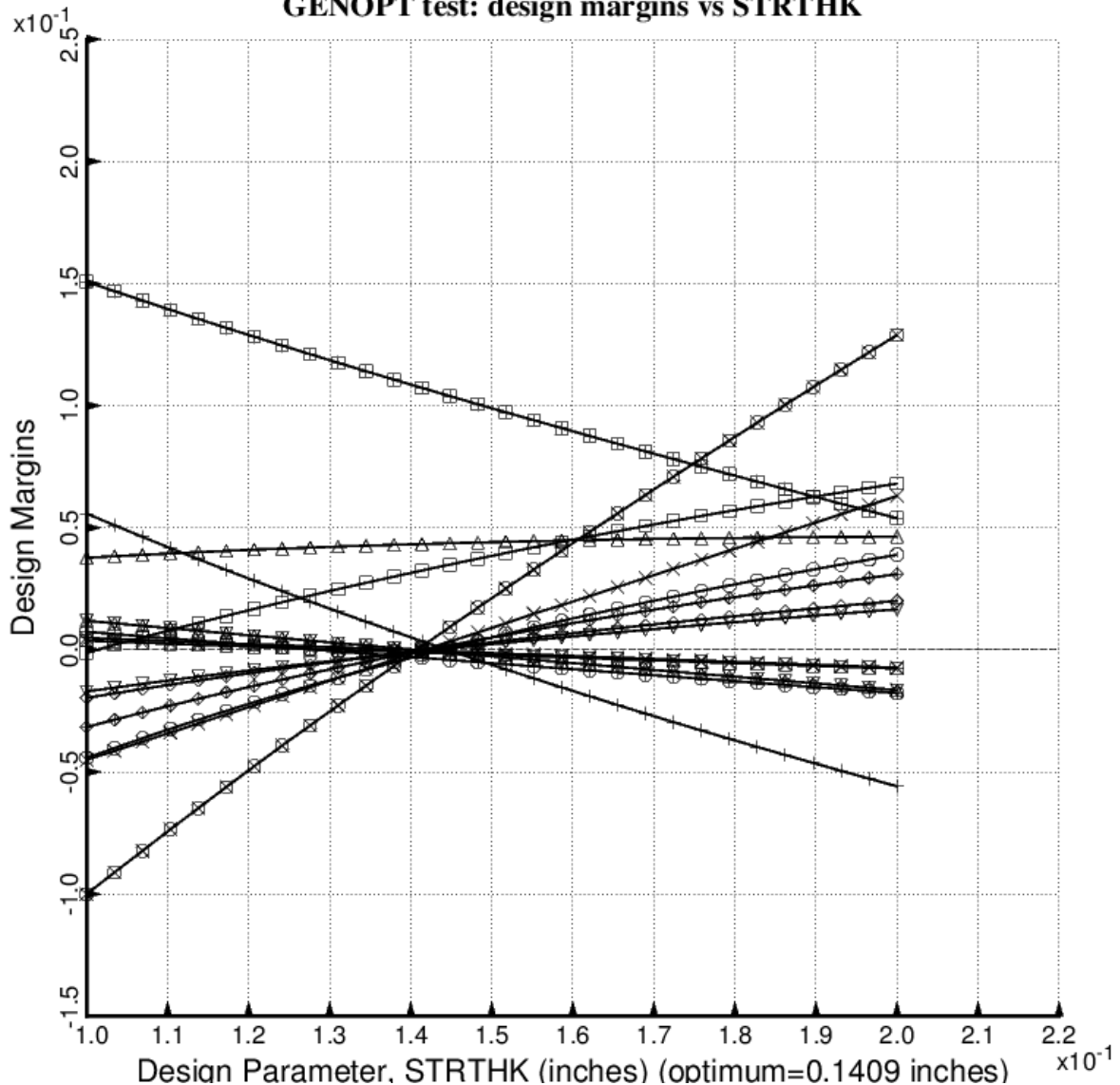


Fig. 36 (old) Design sensitivity of the optimized long propellant tank with aft and forward struts, 4 strut pairs in each set of struts. Here we have the design sensitivity with respect to the decision variable, STRTHK = uniform thickness of the stiffeners in the internal smeared orthogrid “layer” of the propellant tank.

- $\square$  (FREQ(1,1)/FREQA(1,1)) / FREQF(1,1)-1; F.S.= 1.20
- $\circ$  (FREQ(1,2)/FREQA(1,2)) / FREQF(1,2)-1; F.S.= 1.20
- $\triangle$  (STRES2A(1,3)/STRES2(1,3)) / STRES2F(1,3)-1; F.S.= 1.50
- $+$  (FORCEA(1,2)/FORCE(1,2)) / FORCEF(1,2)-1; F.S.= 1.00
- $\times$  (TNKSTRA(1,1)/TNKSTR(1,1)) / TNKSTRF(1,1)-1; F.S.= 1.00
- $\diamond$  (FREQ(2,1)/FREQA(2,1)) / FREQF(2,1)-1; F.S.= 1.20
- $\triangledown$  (FREQ(2,2)/FREQA(2,2)) / FREQF(2,2)-1; F.S.= 1.20
- $\blacksquare$  (STRES1A(2,3)/STRES1(2,3)) / STRES1F(2,3)-1; F.S.= 1.50
- $\times$  (STRES2A(2,3)/STRES2(2,3)) / STRES2F(2,3)-1; F.S.= 1.50
- $\diamond$  (COLBUK(2,2)/COLBUKA(2,2)) / COLBUKF(2,2)-1; F.S.= 1.00
- $\oplus$  (SHLBUK(2,1)/SHLBUKA(2,1)) / SHLBUKF(2,1)-1; F.S.= 2.00
- $\boxtimes$  (SHLBUK(2,2)/SHLBUKA(2,2)) / SHLBUKF(2,2)-1; F.S.= 2.00
- $\blacksquare$  (FORCEA(2,2)/FORCE(2,2)) / FORCEF(2,2)-1; F.S.= 1.00
- $\blacksquare$  (TNKSTRA(2,1)/TNKSTR(2,1)) / TNKSTRF(2,1)-1; F.S.= 1.00

**GENOPT test: design margins vs STRHI**

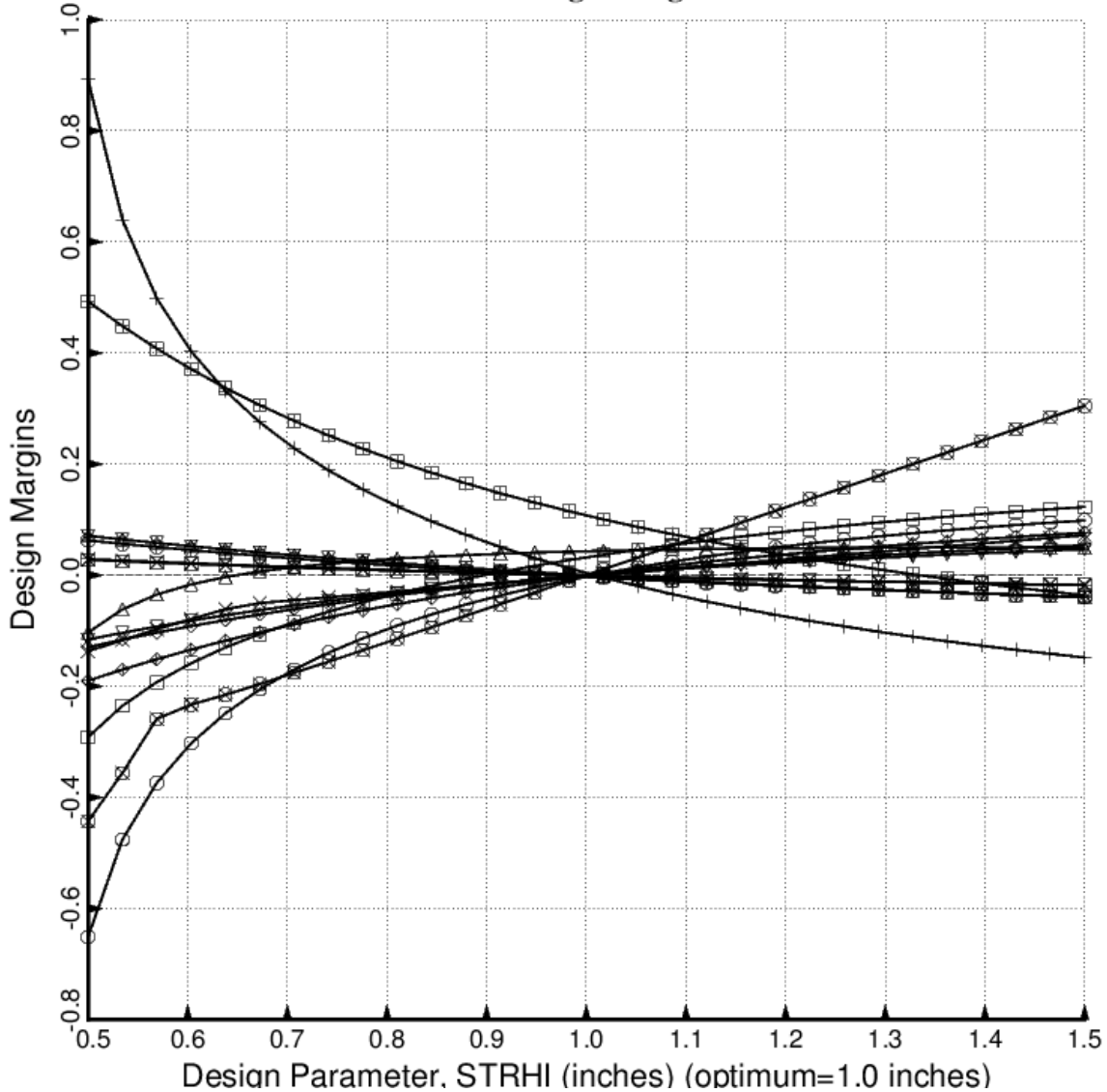


Fig. 37 (old) Design sensitivity of the optimized long propellant tank with aft and forward struts, 4 strut pairs in each set of struts. Here we have the design sensitivity with respect to the decision variable, STRHI = uniform height of the stiffeners in the internal smeared orthogrid “layer” of the propellant tank.

□ (FREQ(1,1)/FREQA(1,1)) / FREQF(1,1)-1; F.S.= 1.20  
 ○ (FREQ(1,2)/FREQA(1,2)) / FREQF(1,2)-1; F.S.= 1.20  
 △ (STRES2A(1,3)/STRES2(1,3)) / STRES2F(1,3)-1; F.S.= 1.50  
 + (FORCEA(1,2)/FORCE(1,2)) / FORCEF(1,2)-1; F.S.= 1.00  
 × (TNKSTRA(1,1)/TNKSTR(1,1)) / TNKSTRF(1,1)-1; F.S.= 1.00  
 ◇ (FREQ(2,1)/FREQA(2,1)) / FREQF(2,1)-1; F.S.= 1.20  
 ▽ (FREQ(2,2)/FREQA(2,2)) / FREQF(2,2)-1; F.S.= 1.20  
 ▨ (STRES1A(2,3)/STRES1(2,3)) / STRES1F(2,3)-1; F.S.= 1.50  
 ✕ (STRES2A(2,3)/STRES2(2,3)) / STRES2F(2,3)-1; F.S.= 1.50  
 ♦ (COLBUK(2,2)/COLBUKA(2,2)) / COLBUKF(2,2)-1; F.S.= 1.00  
 ⊕ (SHLBUK(2,1)/SHLBUKA(2,1)) / SHLBUKF(2,1)-1; F.S.= 2.00  
 ✲ (SHLBUK(2,2)/SHLBUKA(2,2)) / SHLBUKF(2,2)-1; F.S.= 2.00  
 ■ (FORCEA(2,2)/FORCE(2,2)) / FORCEF(2,2)-1; F.S.= 1.00  
 ☒ (TNKSTRA(2,1)/TNKSTR(2,1)) / TNKSTRF(2,1)-1; F.S.= 1.00

**GENOPT test: design margins vs ZGRND(1)**

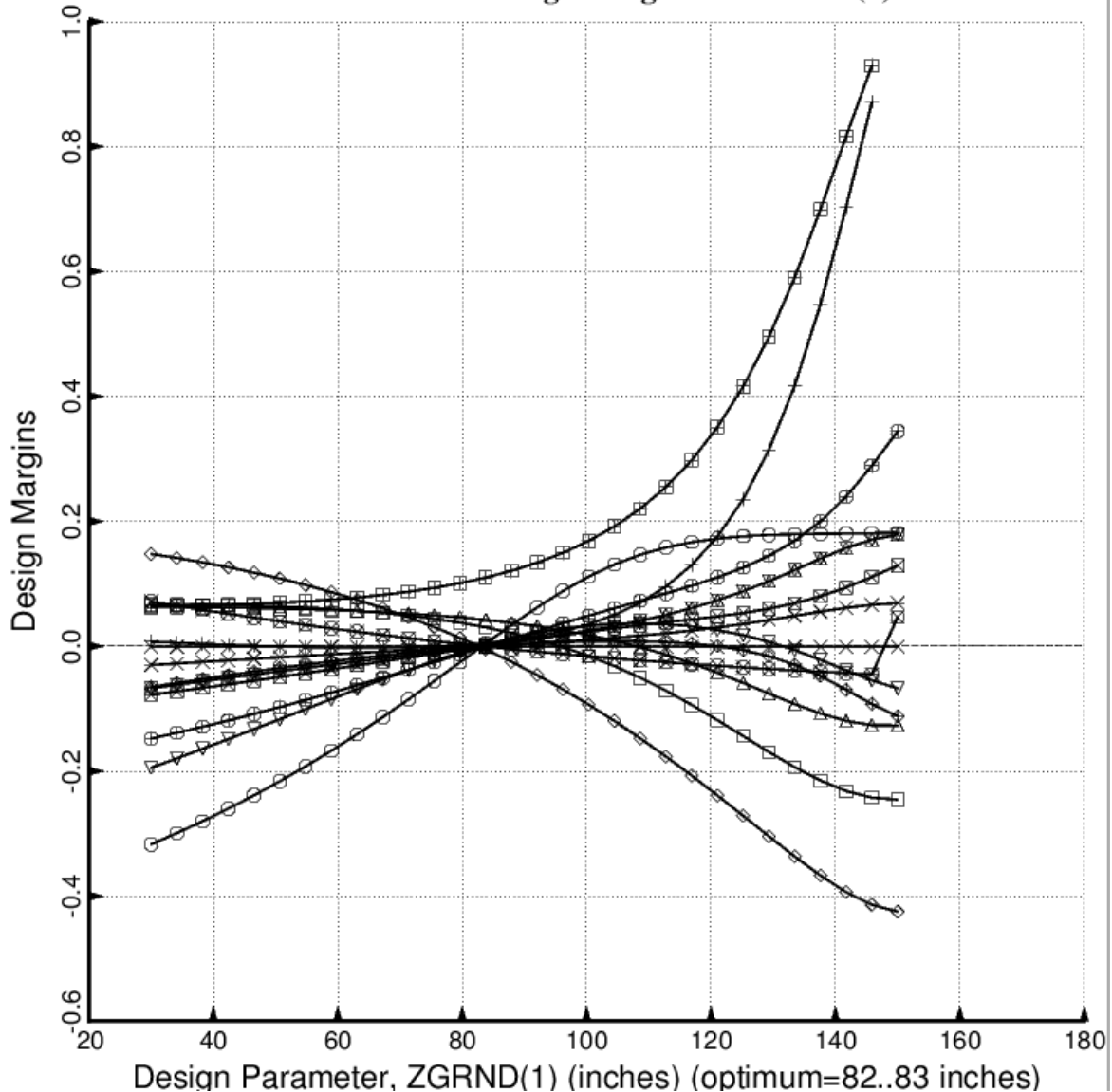


Fig. 38 (old) Design sensitivity of the optimized long propellant tank with aft and forward struts, 4 strut pairs in each set of struts. Here we have the design sensitivity with respect to the decision variable, ZGRND(1) = axial coordinate of “ground” for the aft set of struts.

- 
- (FREQ(1,1)/FREQA(1,1))/FREQF(1,1)-1; F.S.= 1.20  
 ○ (FREQ(1,2)/FREQA(1,2))/FREQF(1,2)-1; F.S.= 1.20  
 △ (STRES2A(1,3)/STRES2(1,3))/STRES2F(1,3)-1; F.S.= 1.50  
 + (FORCEA(1,2)/FORCE(1,2))/FORCEF(1,2)-1; F.S.= 1.00  
 × (TNKSTRA(1,1)/TNKSTR(1,1))/TNKSTRF(1,1)-1; F.S.= 1.00  
 ◇ (FREQ(2,1)/FREQA(2,1))/FREQF(2,1)-1; F.S.= 1.20  
 ▽ (FREQ(2,2)/FREQA(2,2))/FREQF(2,2)-1; F.S.= 1.20  
 ▨ (STRES1A(2,3)/STRES1(2,3))/STRES1F(2,3)-1; F.S.= 1.50  
 ✕ (STRES2A(2,3)/STRES2(2,3))/STRES2F(2,3)-1; F.S.= 1.50  
 ♦ (COLBUK(2,2)/COLBUKA(2,2))/COLBUKF(2,2)-1; F.S.= 1.00  
 ⊕ (SHLBUK(2,1)/SHLBUKA(2,1))/SHLBUKF(2,1)-1; F.S.= 2.00  
 ✂ (SHLBUK(2,2)/SHLBUKA(2,2))/SHLBUKF(2,2)-1; F.S.= 2.00  
 ▨ (FORCEA(2,2)/FORCE(2,2))/FORCEF(2,2)-1; F.S.= 1.00  
 ✕ (TNKSTRA(2,1)/TNKSTR(2,1))/TNKSTRF(2,1)-1; F.S.= 1.00

**GENOPT test: design margins vs ZGRND(2)**

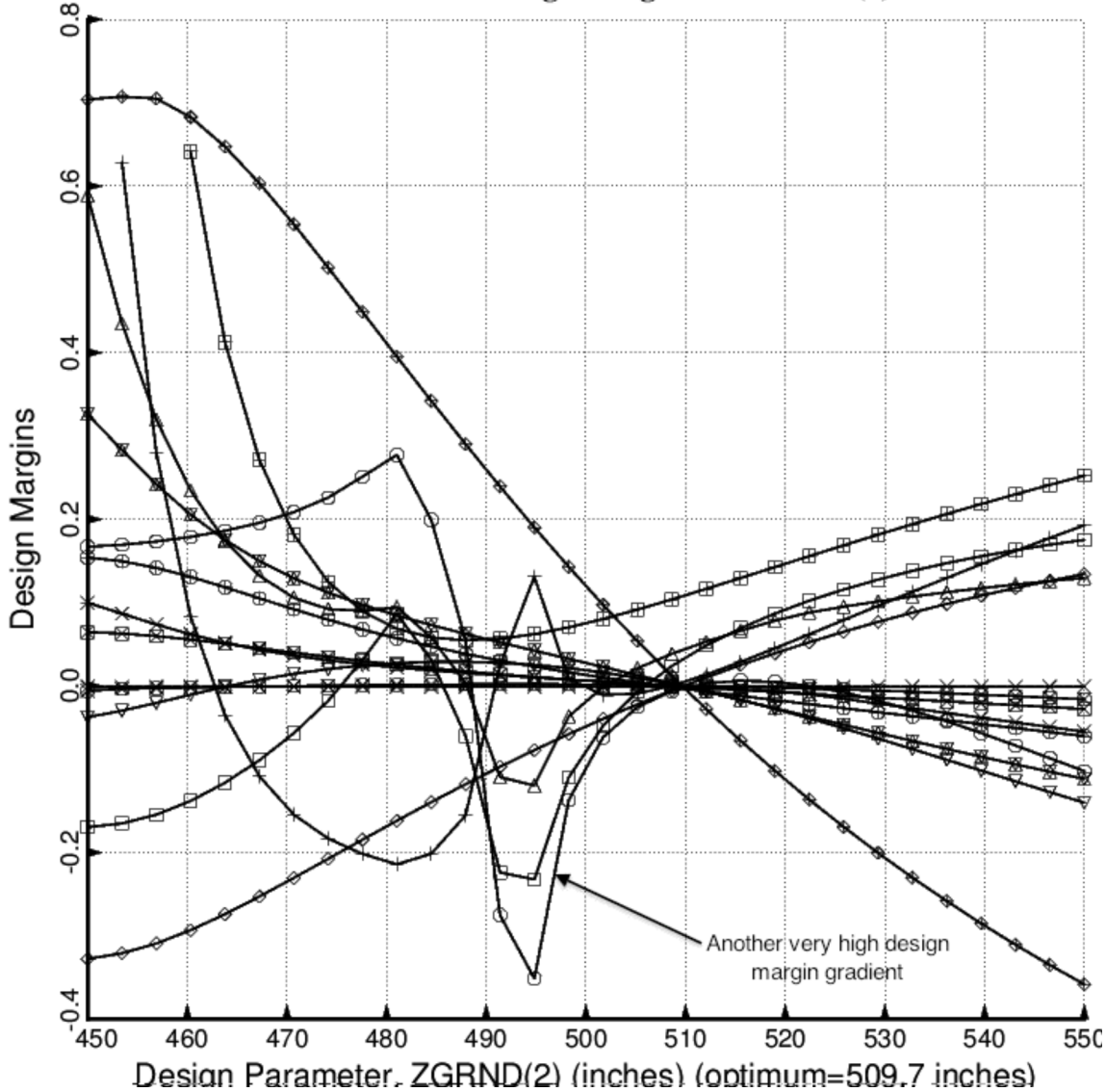


Fig. 39 (old) Design sensitivity of the optimized long propellant tank with aft and forward struts, 4 strut pairs in each set of struts. Here we have the design sensitivity with respect to the decision variable, ZGRND(2) = axial coordinate of “ground” for the forward set of struts.

- $\square$   $(\text{FREQ}(1,1)/\text{FREQA}(1,1)) / \text{FREQF}(1,1)-1$ ; F.S.= 1.20
- $\circ$   $(\text{FREQ}(1,2)/\text{FREQA}(1,2)) / \text{FREQF}(1,2)-1$ ; F.S.= 1.20
- $\triangle$   $(\text{STRES2A}(1,3) / \text{STRES2}(1,3)) / \text{STRES2F}(1,3)-1$ ; F.S.= 1.50
- $+$   $(\text{FORCEA}(1,2) / \text{FORCE}(1,2)) / \text{FORCEF}(1,2)-1$ ; F.S.= 1.00
- $\times$   $(\text{TNKSTR}(1,1) / \text{TNKSTR}(1,1)) / \text{TNKSTRF}(1,1)-1$ ; F.S.= 1.00
- $\diamond$   $(\text{FREQ}(2,1)/\text{FREQA}(2,1)) / \text{FREQF}(2,1)-1$ ; F.S.= 1.20
- $\triangledown$   $(\text{FREQ}(2,2)/\text{FREQA}(2,2)) / \text{FREQF}(2,2)-1$ ; F.S.= 1.20
- $\blacksquare$   $(\text{STRES1A}(2,3) / \text{STRES1}(2,3)) / \text{STRES1F}(2,3)-1$ ; F.S.= 1.50
- $\times$   $(\text{STRES2A}(2,3) / \text{STRES2}(2,3)) / \text{STRES2F}(2,3)-1$ ; F.S.= 1.50
- $\diamond$   $(\text{COLBUK}(2,2) / \text{COLBUKA}(2,2)) / \text{COLBUKF}(2,2)-1$ ; F.S.= 1.00
- $\blacksquare$   $(\text{SHLBUK}(2,1) / \text{SHLBUKA}(2,1)) / \text{SHLBUKF}(2,1)-1$ ; F.S.= 2.00
- $\times$   $(\text{SHLBUK}(2,2) / \text{SHLBUKA}(2,2)) / \text{SHLBUKF}(2,2)-1$ ; F.S.= 2.00
- $\blacksquare$   $(\text{FORCEA}(2,2) / \text{FORCE}(2,2)) / \text{FORCEF}(2,2)-1$ ; F.S.= 1.00
- $\blacksquare$   $(\text{TNKSTR}(2,1) / \text{TNKSTR}(2,1)) / \text{TNKSTRF}(2,1)-1$ ; F.S.= 1.00

**GENOPT test: design margins vs AGRND(1)**

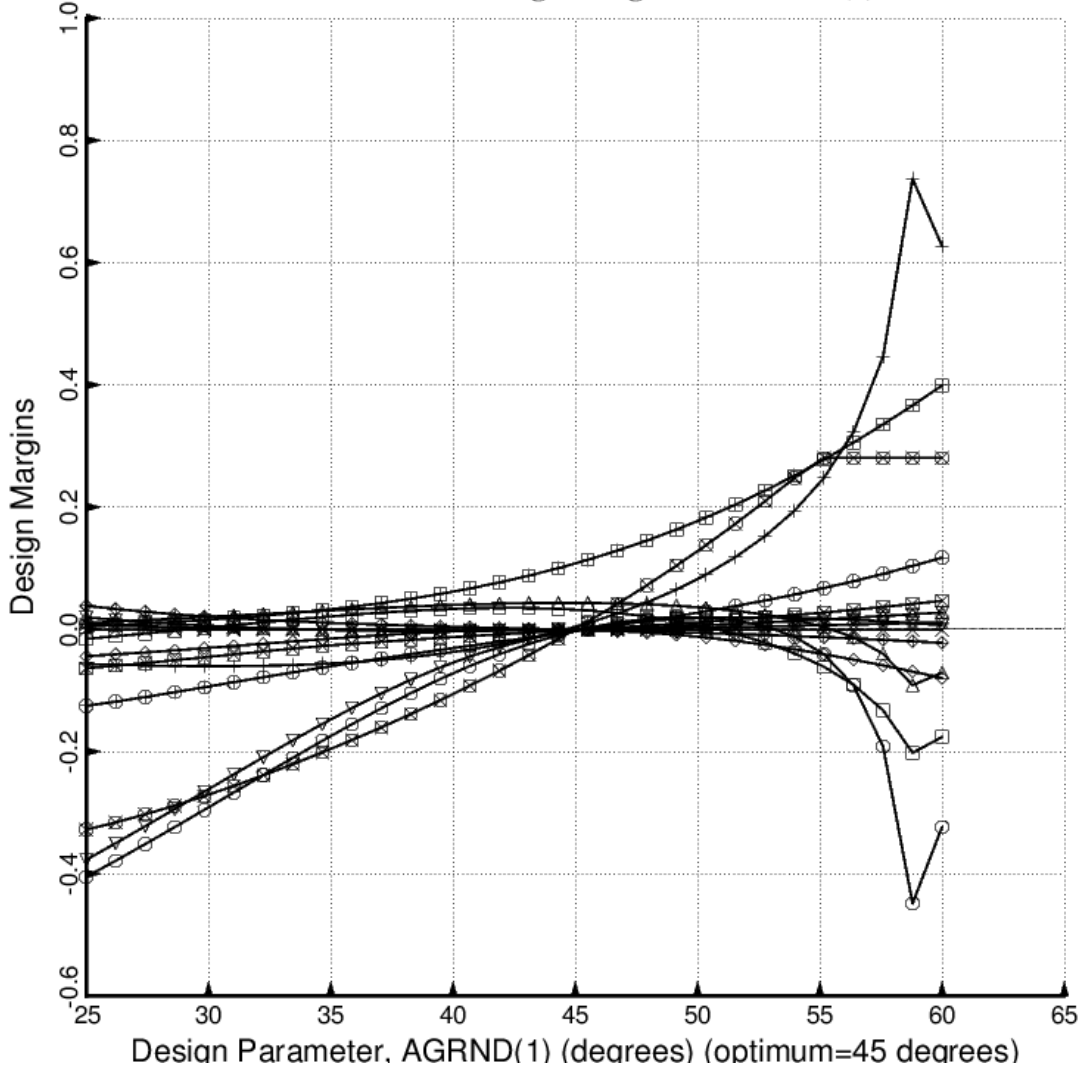


Fig. 40 (old) Design sensitivity of the optimized long propellant tank with aft and forward struts, 4 strut pairs in each set of struts. Here we have the design sensitivity with respect to the decision variable,  $\text{AGRND}(1)$  = azimuthal angle to the “ground” end of the forward-slanting struts in the aft set of struts. [The backward-slanting aft struts have  $-\text{AGRND}(1)$ ]

- 
- $(\text{FREQ}(1,1)/\text{FREQA}(1,1)) / \text{FREQF}(1,1)-1$ ; F.S.= 1.20  
 ○  $(\text{FREQ}(1,2)/\text{FREQA}(1,2)) / \text{FREQF}(1,2)-1$ ; F.S.= 1.20  
 △  $(\text{STRES2A}(1,3)/\text{STRES2}(1,3)) / \text{STRES2F}(1,3)-1$ ; F.S.= 1.50  
 +  $(\text{FORCEA}(1,2)/\text{FORCE}(1,2)) / \text{FORCEF}(1,2)-1$ ; F.S.= 1.00  
 ×  $(\text{TNKSTRA}(1,1)/\text{TNKSTR}(1,1)) / \text{TNKSTRF}(1,1)-1$ ; F.S.= 1.00  
 ◇  $(\text{FREQ}(2,1)/\text{FREQA}(2,1)) / \text{FREQF}(2,1)-1$ ; F.S.= 1.20  
 ▽  $(\text{FREQ}(2,2)/\text{FREQA}(2,2)) / \text{FREQF}(2,2)-1$ ; F.S.= 1.20  
 ▨  $(\text{STRES1A}(2,3)/\text{STRES1}(2,3)) / \text{STRES1F}(2,3)-1$ ; F.S.= 1.50  
 ✕  $(\text{STRES2A}(2,3)/\text{STRES2}(2,3)) / \text{STRES2F}(2,3)-1$ ; F.S.= 1.50  
 ♦  $(\text{COLBUK}(2,2)/\text{COLBUKA}(2,2)) / \text{COLBUKF}(2,2)-1$ ; F.S.= 1.00  
 ⊕  $(\text{SHLBUK}(2,1)/\text{SHLBUKA}(2,1)) / \text{SHLBUKF}(2,1)-1$ ; F.S.= 2.00  
 ■  $(\text{SHLBUK}(2,2)/\text{SHLBUKA}(2,2)) / \text{SHLBUKF}(2,2)-1$ ; F.S.= 2.00  
 ▨  $(\text{FORCEA}(2,2)/\text{FORCE}(2,2)) / \text{FORCEF}(2,2)-1$ ; F.S.= 1.00  
 ▨  $(\text{TNKSTRA}(2,1)/\text{TNKSTR}(2,1)) / \text{TNKSTRF}(2,1)-1$ ; F.S.= 1.00

**GENOPT test: design margins vs AGRND(2)**

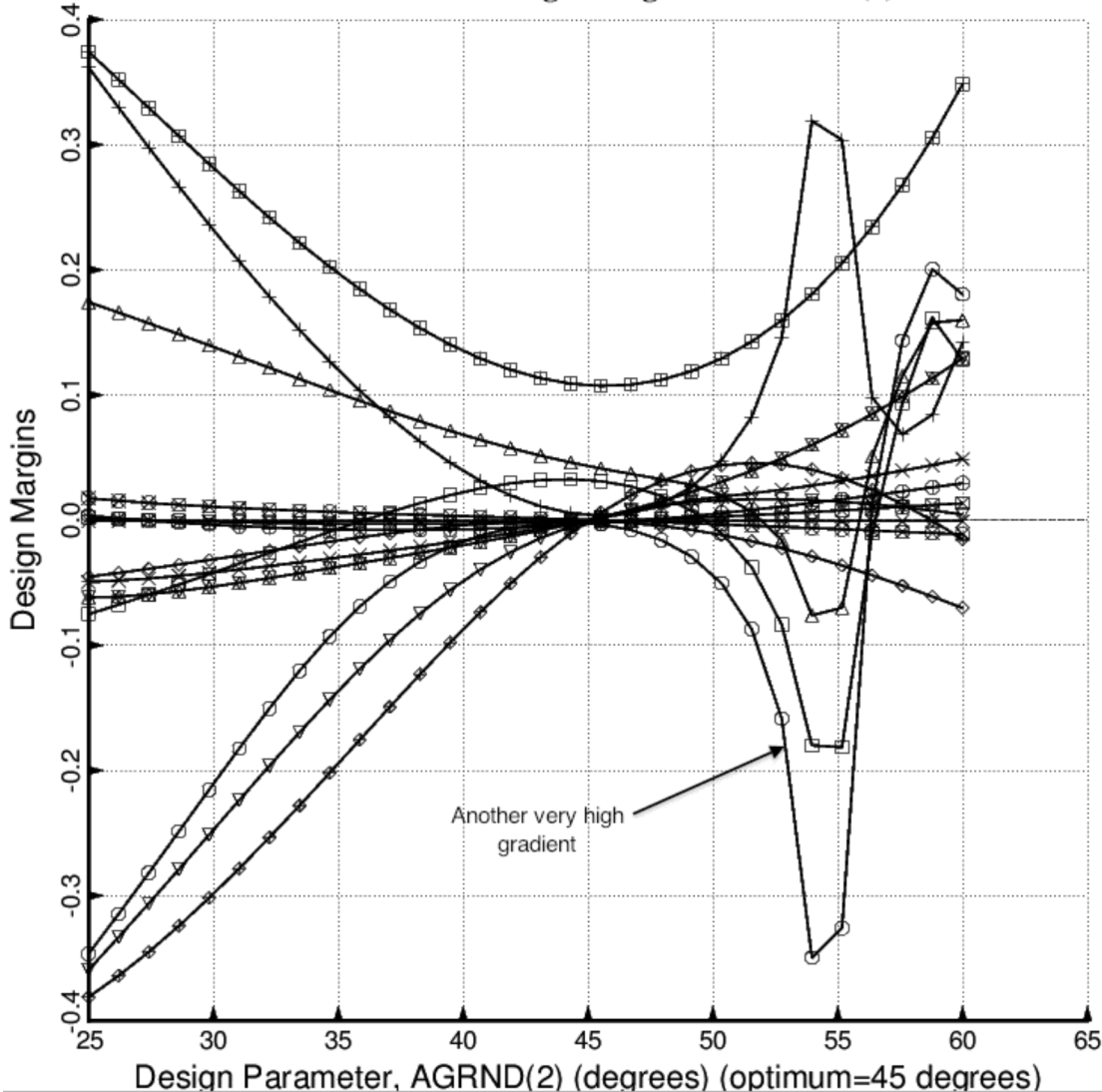


Fig. 41 (old) Design sensitivity of the optimized long propellant tank with aft and forward struts, 4 strut pairs in each set of struts. Here we have the design sensitivity with respect to the decision variable, AGRND(2) = azimuthal angle to the “ground” end of the forward-slanting struts in the forward set of struts. [The backward-slanting forward struts have  $-AGRND(2)$ ]

---

□ (FREQ(1,1)/FREQA(1,1)) / FREQF(1,1)-1; F.S.= 1.20  
 ○ (FREQ(1,2)/FREQA(1,2)) / FREQF(1,2)-1; F.S.= 1.20  
 △ (STRES2A(1,3)/STRES2(1,3)) / STRES2F(1,3)-1; F.S.= 1.50  
 + (FORCEA(1,2)/FORCE(1,2)) / FORCEF(1,2)-1; F.S.= 1.00  
 × (TNKSTR(1,1)/TNKSTR(1,1)) / TNKSTRF(1,1)-1; F.S.= 1.00  
 ◇ (FREQ(2,1)/FREQA(2,1)) / FREQF(2,1)-1; F.S.= 1.20  
 ▽ (FREQ(2,2)/FREQA(2,2)) / FREQF(2,2)-1; F.S.= 1.20  
 ▨ (STRES1A(2,3)/STRES1(2,3)) / STRES1F(2,3)-1; F.S.= 1.50  
 ✕ (STRES2A(2,3)/STRES2(2,3)) / STRES2F(2,3)-1; F.S.= 1.50  
 ♦ (COLBUK(2,2)/COLBUKA(2,2)) / COLBUKF(2,2)-1; F.S.= 1.00  
 ⊕ (SHLBUK(2,1)/SHLBUKA(2,1)) / SHLBUKF(2,1)-1; F.S.= 2.00  
 ■ (SHLBUK(2,2)/SHLBUKA(2,2)) / SHLBUKF(2,2)-1; F.S.= 2.00  
 ▨ (FORCEA(2,2)/FORCE(2,2)) / FORCEF(2,2)-1; F.S.= 1.00  
 ▨ (TNKSTR(2,1)/TNKSTR(2,1)) / TNKSTRF(2,1)-1; F.S.= 1.00

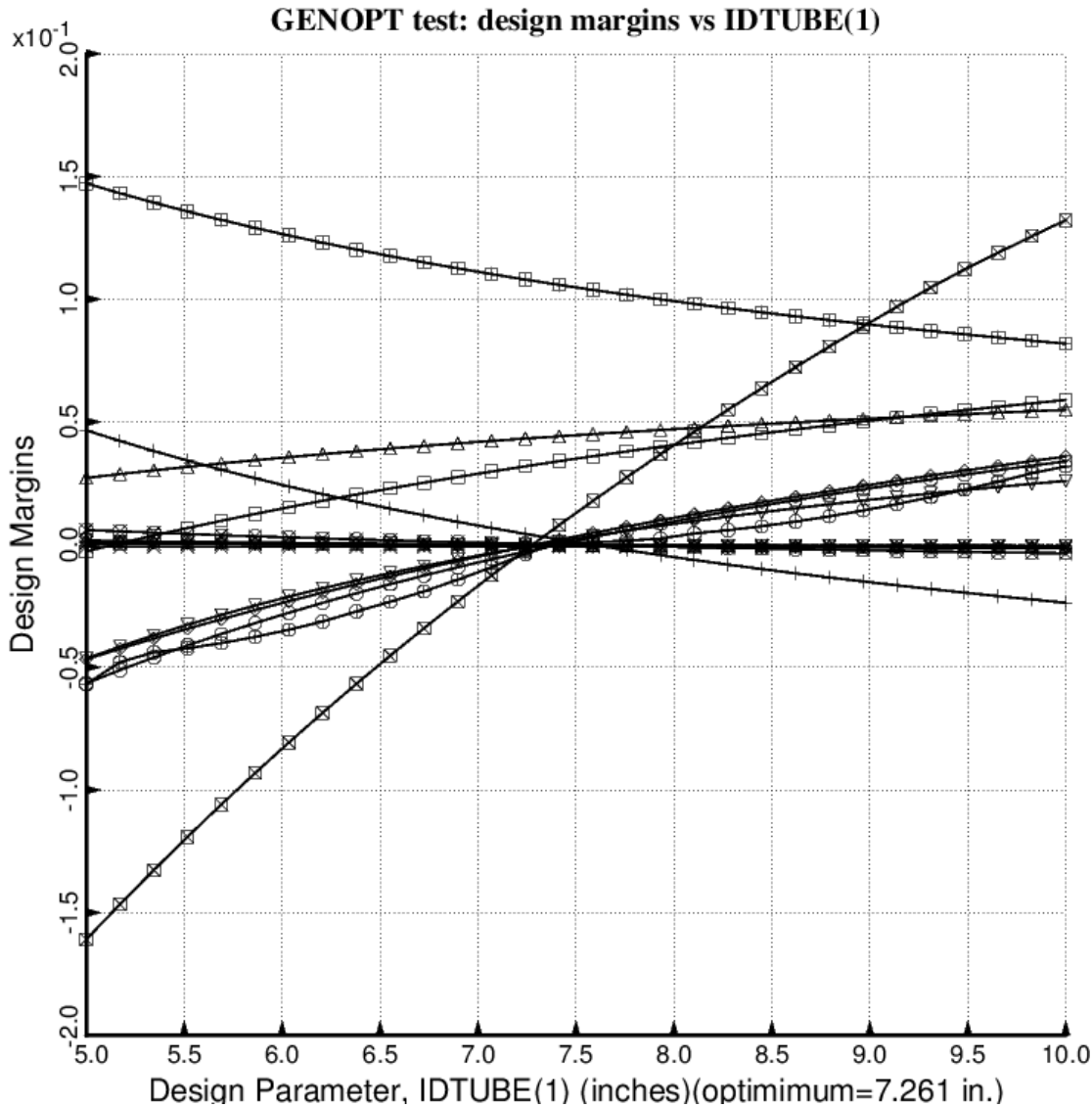


Fig. 42 (old) Design sensitivity of the optimized long propellant tank with aft and forward struts, 4 strut pairs in each set of struts. Here we have the design sensitivity with respect to the decision variable, IDTUBE(1) = inner diameter of each strut tube in the aft set of struts.

□ (FREQ(1,1)/FREQA(1,1)) / FREQH(1,1)-1; F.S.= 1.20  
 ○ (FREQ(1,2)/FREQA(1,2)) / FREQF(1,2)-1; F.S.= 1.20  
 △ (STRES2A(1,3)/STRES2(1,3)) / STRES2F(1,3)-1; F.S.= 1.50  
 + (FORCEA(1,2)/FORCE(1,2)) / FORCEF(1,2)-1; F.S.= 1.00  
 × (TNKSTRA(1,1)/TNKSTR(1,1)) / TNKSTRF(1,1)-1; F.S.= 1.00  
 ◇ (FREQ(2,1)/FREQA(2,1)) / FREQF(2,1)-1; F.S.= 1.20  
 ▽ (FREQ(2,2)/FREQA(2,2)) / FREQF(2,2)-1; F.S.= 1.20  
 ▨ (STRES1A(2,3)/STRES1(2,3)) / STRES1F(2,3)-1; F.S.= 1.50  
 ✕ (STRES2A(2,3)/STRES2(2,3)) / STRES2F(2,3)-1; F.S.= 1.50  
 ♦ (COLBUK(2,2)/COLBUKA(2,2)) / COLBUKF(2,2)-1; F.S.= 1.00  
 ⊕ (SHLBUK(2,1)/SHLBUKA(2,1)) / SHLBUKF(2,1)-1; F.S.= 2.00  
 ✖ (SHLBUK(2,2)/SHLBUKA(2,2)) / SHLBUKF(2,2)-1; F.S.= 2.00  
 ■ (FORCEA(2,2)/FORCE(2,2)) / FORCEF(2,2)-1; F.S.= 1.00  
 ✣ (TNKSTRA(2,1)/TNKSTR(2,1)) / TNKSTRF(2,1)-1; F.S.= 1.00

**GENOPT test: design margins vs IDTUBE(2)**

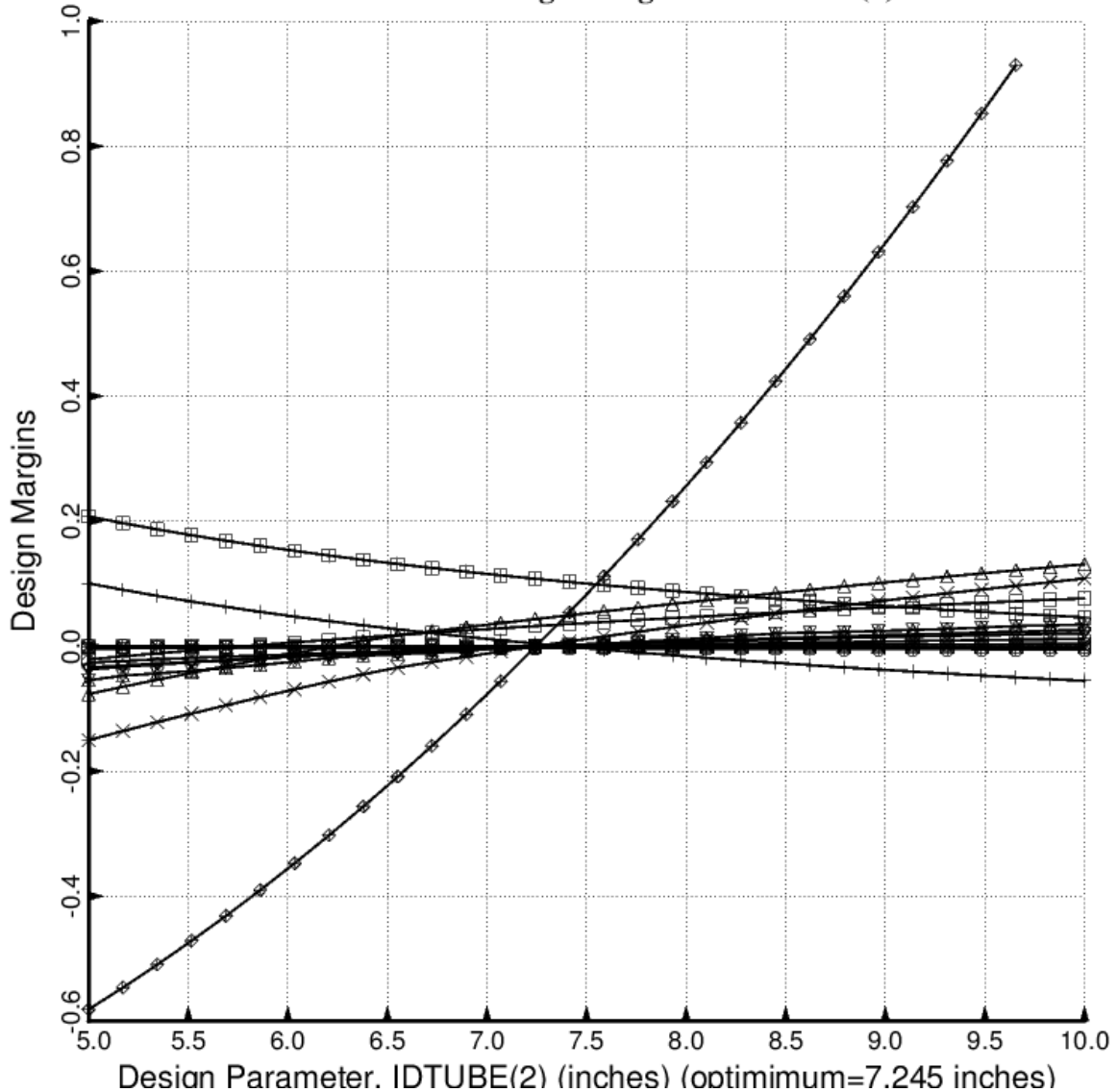


Fig. 43 (old) Design sensitivity of the optimized long propellant tank with aft and forward struts, 4 strut pairs in each set of struts. Here we have the design sensitivity with respect to the decision variable, IDTUBE(2) = inner diameter of each strut tube in the forward set of struts.

- $\square$  (FREQ(1,1)/FREQA(1,1)) / FREQF(1,1)-1; F.S.= 1.20
- $\circ$  (FREQ(1,2)/FREQA(1,2)) / FREQF(1,2)-1; F.S.= 1.20
- $\triangle$  (STRES2A(1,3)/STRES2(1,3)) / STRES2F(1,3)-1; F.S.= 1.50
- $+$  (FORCEA(1,2)/FORCE(1,2)) / FORCEF(1,2)-1; F.S.= 1.00
- $\times$  (TNKSTRA(1,1)/TNKSTR(1,1)) / TNKSTRF(1,1)-1; F.S.= 1.00
- $\diamond$  (FREQ(2,1)/FREQA(2,1)) / FREQF(2,1)-1; F.S.= 1.20
- $\triangledown$  (FREQ(2,2)/FREQA(2,2)) / FREQF(2,2)-1; F.S.= 1.20
- $\blacksquare$  (STRES1A(2,3)/STRES1(2,3)) / STRES1F(2,3)-1; F.S.= 1.50
- $\times$  (STRES2A(2,3)/STRES2(2,3)) / STRES2F(2,3)-1; F.S.= 1.50
- $\diamond$  (COLBUK(2,2)/COLBUKA(2,2)) / COLBUKF(2,2)-1; F.S.= 1.00
- $\blacksquare$  (SHLBUK(2,1)/SHLBUKA(2,1)) / SHLBUKF(2,1)-1; F.S.= 2.00
- $\blacksquare$  (SHLBUK(2,2)/SHLBUKA(2,2)) / SHLBUKF(2,2)-1; F.S.= 2.00
- $\blacksquare$  (FORCEA(2,2)/FORCE(2,2)) / FORCEF(2,2)-1; F.S.= 1.00
- $\blacksquare$  (TNKSTRA(2,1)/TNKSTR(2,1)) / TNKSTRF(2,1)-1; F.S.= 1.00

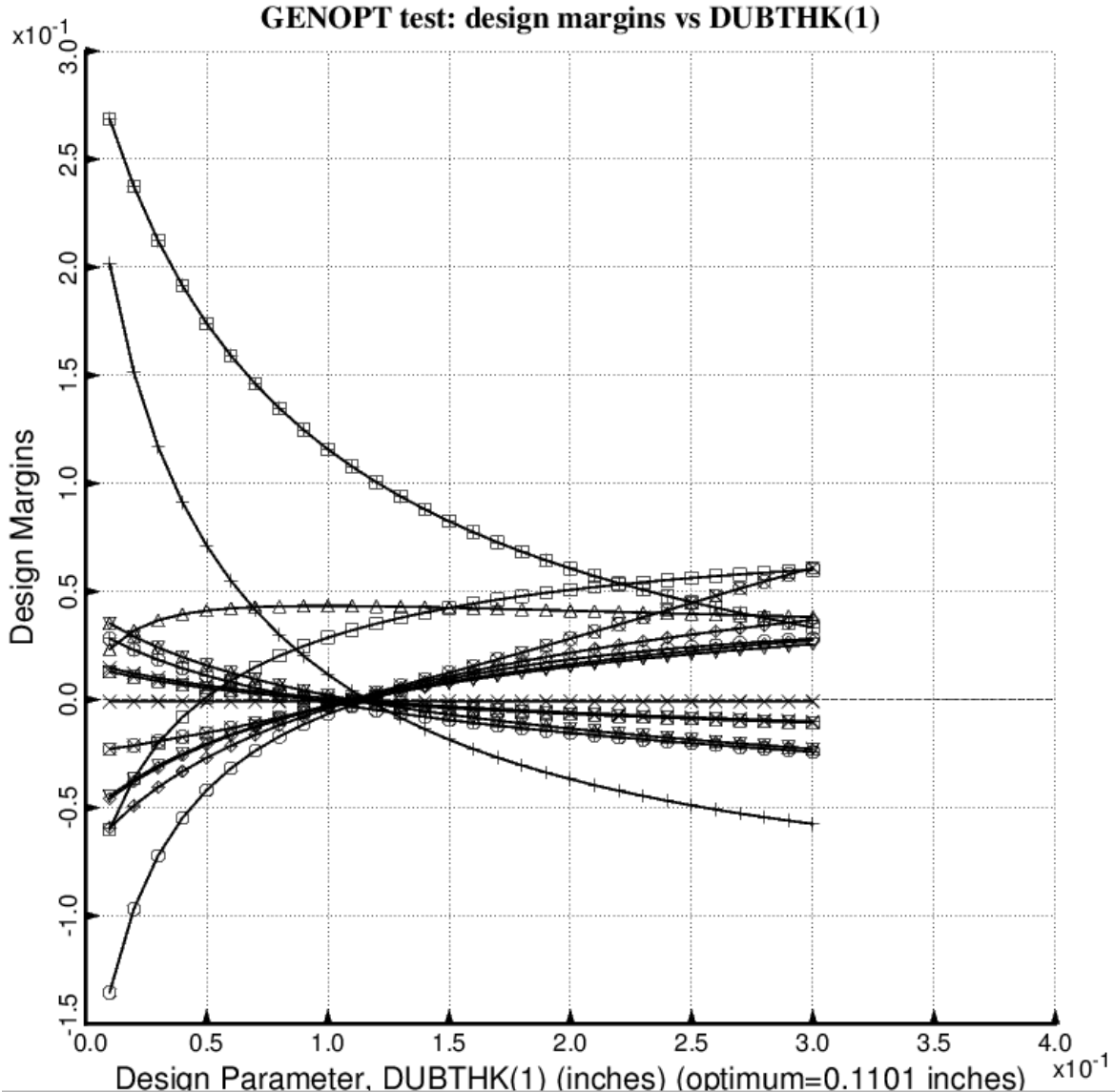


Fig. 44 (old) Design sensitivity of the optimized long propellant tank with aft and forward struts, 4 strut pairs in each set of struts. Here we have the design sensitivity with respect to the decision variable, DUBTHK(1) = maximum thickness of the external tapered doubler, which is part of the tank reinforcement type 1.

- $\square$  (FREQ(1,1)/FREQA(1,1)) / FREQF(1,1)-1; F.S.= 1.20
- $\circ$  (FREQ(1,2)/FREQA(1,2)) / FREQF(1,2)-1; F.S.= 1.20
- $\triangle$  (STRES2A(1,3)/STRES2(1,3)) / STRES2F(1,3)-1; F.S.= 1.50
- $+$  (FORCEA(1,2)/FORCE(1,2)) / FORCEF(1,2)-1; F.S.= 1.00
- $\times$  (TNKSTR(1,1)/TNKSTR(1,1)) / TNKSTRF(1,1)-1; F.S.= 1.00
- $\diamond$  (FREQ(2,1)/FREQA(2,1)) / FREQF(2,1)-1; F.S.= 1.20
- $\triangledown$  (FREQ(2,2)/FREQA(2,2)) / FREQF(2,2)-1; F.S.= 1.20
- $\blacksquare$  (STRES1A(2,3)/STRES1(2,3)) / STRES1F(2,3)-1; F.S.= 1.50
- $\times$  (STRES2A(2,3)/STRES2(2,3)) / STRES2F(2,3)-1; F.S.= 1.50
- $\diamond$  (COLBUK(2,2)/COLBUKA(2,2)) / COLBUKF(2,2)-1; F.S.= 1.00
- $\oplus$  (SHLBUK(2,1)/SHLBUKA(2,1)) / SHLBUKF(2,1)-1; F.S.= 2.00
- $\blacksquare$  (SHLBUK(2,2)/SHLBUKA(2,2)) / SHLBUKF(2,2)-1; F.S.= 2.00
- $\blacksquare$  (FORCEA(2,2)/FORCE(2,2)) / FORCEF(2,2)-1; F.S.= 1.00
- $\blacksquare$  (TNKSTR(2,1)/TNKSTR(2,1)) / TNKSTRF(2,1)-1; F.S.= 1.00

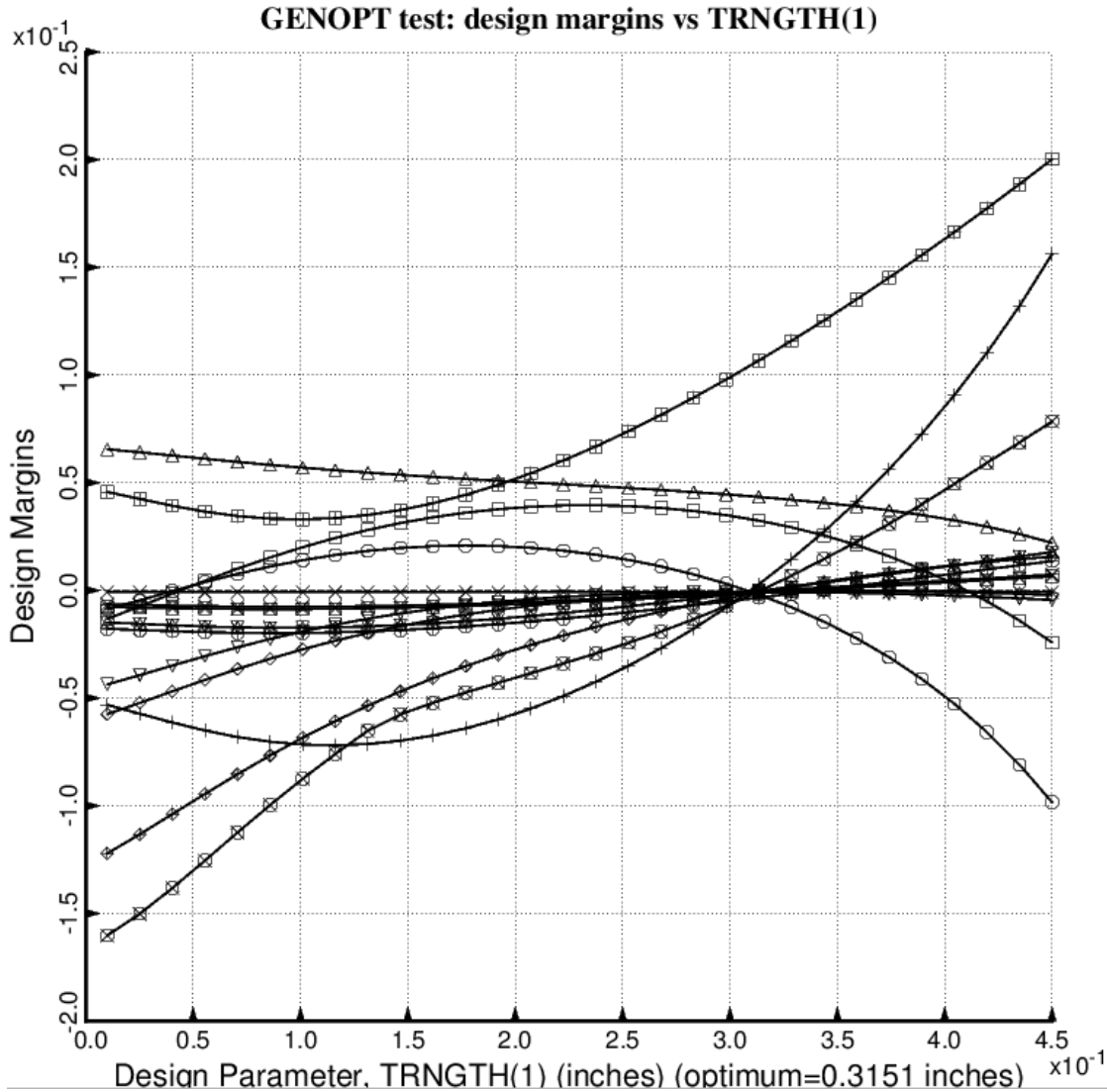


Fig. 45 (old) Design sensitivity of the optimized long propellant tank with aft and forward struts, 4 strut pairs in each set of struts. Here we have the design sensitivity with respect to the decision variable, TRNGTH(1) = thickness of the external propellant tank ring, which is part of the tank reinforcement type 1. The cross section of the ring is rectangular with ring height equal to five times the ring thickness, a linking established by the End user during the interactive session with the GENOPT processor, DECIDE. (See Table 5).

- 
- (FREQ(1,1)/FREQA(1,1)) / FREQF(1,1)-1; F.S.= 1.20
  - (FREQ(1,2)/FREQA(1,2)) / FREQF(1,2)-1; F.S.= 1.20
  - △ (STRES2A(1,3)/STRES2(1,3)) / STRES2F(1,3)-1; F.S.= 1.50
  - + (FORCEA(1,2)/FORCE(1,2)) / FORCEF(1,2)-1; F.S.= 1.00
  - × (TNKSTR(1,1)/TNKSTR(1,1)) / TNKSTRF(1,1)-1; F.S.= 1.00
  - ◊ (FREQ(2,1)/FREQA(2,1)) / FREQF(2,1)-1; F.S.= 1.20
  - ▽ (FREQ(2,2)/FREQA(2,2)) / FREQF(2,2)-1; F.S.= 1.20
  - ⊗ (STRES1A(2,3)/STRES1(2,3)) / STRES1F(2,3)-1; F.S.= 1.50
  - ※ (STRES2A(2,3)/STRES2(2,3)) / STRES2F(2,3)-1; F.S.= 1.50
  - ♦ (COLBUK(2,2)/COLBUKA(2,2)) / COLBUKF(2,2)-1; F.S.= 1.00
  - ⊕ (SHLBUK(2,1)/SHLBUKA(2,1)) / SHLBUKF(2,1)-1; F.S.= 2.00
  - ⊗ (SHLBUK(2,2)/SHLBUKA(2,2)) / SHLBUKF(2,2)-1; F.S.= 2.00
  - ⊗ (FORCEA(2,2)/FORCE(2,2)) / FORCEF(2,2)-1; F.S.= 1.00
  - ⊗ (TNKSTR(2,1)/TNKSTR(2,1)) / TNKSTRF(2,1)-1; F.S.= 1.00

**GENOPT test: design margins vs THICK(1)**

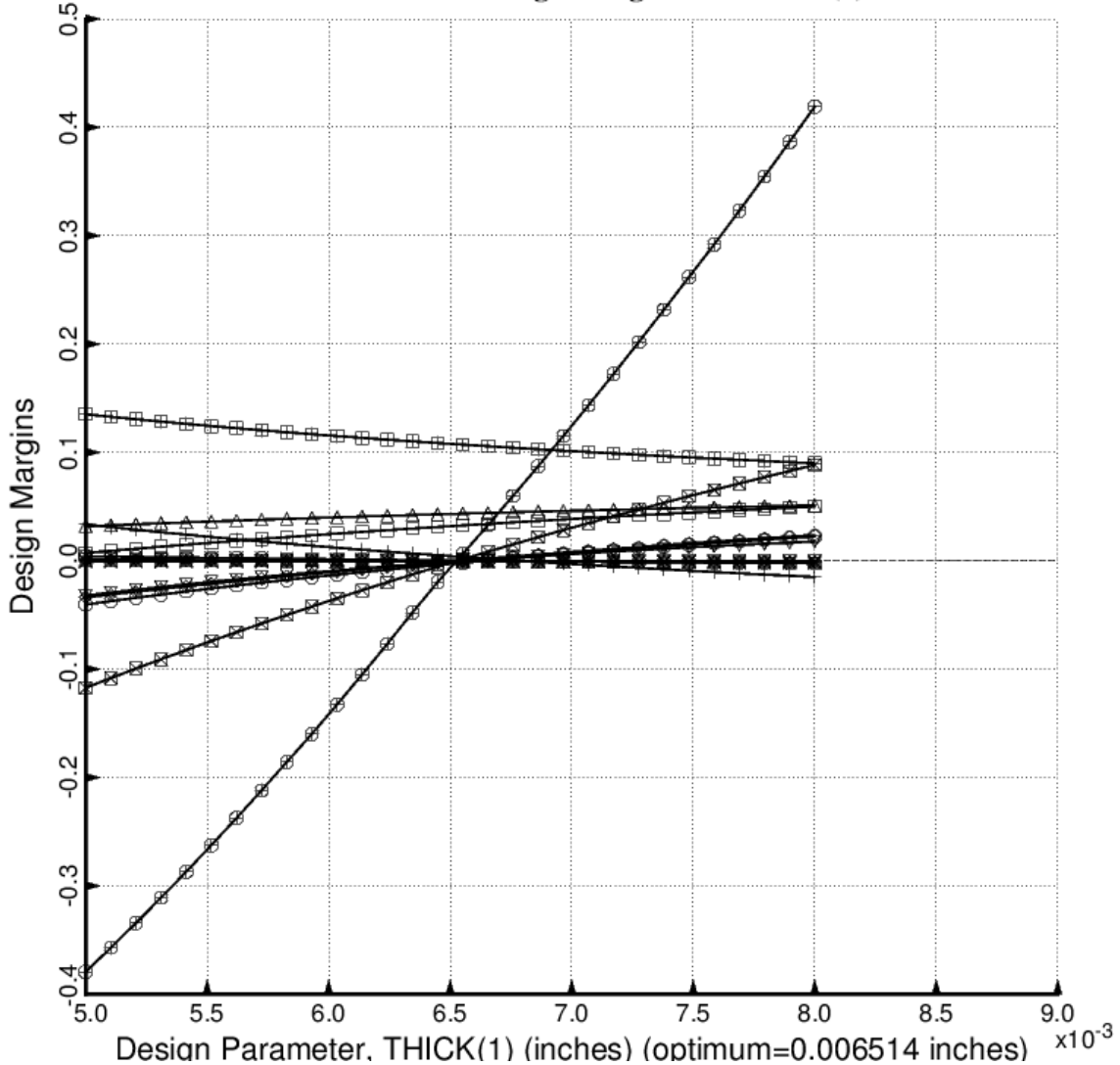


Fig. 46 (old) Design sensitivity of the optimized long propellant tank with aft and forward struts, 4 strut pairs in each set of struts. Here we have the design sensitivity with respect to the decision variable, THICK(1)= thickness of inner and outer layer of each aft laminated composite strut tube. All other layers in the aft strut tube are linked to THICK(1).

□ (FREQ(1,1)/FREQA(1,1)) / FREQF(1,1)-1; F.S.= 1.20  
 ○ (FREQ(1,2)/FREQA(1,2)) / FREQF(1,2)-1; F.S.= 1.20  
 △ (STRES2A(1,3)/STRES2(1,3)) / STRES2F(1,3)-1; F.S.= 1.50  
 + (FORCEA(1,2)/FORCE(1,2)) / FORCEF(1,2)-1; F.S.= 1.00  
 × (TNKSTR(1,1)/TNKSTR(1,1)) / TNKSTRF(1,1)-1; F.S.= 1.00  
 ◇ (FREQ(2,1)/FREQA(2,1)) / FREQF(2,1)-1; F.S.= 1.20  
 ▽ (FREQ(2,2)/FREQA(2,2)) / FREQF(2,2)-1; F.S.= 1.20  
 ▨ (STRES1A(2,3)/STRES1(2,3)) / STRES1F(2,3)-1; F.S.= 1.50  
 ✕ (STRES2A(2,3)/STRES2(2,3)) / STRES2F(2,3)-1; F.S.= 1.50  
 ♦ (COLBUK(2,2)/COLBUKA(2,2)) / COLBUKF(2,2)-1; F.S.= 1.00  
 ☐ (SHLBUK(2,1)/SHLBUKA(2,1)) / SHLBUKF(2,1)-1; F.S.= 2.00  
 ✕ (SHLBUK(2,2)/SHLBUKA(2,2)) / SHLBUKF(2,2)-1; F.S.= 2.00  
 ▨ (FORCEA(2,2)/FORCE(2,2)) / FORCEF(2,2)-1; F.S.= 1.00  
 ✕ (TNKSTR(2,1)/TNKSTR(2,1)) / TNKSTRF(2,1)-1; F.S.= 1.00

**GENOPT test: design margins vs THICK(7)**

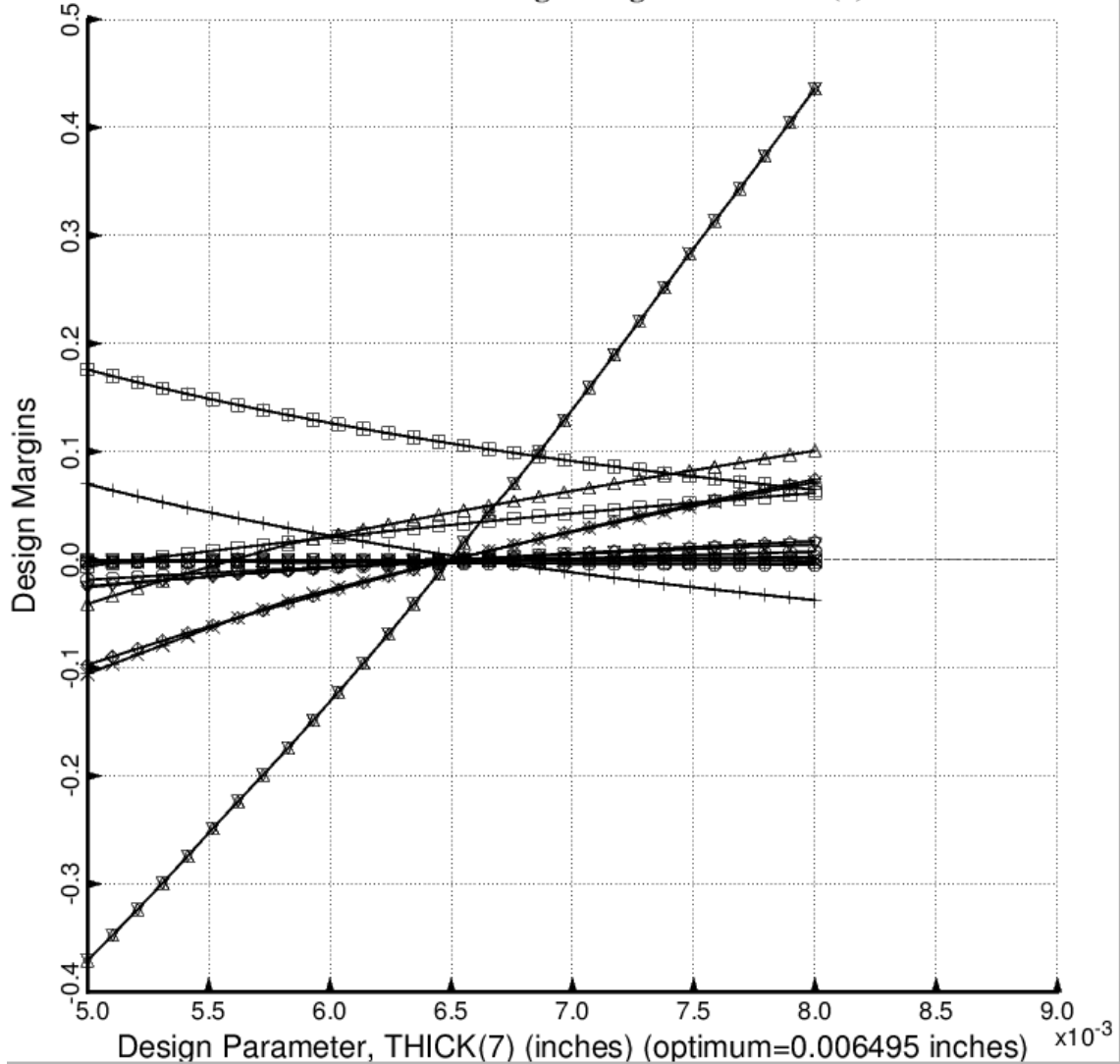


Fig. 47 (old) Design sensitivity of the optimized long propellant tank with aft and forward struts, 4 strut pairs in each set of struts. Here we have the design sensitivity with respect to the decision variable, THICK(7)= thickness of inner and outer layer of each forward laminated composite strut tube. All other layers in the forward strut tube are linked to THICK(7).

- 
- (FREQ(1,1)/FREQA(1,1)) / FREQF(1,1)-1; F.S.= 1.20  
 ○ (FREQ(1,2)/FREQA(1,2)) / FREQF(1,2)-1; F.S.= 1.20  
 △ (STRES2A(1,3)/STRES2(1,3)) / STRES2F(1,3)-1; F.S.= 1.50  
 + (FORCEA(1,2)/FORCE(1,2)) / FORCEF(1,2)-1; F.S.= 1.00  
 × (TNKSTRA(1,1)/TNKSTR(1,1)) / TNKSTRF(1,1)-1; F.S.= 1.00  
 ◇ (FREQ(2,1)/FREQA(2,1)) / FREQF(2,1)-1; F.S.= 1.20  
 ▽ (FREQ(2,2)/FREQA(2,2)) / FREQF(2,2)-1; F.S.= 1.20  
 ▨ (STRES1A(2,3)/STRES1(2,3)) / STRES1F(2,3)-1; F.S.= 1.50  
 ✕ (STRES2A(2,3)/STRES2(2,3)) / STRES2F(2,3)-1; F.S.= 1.50  
 ♦ (COLBUK(2,2)/COLBUKA(2,2)) / COLBUKF(2,2)-1; F.S.= 1.00  
 ⊕ (SHLBUK(2,1)/SHLBUKA(2,1)) / SHLBUKF(2,1)-1; F.S.= 2.00  
 ✖ (SHLBUK(2,2)/SHLBUKA(2,2)) / SHLBUKF(2,2)-1; F.S.= 2.00  
 ▨ (FORCEA(2,2)/FORCE(2,2)) / FORCEF(2,2)-1; F.S.= 1.00  
 ✕ (TNKSTRA(2,1)/TNKSTR(2,1)) / TNKSTRF(2,1)-1; F.S.= 1.00

**GENOPT test: design margins vs ANGLE(1)**

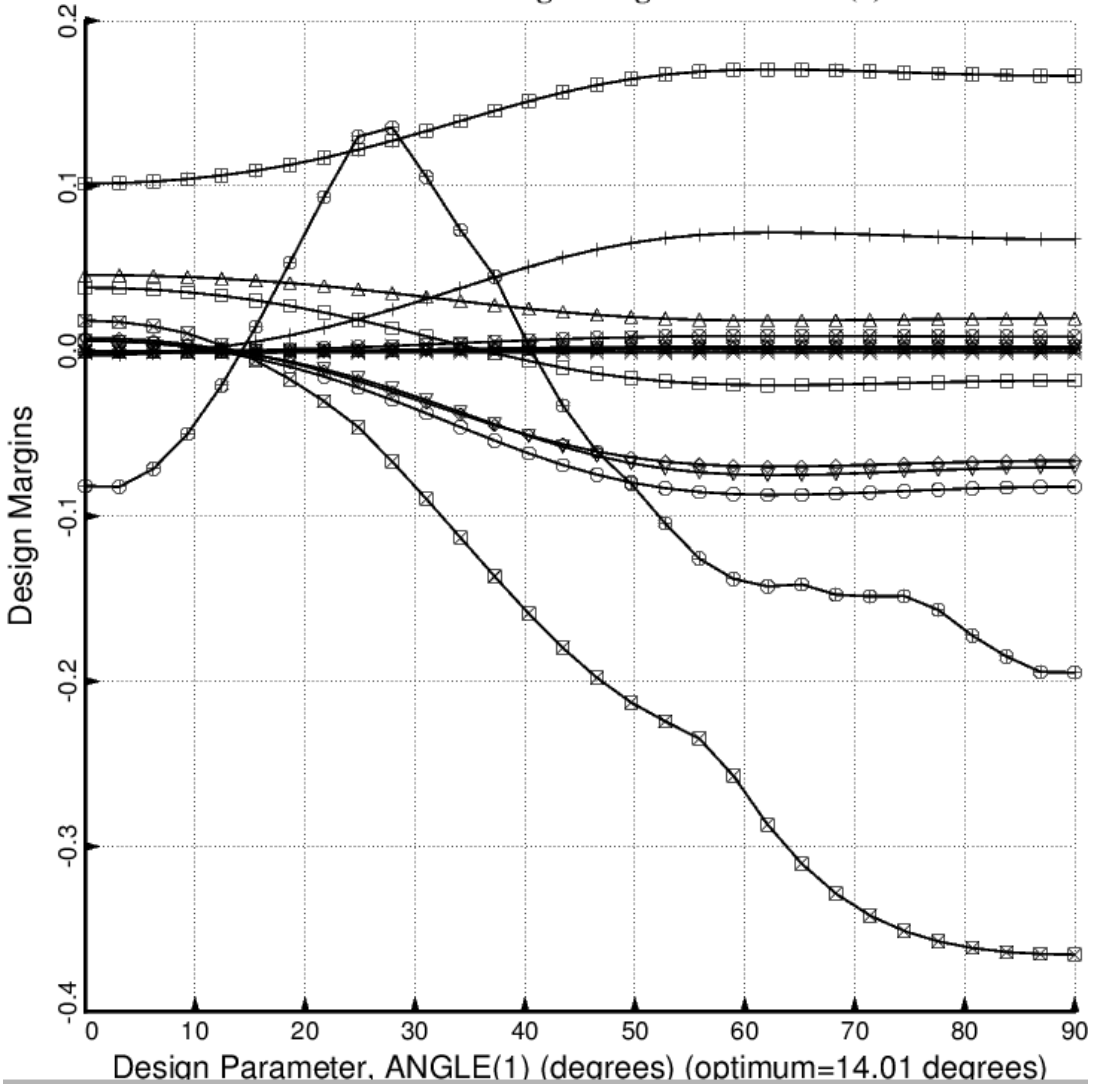


Fig. 48 (old) Design sensitivity of the optimized long propellant tank with aft and forward struts, 4 strut pairs in each set of struts. Here we have the design sensitivity with respect to the decision variable, ANGLE(1) = layup angle of the inner and outer layer of each aft laminated composite strut tube. ANGLE(2) is linked to ANGLE(1) with a linking coefficient equal to -1.0.

- $\square$  (FREQ(1,1)/FREQA(1,1)) / FREQF(1,1)-1; F.S.= 1.20
- $\circ$  (FREQ(1,2)/FREQA(1,2)) / FREQF(1,2)-1; F.S.= 1.20
- $\triangle$  (STRES2A(1,3)/STRES2(1,3)) / STRES2F(1,3)-1; F.S.= 1.50
- $+$  (FORCEA(1,2)/FORCE(1,2)) / FORCEF(1,2)-1; F.S.= 1.00
- $\times$  (TNKSTRA(1,1)/TNKSTR(1,1)) / TNKSTRF(1,1)-1; F.S.= 1.00
- $\diamond$  (FREQ(2,1)/FREQA(2,1)) / FREQF(2,1)-1; F.S.= 1.20
- $\triangledown$  (FREQ(2,2)/FREQA(2,2)) / FREQF(2,2)-1; F.S.= 1.20
- $\blacksquare$  (STRES1A(2,3)/STRES1(2,3)) / STRES1F(2,3)-1; F.S.= 1.50
- $\times$  (STRES2A(2,3)/STRES2(2,3)) / STRES2F(2,3)-1; F.S.= 1.50
- $\diamond$  (COLBUK(2,2)/COLBUKA(2,2)) / COLBUKF(2,2)-1; F.S.= 1.00
- $\blacksquare$  (SHLBUK(2,1)/SHLBUKA(2,1)) / SHLBUKF(2,1)-1; F.S.= 2.00
- $\blacksquare$  (SHLBUK(2,2)/SHLBUKA(2,2)) / SHLBUKF(2,2)-1; F.S.= 2.00
- $\blacksquare$  (FORCEA(2,2)/FORCE(2,2)) / FORCEF(2,2)-1; F.S.= 1.00
- $\blacksquare$  (TNKSTRA(2,1)/TNKSTR(2,1)) / TNKSTRF(2,1)-1; F.S.= 1.00

GENOPT test: design margins vs ANGLE(3)

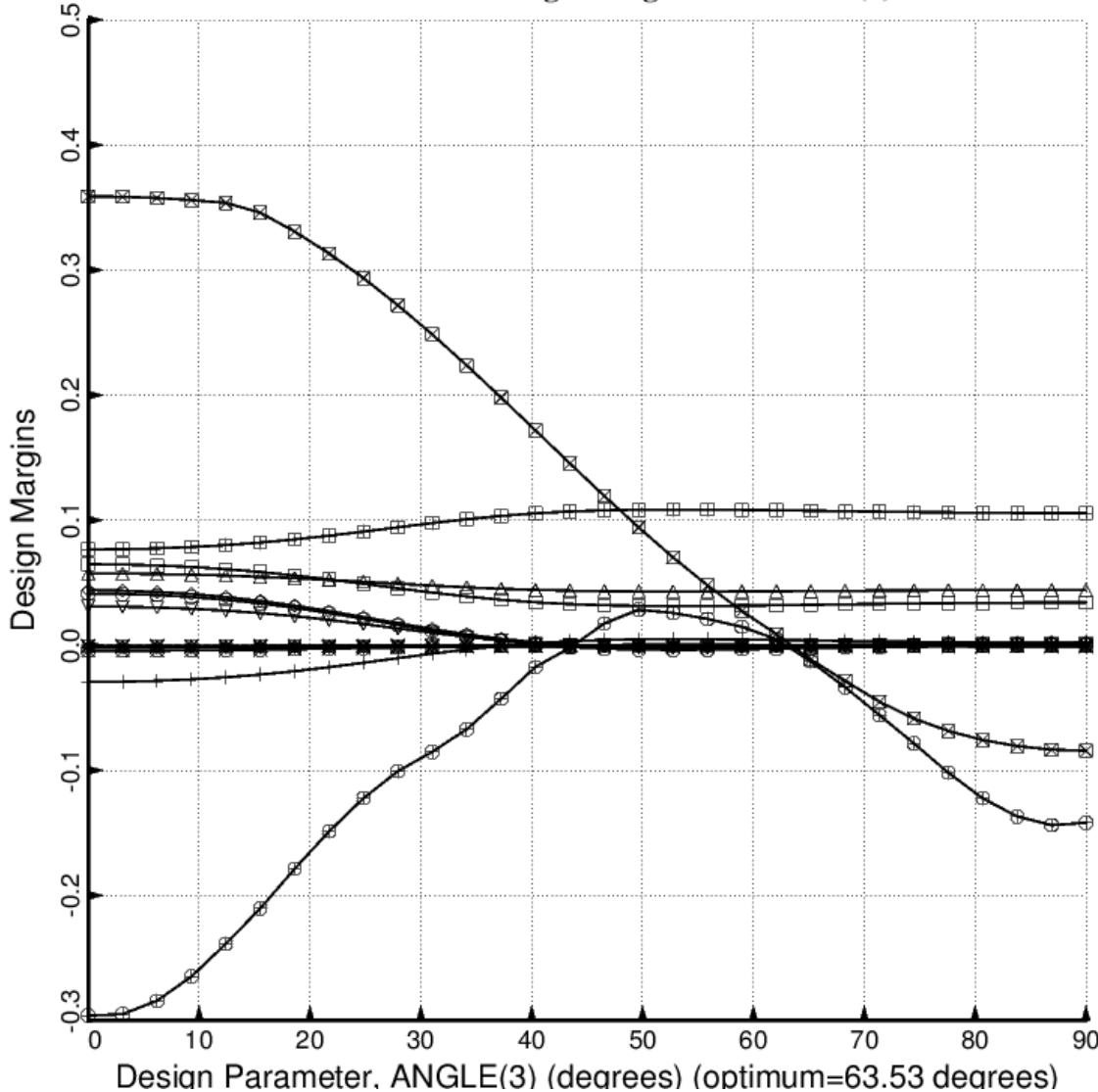


Fig. 49 (old) Design sensitivity of the optimized long propellant tank with aft and forward struts, 4 strut pairs in each set of struts. Here we have the design sensitivity with respect to the decision variable, ANGLE(3) = layup angle of the third and tenth layer of each aft laminated composite strut tube. ANGLE(4) is linked to ANGLE(3) with a linking coefficient equal to -1.0.

- 
- (FREQ(1,1)/FREQA(1,1)) / FREQF(1,1)-1; F.S.= 1.20
  - (FREQ(1,2)/FREQA(1,2)) / FREQF(1,2)-1; F.S.= 1.20
  - (STRES2A(1,3)/STRES2(1,3)) / STRES2F(1,3)-1; F.S.= 1.50
  - (FORCEA(1,2)/FORCE(1,2)) / FORCEF(1,2)-1; F.S.= 1.00
  - (TNKSTR(1,1)/TNKSTR(1,1)) / TNKSTRF(1,1)-1; F.S.= 1.00
  - (FREQ(2,1)/FREQA(2,1)) / FREQF(2,1)-1; F.S.= 1.20
  - (FREQ(2,2)/FREQA(2,2)) / FREQF(2,2)-1; F.S.= 1.20
  - (STRES1A(2,3)/STRES1(2,3)) / STRES1F(2,3)-1; F.S.= 1.50
  - (STRES2A(2,3)/STRES2(2,3)) / STRES2F(2,3)-1; F.S.= 1.50
  - (COLBUK(2,2)/COLBUKA(2,2)) / COLBUKF(2,2)-1; F.S.= 1.00
  - (SHLBUK(2,1)/SHLBUKA(2,1)) / SHLBUKF(2,1)-1; F.S.= 2.00
  - (SHLBUK(2,2)/SHLBUKA(2,2)) / SHLBUKF(2,2)-1; F.S.= 2.00
  - (FORCEA(2,2)/FORCE(2,2)) / FORCEF(2,2)-1; F.S.= 1.00
  - (TNKSTR(2,1)/TNKSTR(2,1)) / TNKSTRF(2,1)-1; F.S.= 1.00

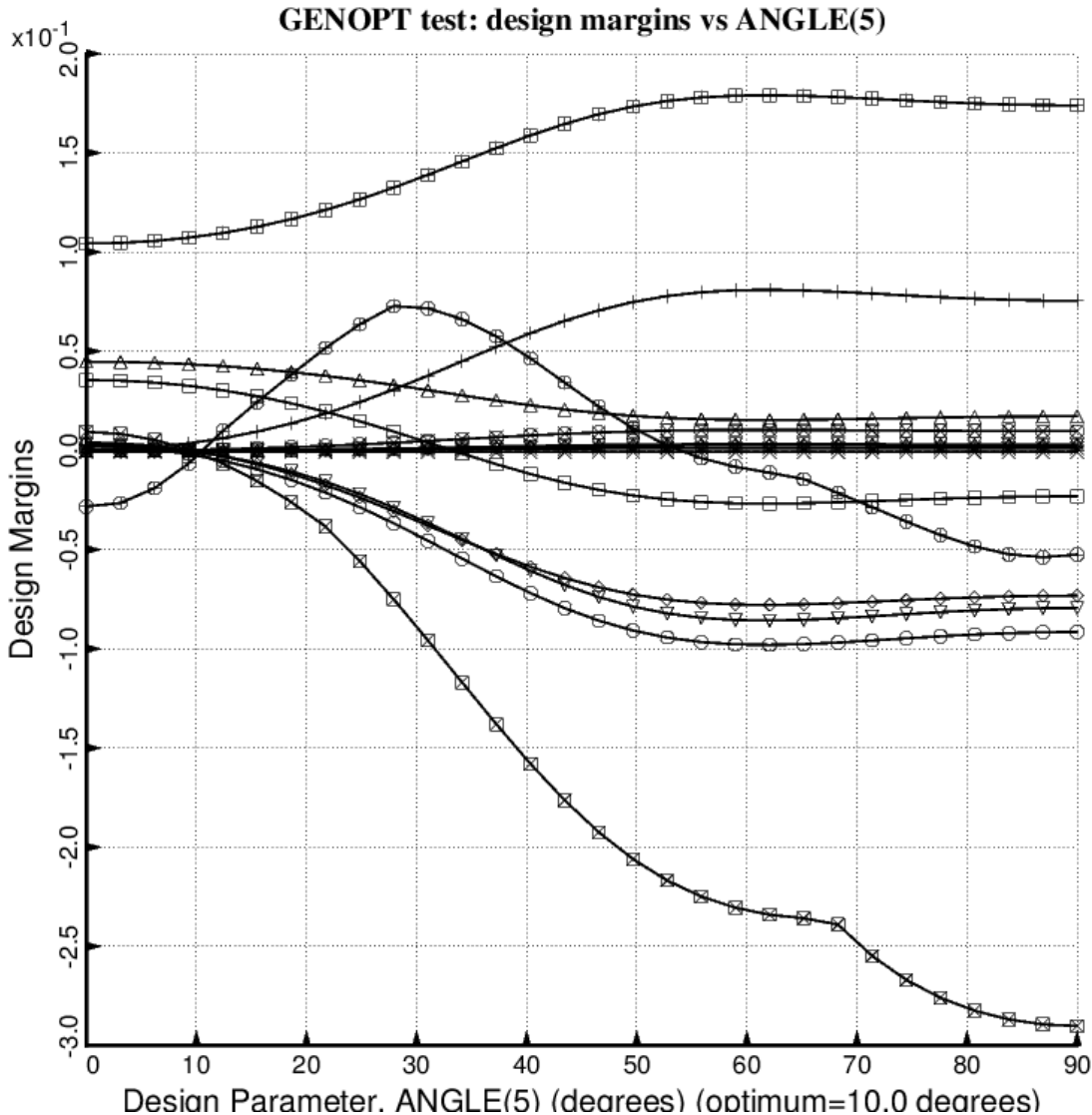


Fig. 50 (old) Design sensitivity of the optimized long propellant tank with aft and forward struts, 4 strut pairs in each set of struts. Here we have the design sensitivity with respect to the decision variable, ANGLE(5) = layup angle of the fifth and eighth layer of each aft laminated composite strut tube. ANGLE(6) is linked to ANGLE(5) with a linking coefficient equal to -1.0.

○ □ (FREQ(1,1)/FREQA(1,1)) / FREQF(1,1)-1; F.S.= 1.20  
 ○ △ (FREQ(1,2)/FREQA(1,2)) / FREQF(1,2)-1; F.S.= 1.20  
 △ (STRES2A(1,3)/STRES2(1,3)) / STRES2F(1,3)-1; F.S.= 1.50  
 + (FORCEA(1,2)/FORCE(1,2)) / FORCEF(1,2)-1; F.S.= 1.00  
 × (TNKSTRA(1,1)/TNKSTR(1,1)) / TNKSTRF(1,1)-1; F.S.= 1.00  
 ◊ (FREQ(2,1)/FREQA(2,1)) / FREQF(2,1)-1; F.S.= 1.20  
 ▽ (FREQ(2,2)/FREQA(2,2)) / FREQF(2,2)-1; F.S.= 1.20  
 × (STRES1A(2,3)/STRES1(2,3)) / STRES1F(2,3)-1; F.S.= 1.50  
 (STRES2A(2,3)/STRES2(2,3)) / STRES2F(2,3)-1; F.S.= 1.50  
 ◆ (COLBUK(2,2)/COLBUKA(2,2)) / COLBUKF(2,2)-1; F.S.= 1.00  
 (SHLBUK(2,1)/SHLBUKA(2,1)) / SHLBUKF(2,1)-1; F.S.= 2.00  
 ◇ (SHLBUK(2,2)/SHLBUKA(2,2)) / SHLBUKF(2,2)-1; F.S.= 2.00  
 ▨ (FORCEA(2,2)/FORCE(2,2)) / FORCEF(2,2)-1; F.S.= 1.00  
 ▨ (TNKSTRA(2,1)/TNKSTR(2,1)) / TNKSTRF(2,1)-1; F.S.= 1.00

**GENOPT test: design margins vs ANGLE(7)**

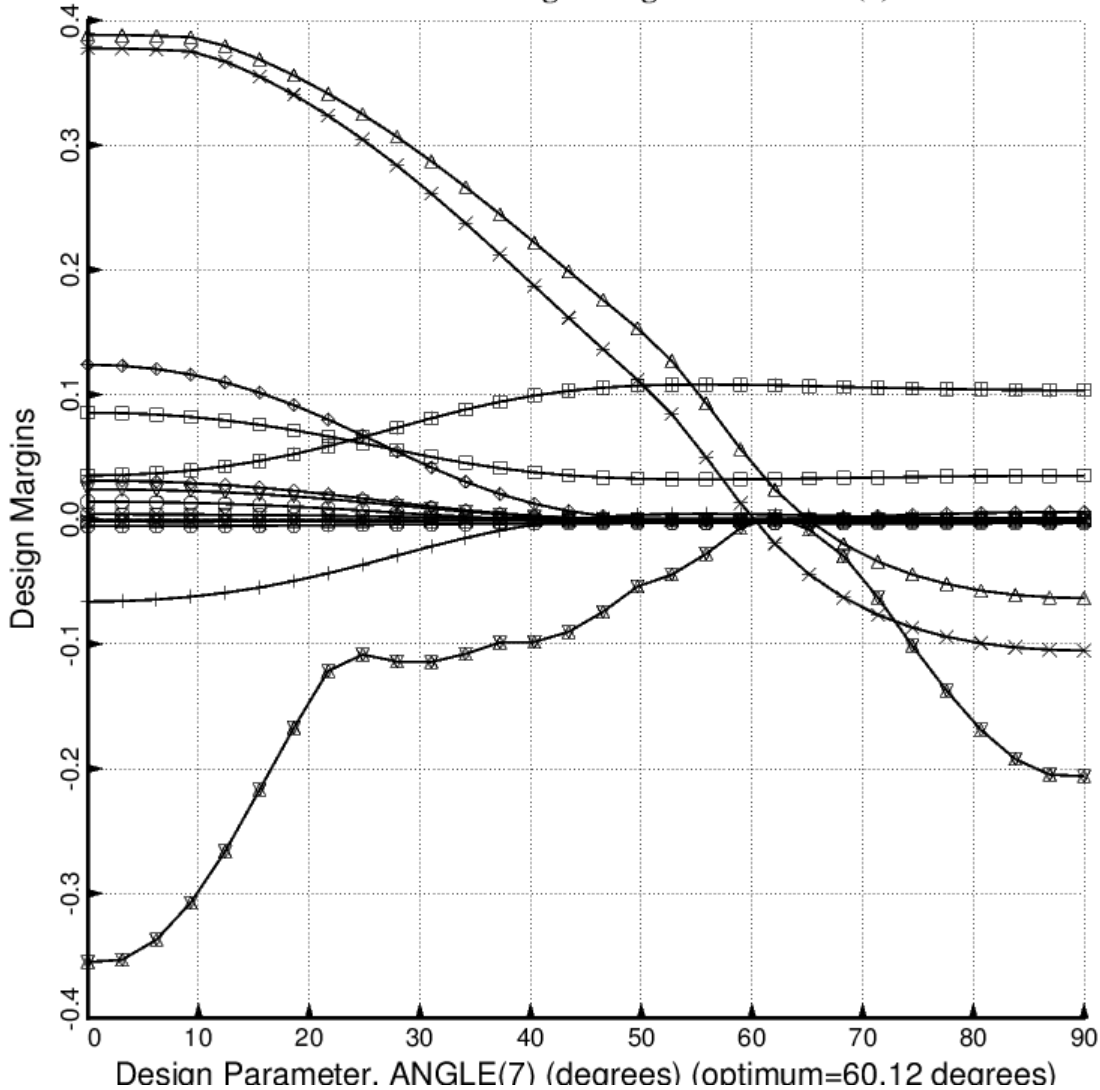


Fig. 51 (old) Design sensitivity of the optimized long propellant tank with aft and forward struts, 4 strut pairs in each set of struts. Here we have the design sensitivity with respect to the decision variable, ANGLE(7) = layup angle of the inner and outer layer of each forward laminated composite strut tube. ANGLE(8) is linked to ANGLE(7) with a linking coefficient equal to -1.0.

○ □ (FREQ(1,1)/FREQA(1,1)) / FREQF(1,1)-1; F.S.= 1.20  
 ○ △ (FREQ(1,2)/FREQA(1,2)) / FREQF(1,2)-1; F.S.= 1.20  
 △ (STRES2A(1,3)/STRES2(1,3)) / STRES2F(1,3)-1; F.S.= 1.50  
 + (FORCEA(1,2)/FORCE(1,2)) / FORCEF(1,2)-1; F.S.= 1.00  
 × (TNKSTR(1,1)/TNKSTR(1,1)) / TNKSTRF(1,1)-1; F.S.= 1.00  
 ◊ (FREQ(2,1)/FREQA(2,1)) / FREQF(2,1)-1; F.S.= 1.20  
 ▽ (FREQ(2,2)/FREQA(2,2)) / FREQF(2,2)-1; F.S.= 1.20  
 ▨ (STRES1A(2,3)/STRES1(2,3)) / STRES1F(2,3)-1; F.S.= 1.50  
 ✕ (STRES2A(2,3)/STRES2(2,3)) / STRES2F(2,3)-1; F.S.= 1.50  
 ♦ (COLBUK(2,2)/COLBUKA(2,2)) / COLBUKF(2,2)-1; F.S.= 1.00  
 (SHLBUK(2,1)/SHLBUKA(2,1)) / SHLBUKF(2,1)-1; F.S.= 2.00  
 ✣ (SHLBUK(2,2)/SHLBUKA(2,2)) / SHLBUKF(2,2)-1; F.S.= 2.00  
 ▨ (FORCEA(2,2)/FORCE(2,2)) / FORCEF(2,2)-1; F.S.= 1.00  
 ✕ (TNKSTR(2,1)/TNKSTR(2,1)) / TNKSTRF(2,1)-1; F.S.= 1.00

**GENOPT test: design margins vs ANGLE(9)**

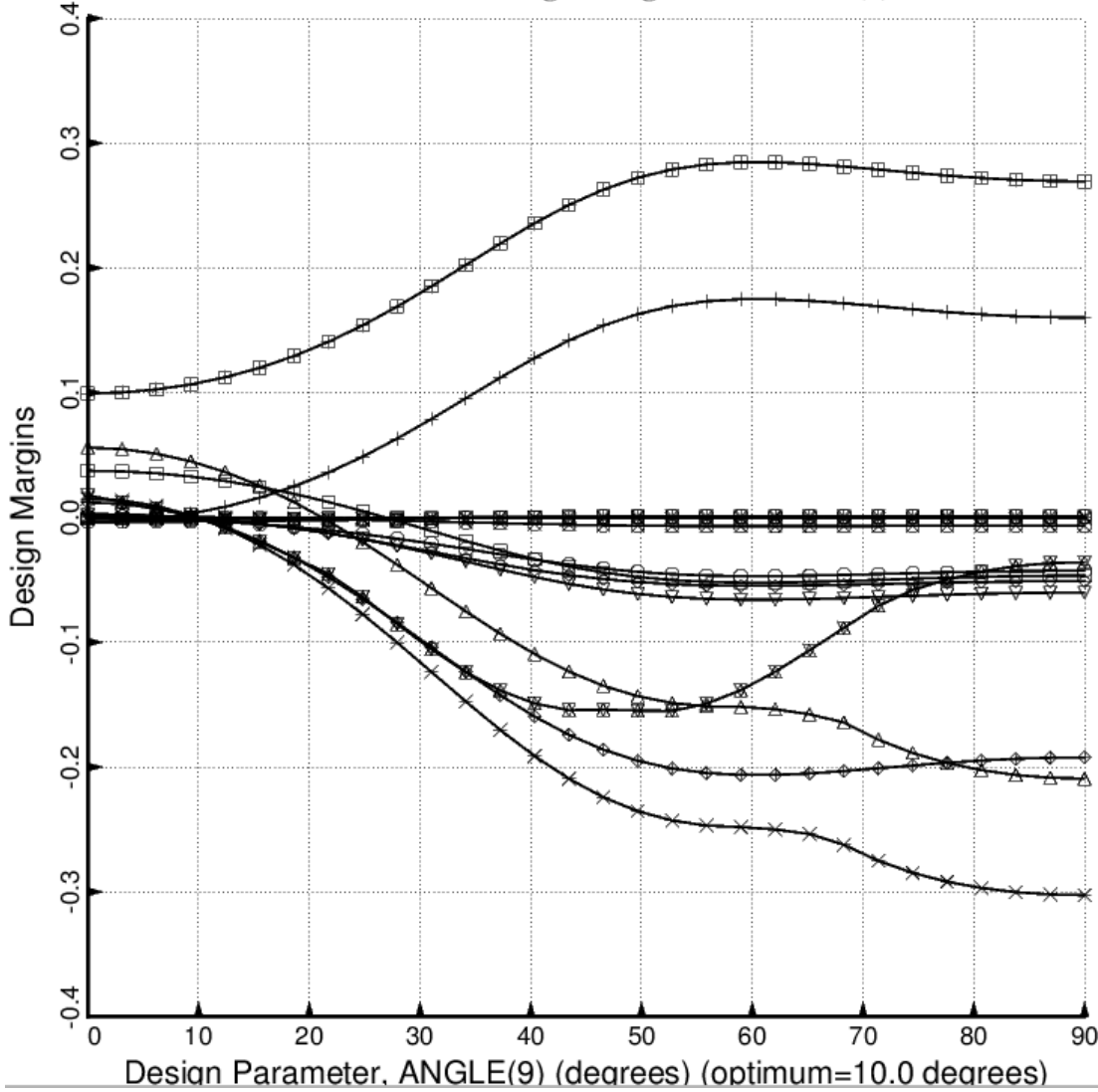


Fig. 52 (old) Design sensitivity of the optimized long propellant tank with aft and forward struts, 4 strut pairs in each set of struts. Here we have the design sensitivity with respect to the decision variable, ANGLE(9) = layup angle of the third and tenth layer of each forward laminated composite strut tube. ANGLE(10) is linked to ANGLE(9) with a linking coefficient equal to -1.0.

- 
- (FREQ(1,1)/FREQA(1,1)) / FREQF(1,1)-1; F.S.= 1.20  
 ○ (FREQ(1,2)/FREQA(1,2)) / FREQF(1,2)-1; F.S.= 1.20  
 △ (STRES2A(1,3)/STRES2(1,3)) / STRES2F(1,3)-1; F.S.= 1.50  
 + (FORCEA(1,2)/FORCE(1,2)) / FORCEF(1,2)-1; F.S.= 1.00  
 × (TNKSTR(1,1)/TNKSTR(1,1)) / TNKSTRF(1,1)-1; F.S.= 1.00  
 ◇ (FREQ(2,1)/FREQA(2,1)) / FREQF(2,1)-1; F.S.= 1.20  
 ▽ (FREQ(2,2)/FREQA(2,2)) / FREQF(2,2)-1; F.S.= 1.20  
 ▨ (STRES1A(2,3)/STRES1(2,3)) / STRES1F(2,3)-1; F.S.= 1.50  
 ✕ (STRES2A(2,3)/STRES2(2,3)) / STRES2F(2,3)-1; F.S.= 1.50  
 ♦ (COLBUK(2,2)/COLBUKA(2,2)) / COLBUKF(2,2)-1; F.S.= 1.00  
 ⊕ (SHLBUK(2,1)/SHLBUKA(2,1)) / SHLBUKF(2,1)-1; F.S.= 2.00  
 ✖ (SHLBUK(2,2)/SHLBUKA(2,2)) / SHLBUKF(2,2)-1; F.S.= 2.00  
 ▨ (FORCEA(2,2)/FORCE(2,2)) / FORCEF(2,2)-1; F.S.= 1.00  
 ✕ (TNKSTR(2,1)/TNKSTR(2,1)) / TNKSTRF(2,1)-1; F.S.= 1.00

**GENOPT test: design margins vs ANGLE(11)**

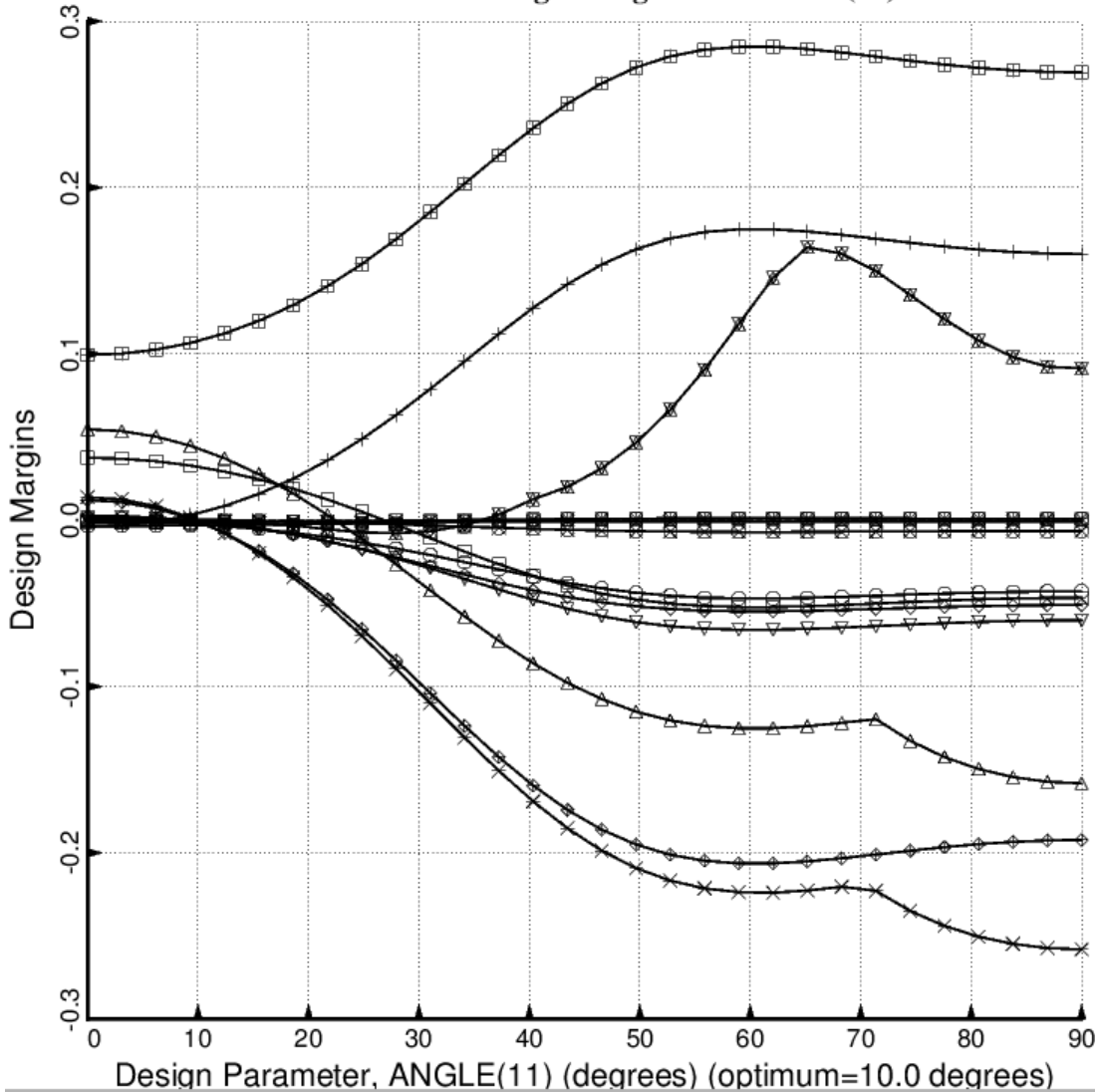


Fig. 53 (old) Design sensitivity of the optimized long propellant tank with aft and forward struts, 4 strut pairs in each set of struts. Here we have the design sensitivity with respect to the decision variable, ANGLE(11) = layup angle of the fifth and eighth layer of each forward laminated composite strut tube. ANGLE(12) is linked to ANGLE(11) with a linking coefficient equal to -1.0.

□ total conductance into the tank: CONDCT

### test: objective vs ANGLE(3) for the optimized tank/strut system

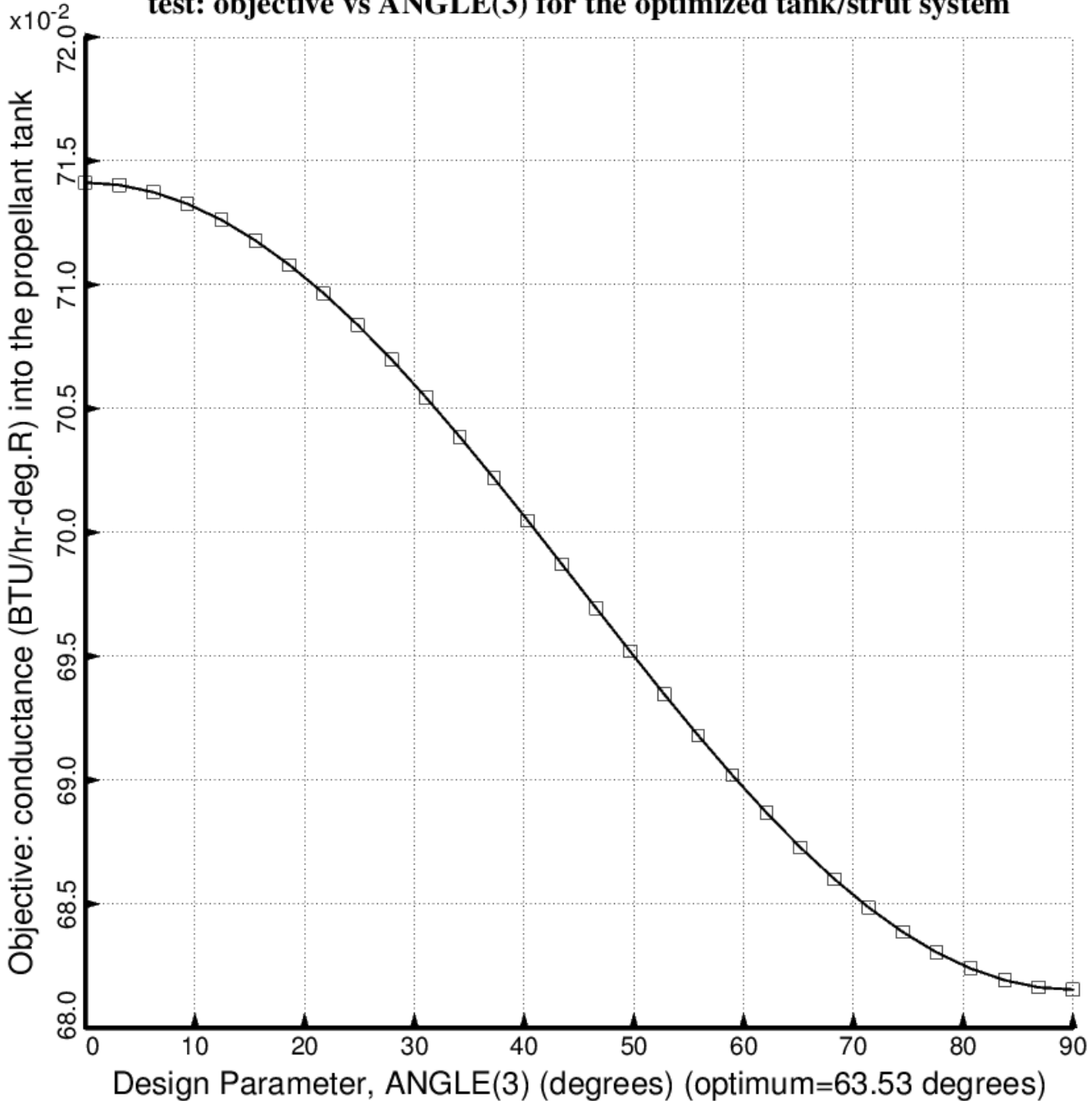


Fig. 54 (old) Design sensitivity of the optimized long propellant tank with aft and forward struts, 4 strut pairs in each set of struts. Here we have the design sensitivity of the objective =  $WGT \times TOTMAS/TNKNRM + (1-WGT) \times CONDCT/CONNRM$  with respect to the decision variable, ANGLE(3) = layup angle of the third and tenth layer of each aft laminated composite strut tube. NOTE: the vertical axis is mis-labeled in this figure. The label should be: objective =  $WGT \times TOTMAS/TNKNRM + (1-WGT) \times CONDCT/CONNRM$ . Also, the legend is mis-labeled. It should be: objective =  $WGT \times TOTMAS/TNKNRM + (1-WGT) \times CONDCT/CONNRM$ .

- Optimized conductance into long propellant tank from permanent BIGBOSOR4/BOSDEC; TEMTUR=0 deg.
- Optimized conductance, permanent BIGBOSOR4/BOSDEC, composite strut tube cure temperature=170 deg.
- Optimized conductance into long propellant tank from temporary BIGBOSOR4/BOSDEC; TEMTUR=0 deg.
- Optimized conductance, temporary BIGBOSOR4/BOSDEC, composite strut tube cure temperature=170 deg.
- Optimized mass, temporary BIGBOSOR4/BOSDEC, cure temperature=170 deg., starting from scratch

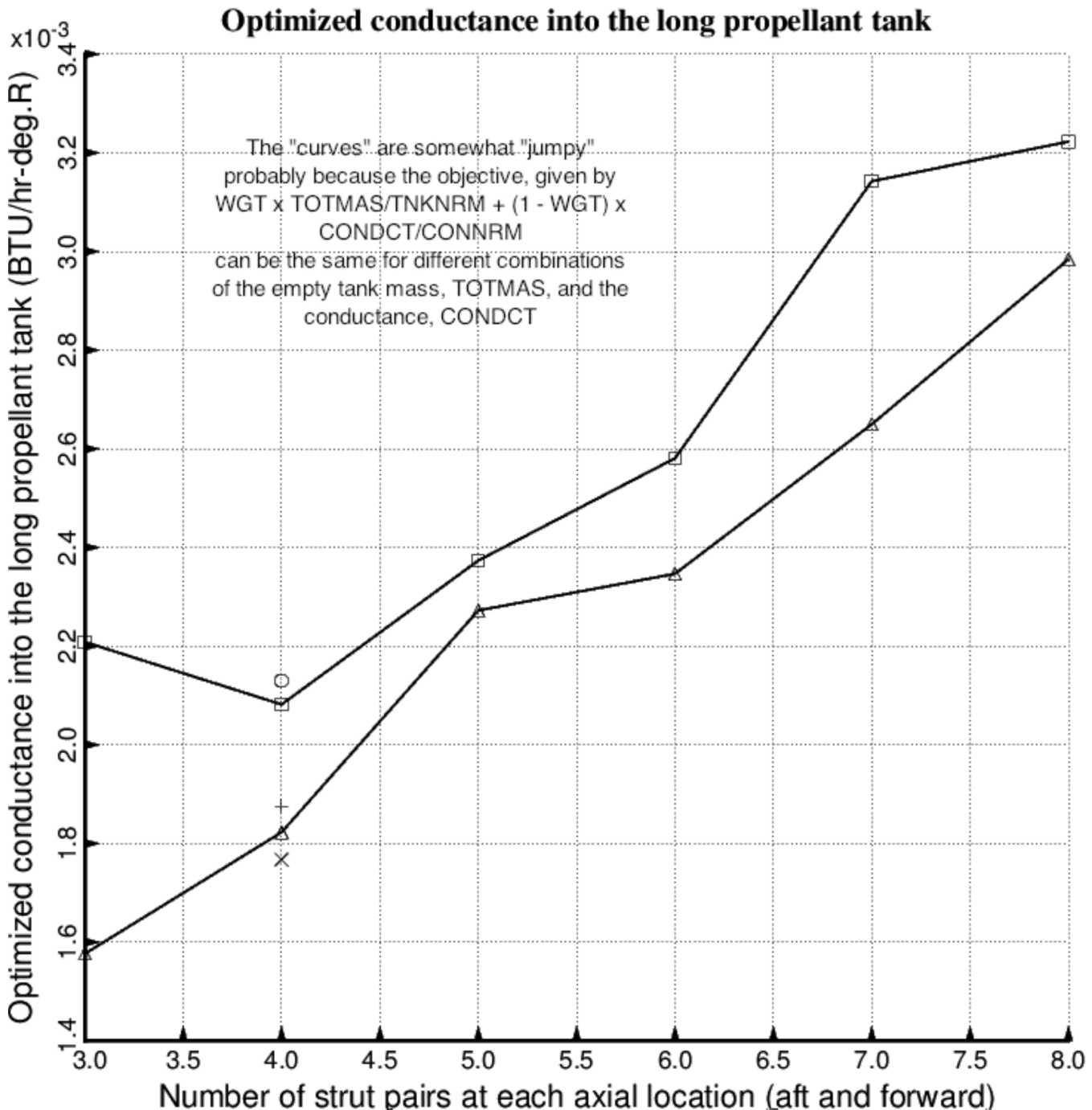


Fig. 55 (old) Optimized conductance into the long propellant tank with aft and forward sets of struts as functions of the number of strut pairs at each axial location.

- Optimized mass of long empty propellant tank; permanent BIGBOSOR4/BOSDEC; TEMTUR=0 deg.
- Optimized mass, permanent BIGBOSOR4/BOSDEC, composite strut tube cure temperature=170 deg.
- △ Optimized mass of long empty propellant tank; temporary BIGBOSOR4/BOSDEC; TEMTUR=0 deg.
- + Optimized mass, temporary BIGBOSOR4/BOSDEC, composite strut tube cure temperature=170 deg.
- × Optimized mass, temporary BIGBOSOR4/BOSDEC, cure temperature=170 deg., starting from scratch

### Optimized mass of the long empty propellant tank

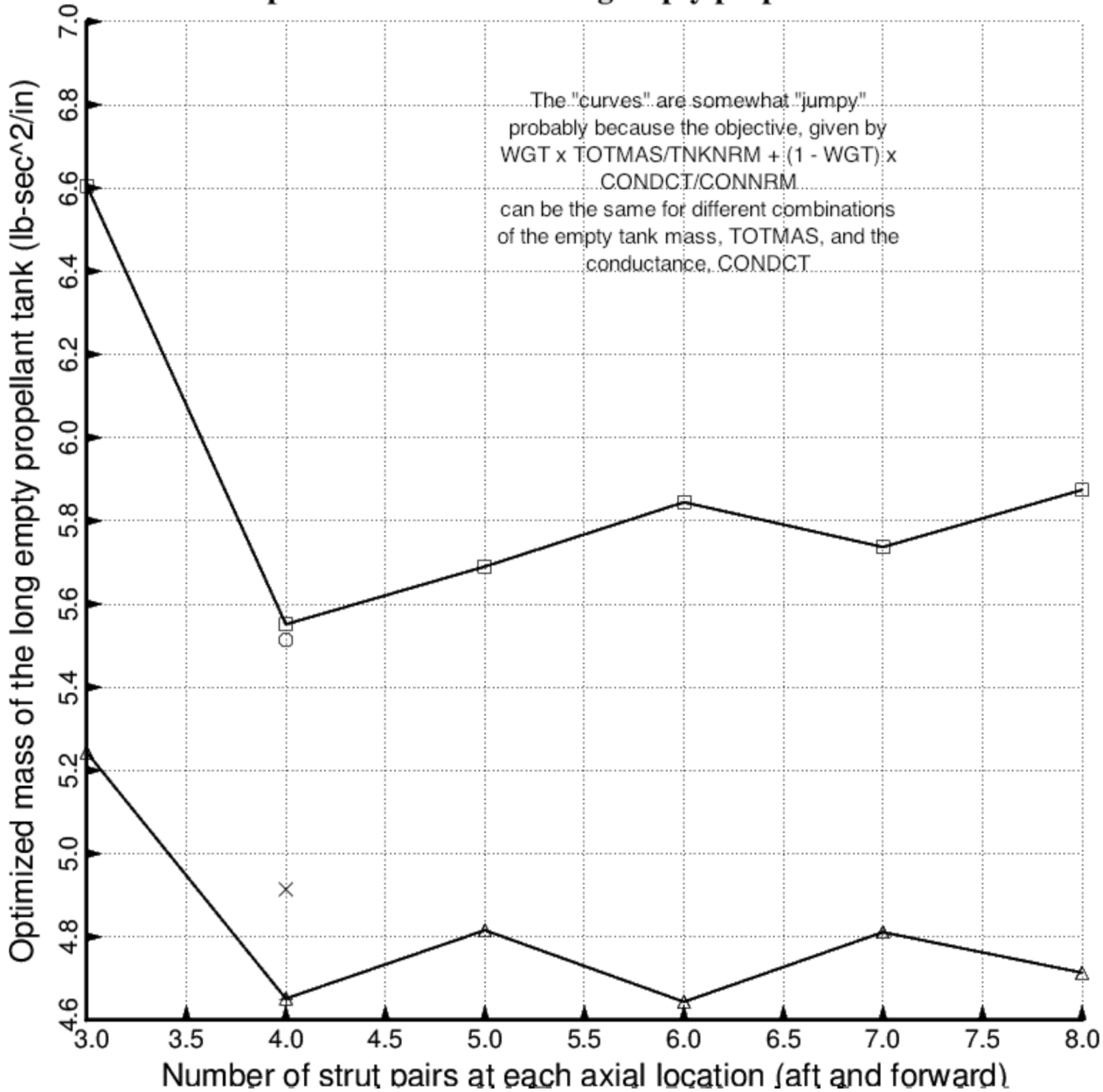


Fig. 56 (old) Optimized empty tank mass of the long propellant tank with aft and forward sets of struts as functions of the number of strut pairs at each axial location.

□ objective:  $0.5x(TOTMAS/3.0) + (1.-0.5)x(CONDCT/0.0006)$ ; cure temperature, TEMTUR=170 deg.

### test2: objective vs design iterations (temporary BIGBOSOR4/BOSDEC)

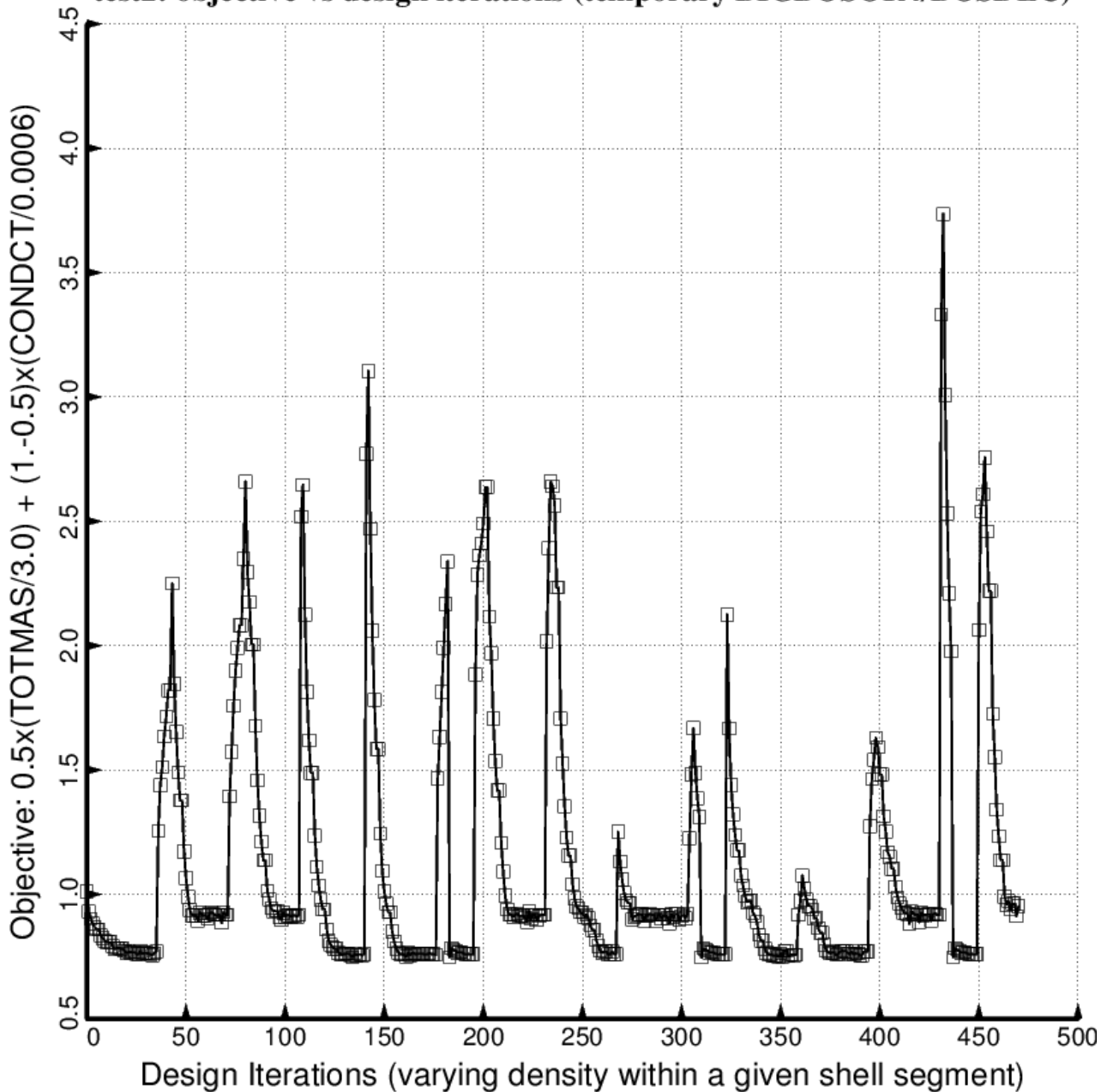


Fig. 57 (old) “Temporary” BIGBOSOR4/BOSDEC: Evolution of the objective during the first execution of the GENOPT processor, SUPEROPT, for the short tank/strut system with only one set of struts attached to the propellant tank at the midlength of the short cylindrical part of the tank. Notice that during the long SUPEROPT process (about 15 hours of computer time on the writer’s very fast computer) the objective converges to more than one local minimum. This behavior makes it difficult to find a “global” optimum design. Compare with Fig. 58 which pertains to optimization with use of the “permanent” version of BIGBOSOR4/BOSDEC.

□ WGTxTOTMAS/TNKNRM +(1-WGT)xCONDCT/CONNRM: CONDCT

### GENOPT test2: objective vs design iterations

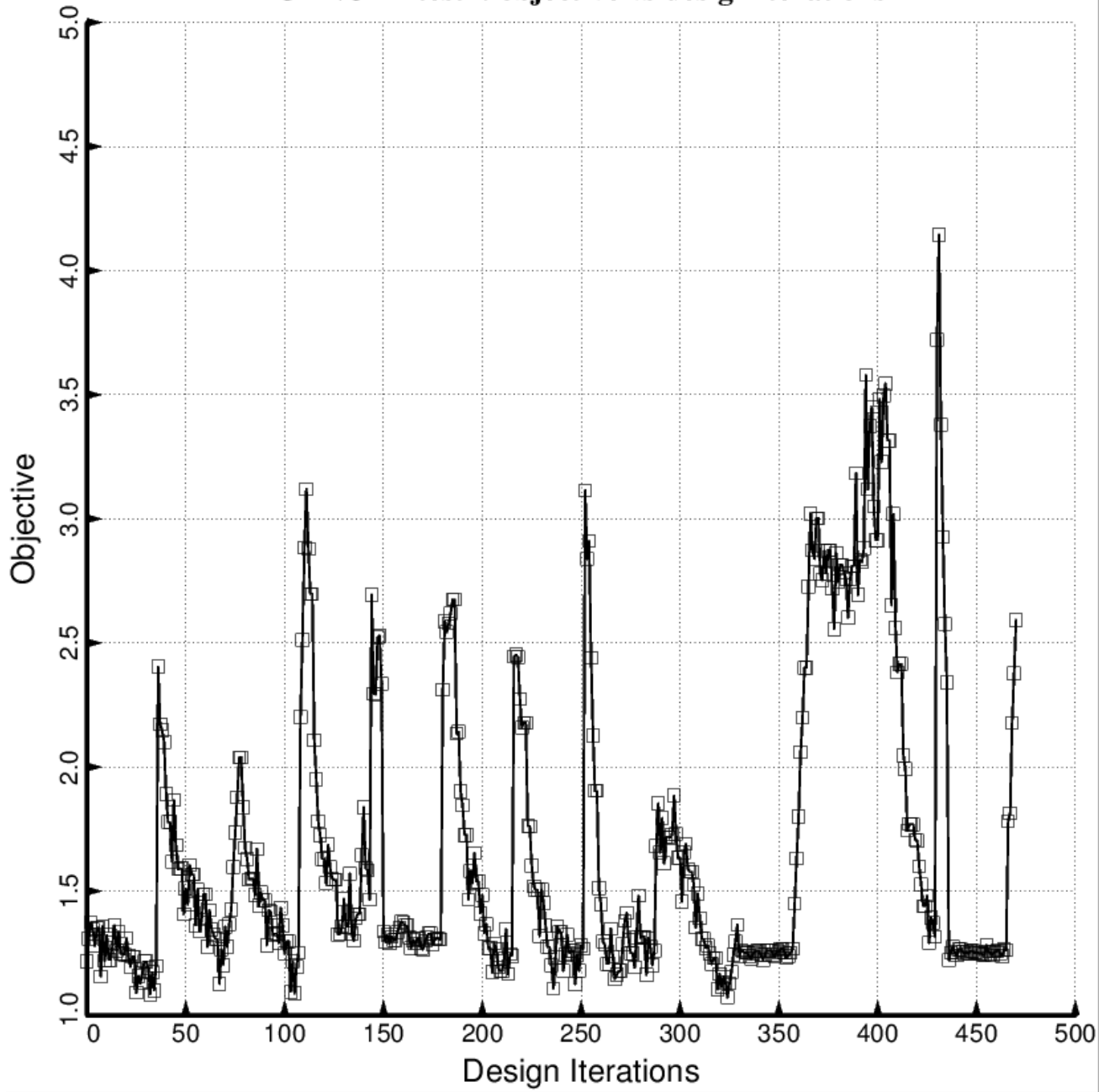


Fig. 57 (new) “Temporary” BIGBOSOR4/BOSDEC: Evolution of the objective during the first execution of the GENOPT processor, SUPEROPT, for the short tank/strut system with only one set of struts attached to the propellant tank at the midlength of the short cylindrical part of the tank. Notice that during the long SUPEROPT process (about 15 hours of computer time on the writer’s very fast computer) the objective is very “zig-zaggy” from iteration to iteration. This behavior makes it difficult to find a “global” optimum design. Compare with Fig. 58, which pertains to optimization with use of the “permanent” version of BIGBOSOR4/BOSDEC.

$\square$  objective =  $0.5x(TOTMAS/3.0) + (1-0.5)x(CONDCT/0.0006)$ ; cure temperature, TEMTUR=170 deg.

### test2: objective vs design iterations (permanent BIGBOSOR4/BOSDEC)

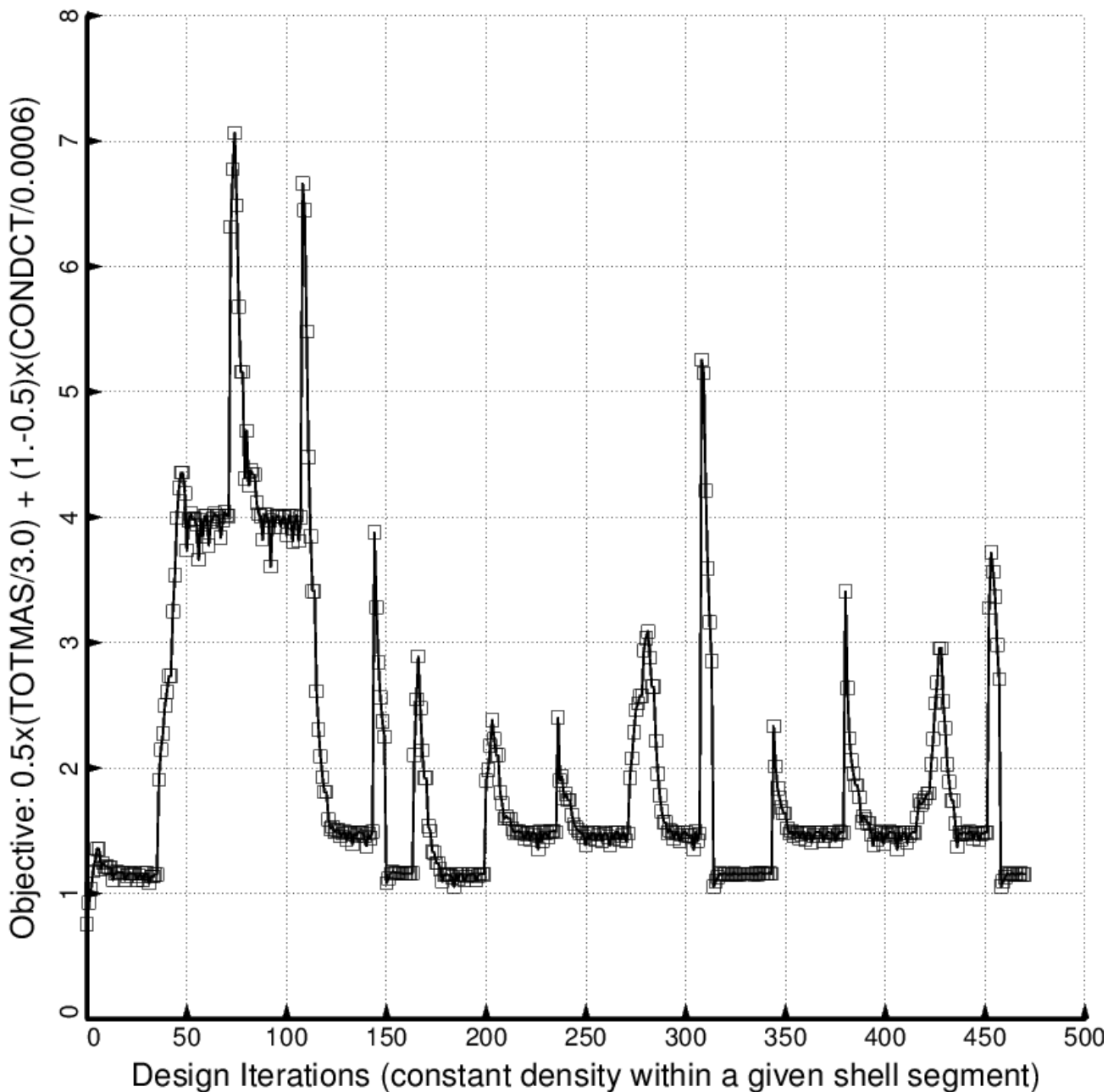


Fig. 58 (old) “Permanent” BIGBOSOR4/BOSDEC: Evolution of the objective during the first execution of the GENOPT processor, SUPEROPT, for the short tank/strut system with only one set of struts attached to the propellant tank at the midlength of the short cylindrical part of the tank. Notice that during the long SUPEROPT process (about 15 hours of computer time on the writer’s very fast computer) the objective converges to more than one local minimum. This behavior makes it difficult to find a “global” optimum design. Compare with Fig. 57, which pertains to optimization with use of the “temporary” version of BIGBOSOR4/BOSDEC.

□ Objective=0.5x(TOTMAS/10.) +0.5x(CONDCT/0.002); temporary bigbosor4/bosdec; TEMTUR=0 deg.

### test: objective vs design iterations; curing temperature=0 degrees

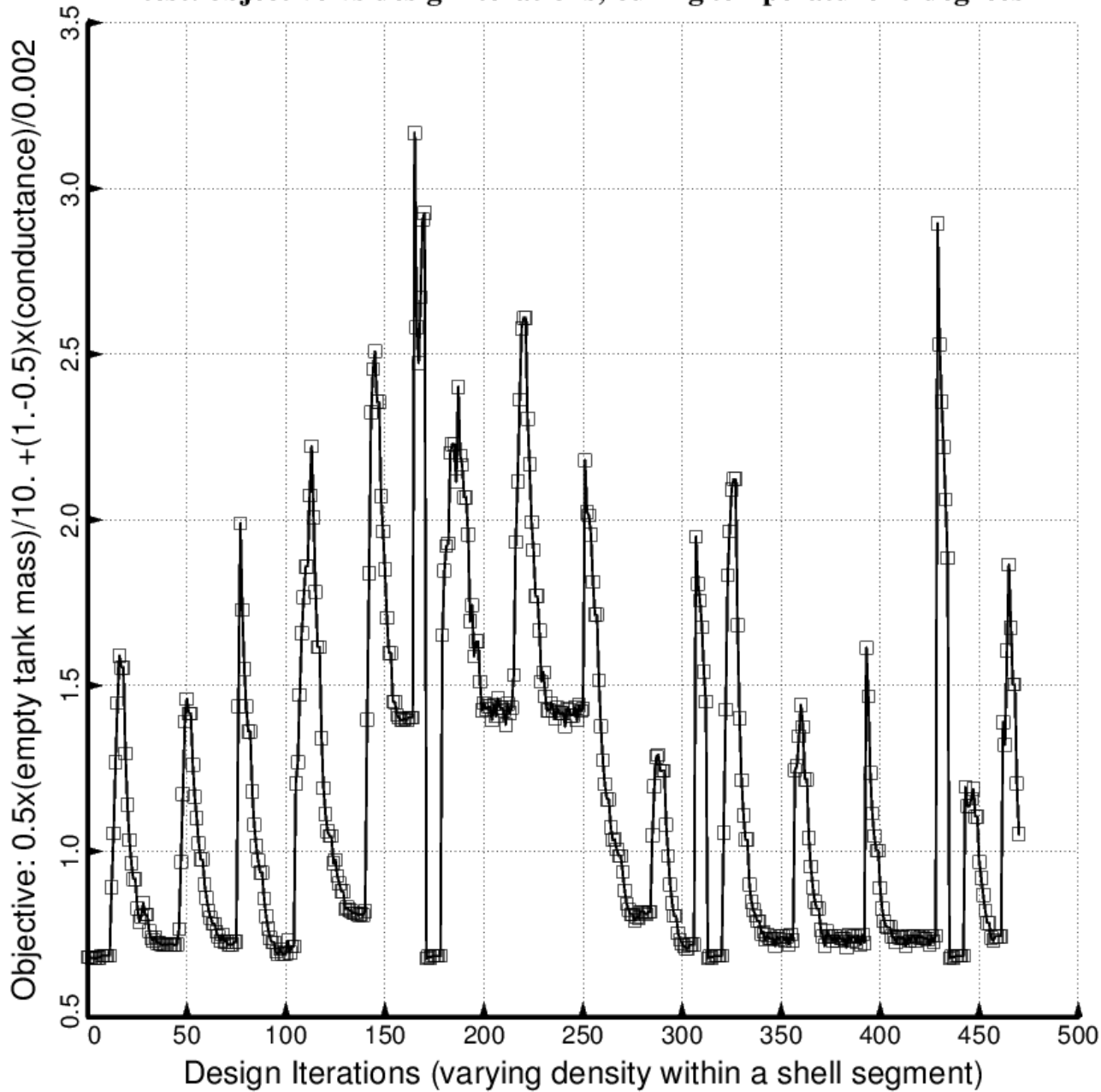


Fig. 59a (old) “Temporary” BIGBOSOR4/BOSDEC: Evolution of the objective during the second execution of the GENOPT processor, SUPEROPT, for the long tank/strut system with aft and forward sets of struts attached to the propellant tank at the dome/cylinder junctions of the tank. Notice that during the long SUPEROPT process (about 24 hours of computer time on the writer’s very fast computer) the objective converges to more than one local minimum. This behavior makes it difficult to find a “global” optimum design. Compare with the next figure, which was generated with strut tube layup angles, ANGLE(5) and ANGLE(11), fixed at 10 degrees.

□ Objective=0.5x(TOTMAS/10.) +0.5x(CONDCT/0.002); temporary bigbosor4/bosdec; TEMTUR=0 deg.

**test: curing temperature=0 degrees; ANGLE(5)=ANGLE(11)=10 deg.**

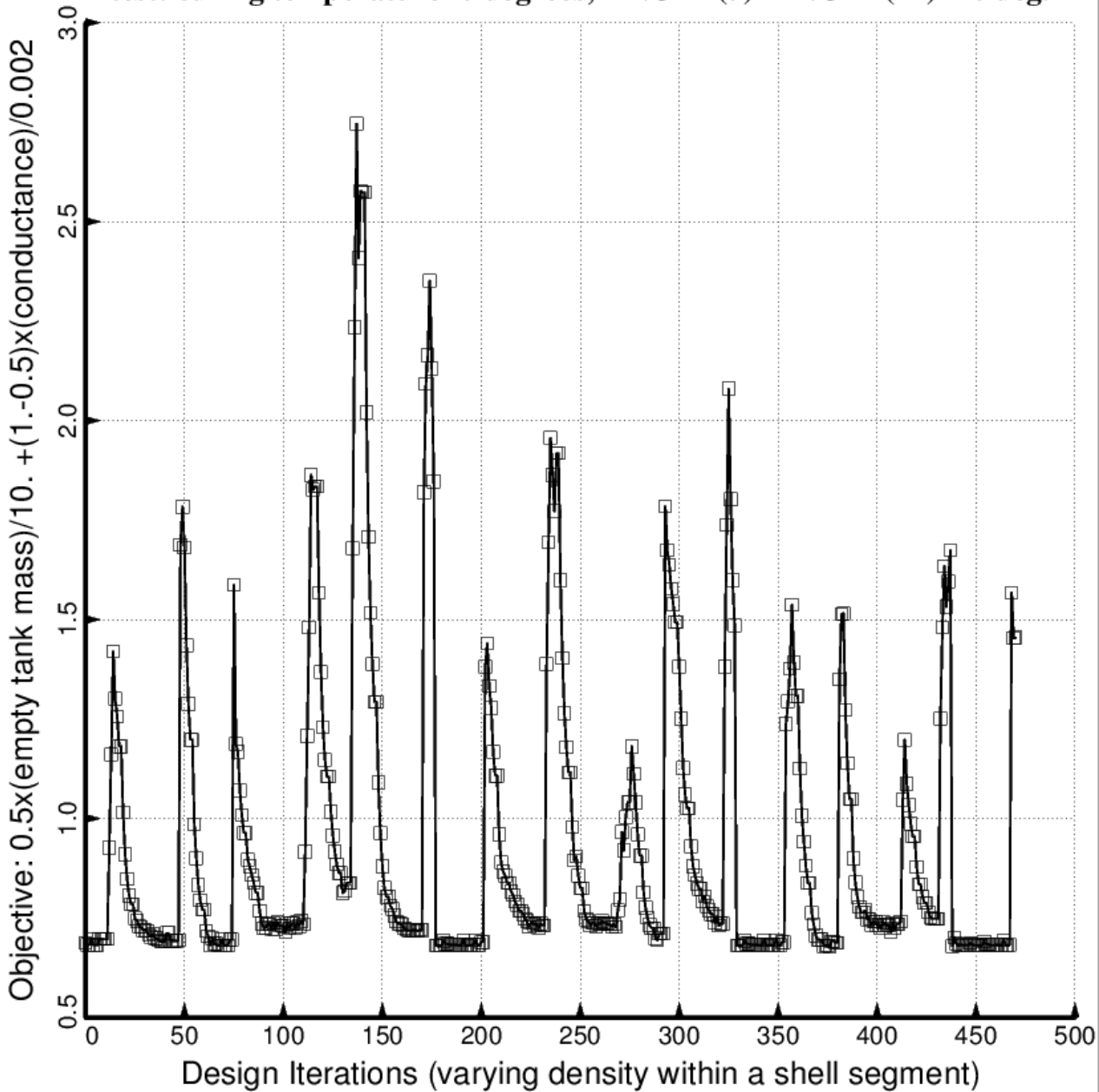


Fig. 59b (old) “Temporary” BIGBOSOR4/BOSDEC: Evolution of the objective during the second execution of the GENOPT processor, SUPEROPT, for the long tank/strut system with aft and forward sets of struts attached to the propellant tank at the dome/cylinder junctions of the tank. Notice that during the long SUPEROPT process (about 24 hours of computer time on the writer’s very fast computer) the objective converges to more than one local minimum. This behavior makes it difficult to find a “global” optimum design. Compare with the previous figure, which was generated with strut tube layup angles, ANGLE(5) and ANGLE(11), established as decision variables.

□ thickness of the tank aft dome skin: THKAFT

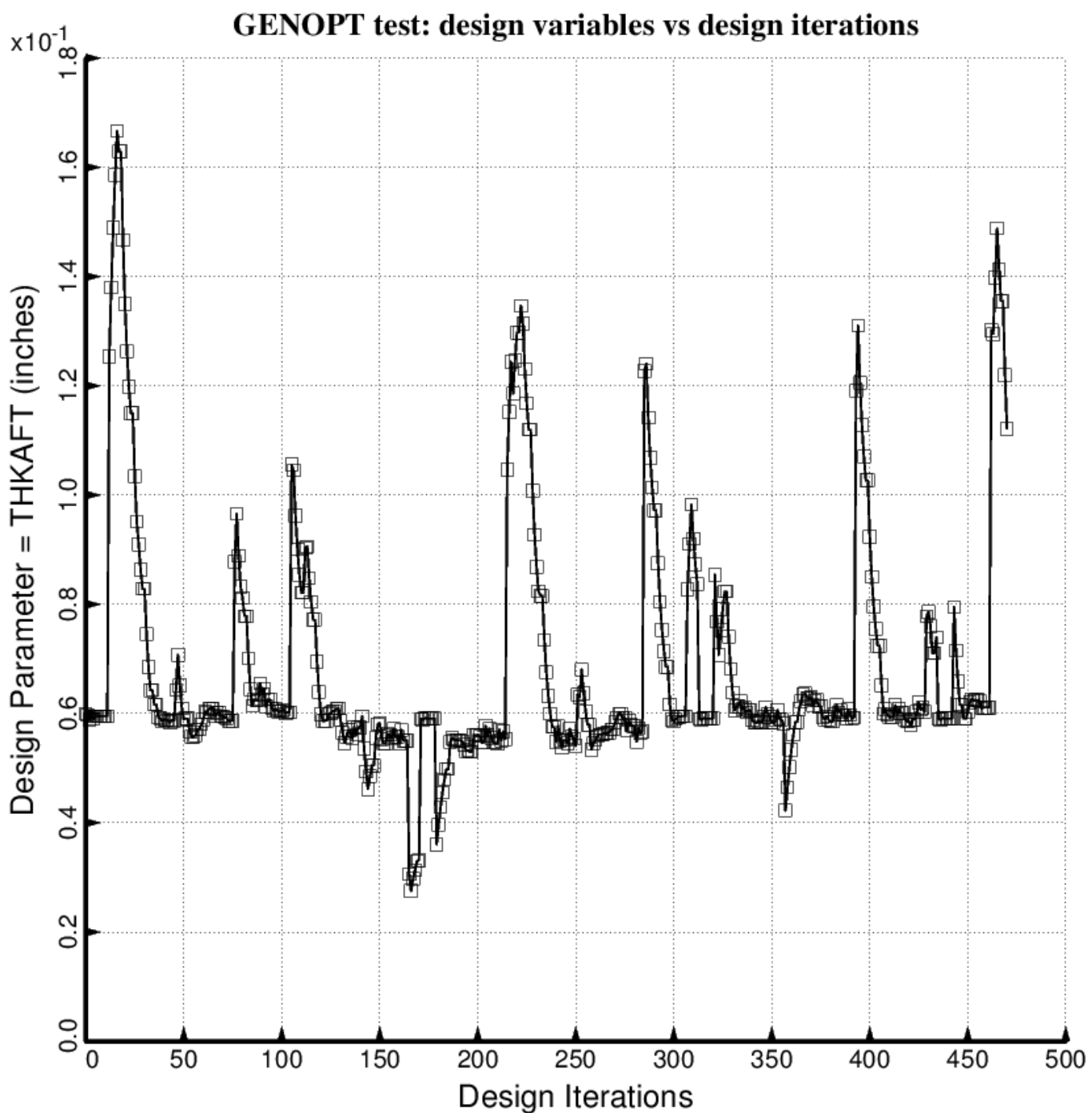


Fig. 60 (old) Temporary BIGBOSOR4/BOSDEC: Evolution of the decision variable, THKAFT = uniform thickness of the middle layer of the 3-layered aft ellipsoidal dome, during the first SUPEROPT execution involving the long propellant tank with aft and forward sets of struts, 4 strut pairs per set. This figure corresponds to the objective plotted in Fig. 59.

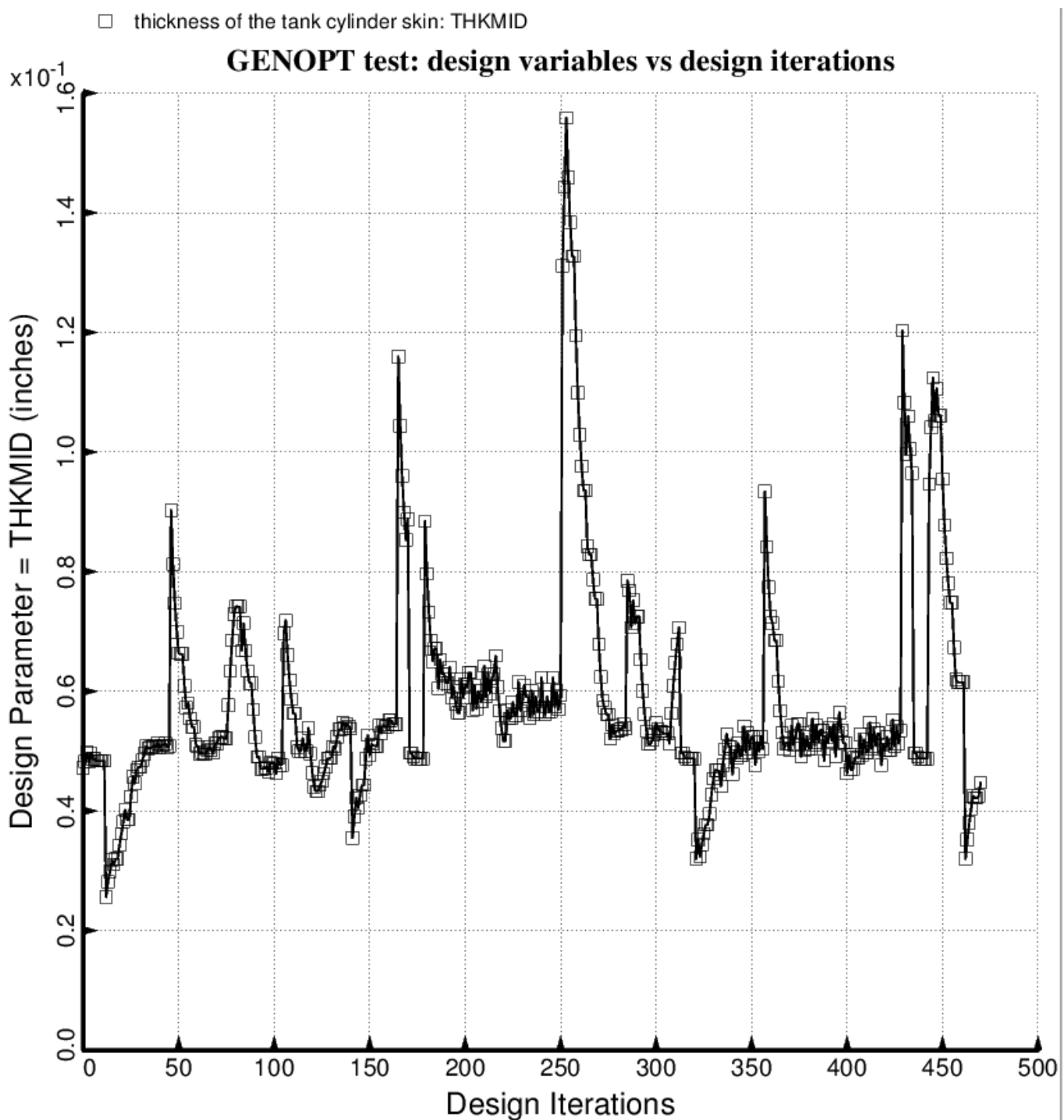


Fig. 61 (old) Temporary BIGBOSOR4/BOSDEC: Evolution of the decision variable, THKMID = uniform thickness of the middle layer of the 3-layered cylindrical part of the propellant tank, during the first SUPEROPT execution involving the long propellant tank with aft and forward sets of struts, 4 strut pairs per set. This figure corresponds to the objective plotted in Fig. 59.

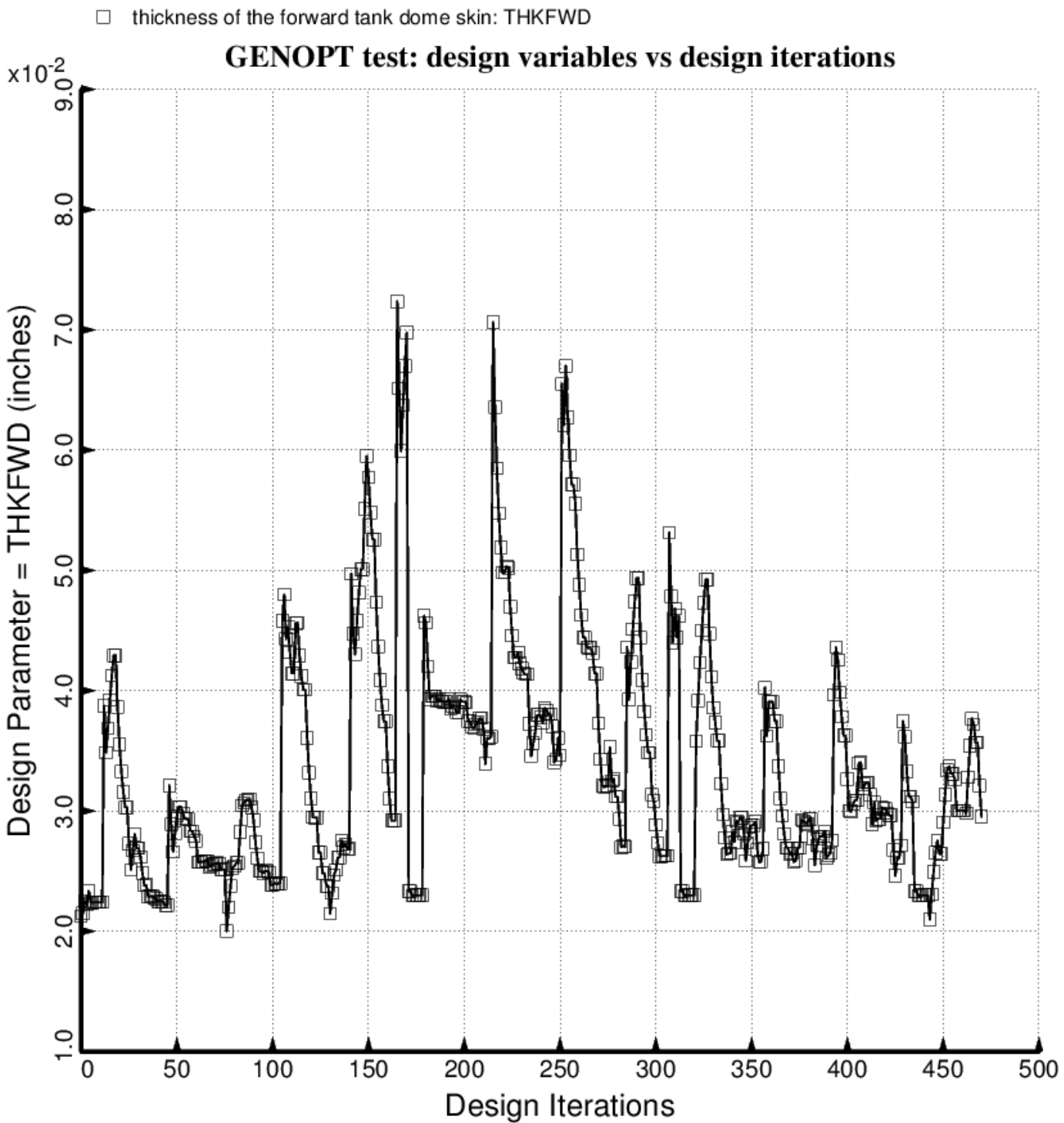


Fig. 62 (old) Temporary BIGBOSOR4/BOSDEC: Evolution of the decision variable, THKFWD = uniform thickness of the middle layer of the 3-layered forward ellipsoidal dome, during the first SUPEROPT execution involving the long propellant tank with aft and forward sets of struts, 4 strut pairs per set. This figure corresponds to the objective plotted in Fig. 59.

□ spacing of the tank orthogrid stringers: STRSPC

### GENOPT test: design variables vs design iterations

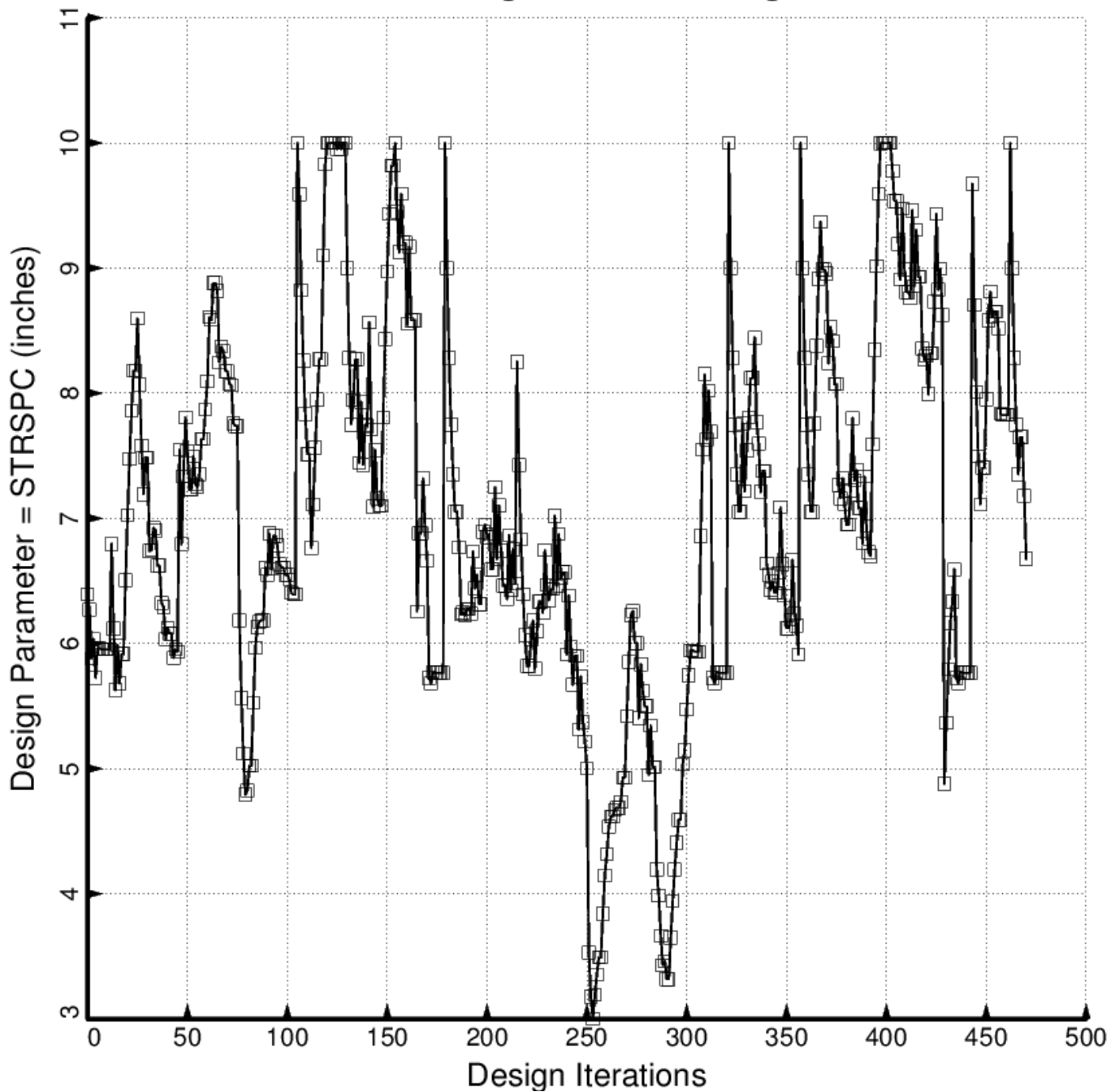


Fig. 63 (old) Temporary BIGBOSOR4/BOSDEC: Evolution of the decision variable, STRSPC = uniform spacing of the stiffeners in the internal smeared orthogrid “layer” of the propellant tank, during the first SUPEROPT execution involving the long propellant tank with aft and forward sets of struts, 4 strut pairs per set. This figure corresponds to the objective plotted in Fig. 59.

□ thickness of the tank orthogrid stringers: STRTHK

### GENOPT test: design variables vs design iterations

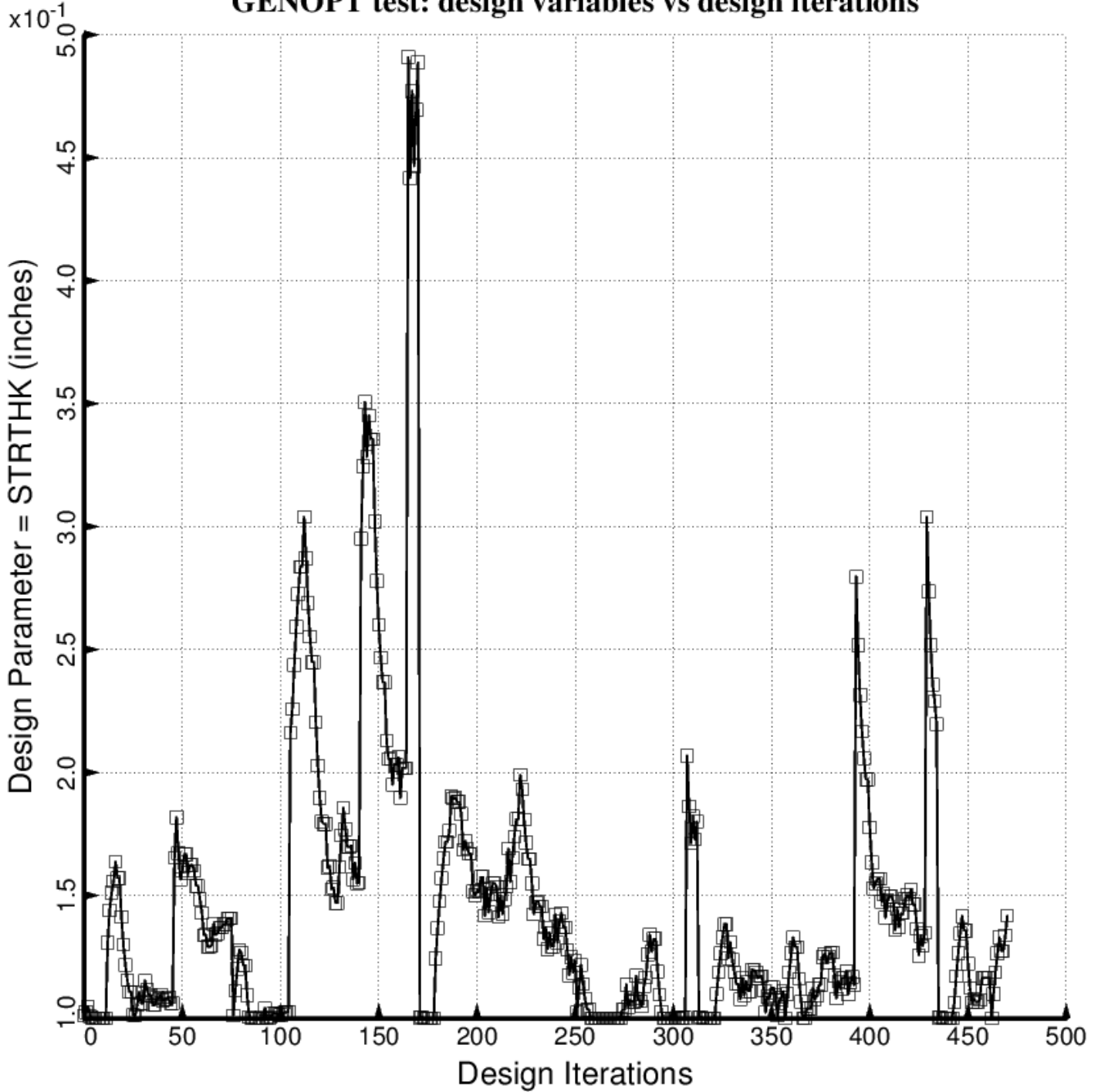


Fig. 64 (old) Temporary BIGBOSOR4/BOSDEC: Evolution of the decision variable,  $\text{STRTHK} = \text{uniform thickness of the stiffeners in the internal smeared orthogrid "layer" of the propellant tank}$ , during the first SUPEROPT execution involving the long propellant tank with aft and forward sets of struts, 4 strut pairs per set. This figure corresponds to the objective plotted in Fig. 59.

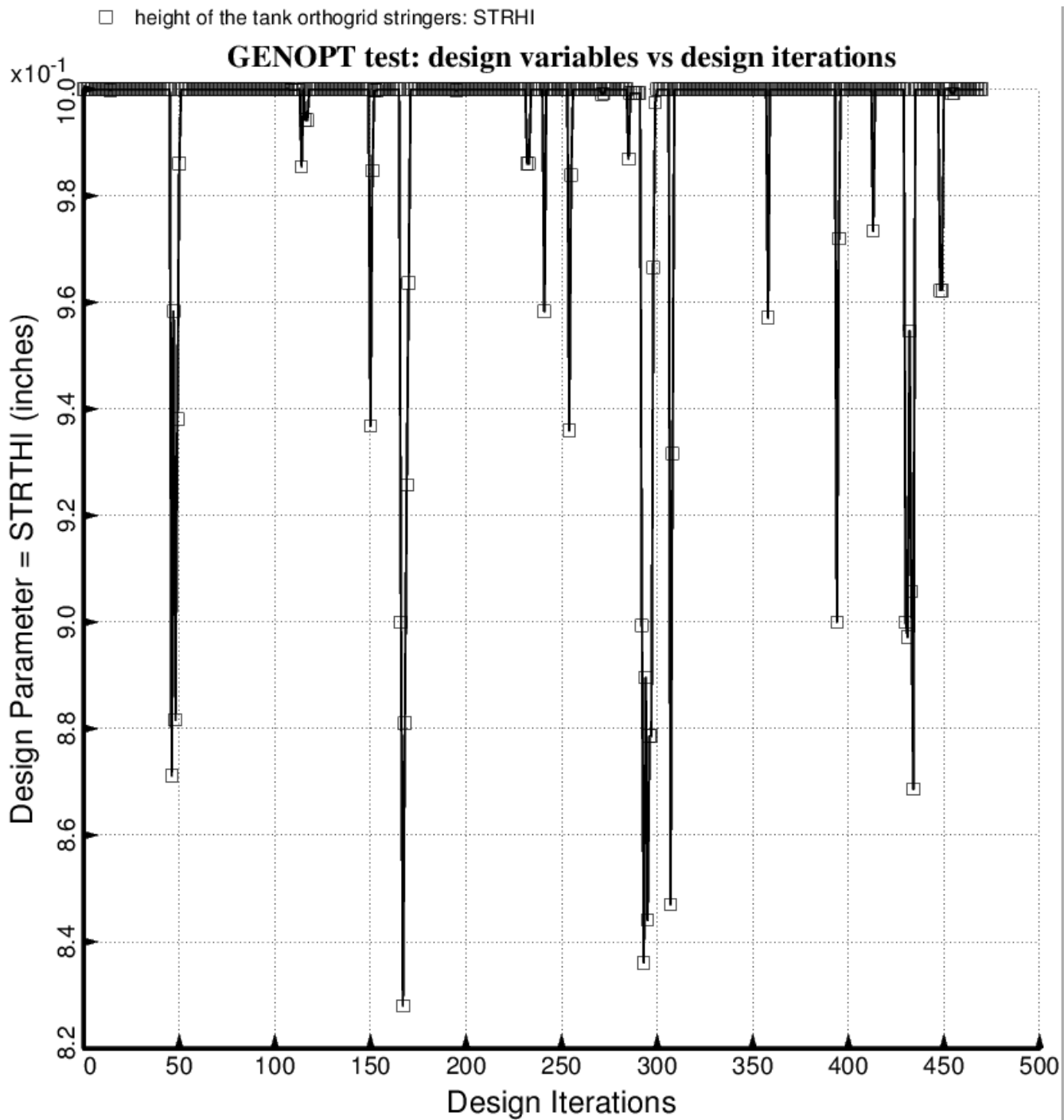


Fig. 65 (old) Temporary BIGBOSOR4/BOSDEC: Evolution of the decision variable,  $\text{STRHI}$  = uniform height of the stiffeners in the internal smeared orthogrid “layer” of the propellant tank, during the first SUPEROPT execution involving the long propellant tank with aft and forward sets of struts, 4 strut pairs per set. This figure corresponds to the objective plotted in Fig. 59.

□ global axial coordinate of "ground": ZGRND(1)

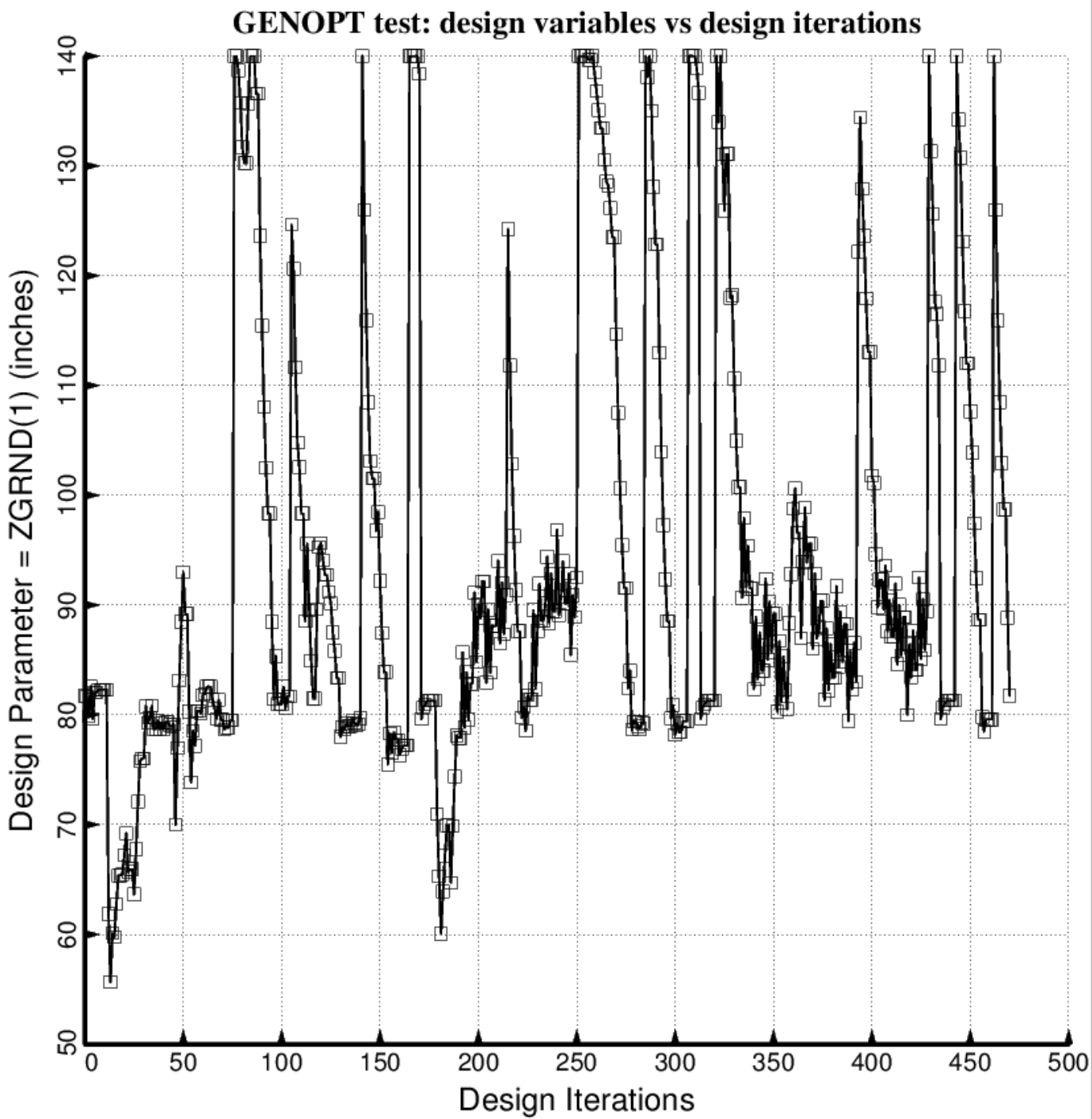


Fig. 66 (old) Temporary BIGBOSOR4/BOSDEC: Evolution of the decision variable,  $ZGRND(1)$  = axial coordinate of “ground” for the aft set of struts, during the first SUPEROPT execution involving the long propellant tank with aft and forward sets of struts, 4 strut pairs per set. This figure corresponds to the objective plotted in Fig. 59.

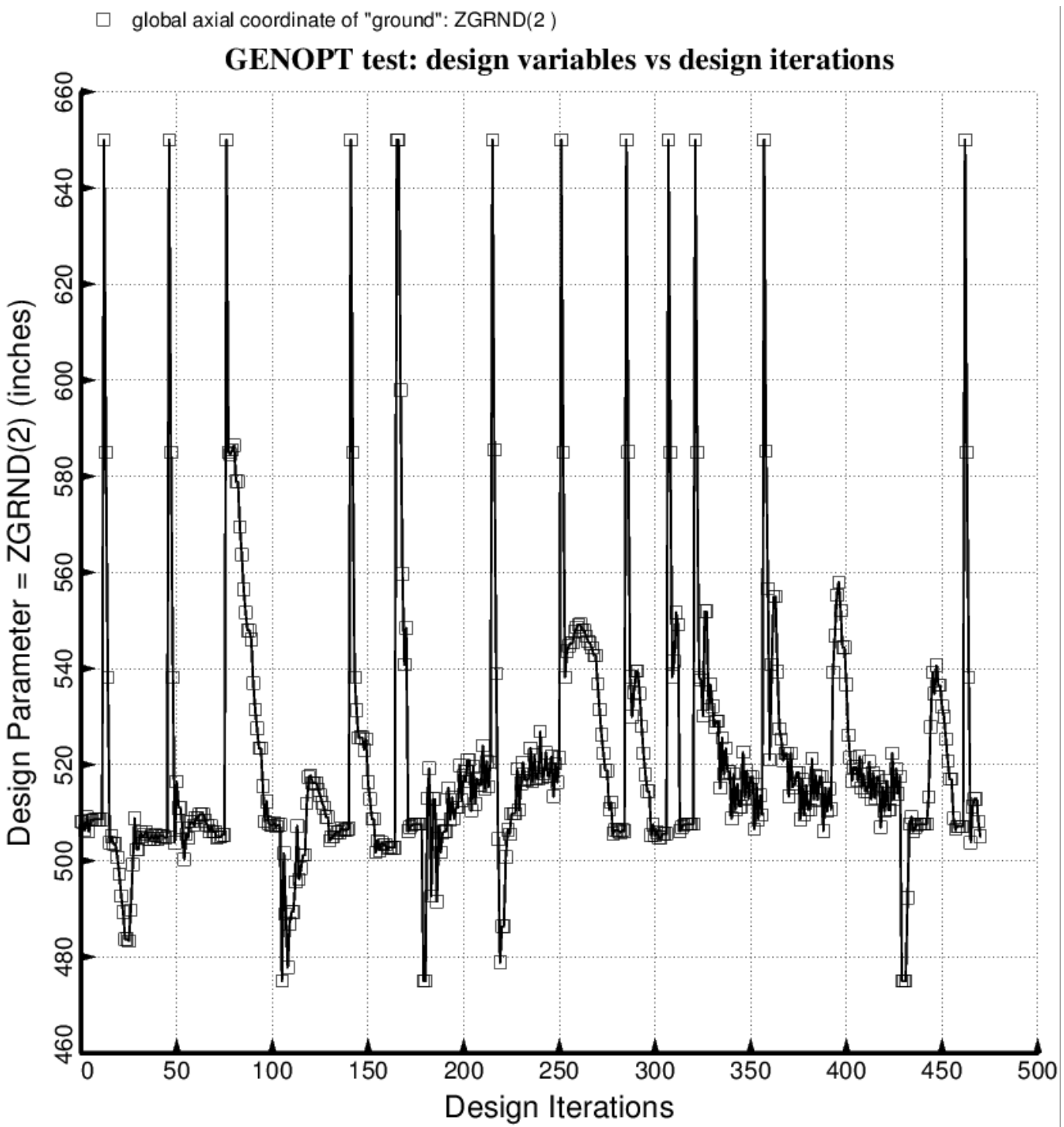


Fig. 67 (old) Temporary BIGBOSOR4/BOSDEC: Evolution of the decision variable,  $ZGRND(2)$  = axial coordinate of “ground” for the forward set of struts, during the first SUPEROPT execution involving the long propellant tank with aft and forward sets of struts, 4 strut pairs per set. This figure corresponds to the objective plotted in Fig. 59.

□ circ.angle (deg.) to pinned tank end of strut: ATANK(1)

### GENOPT test: design variables vs design iterations

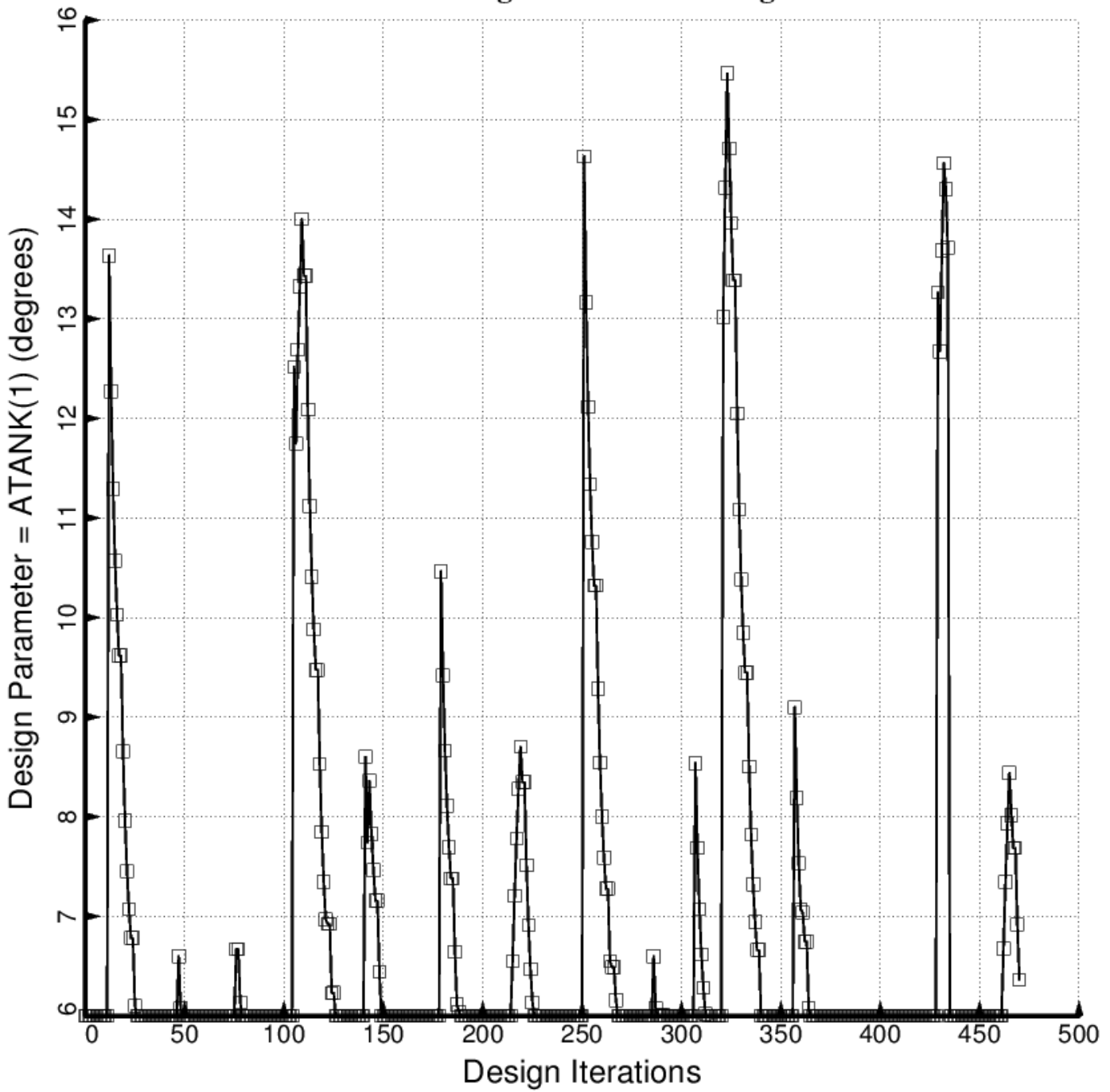


Fig. 68 (old) Temporary BIGBOSOR4/BOSDEC: Evolution of the decision variable,  $ATANK(1)$  = azimuthal angle to the tank end of the forward-slanting struts in the aft set of struts [the backward-slanting aft struts have  $-ATANK(1)$ ], during the first SUPEROPT execution involving the long propellant tank with aft and forward sets of struts, 4 strut pairs per set. This figure corresponds to the objective plotted in Fig. 59.

□ circ.angle (deg.) to pinned tank end of strut: ATANK(2)

### GENOPT test: design variables vs design iterations

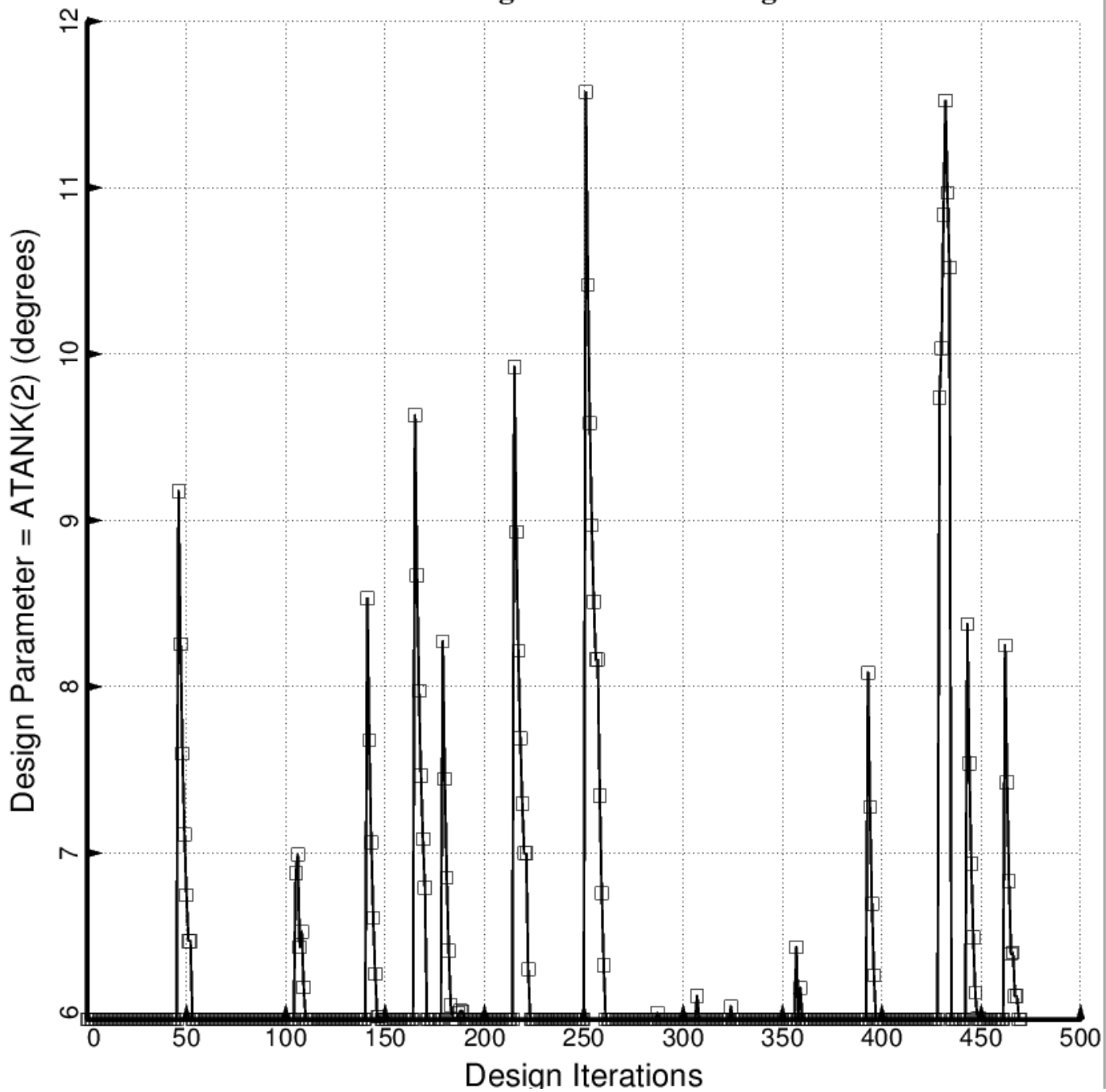


Fig. 69 (old) Temporary BIGBOSOR4/BOSDEC: Evolution of the decision variable,  $ATANK(2)$  = azimuthal angle to the tank end of the forward-slanting struts in the forward set of struts [the backward-slanting forward struts have  $-ATANK(2)$ ], during the first SUPEROPT execution involving the long propellant tank with aft and forward sets of struts, 4 strut pairs per set. This figure corresponds to the objective plotted in Fig. 59.

□ circ.angle to pinned "ground" end of strut: AGRND(1 )

### GENOPT test: design variables vs design iterations

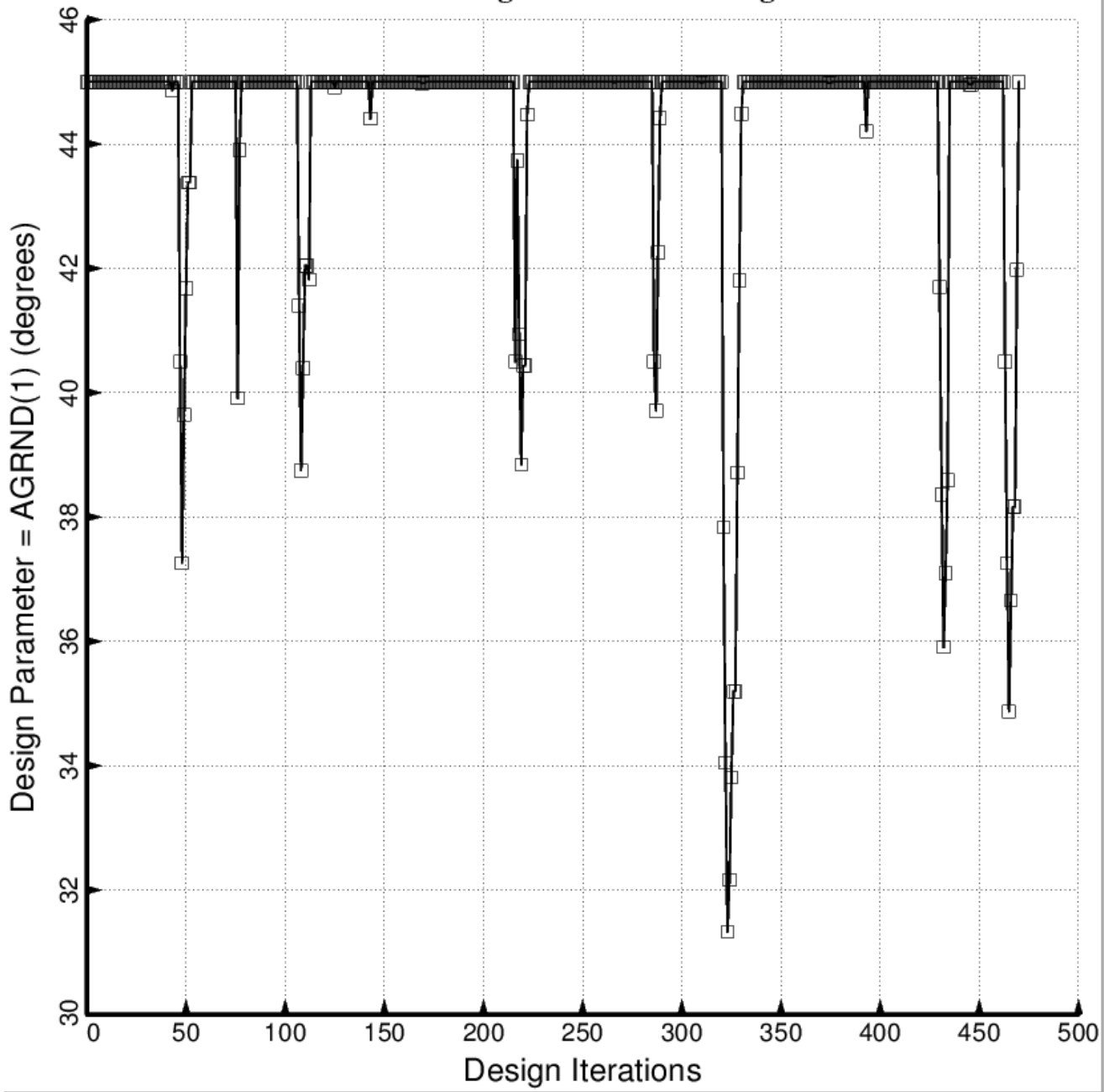


Fig. 70 (old) Temporary BIGBOSOR4/BOSDEC: Evolution of the decision variable,  $AGRND(1)$  = azimuthal angle to the “ground” end of the forward-slanting struts in the aft set of struts [the backward-slanting aft struts have  $-AGRND(1)$ ], during the first SUPEROPT execution involving the long propellant tank with aft and forward sets of struts, 4 strut pairs per set. This figure corresponds to the objective plotted in Fig. 59.

□ circ.angle to pinned "ground" end of strut: AGRND(2 )

### GENOPT test: design variables vs design iterations

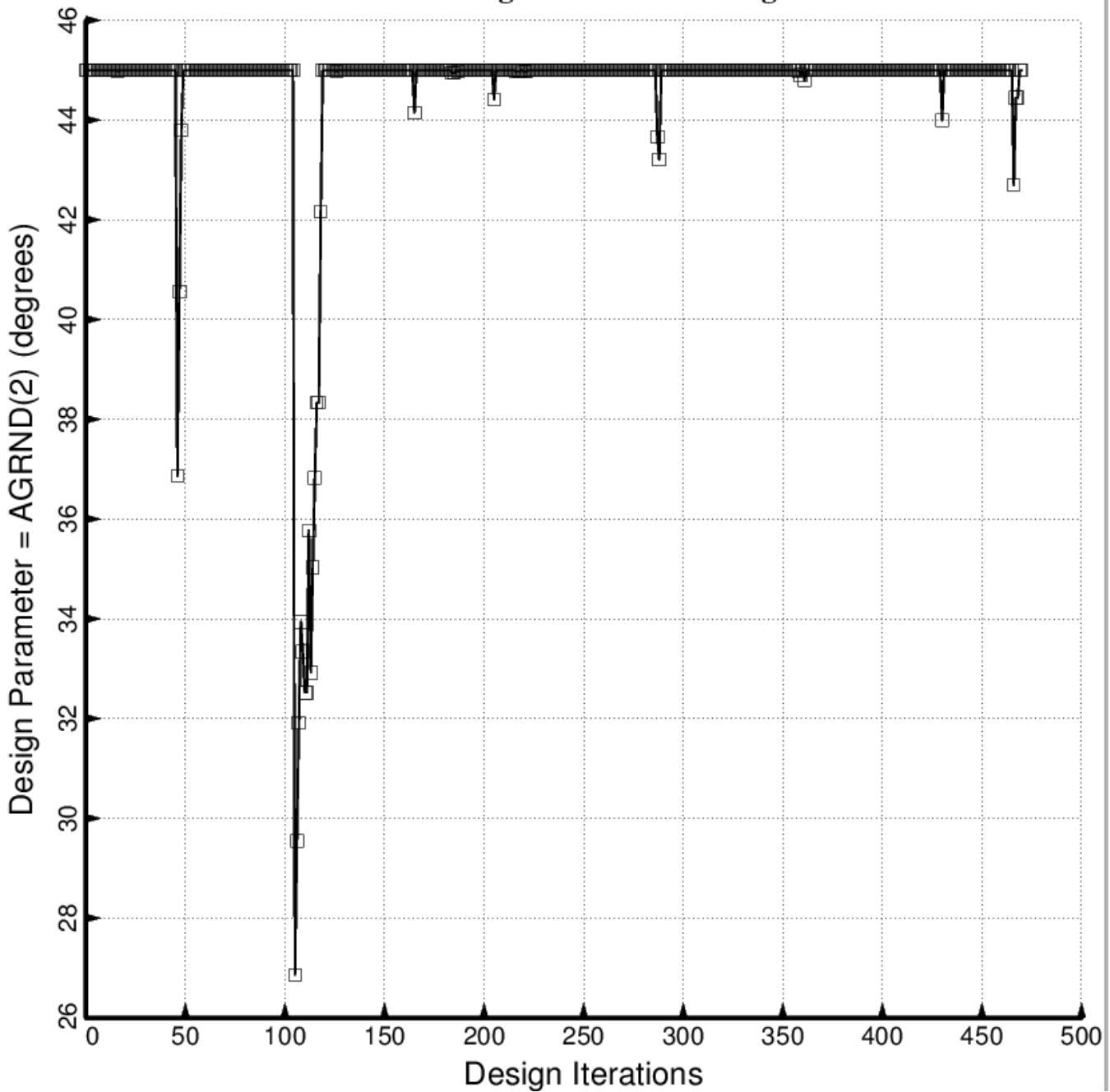


Fig. 71 (old) Temporary BIGBOSOR4/BOSDEC: Evolution of the decision variable,  $AGRND(2)$  = azimuthal angle to the “ground” end of the forward-slanting struts in the forward set of struts [the backward-slanting forward struts have  $-AGRND(2)$ ], during the first SUPEROPT execution involving the long propellant tank with aft and forward sets of struts, 4 strut pairs per set. This figure corresponds to the objective plotted in Fig. 59.

□ inner diam. of support tube active at launch: IDTUBE(1)

### GENOPT test: design variables vs design iterations

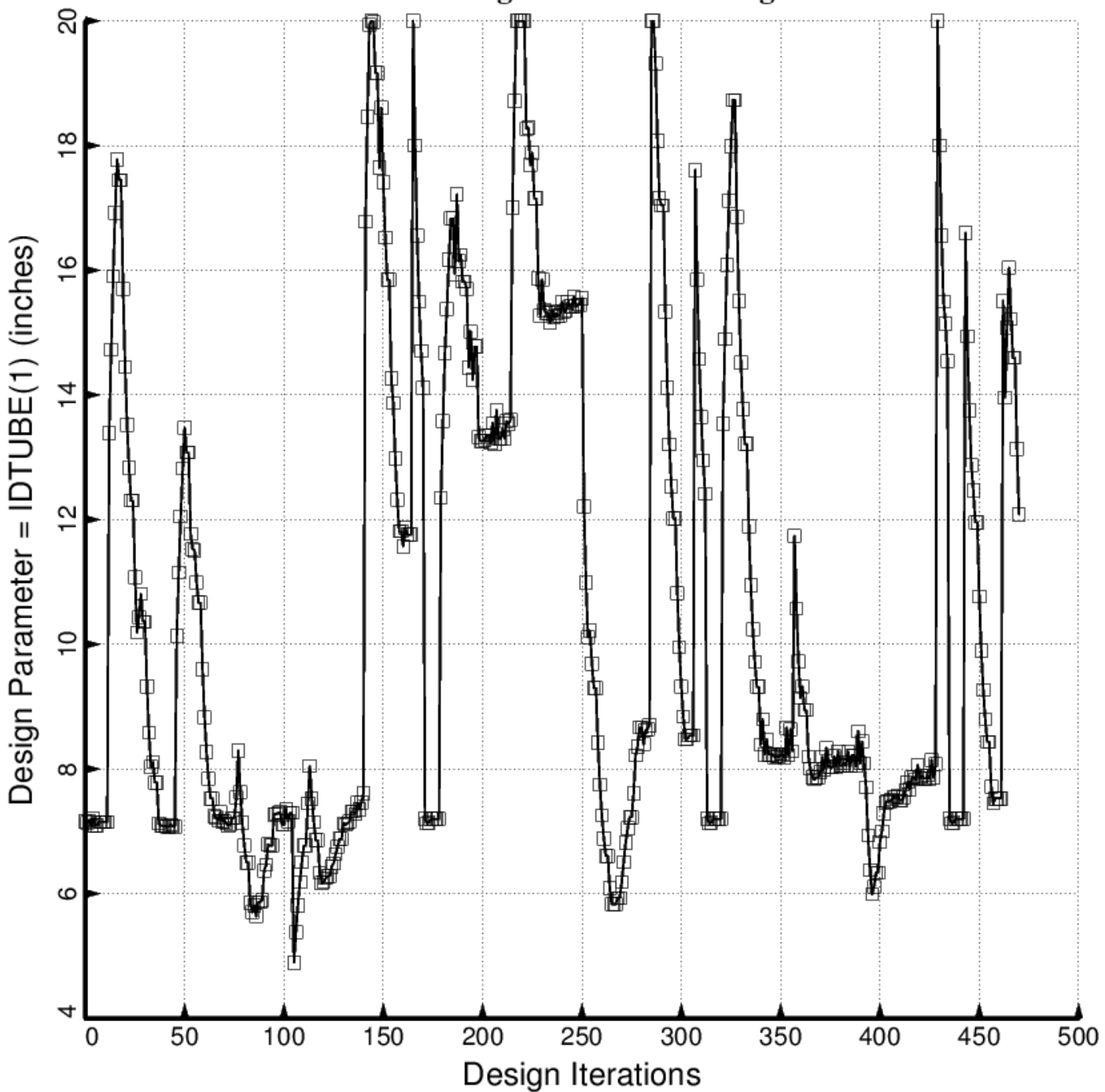


Fig. 72 (old) Temporary BIGBOSOR4/BOSDEC: Evolution of the decision variable,  $IDTUBE(1)$  = inner diameter of each aft strut tube, during the first SUPEROPT execution involving the long propellant tank with aft and forward sets of struts, 4 strut pairs per set. This figure corresponds to the objective plotted in Fig. 59.

□ inner diam. of support tube active at launch: IDTUBE(2)

### GENOPT test: design variables vs design iterations

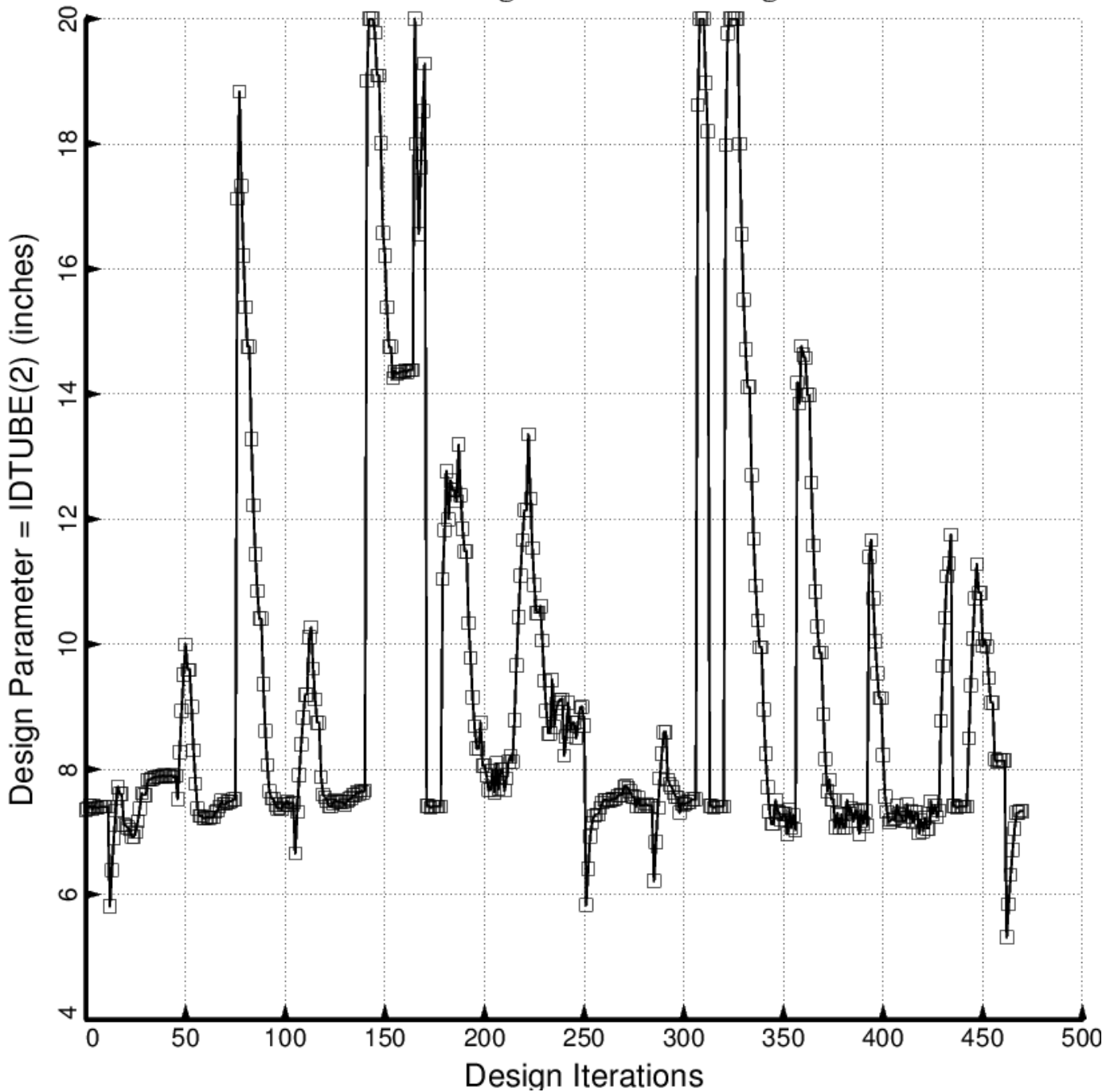


Fig. 73 (old) Temporary BIGBOSOR4/BOSDEC: Evolution of the decision variable,  $IDTUBE(2)$  = inner diameter of each forward strut tube, during the first SUPEROPT execution involving the long propellant tank with aft and forward sets of struts, 4 strut pairs per set. This figure corresponds to the objective plotted in Fig. 59.

□ max.thickness of the propellant tank doubler: DUBTHK(1 )

### GENOPT test: design variables vs design iterations

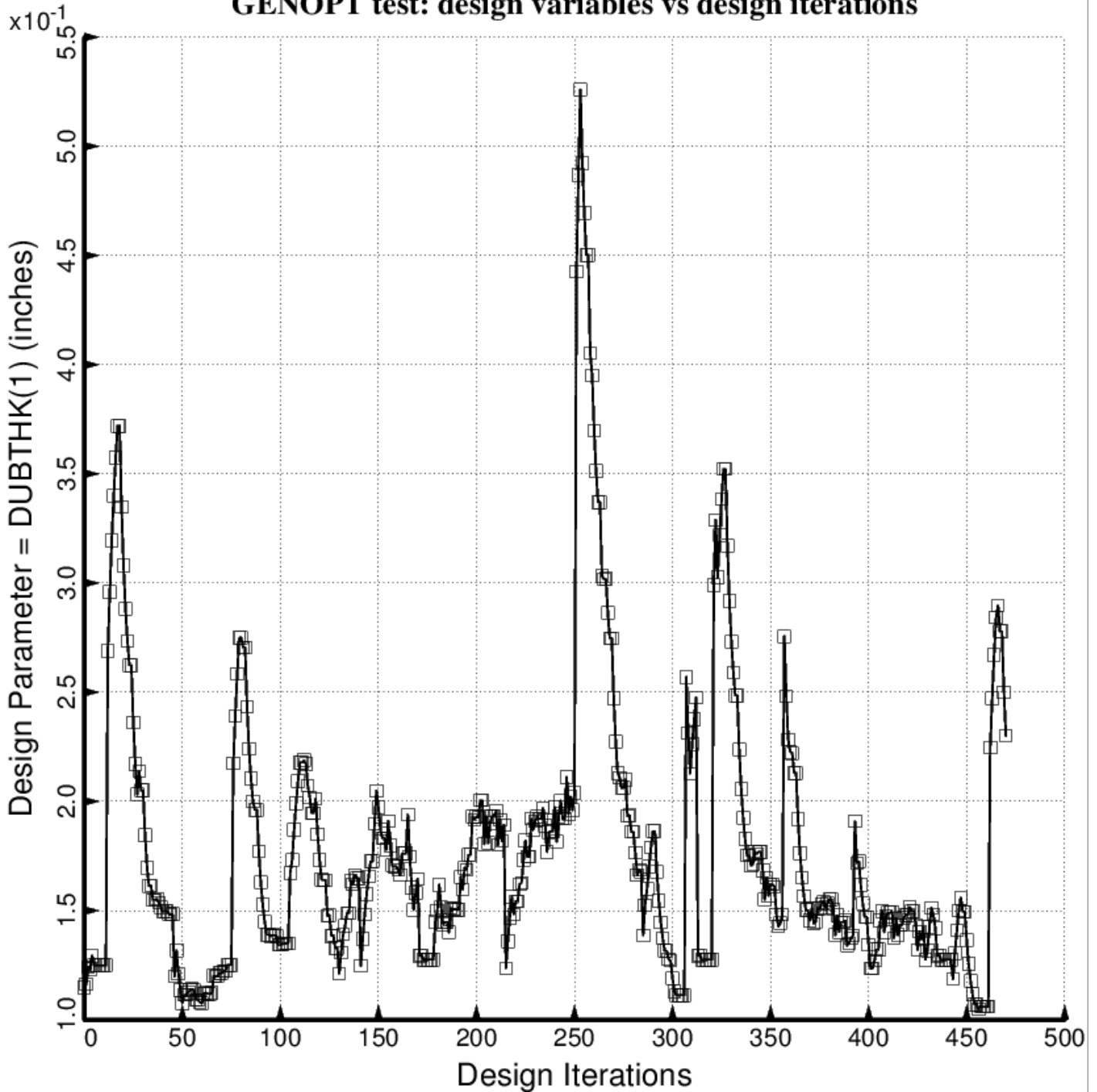


Fig. 74 (old) Temporary BIGBOSOR4/BOSDEC: Evolution of the decision variable,  $DUBTHK(1)$  = maximum thickness of the external tapered doubler, which is part of the tank reinforcement type 1, during the first SUPEROPT execution involving the long propellant tank with aft and forward sets of struts, 4 strut pairs per set. This figure corresponds to the objective plotted in Fig. 59.

□ thickness of the tank reinforcement ring: TRNGTH(1 )

### GENOPT test: design variables vs design iterations

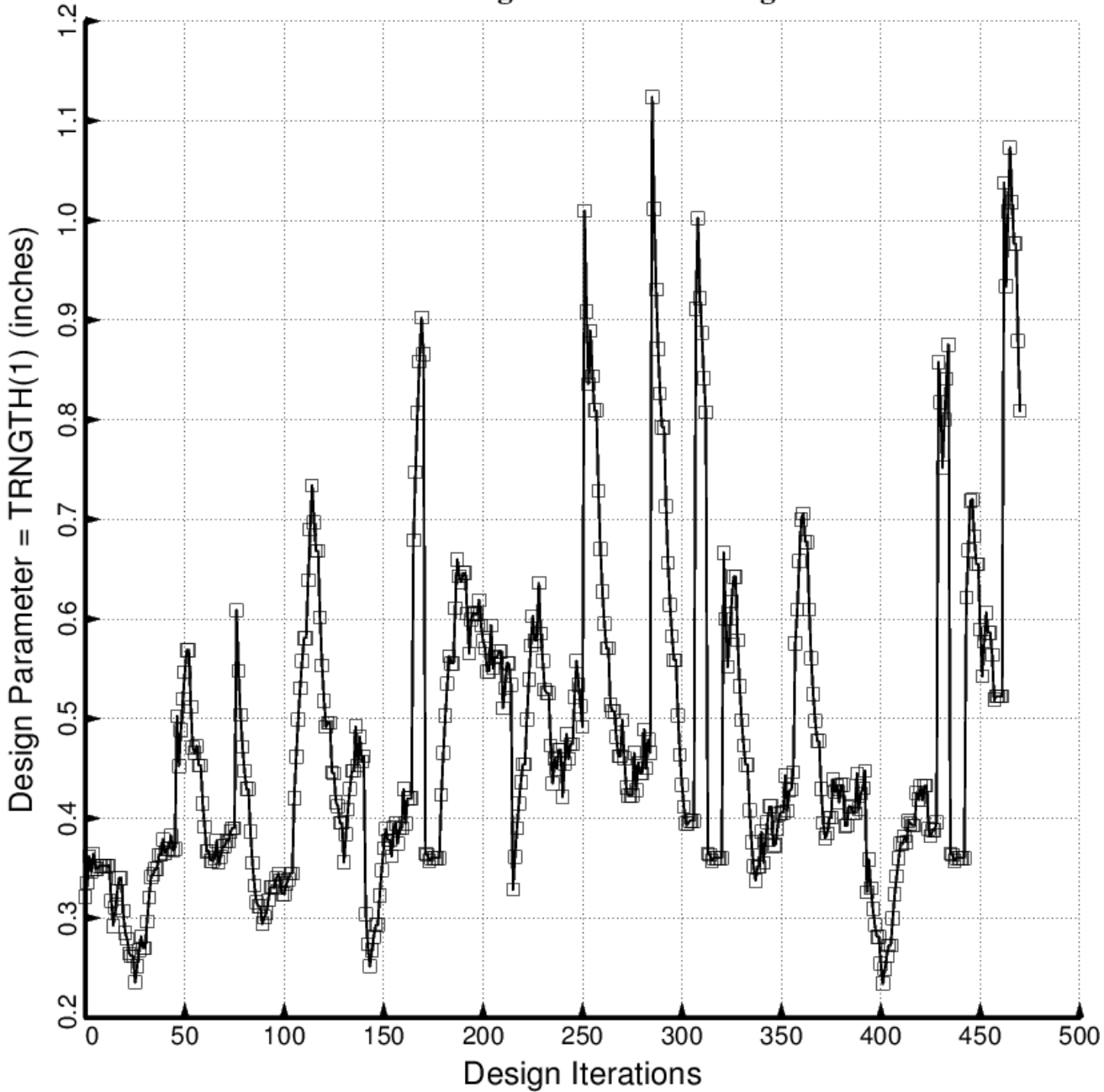


Fig. 75 (old) Temporary BIGBOSOR4/BOSDEC: Evolution of the decision variable,  $\text{TRNGTH}(1)$  = thickness of the external propellant tank ring, which is part of the tank reinforcement type 1. during the first SUPEROPT execution involving the long propellant tank with aft and forward sets of struts, 4 strut pairs per set. This figure corresponds to the objective plotted in Fig. 59. The cross section of the propellant tank support ring is rectangular with ring height equal to five times the ring thickness, a linking established by the End user during the interactive session with the GENOPT processor, DECIDE. (See Table 5).

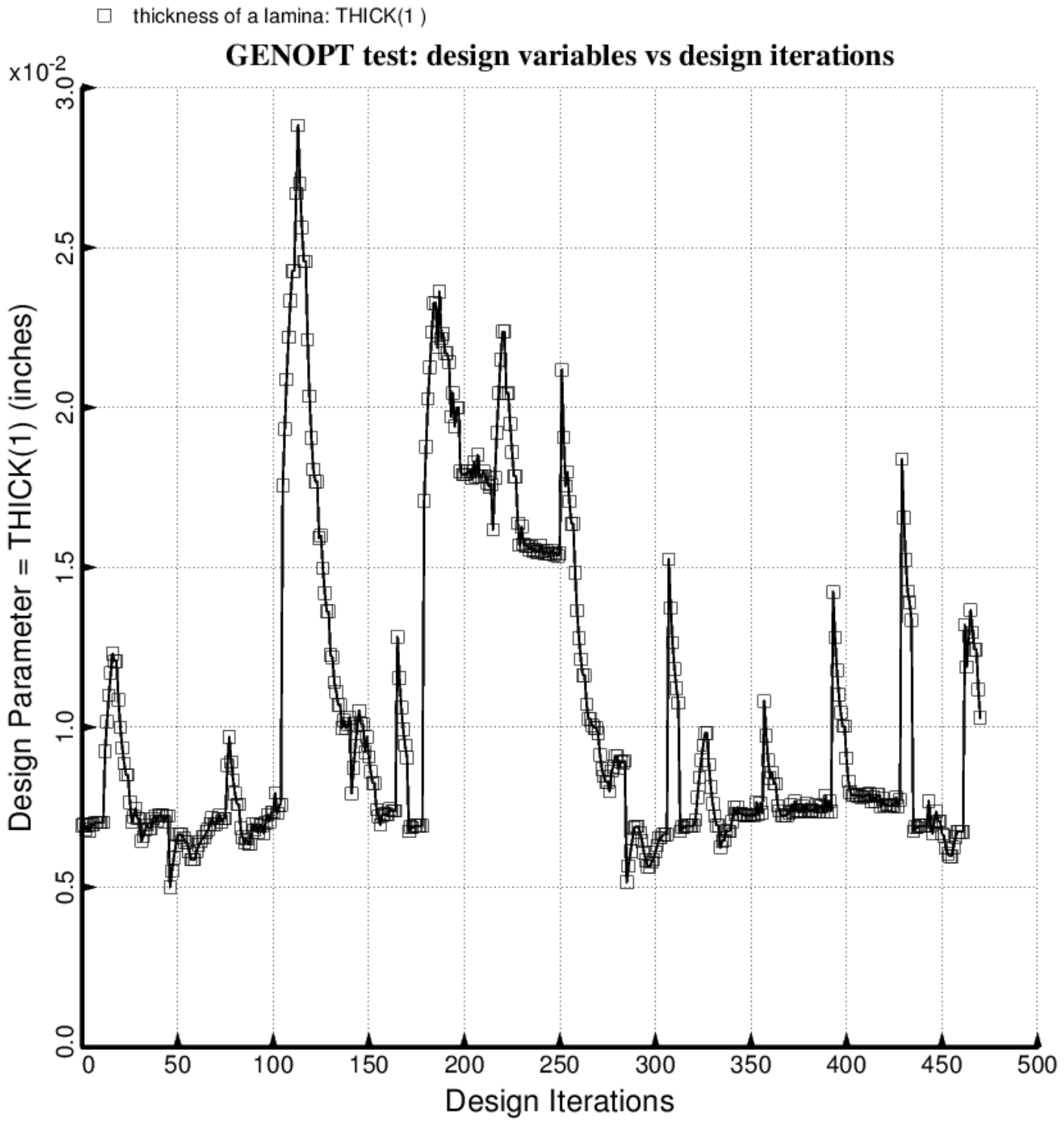


Fig. 76 (old) Temporary BIGBOSOR4/BOSDEC: Evolution of the decision variable, THICK(1) = thickness of inner and outer layer of each aft laminated composite strut tube, during the first SUPEROPT execution involving the long propellant tank with aft and forward sets of struts, 4 strut pairs per set. This figure corresponds to the objective plotted in Fig. 59. All other layers in the aft strut tube are linked to THICK(1).

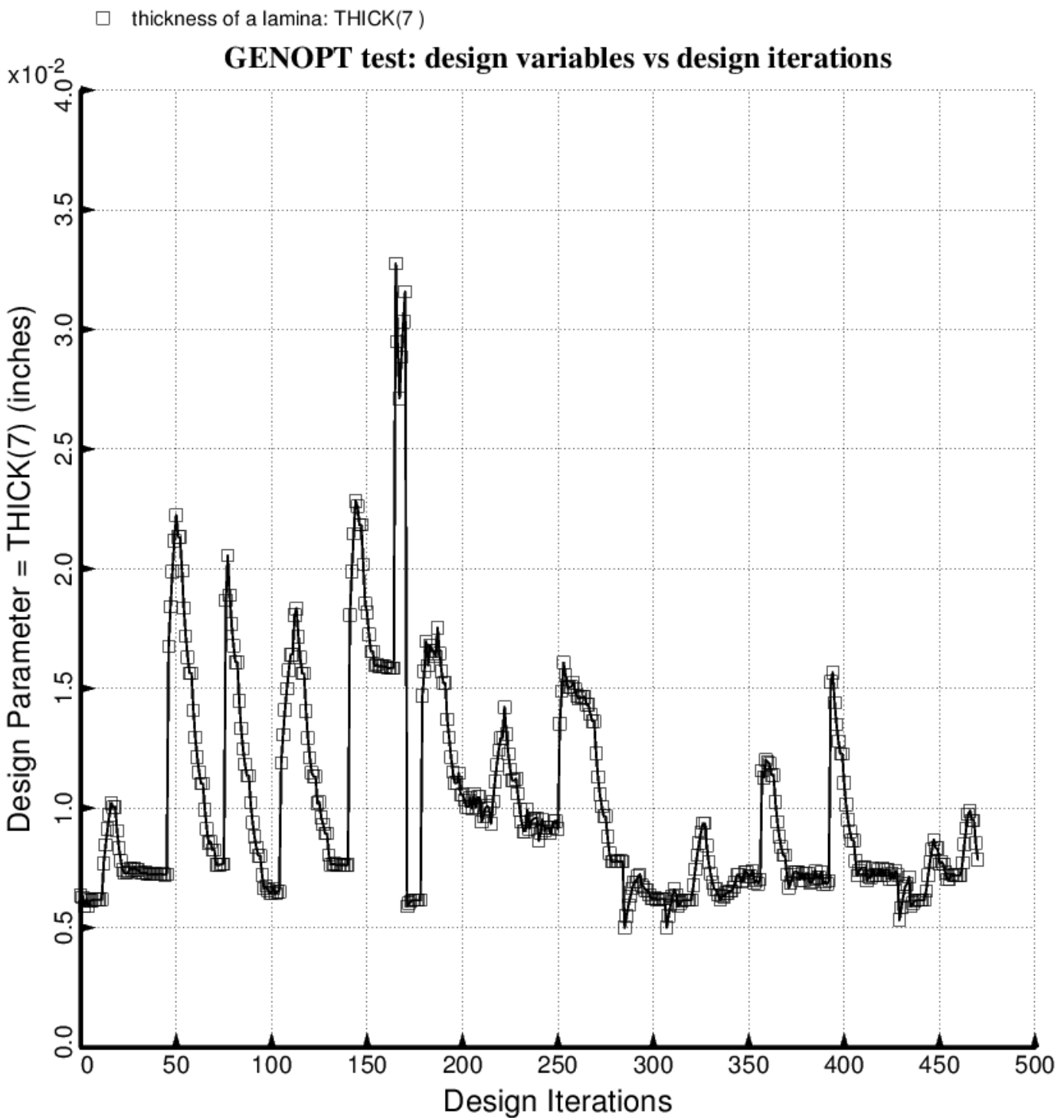


Fig. 77 (old) Temporary BIGBOSOR4/BOSDEC: Evolution of the decision variable, THICK(7) = thickness of inner and outer layer of each forward laminated composite strut tube, during the first SUPEROPT execution involving the long propellant tank with aft and forward sets of struts, 4 strut pairs per set. This figure corresponds to the objective plotted in Fig. 59. All other layers in the forward strut tube are linked to THICK(7).

□ layup angle: ANGLE(1 )

### GENOPT test: design variables vs design iterations

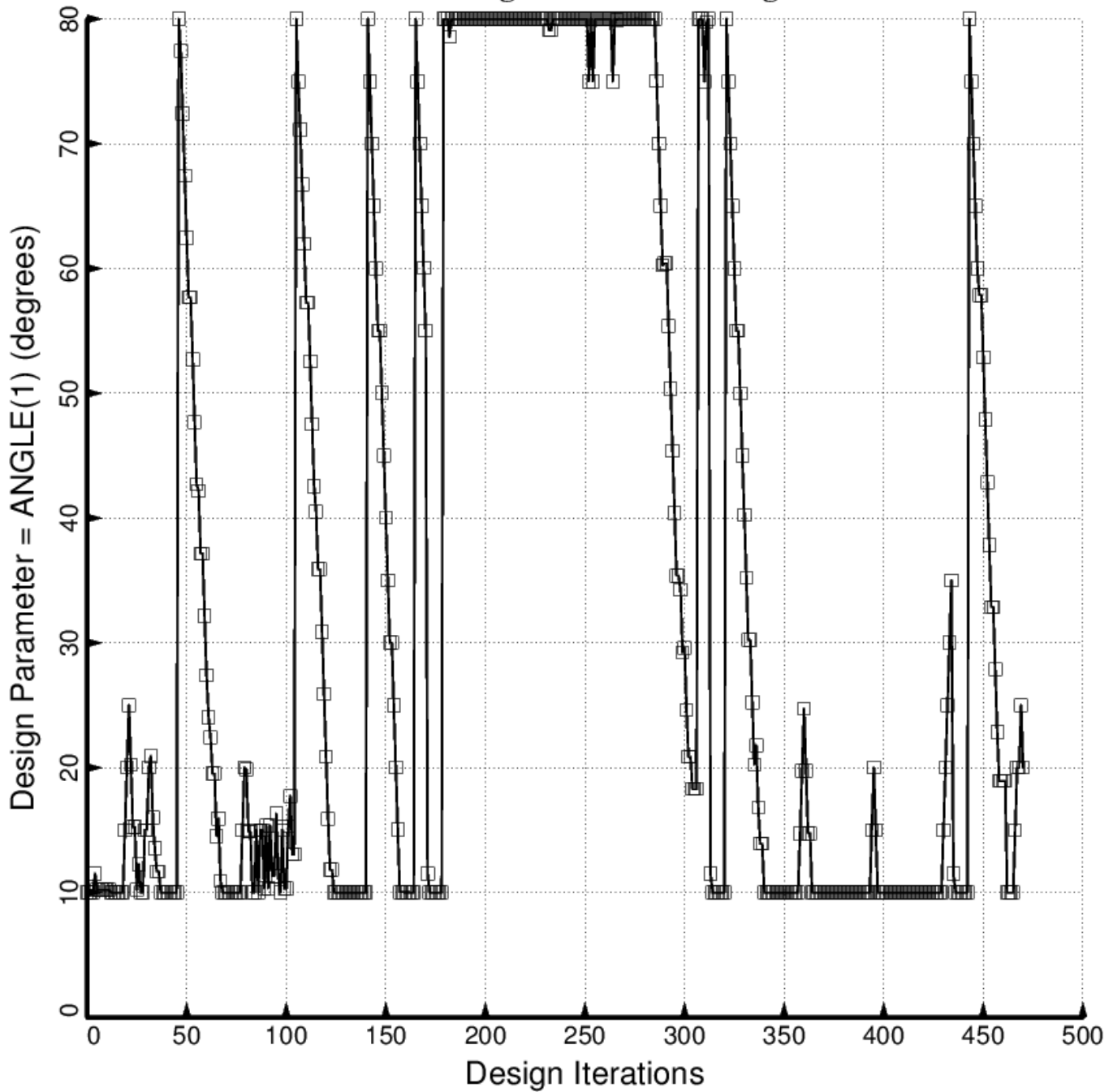


Fig. 78 (old) Temporary BIGBOSOR4/BOSDEC: Evolution of the decision variable, ANGLE(1) = layup angle of inner and outer layer of each aft laminated composite strut tube, during the first SUPEROPT execution involving the long propellant tank with aft and forward sets of struts, 4 strut pairs per set. This figure corresponds to the objective plotted in Fig. 59. ANGLE(2) is linked to ANGLE(1) with a linking coefficient equal to -1.0.

□ layup angle: ANGLE(3 )

### GENOPT test: design variables vs design iterations

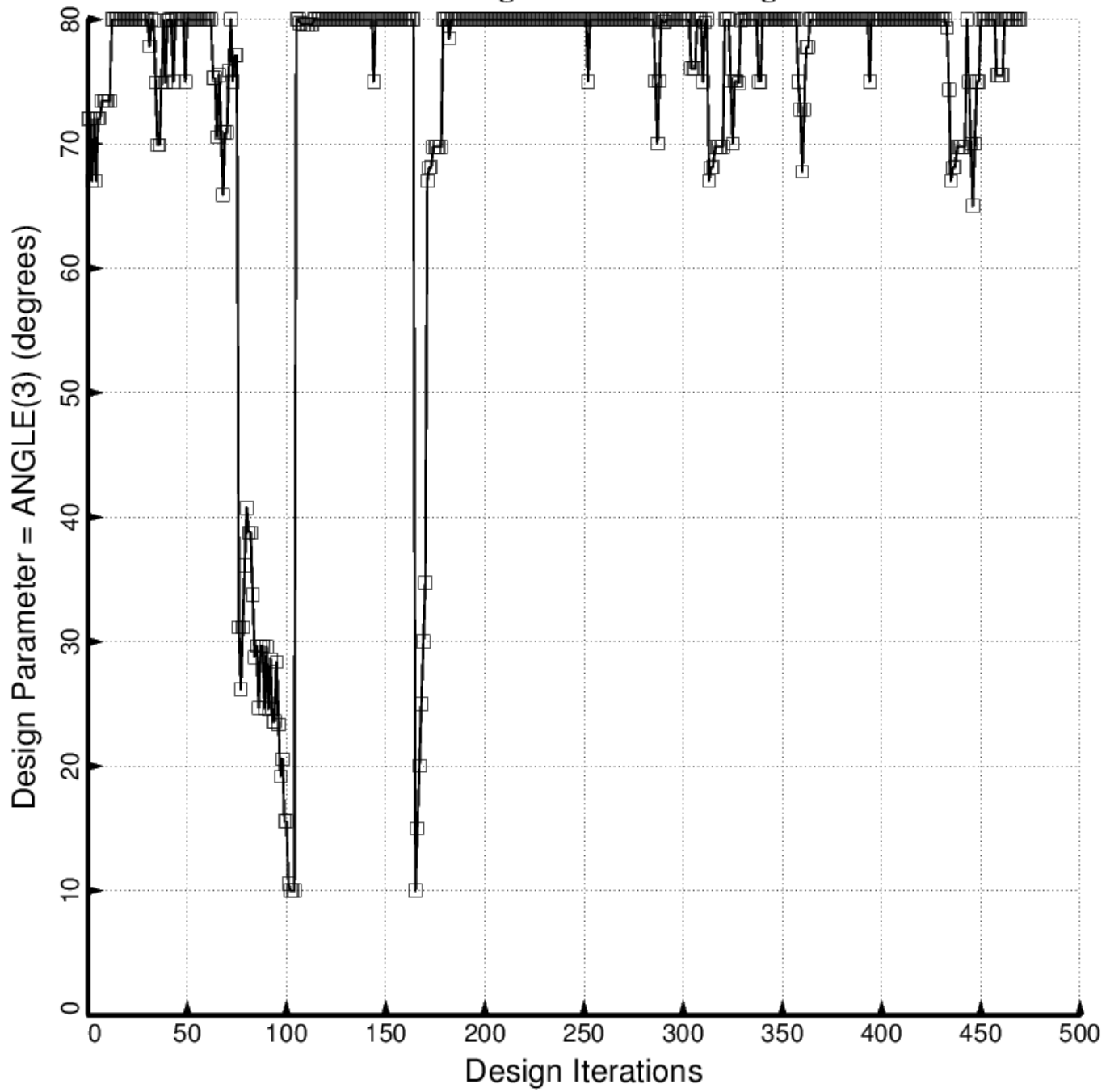


Fig. 79 (old) Temporary BIGBOSOR4/BOSDEC: Evolution of the decision variable,  $\text{ANGLE}(3)$  = layup angle of third and 10th layer of each aft laminated composite strut tube, during the first SUPEROPT execution involving the long propellant tank with aft and forward sets of struts, 4 strut pairs per set. This figure corresponds to the objective plotted in Fig. 59.  $\text{ANGLE}(4)$  is linked to  $\text{ANGLE}(3)$  with a linking coefficient equal to  $-1.0$ .

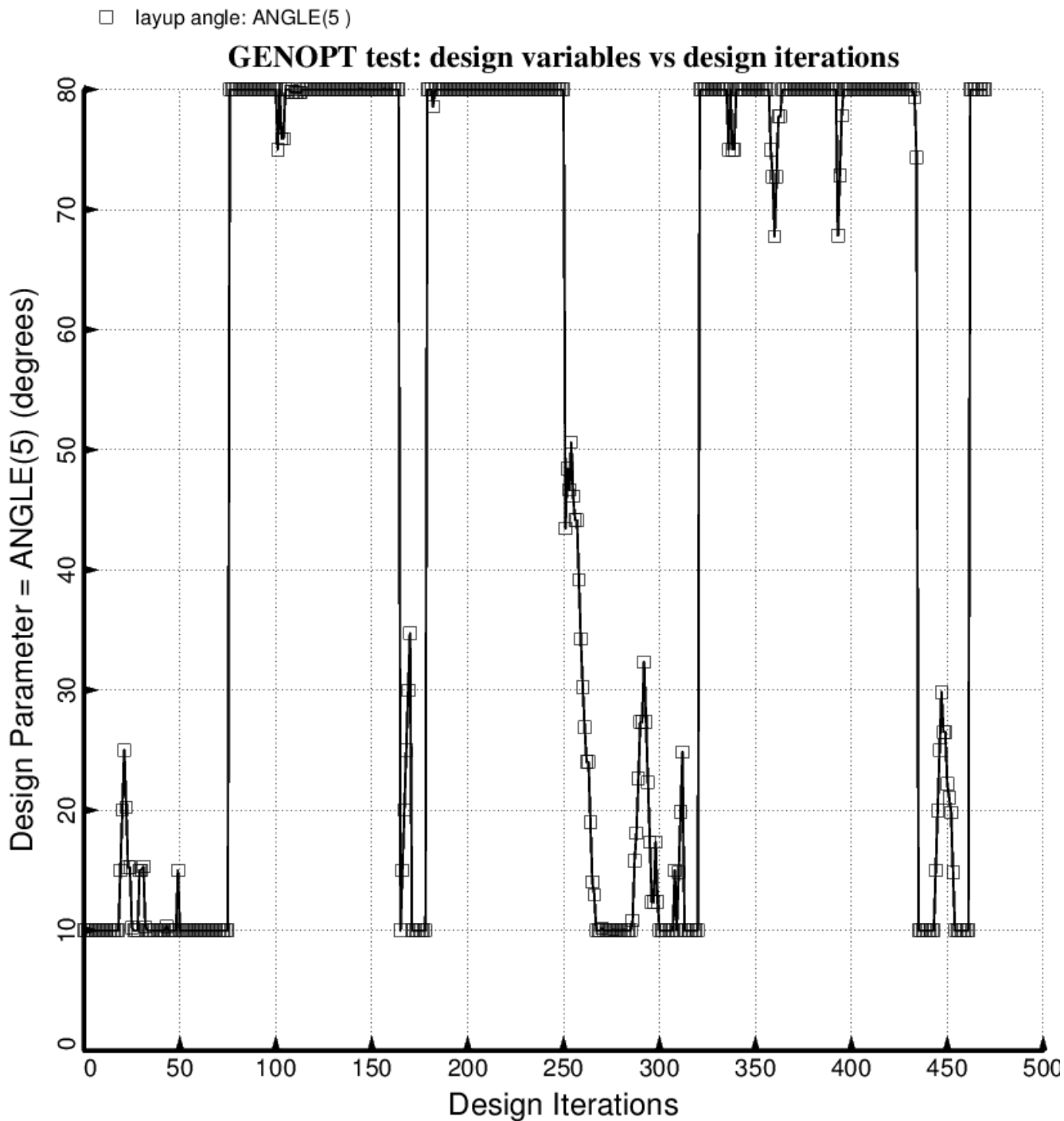


Fig. 80 (old) Temporary BIGBOSOR4/BOSDEC: Evolution of the decision variable,  $\text{ANGLE}(5) = \text{layup angle}$  of fifth and 8th layer of each aft laminated composite strut tube, during the first SUPEROPT execution involving the long propellant tank with aft and forward sets of struts, 4 strut pairs per set. This figure corresponds to the objective plotted in Fig. 59.  $\text{ANGLE}(6)$  is linked to  $\text{ANGLE}(5)$  with a linking coefficient equal to -1.0.

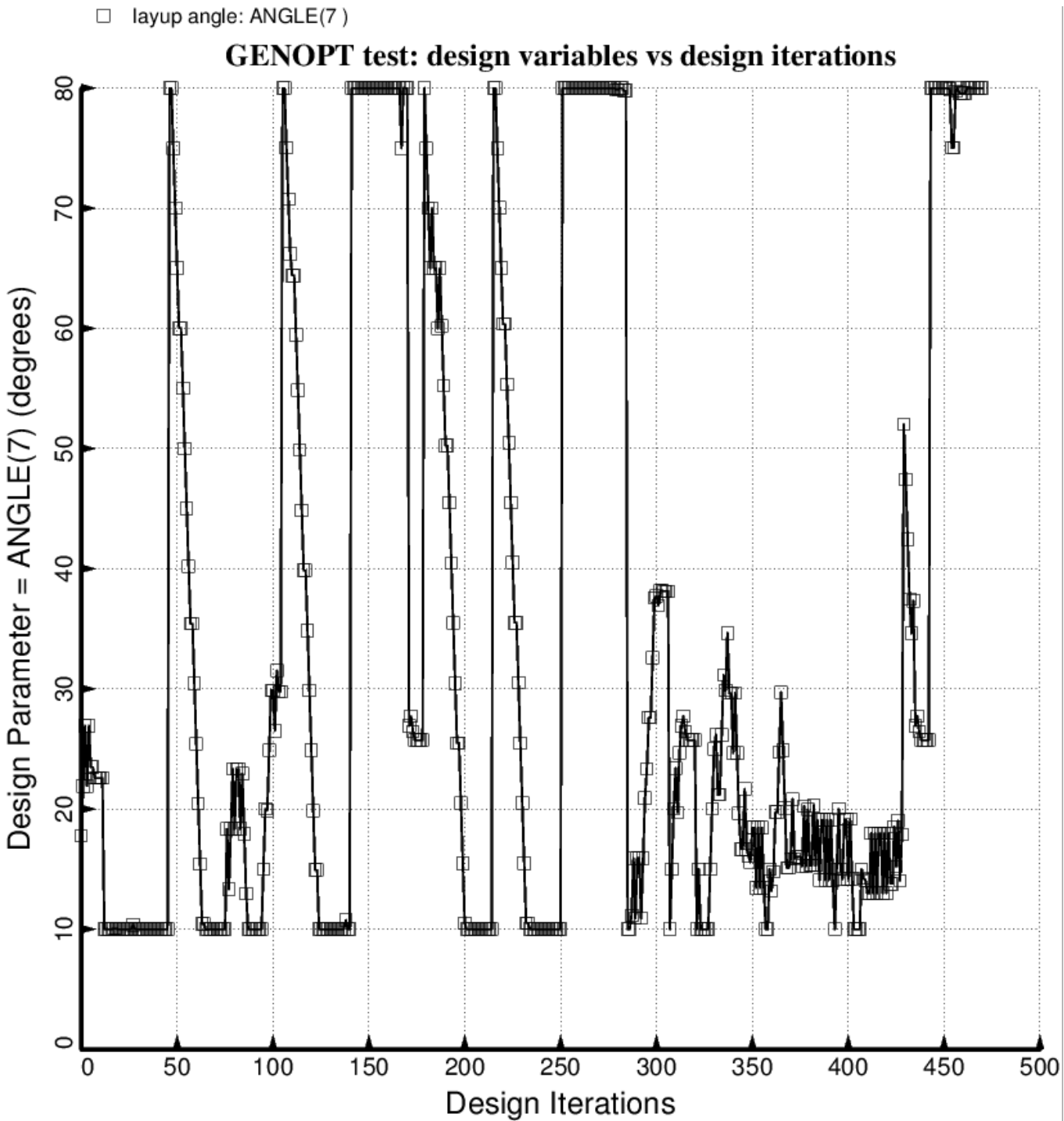


Fig. 81 (old) Temporary BIGBOSOR4/BOSDEC: Evolution of the decision variable,  $\text{ANGLE}(7) = \text{layup angle}$  of inner and outer layer of each forward laminated composite strut tube, during the first SUPEROPT execution involving the long propellant tank with aft and forward sets of struts, 4 strut pairs per set. This figure corresponds to the objective plotted in Fig. 59.  $\text{ANGLE}(8)$  is linked to  $\text{ANGLE}(7)$  with a linking coefficient equal to  $-1.0$ .

□ layup angle: ANGLE(9 )

### GENOPT test: design variables vs design iterations

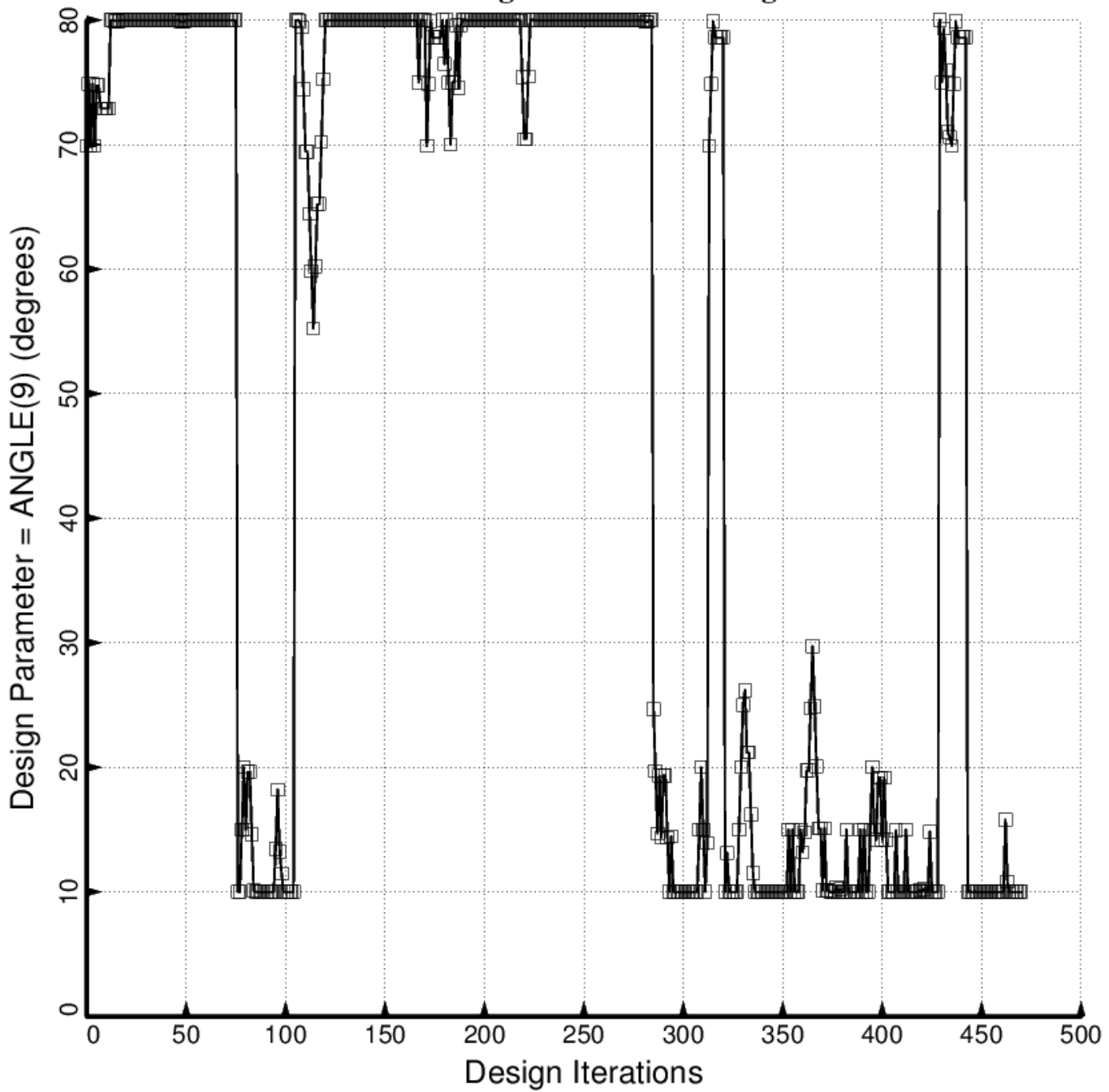


Fig. 82 (old) Temporary BIGBOSOR4/BOSDEC: Evolution of the decision variable,  $\text{ANGLE}(9)$  = layup angle of third and tenth layer of each forward laminated composite strut tube, during the first SUPEROPT execution involving the long propellant tank with aft and forward sets of struts, 4 strut pairs per set. This figure corresponds to the objective plotted in Fig. 59.  $\text{ANGLE}(10)$  is linked to  $\text{ANGLE}(9)$  with a linking coefficient equal to  $-1.0$ .

□ layup angle: ANGLE(11)

### GENOPT test: design variables vs design iterations

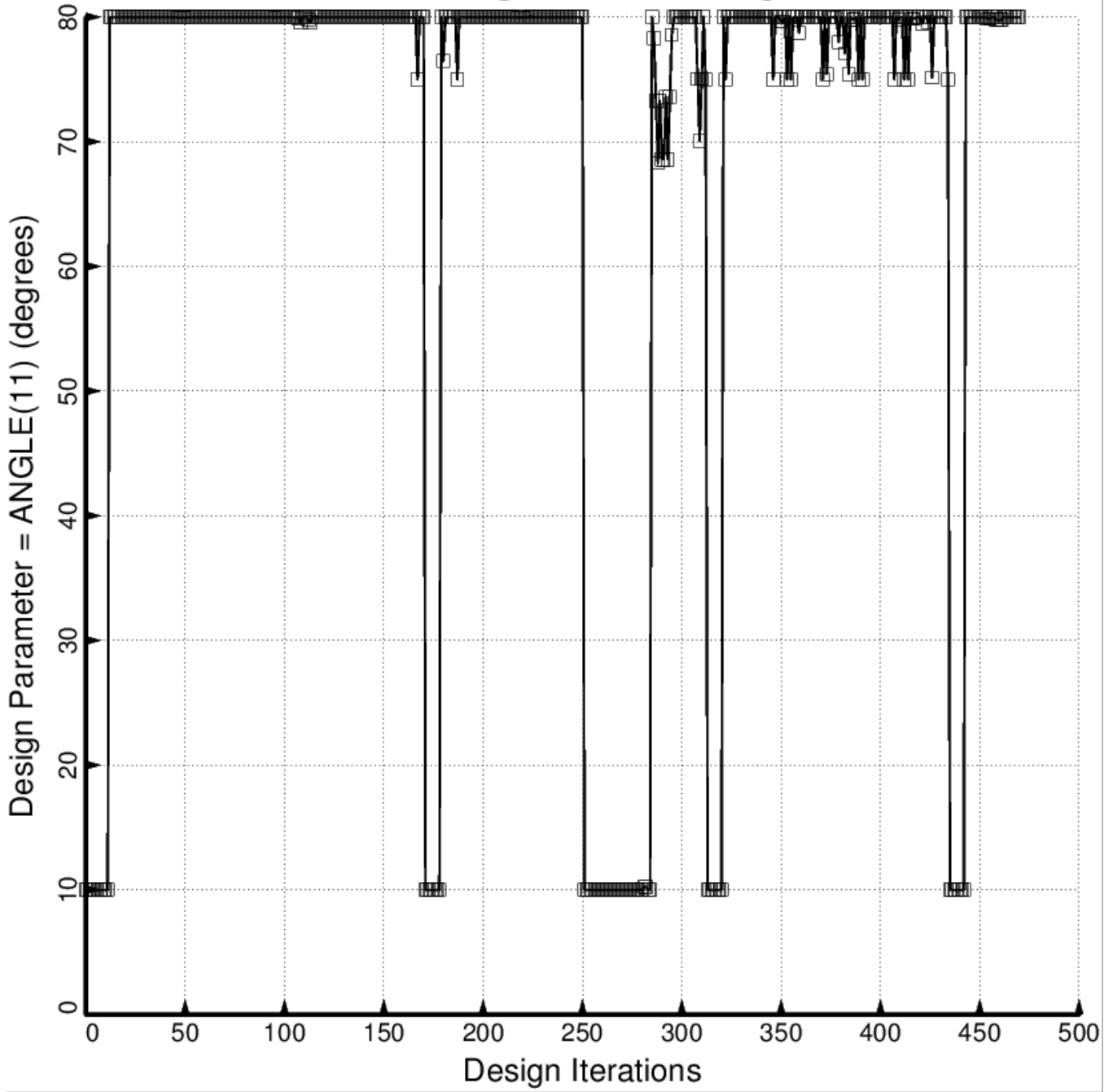


Fig. 83 (old) Temporary BIGBOSOR4/BOSDEC: Evolution of the decision variable,  $\text{ANGLE}(11) = \text{layup angle}$  of fifth and eighth layer of each forward laminated composite strut tube, during the first SUPEROPT execution involving the long propellant tank with aft and forward sets of struts, 4 strut pairs per set. This figure corresponds to the objective plotted in Fig. 59.  $\text{ANGLE}(12)$  is linked to  $\text{ANGLE}(11)$  with a linking coefficient equal to  $-1.0$ .

- $\square$  (FREQ(1,1)/FREQA(1,1)) / FREQF(1,1)-1; F.S.= 1.20
- $\circ$  (FREQ(1,2)/FREQA(1,2)) / FREQF(1,2)-1; F.S.= 1.20
- $\triangle$  (FREQ(1,3)/FREQA(1,3)) / FREQF(1,3)-1; F.S.= 1.20
- $+$  (FREQ(1,4)/FREQA(1,4)) / FREQF(1,4)-1; F.S.= 1.20
- $\times$  (STRES2A(1,3)/STRES2(1,3)) / STRES2F(1,3)-1; F.S.= 1.50
- $\diamond$  (FORCEA(1,2)/FORCE(1,2)) / FORCEF(1,2)-1; F.S.= 1.00
- $\nabla$  (TNKSTRA(1,1)/TNKSTR(1,1)) / TNKSTRF(1,1)-1; F.S.= 1.00

GENOPT test: design margins vs design iterations

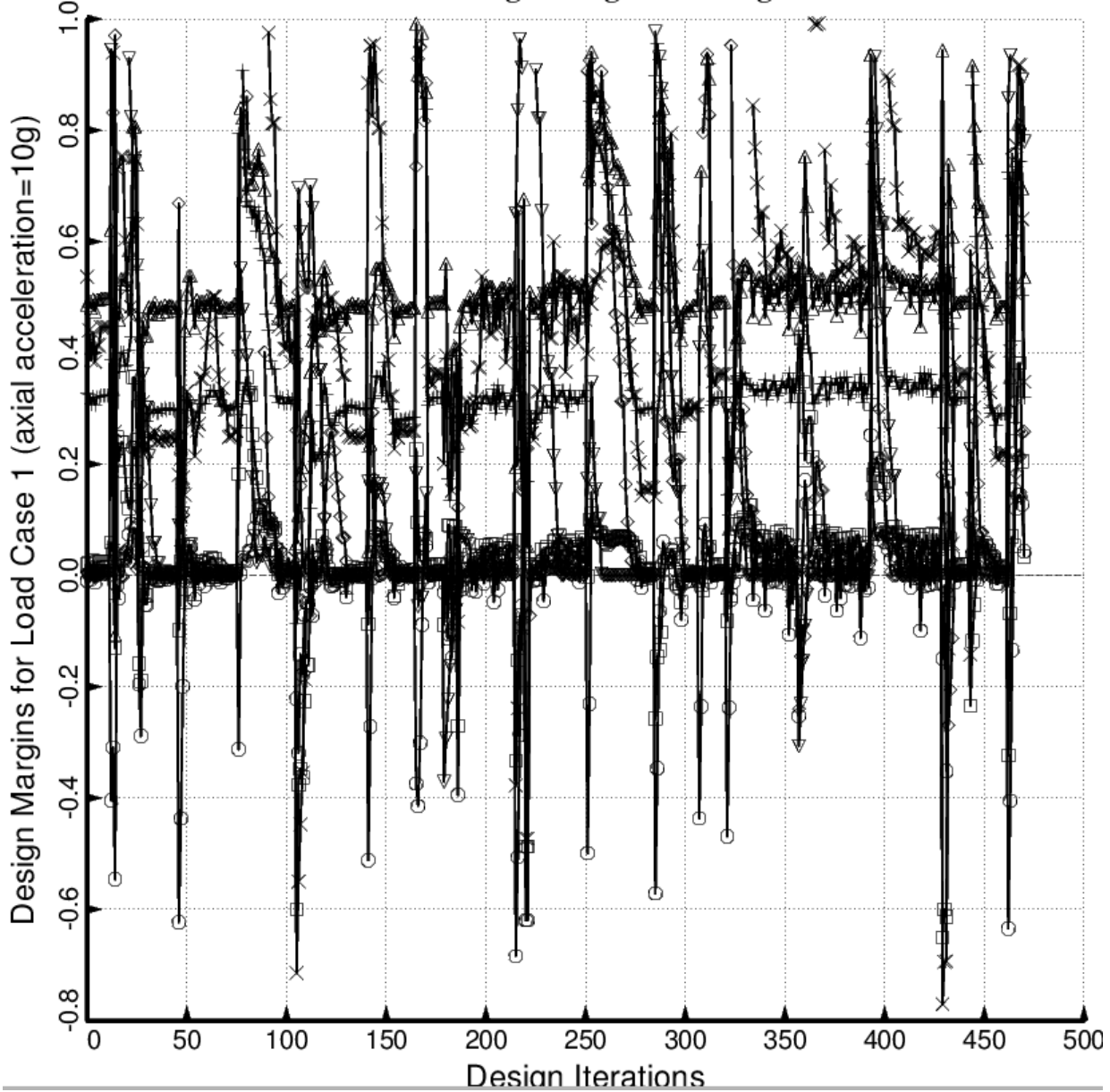


Fig. 84 (old) Temporary BIGBOSOR4/BOSDEC: Evolution of the most critical design margins for Load Case 1 (10g axial acceleration, 25 psi ullage pressure, 200 degree tank cool-down), during the first SUPEROPT execution involving the long propellant tank with aft and forward sets of struts, 4 strut pairs per set. This figure corresponds to the objective plotted in Fig. 59.

□ (FREQ(2,1)/FREQA(2,1)) / FREQF(2,1)-1; F.S.= 1.20  
 ○ (FREQ(2,2)/FREQA(2,2)) / FREQF(2,2)-1; F.S.= 1.20  
 △ (FREQ(2,3)/FREQA(2,3)) / FREQF(2,3)-1; F.S.= 1.20  
 + (FREQ(2,4)/FREQA(2,4)) / FREQF(2,4)-1; F.S.= 1.20  
 × (STRES1A(2,2)/STRES1(2,2)) / STRES1F(2,2)-1; F.S.= 1.50  
 ◇ (STRES1A(2,3)/STRES1(2,3)) / STRES1F(2,3)-1; F.S.= 1.50  
 ▽ (STRES2A(2,1)/STRES2(2,1)) / STRES2F(2,1)-1; F.S.= 1.50  
 ▨ (STRES2A(2,2)/STRES2(2,2)) / STRES2F(2,2)-1; F.S.= 1.50  
 × (STRES2A(2,3)/STRES2(2,3)) / STRES2F(2,3)-1; F.S.= 1.50  
 ♦ (COLBUK(2,2)/COLBUKA(2,2)) / COLBUKF(2,2)-1; F.S.= 1.00  
 ⊕ (SHLBUK(2,1)/SHLBUKA(2,1)) / SHLBUKF(2,1)-1; F.S.= 2.00  
 □ (SHLBUK(2,2)/SHLBUKA(2,2)) / SHLBUKF(2,2)-1; F.S.= 2.00  
 ▨ (FORCEA(2,2)/FORCE(2,2)) / FORCEF(2,2)-1; F.S.= 1.00  
 ▨ (TNKSTR(2,1)/TNKSTR(2,1)) / TNKSTRF(2,1)-1; F.S.= 1.00  
 □ (TNKSTR(2,2)/TNKSTR(2,2)) / TNKSTRF(2,2)-1; F.S.= 1.00

**GENOPT test: design margins vs design iterations**

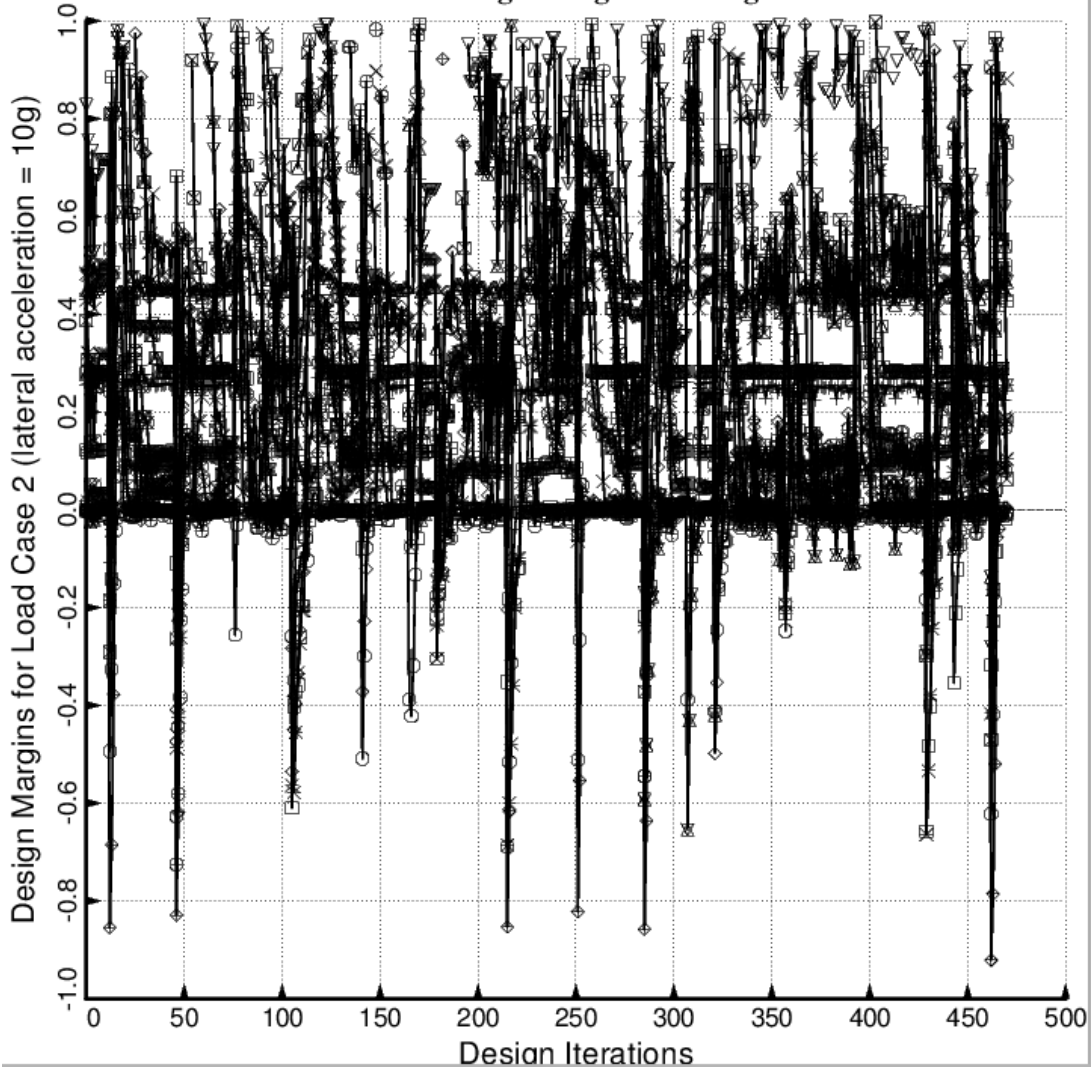


Fig. 85 (old) Temporary BIGBOSOR4/BOSDEC: Evolution of the most critical design margins for Load Case 2 (10g lateral acceleration, 25 psi ullage pressure, 200 degree tank cool-down), during the first SUPEROPT execution involving the long propellant tank with aft and forward sets of struts, 4 strut pairs per set. This figure corresponds to the objective plotted in Fig. 59.

$\square$  objective =  $0.5 \times (\text{TOTMAS}/3.0) + (1 - 0.5) \times (\text{CONDCT}/0.0006)$

### test2: objective vs design iterations (temporary BIGBOSOR4/BOSDEC)

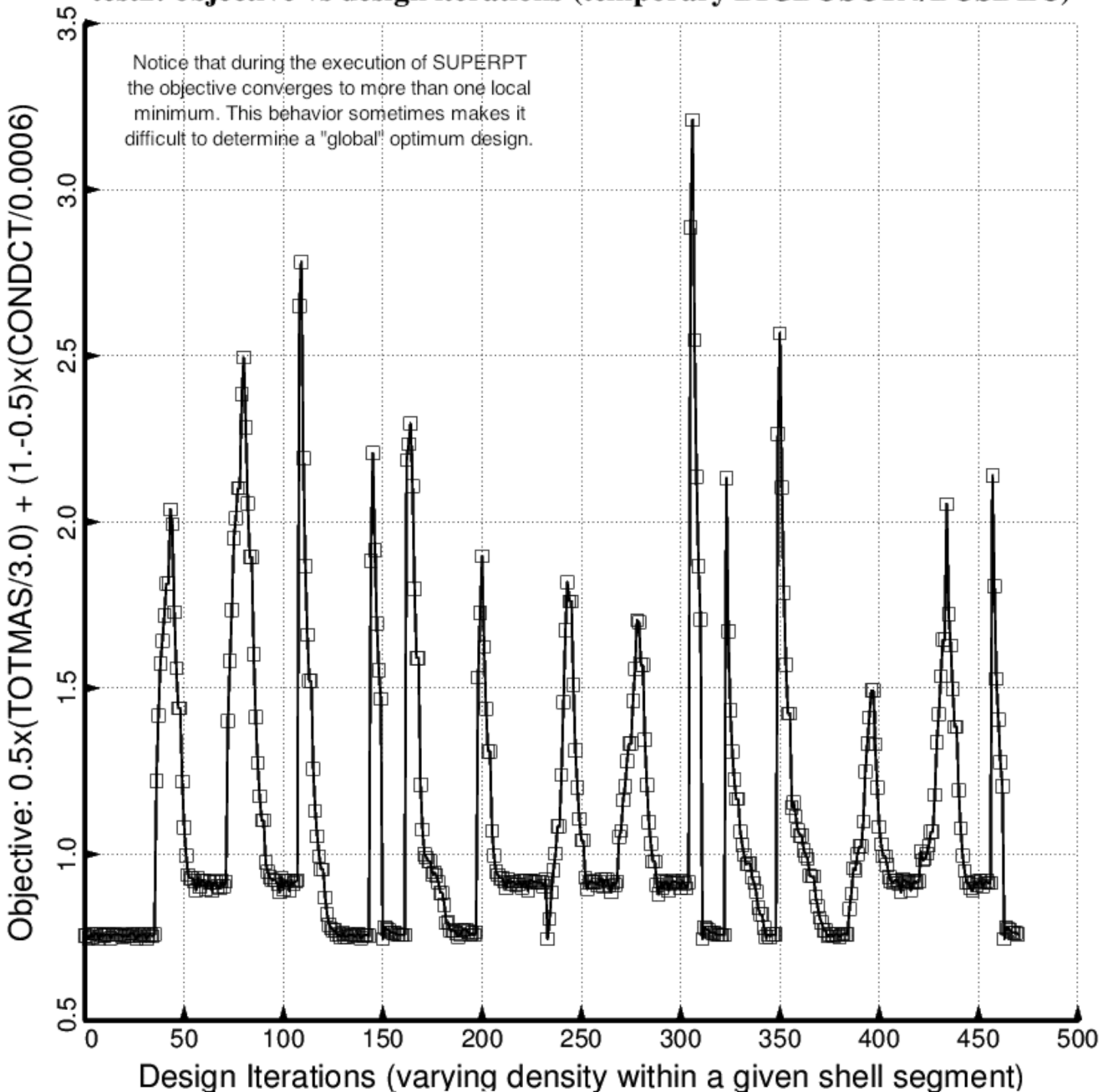


Fig. 86 (old) “Temporary” BIGBOSOR4/BOSDEC: Evolution of the objective during the second execution of the GENOPT processor, SUPEROPT, for the short tank/strut system with only one set of struts attached to the propellant tank at the midlength of the short cylindrical part of the tank. Notice that during the long SUPEROPT process (about 15 hours of computer time on the writer’s very fast computer) the objective converges to more than one local minimum. This behavior makes it difficult to find a “global” optimum design. Compare with Fig. 88, which was generated with strut tube layup angle, ANGLE(5), fixed at 10 degrees.

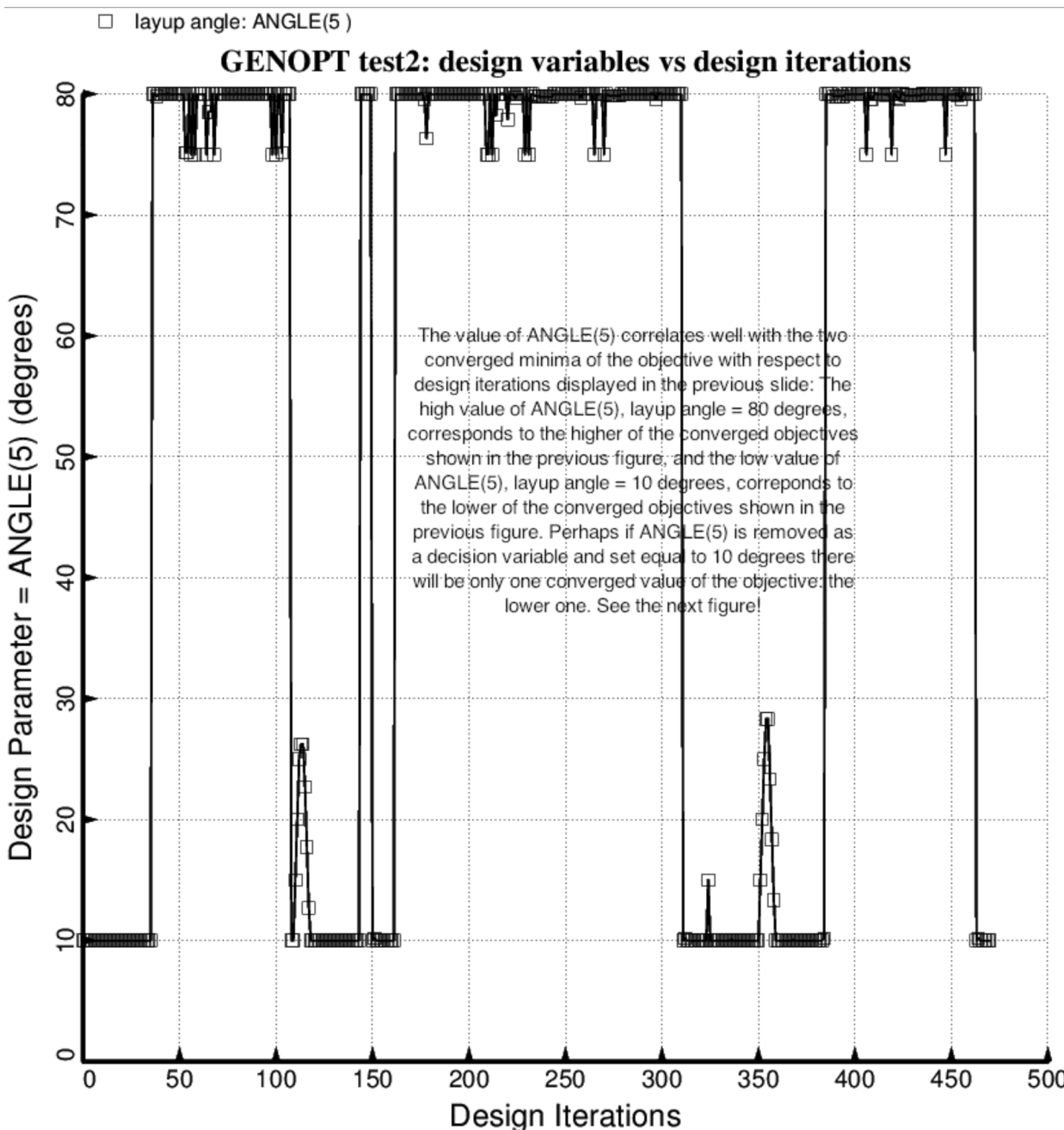


Fig. 87 (old) “Temporary” BIGBOSOR4/BOSDEC: Evolution of the strut tube layup angle, ANGLE(5) = layup angle of layers 3 and 10 of a strut tube, during the second execution of the GENOPT processor, SUPEROPT, for the short tank/strut system with only one set of struts attached to the propellant tank at the midlength of the short cylindrical part of the tank. The behavior of ANGLE(5) during this execution of SUPEROPT correlates well with the higher and lower local minima of the converged objective plotted in the previous figure. Therefore, another execution of SUPEROPT was performed, this time with ANGLE(5) fixed at 10 degrees (which corresponds to the “global” optimum design) rather than being chosen as a decision variable. The result of that SUPERPT run is plotted in the next figure.

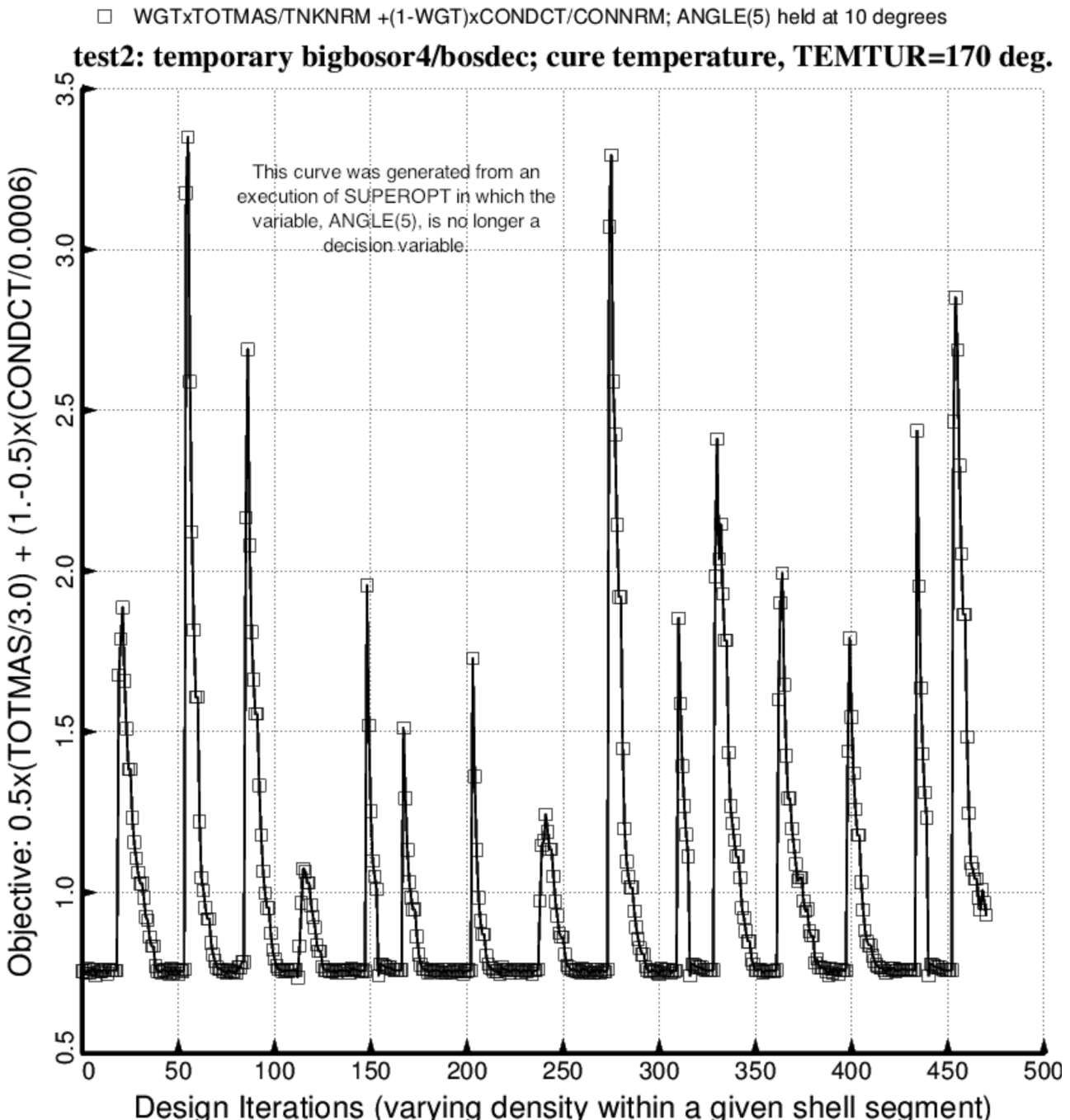


Fig. 88 (old) “Temporary” BIGBOSOR4/BOSDEC: Evolution of the objective during the second execution of the GENOPT processor, SUPEROPT, for the short tank/strut system with only one set of struts attached to the propellant tank at the midlength of the short cylindrical part of the tank. Notice that during the long SUPEROPT process (about 15 hours of computer time on the writer’s very fast computer) the objective converges to only one local minimum. This behavior makes it easier to find a “global” optimum design. Compare with Fig. 86, which was generated with strut tube layup angle, ANGLE(5), chosen as one of the decision variables..

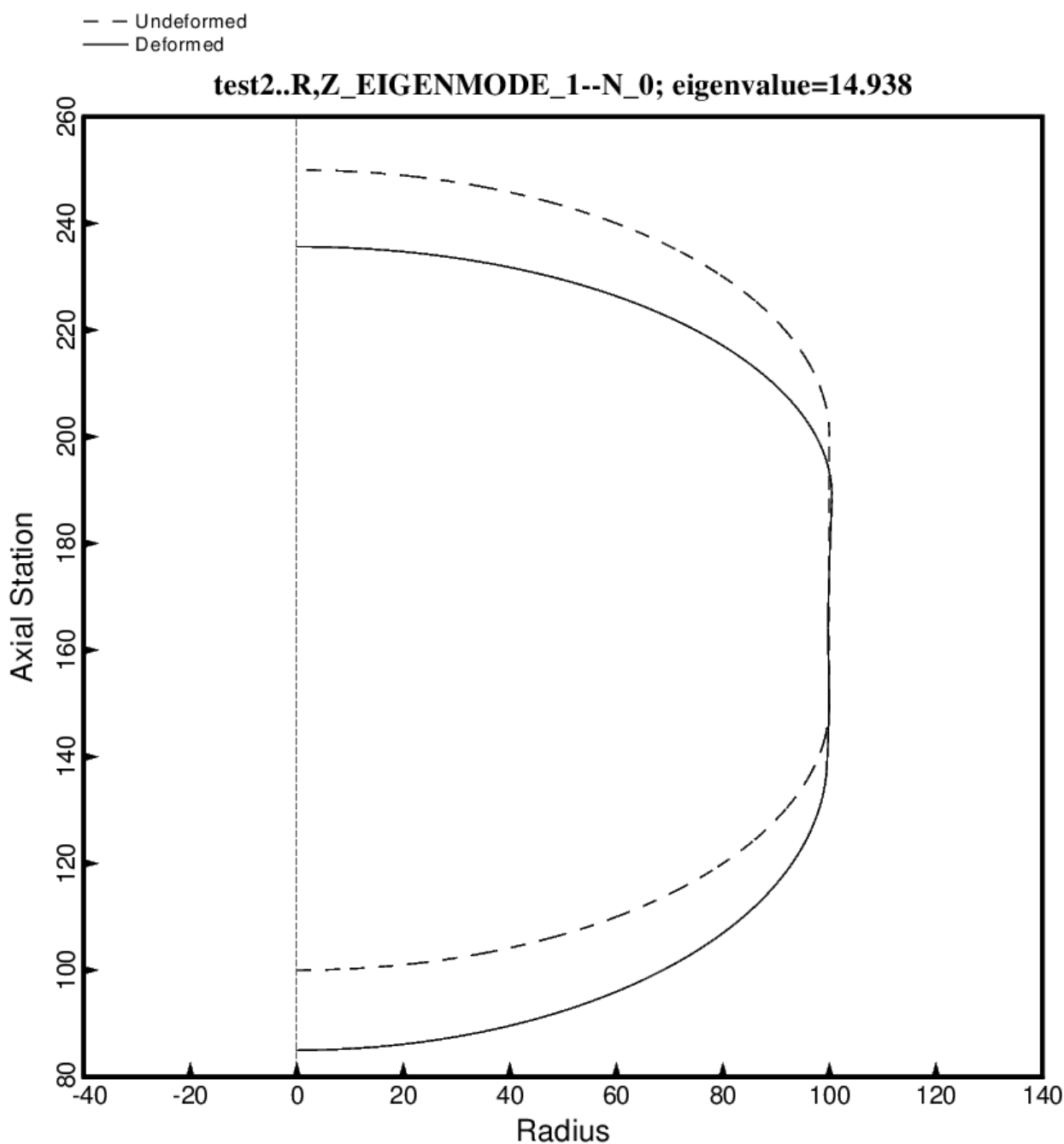


Fig. 89 (new) Free vibration mode of the optimized tank/strut system for the short propellant tank with one set of struts, 4 strut pairs in that set, Load Case 2 (test.BEHX12). The struts are attached to a propellant tank support ring located at the same axial coordinate as the midlength of the propellant tank. The struts are present in the BIGBOSOR4 model but are not plotted here because BIGBOSOR4 does not yet have the capability to plot springs. This first mode with  $n = 0$  circumferential waves corresponds to axial motion. The optimum design was found with use of the “permanent” (constant density) versions of bosdec (bosdec.tank) and addbosor4 (addbosor4.tank). This figure is analogous to Fig. 19.

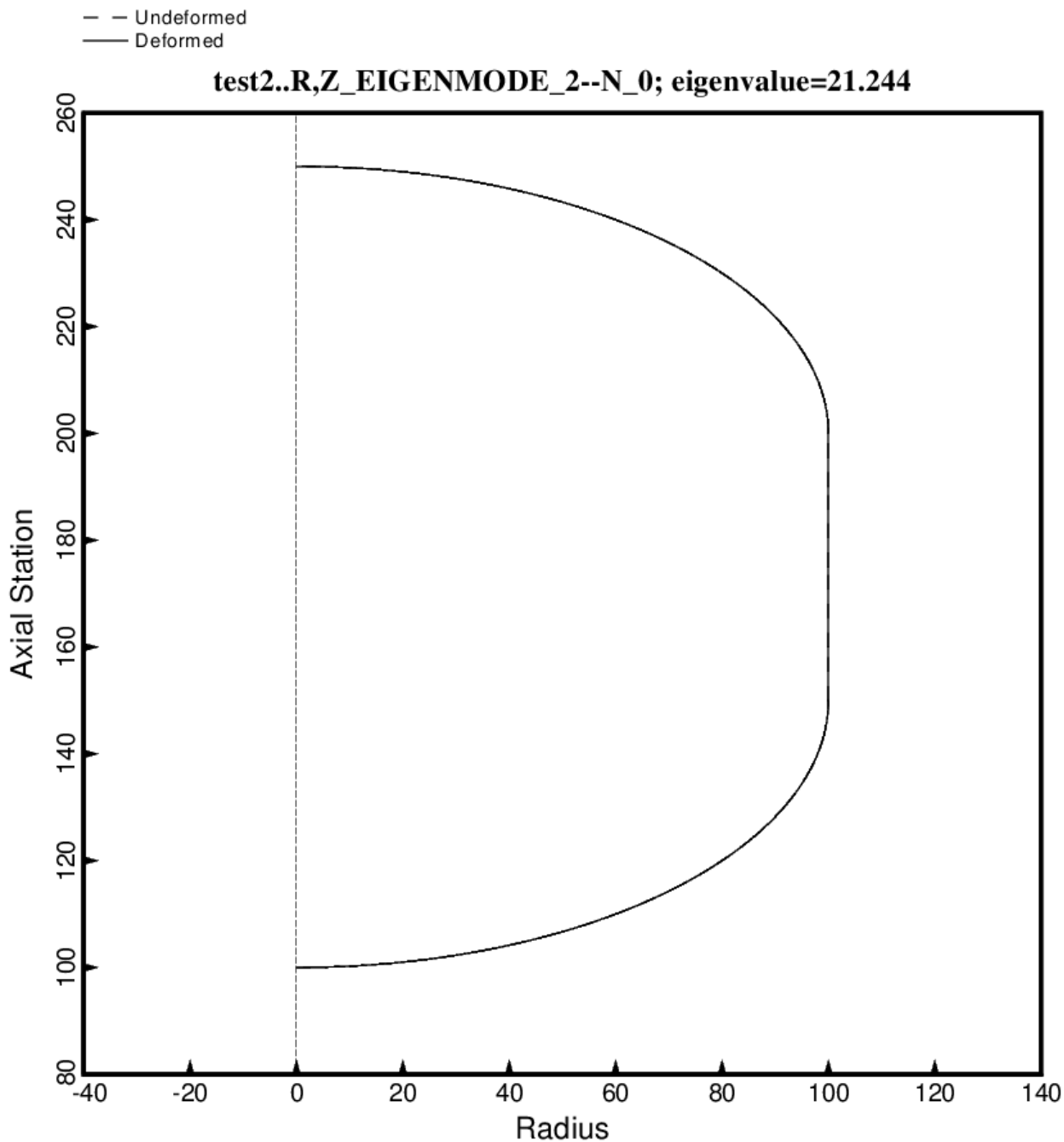


Fig. 90 (new) Free vibration mode of the optimized tank/strut system for the short propellant tank with one set of struts, 4 strut pairs in that set, Load Case 2 (test.BEHX12). The struts are attached to a propellant tank support ring located at the same axial coordinate as the midlength of the propellant tank. The struts are present in the BIGBOSOR4 model but are not plotted here because BIGBOSOR4 does not yet have the capability to plot springs. This second mode with  $n = 0$  circumferential waves corresponds to rolling motion. The optimum design was found with use of the “permanent” (constant density) versions of bosdec (bosdec.tank) and addbosor4 (addbosor4.tank).

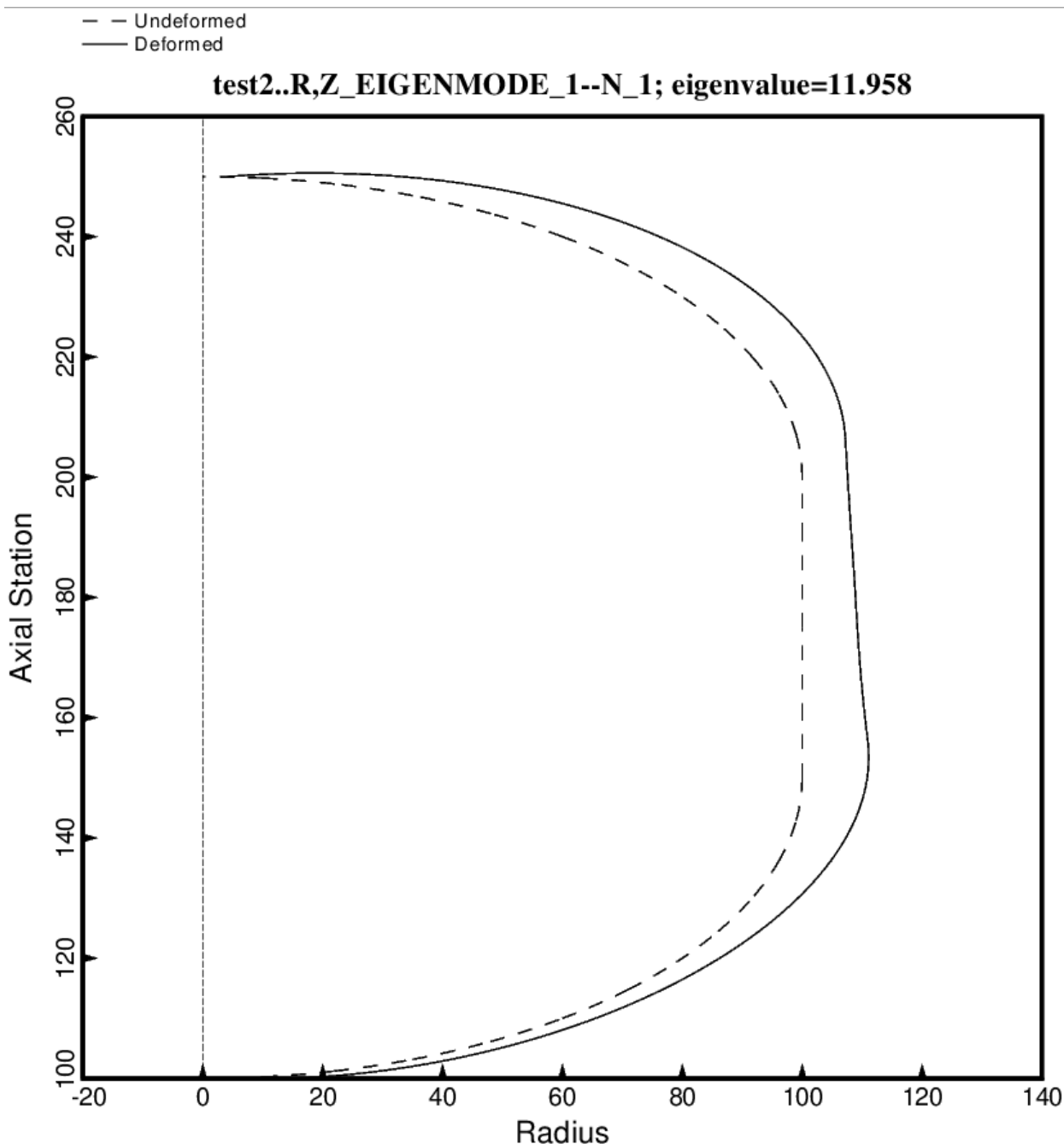


Fig. 91 (new) Free vibration mode of the optimized tank/strut system for the short propellant tank with one set of struts, 4 strut pairs in that set, Load Case 2 (test.BEHX12). The struts are attached to a propellant tank support ring located at the same axial coordinate as the midlength of the propellant tank. The struts are present in the BIGBOSOR4 model but are not plotted here because BIGBOSOR4 does not yet have the capability to plot springs. This first mode with  $n = 1$  circumferential wave corresponds to lateral-pitching motion. The optimum design was found with use of the “permanent” (constant density) versions of bosdec (bosdec.tank) and addbosor4 (addbosor4.tank). This figure is analogous to Fig. 21.

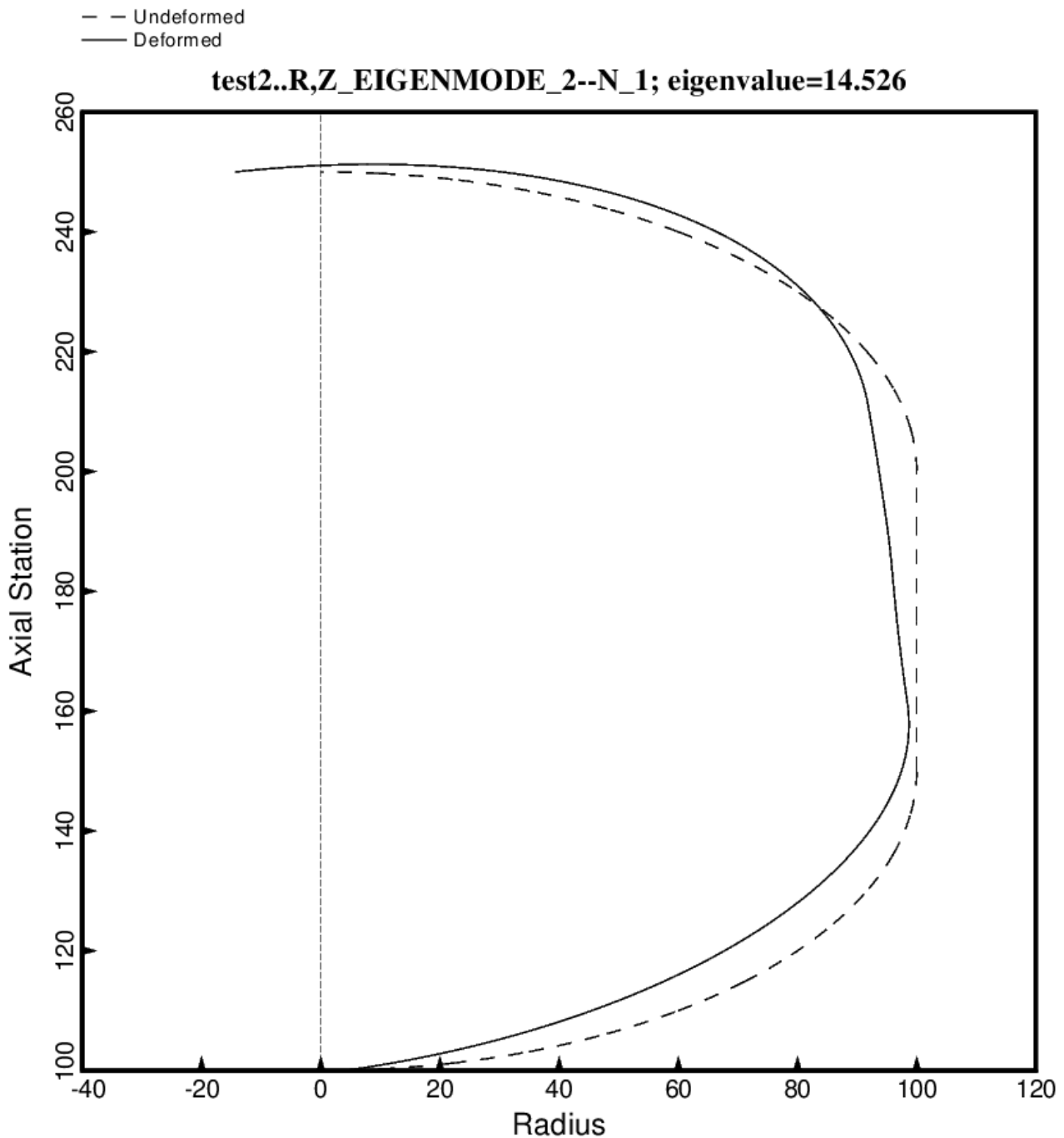


Fig. 92 (new) Free vibration mode of the optimized tank/strut system for the short propellant tank with one set of struts, 4 strut pairs in that set, Load Case 2 (test.BEHX12). The struts are attached to a propellant tank support ring located at the same axial coordinate as the midlength of the propellant tank. The struts are present in the BIGBOSOR4 model but are not plotted here because BIGBOSOR4 does not yet have the capability to plot springs. This second mode with  $n = 1$  circumferential wave corresponds to lateral-pitching motion. The optimum design was found with use of the “permanent” (constant density) versions of bosdec (bosdec.tank) and addbosor4 (addbosor4.tank).

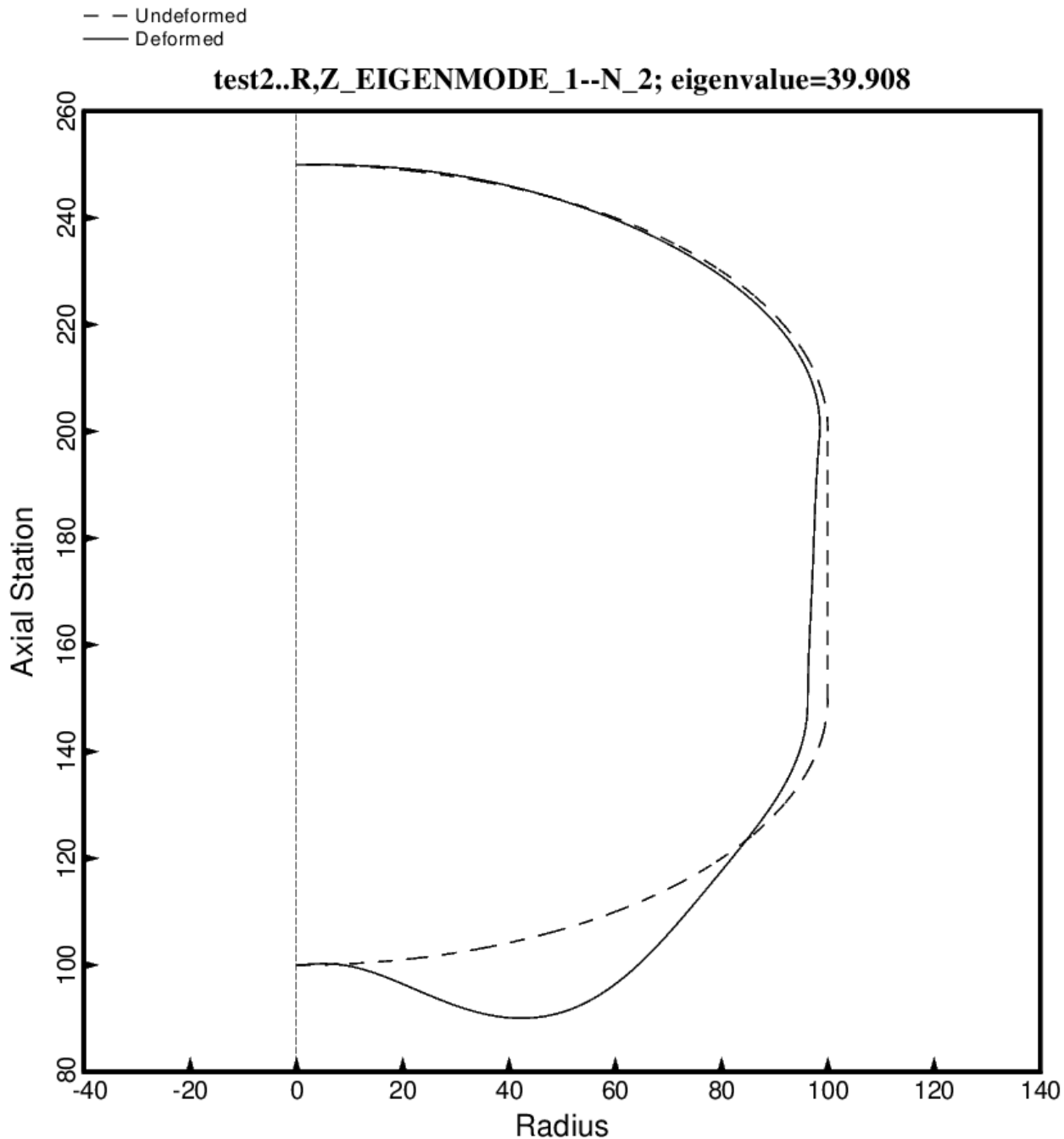


Fig. 93 (new) Free vibration mode of the optimized tank/strut system for the short propellant tank with one set of struts, 4 strut pairs in that set, Load Case 2 (test.BEHX12). The struts are attached to a propellant tank support ring located at the same axial coordinate as the midlength of the propellant tank. The struts are present in the BIGBOSOR4 model but are not plotted here because BIGBOSOR4 does not yet have the capability to plot springs. This first mode with  $n = 2$  circumferential wave corresponds to a flexible “shell” mode in which mainly the aft dome is vibrating. The optimum design was found with use of the “permanent” (constant density) versions of bosdec (bosdec.tank) and addbosor4 (addbosor4.tank). This figure is analogous to Fig. 22bnew.

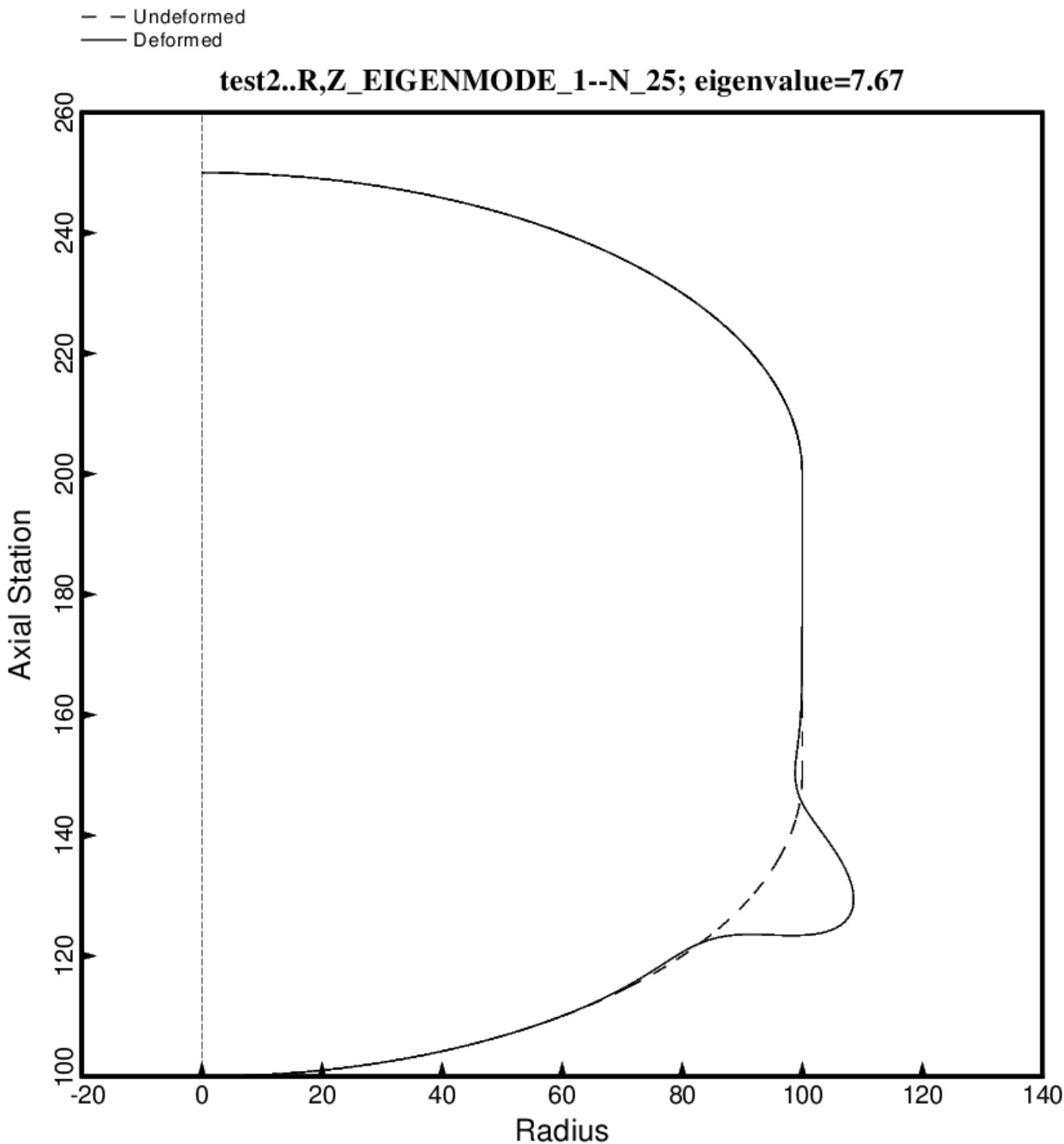


Fig. 94 (new) Buckling of the short optimized tank with one set of struts, 4 strut pairs in that set. The loading is Load Case 1: axial acceleration = 10 g, 25 psi ullage pressure, 200 deg. tank cool-down. Buckling in the aft 2:1 ellipsoidal dome is caused by the narrow band of hoop compression in the dome knuckle region. This optimum design was found with use of the “temporary” (varying density) versions of bosdec (bosdec.density.var) and addbosor4 (addbosor4.density.var). This figure is analogous to Fig. 23.

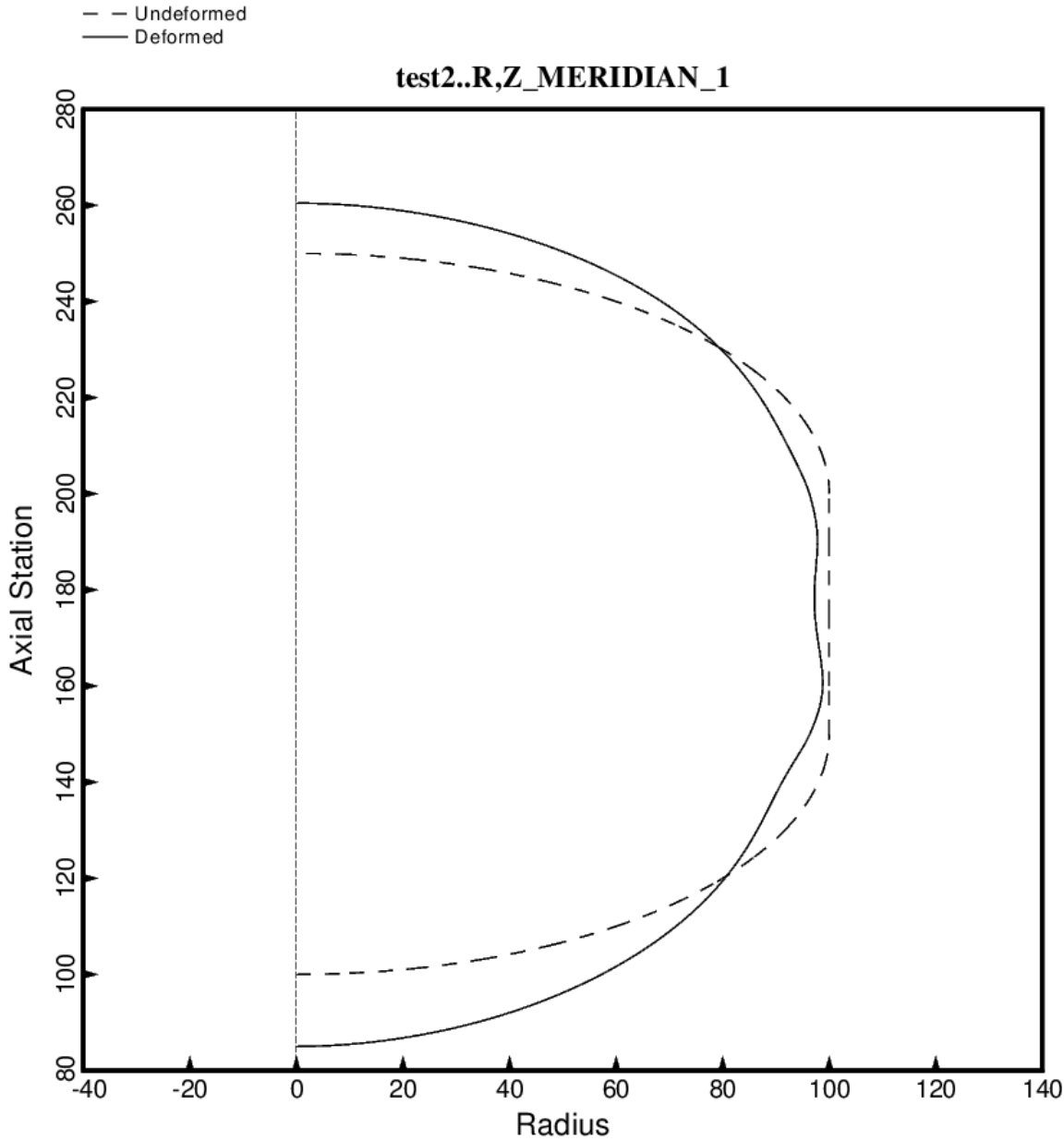


Fig. 95 (new) Load Case 1 (10 g axial acceleration, 25 psi ullage pressure, 200 deg. tank cool-down): Deformation along the meridian at zero degrees of the short propellant tank with one set of struts, 4 strut pairs in that set of struts. In this BIGBOSOR4 model, from which the maximum stresses in the propellant tank are computed, the struts (springs) are replaced by the concentrated loads that these springs apply to the tank. The concentrated loads are represented in the BIGBOSOR4 model as Fourier series expansions of circumferential line loads. The non-axisymmetric linear equilibrium state is obtained by superposition of the displacements and stresses from each Fourier component. This optimum design was found with use of the “temporary” (varying density) versions of bosdec (bosdec.density.var) and addbosor4 (addbosor4.density.var). This figure is analogous to Fig. 27.

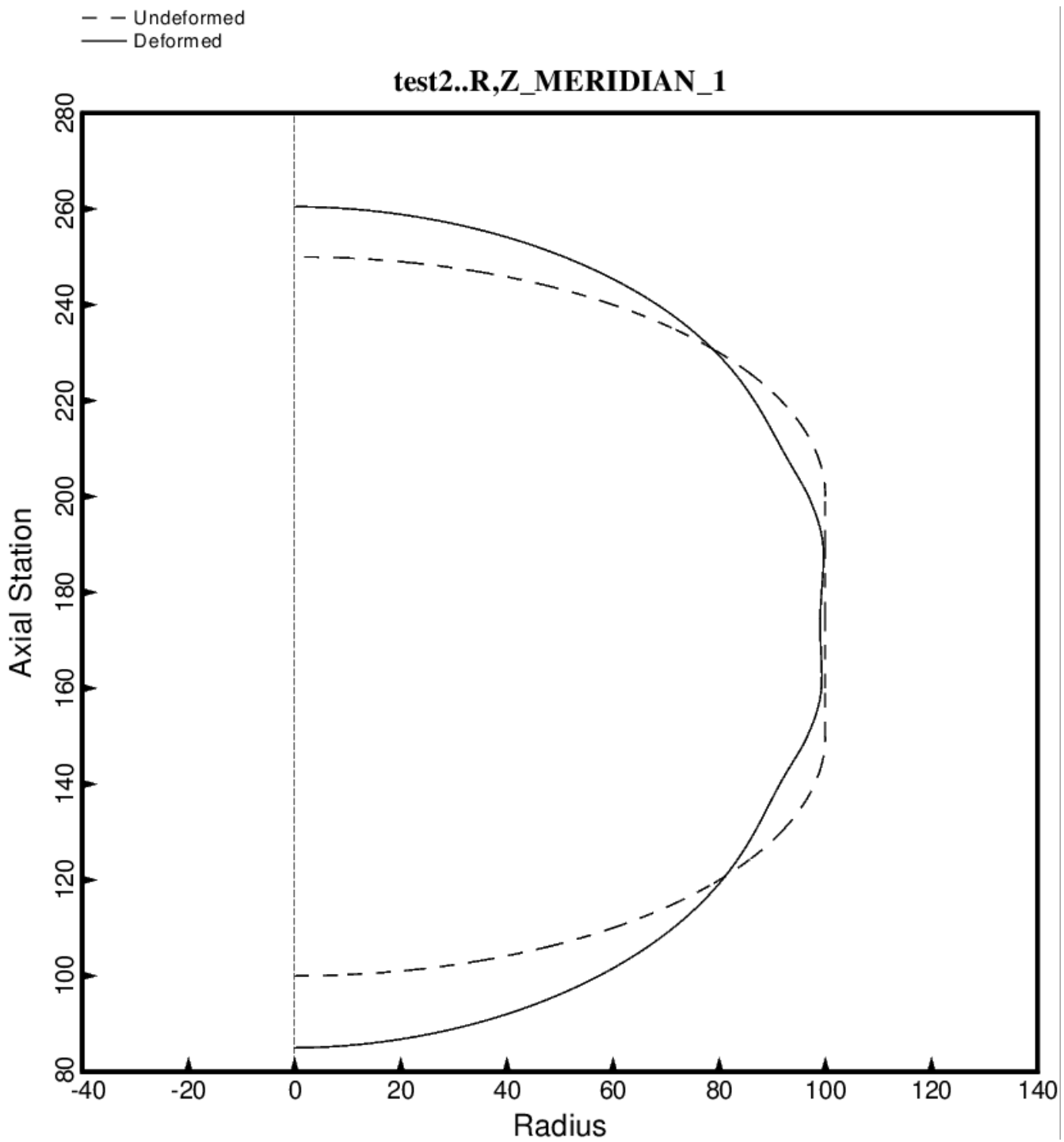


Fig. 96 (new) Load Case 1 (10 g axial acceleration, 25 psi ullage pressure, 200 deg. tank cool-down): Deformation along the meridian at 25 degrees of the short propellant tank with one set of struts, 4 strut pairs in that set of struts. This optimum design was found with use of the “temporary” (varying density) versions of bosdec (bosdec.density.var) and addbosor4 (addbosor4.density.var). This figure is analogous to Fig. 27b.

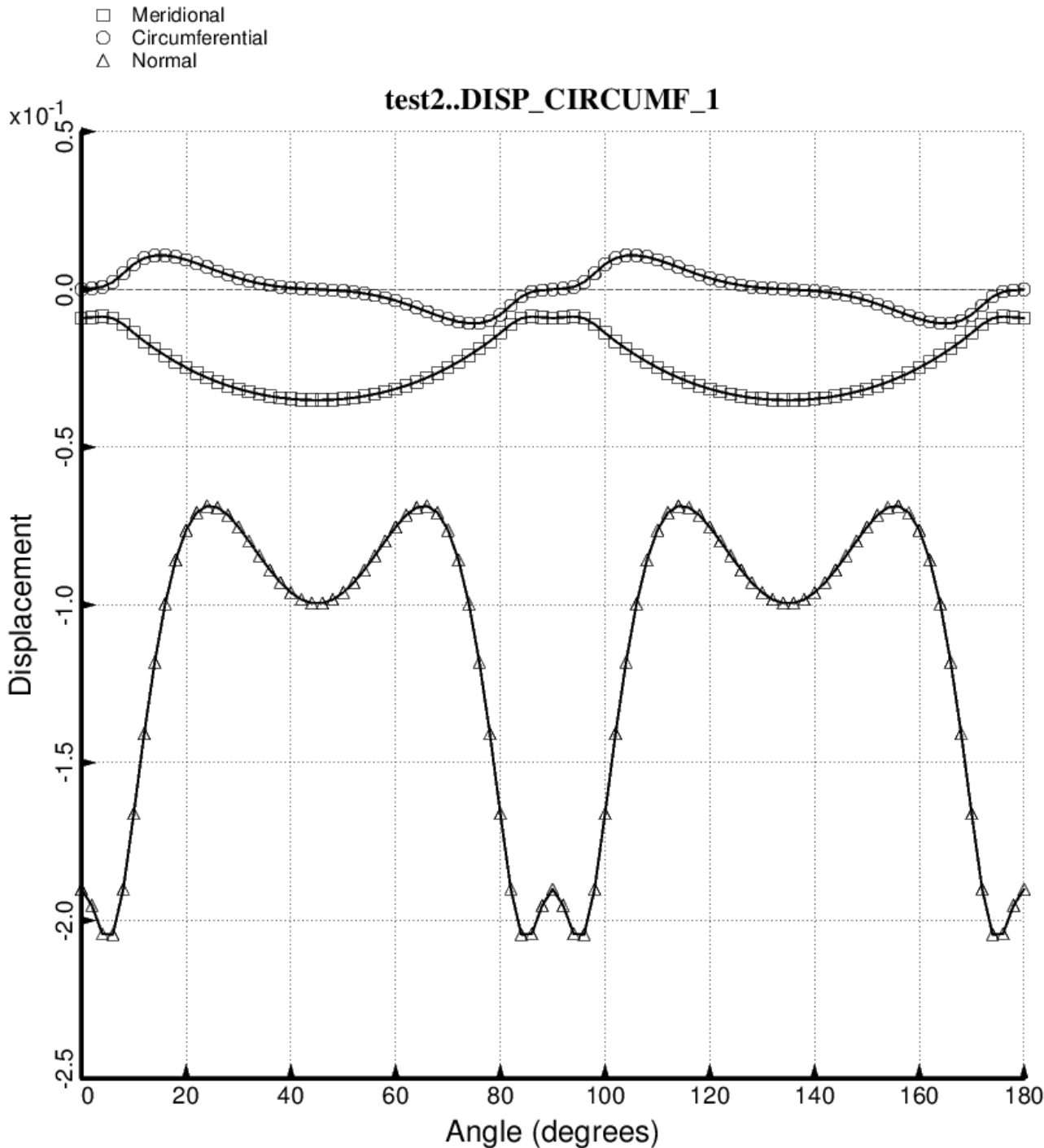


Fig. 97 (new) Load Case 1 (10 g axial acceleration, 25 psi ullage pressure, 200 deg. tank cool-down): Deformation along 180 degrees of the circumference at the midlength of the cylindrical part of the short propellant tank with one set of struts, 4 strut pairs in that set of struts. This optimum design was found with use of the “temporary” (varying density) versions of bosdec (bosdec.density.var) and addbosor4 (addbosor4.density.var). This figure is analogous to Fig. 27d.

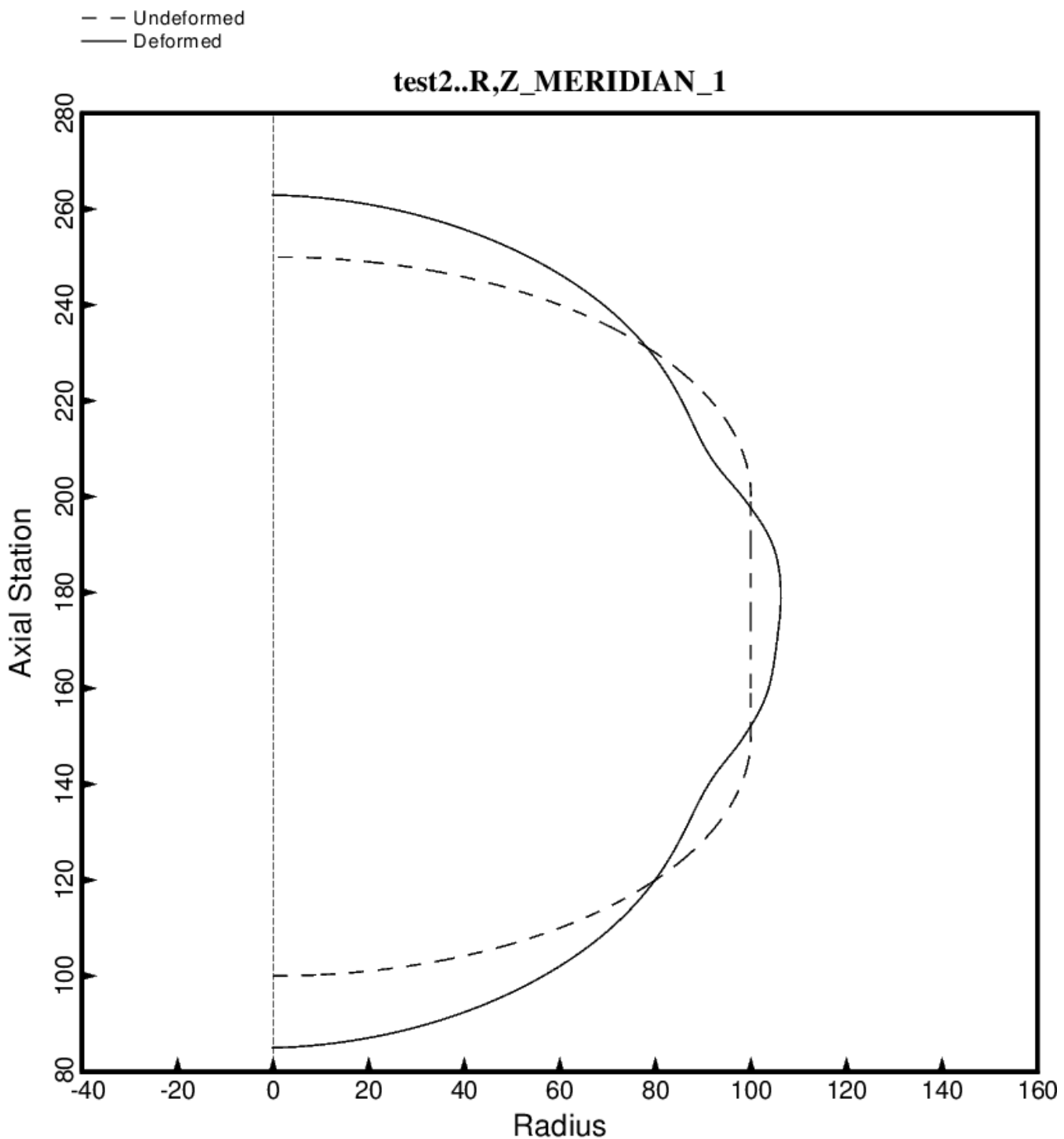


Fig. 98 (new) Load Case 2 (10 g lateral acceleration, 25 psi ullage pressure, 200 deg. tank cool-down): Deformation along the meridian at 80 degrees of the short propellant tank with one set of struts, 4 strut pairs in that set of struts. This optimum design was found with use of the “temporary” (varying density) versions of bosdec (bosdec.density.var) and addbosor4 (addbosor4.density.var). This figure is analogous to Fig. 28b.

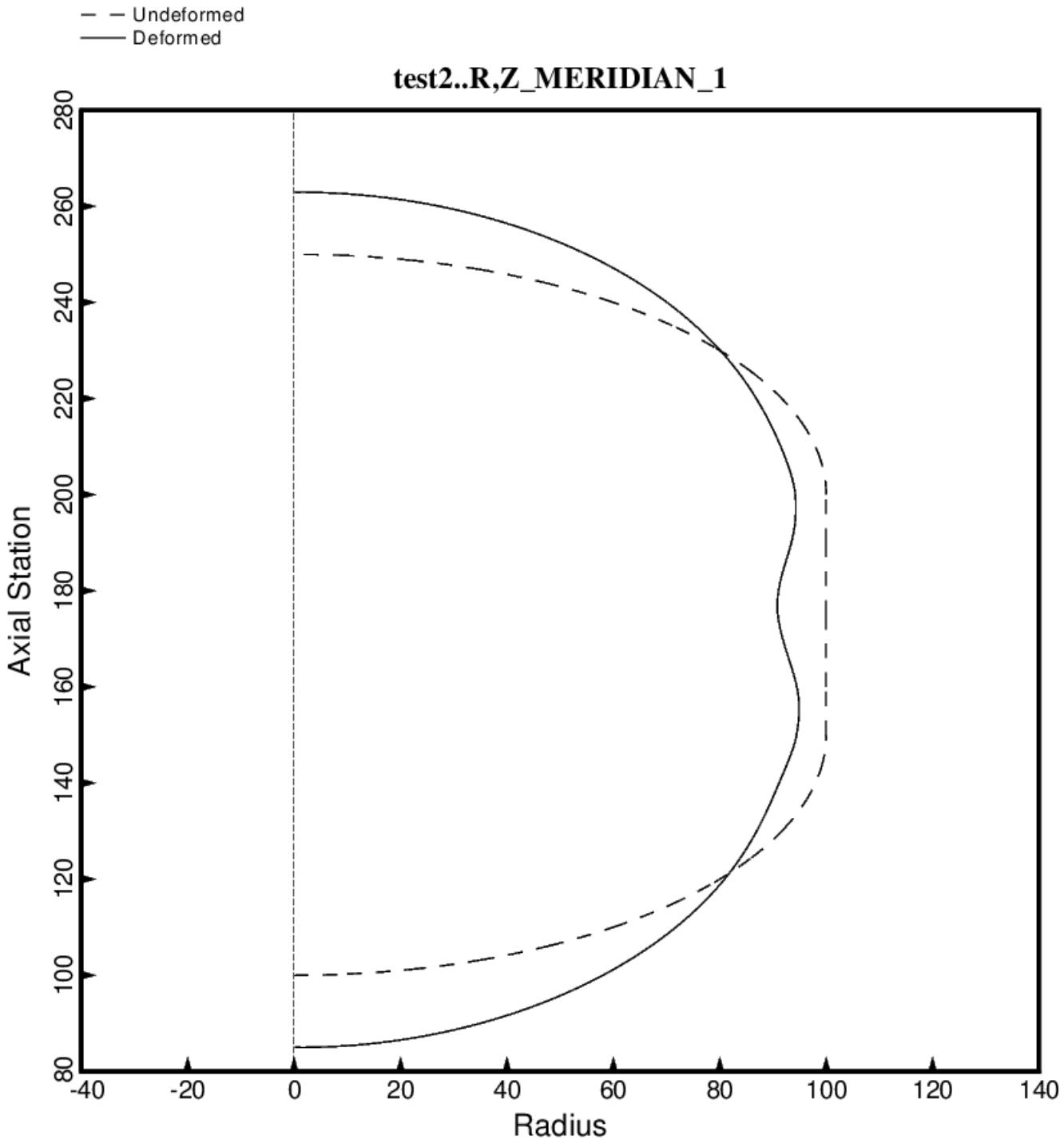


Fig. 99 (new) Load Case 2 (10 g lateral acceleration, 25 psi ullage pressure, 200 deg. tank cool-down): Deformation along the meridian at 100 degrees of the short propellant tank with one set of struts, 4 strut pairs in that set of struts. This optimum design was found with use of the “temporary” (varying density) versions of bosdec (bosdec.density.var) and addbosor4 (addbosor4.density.var). This figure is analogous to Fig. 28c.

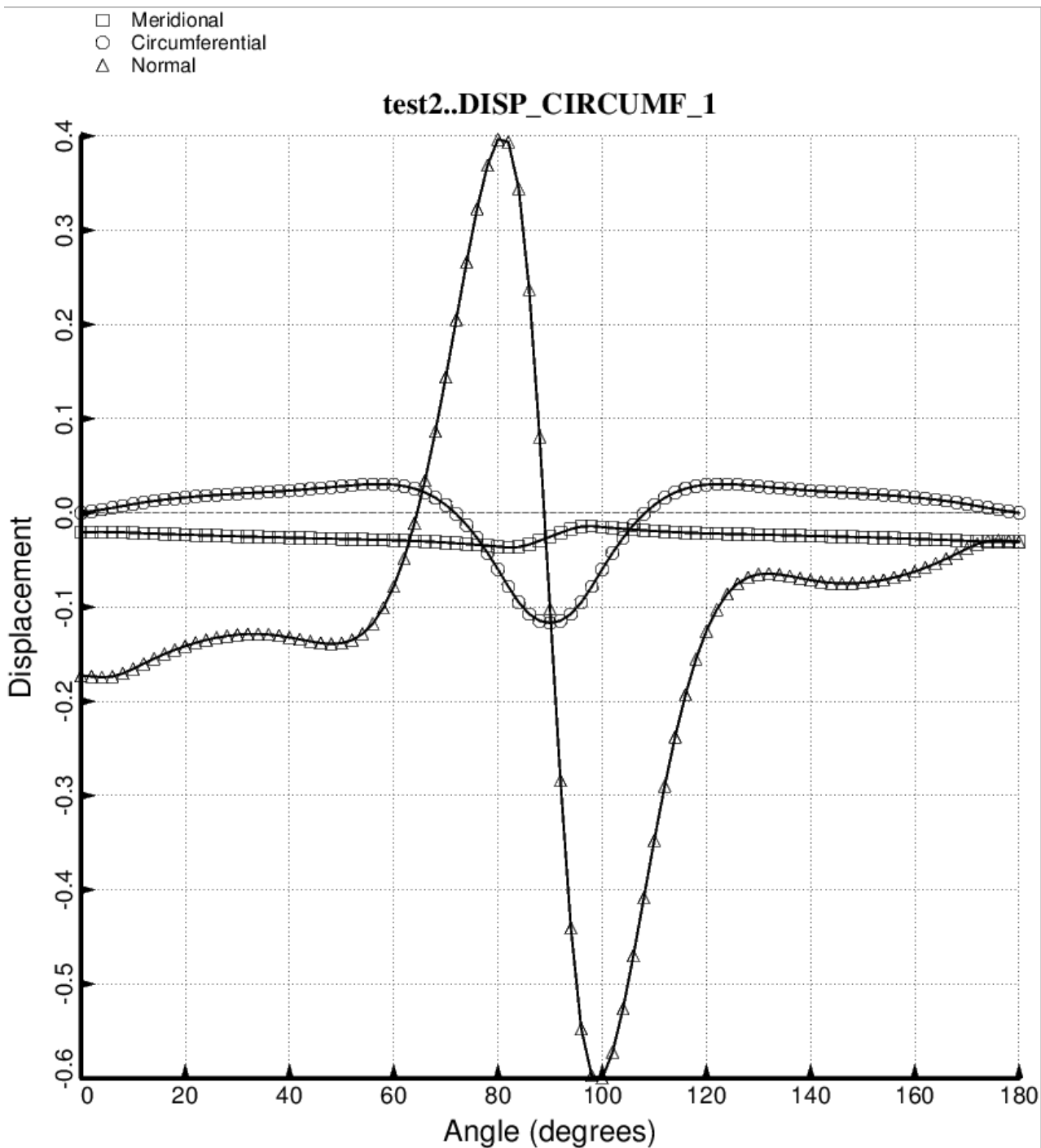


Fig. 100 (new) Load Case 2 (10 g lateral acceleration, 25 psi ullage pressure, 200 deg. tank cool-down): Deformation along 180 degrees of the circumference at the midlength of the cylindrical part of the short propellant tank with one set of struts, 4 strut pairs in that set of struts. This optimum design was found with use of the “temporary” (varying density) versions of bosdec (bosdec.density.var) and addbosor4 (addbosor4.density.var). This figure is analogous to Fig. 28d.

